HAL
open science

Trace metals dynamics in a tropical mangrove-dominated estuary (Can Gio, Viet Nam)

Thanh Nho Nguyen

To cite this version:

Thanh Nho Nguyen. Trace metals dynamics in a tropical mangrove-dominated estuary (Can Gio, Viet Nam). Geochemistry. Université de la Nouvelle-Calédonie, 2018. English. NNT : 2018NCAL0006 . tel-03228268

HAL Id: tel-03228268

https://unc.hal.science/tel-03228268

Submitted on 18 May 2021

HAL is a multi-disciplinary open access archive for the deposit and dissemination of scientific research documents, whether they are published or not. The documents may come from teaching and research institutions in France or abroad, or from public or private research centers.

L'archive ouverte pluridisciplinaire **HAL**, est destinée au dépôt et à la diffusion de documents scientifiques de niveau recherche, publiés ou non, émanant des établissements d'enseignement et de recherche français ou étrangers, des laboratoires publics ou privés.

Institut de Recherche pour le Développement FRANCE

UNIVERSITÉ de la NOUVELLE-CALÉDONIE

ÉCOLE DOCTORALE DU PACIFIQUE

École Doctorale du Pacifique – ED 469

THESE DE DOCTORAT

présentée à l'Université de la Nouvelle-Calédonie

dans la spécialité: Sciences de la terre et de l'environnement

par

NGUYEN THANH NHO

Dynamiques des éléments traces métalliques dans un estuaire tropical à mangroves (Can Gio, Vietnam)

Le 23 juillet 2018

devant un jury composé de:

Prof. Andrea Alfaro	Auckland University of Technology	Rapporteur
Dr. Christian Sanders	Southern Cross University	Rapporteur
Prof. Dr. Michel Allenbach	Université de la Nouvelle-Calédonie	Examinateur
Prof. Shing Yip Joe Lee	The Chinese University of Hong Kong	Examinateur
Dr. Cyril Marchand	IRD Nouvelle Calédonie	Directeur
Dr. Nhu-Trang Tran-Thi	University of Science Ho Chi Minh City-VNU	Directeur
Dr. Emilie Strady	IGE-IRD France	Invitée

Juillet 2018

Institut de Recherche pour le Développement FRANCE

UNIVERSITÉ de la NOUVELLE-CALÉDONIE

ÉCOLE DOCTORALE DU PACIFIQUE

École Doctorale du Pacifique – ED 469

PhD THESIS

Doctor of Philosophy presented at the University of New Caledonia

Specialty: Earth and Environmental Sciences

by

NGUYEN THANH NHO

Trace metals dynamics in a tropical mangrove-dominated estuary (Can Gio, Viet Nam)

Presented the 24th of July 2018

Members of the PhD committee:

Prof. Andrea Alfaro	Auckland University of Technology	Rapporteur
Dr. Christian Sanders	Southern Cross University	Rapporteur
Prof. Dr. Michel Allenbach	Université de la Nouvelle-Calédonie	Examinateur
Prof. Shing Yip Joe Lee	The Chinese University of Hong Kong	Examinateur
Dr. Cyril Marchand	IRD Nouvelle Calédonie	Directeur
Dr. Nhu-Trang Tran-Thi	University of Science Ho Chi Minh City-VNU	Directeur
Dr. Emilie Strady	IGE-IRD France	Invitée

July 2018

ACKNOWLEDGEMENTS

I have spent the last three years studying trace metals dynamics in the mangrove forest. My dissertation would not have been completed without my professors.

Foremost, I am grateful to Dr. Cyril Marchand who has spent a substantial amount of energy to teach me and to guide me in the last 3 years to complete the research work necessary for my dissertation. He has spent a lot of his time to assist me with all that I needed.

I am also grateful to Dr. Nhu-Trang Tran-Thi who has supported to me the best conditions to complete this dissertation during my time at University of Science, Viet Nam National University Ho Chi Minh City. She has given me valuable advices in time of stress during my studying.

I would like to thank Dr. Emilie Strady (IGE-IRD France) who has taught me the valuable knowledge during my writing of the dissertation. She also spent a lot of her time to help me for the corrections.

I would like to thank Prof. Andrea Alfaro, Dr. Christian Sanders, Prof. Dr. Michel Allenbach, Prof. Shing Yip Joe Lee, the members of the jury to have agreed to evaluate my PhD thesis

During these 3 years, I have met and made numerous friends, especially the “mangrove team”: Dr. Adrien Jacotot, Dr. Frank David, Dr. Pierre Tailladart, PhD candidate Carine Bourgeois, PhD candidate Vinh Truong Van, MSc. Joanne Aime” with leader Dr. Cyril Marchand. I would like to thank them to have helped me in one way or another during my thesis.

It is a pleasure to thank the people who helped me with in different aspect, Prof. Michel Allenbach (UNC) for his help during my stay in New Caledonia, Ms. Leocadie (LAMA lab, New Caledonia) for helping with sample preparation and analysis, Benjamin Moreton and Hélène Kaplan (AEL-lab, New Caledonia) for their help with sampling equipment at field and sample preparation at lab, Nguyen Huu Phat for his sample analysis (in Viet Nam), my students Nguyen

Ngoc Hon, Nguyen Truong Giang, To Thi Hong Chuyen, Nguyen Tien Hoa for their help with field sampling.

This research is funded by Vietnam National University Ho Chi Minh City (VNU-HCM) under grand number C2016-18-07, and a BEST grant from IRD.

Contents

1. Chapter 1. General introduction 1
1.1. Mangroves, global distribution and ecological roles 1
1.1.1. Definition of mangroves 1
1.1.2. Global distribution and ecological roles of mangroves 2
1.2. Sources, distribution of trace metals in mangrove. 4
1.2.1. Sources of trace metals 4
1.2.2. Distribution of trace metal in mangroves 5
1.2.2.1 Trace metals in mangrove waters 7
1.2.2.2 Trace metals in mangrove sediments 7
1.2.2.3 Trace metals in mangrove plants 8
1.2.2.4 Heavy metals in mangrove-associated gastropods 9
1.2.3. Geochemistry of trace metals in mangrove sediments. 10
1.2.4. Possible reactions affecting the cycling of trace metals in mangrove sediments 10
1.2.5. Factors controlling the geochemistry of trace metals in mangrove sediments 12
1.2.5.1 Organic matter 12
1.2.5.2 Redox cycling 12
1.2.5.3 Iron and manganese oxihydroxides 14
1.2.5.4 pH and carbonates 16
1.2.5.5 Salinity 17
1.3. The Can Gio Mangrove Biosphere Reserve 17
1.3.1. Geo-physical characteristics 17
1.3.2. The destruction and reforestation of the Can Gio mangrove 20
1.3.3. Research projects conducted in the Can Gio mangrove 23
1.4. Objectives of the dissertation 24
2. Chapter 2 - Trace metals partitioning between particulate and dissolved phases along a tropical mangrove estuary 27
ABSTRACT 28
2.1. Introduction 29
2.2. Materials and Methods 31
2.2.1. Study area 31
2.2.2. Field sampling and measurements 33
2.2.3. Samples analysis 34

2.2.4. Data analysis 36
2.3. Results and discussion 36
2.3.1. Spatial and seasonal variations of physico-chemical parameters 36
2.3.2. Trace metal distributions at the upstream site during the monsoon 40
2.3.3. Trace metal partitioning in the estuarine zone 42
2.3.3.1 Iron 42
2.3.3.2 Manganese 44
2.3.3.3 Chromium 46
2.3.3.4 Arsenic 47
2.3.3.5 Copper 48
2.3.3.6 Nickel 49
2.3.3.7 Cobalt and lead 51
2.4. Conclusions 52
3. Chapter 3 - Trace metal geochemistry and ecological risks in a tropical mangrove 57
ABSTRACT 58
3.1. Introduction 59
3.2. Materials and methods 61
3.2.1. Study site 61
3.2.2. Sample collections and preservations 62
3.2.3. Analytical methods and calculations 63
3.2.3.1 Salinity, pH and redox measurements 63
3.2.3.2 Metal concentrations in pore-waters 63
3.2.3.3 Total metal concentrations in sediments 64
3.2.3.4 Sequential extraction of metal chemical fractions 65
3.2.3.5 Total organic carbon (TOC) 66
3.2.3.6 Sediment bulk density and trace metal stock estimation 66
3.2.3.7 Data analysis 67
3.3. Results 67
3.3.1. Physico-chemical parameters in the sediment cores 67
3.3.2. Total metal concentrations in the sediment cores 68
3.3.3. Trace metal stock estimation 69
3.3.4. Metal partitioning in mangrove sediments 71
3.3.4.1 Fe and Mn 71

3.3.4.2 Ni, Cr, Cu, Co and As 73
3.3.5. Distribution of dissolved metals concentrations in mangroves pore-waters 75
3.4. Discussion 78
3.4.1. Mangrove sediments characteristics 78
3.4.2. Lateritic soil as main source of trace metal in mangrove sediments. 79
3.4.3. Trace metal geochemistry in mangrove sediments. 80
3.4.3.1 Redox sensitive elements (Fe and Mn) 80
3.4.3.2 Geochemistry of Ni, Cr, Cu, Co and As 83
3.4.4. Trace metals stocks and ecological potential risk assessment 88
3.5. Conclusions 90
4. Chapter 4 - Trace metals accumulation in plants and snails of a tropical mangrove (Can Gio, Vietnam) 93
ABSTRACT 94
4.1. Introduction 95
4.2. Materials and methods 97
4.2.1. Study area 97
4.2.2. Field sampling 98
4.2.3. Analytical methods and calculations 99
4.2.3.1 Samples digestion 99
4.2.3.2 Data calculations 100
4.3. Results 102
4.3.1. Plant tissues 102
4.3.2. Snails 104
4.4. Discussions 106
4.4.1. Trace metal bioaccumulation in Avicennia and Rhizophora mangrove tissues 106
4.4.1.1 Essential elements: Fe, Mn, Cu 106
4.4.1.2 Non-essential elements: As, Ni, Cr, Co 109
4.4.2. Trace metal bioaccumulation in snails 112
4.5. Conclusions 115
5. Chapter 5 - Trace metals dynamic in a tropical mangrove tidal creek, influence of pore-water seepage 119
ABSTRACT 120
5.1. Introduction 121
5.2. Materials and Methods 122

5.2.1. Study site 122
5.2.2. Field sampling 124
5.2.3. In situ measurements of physico-chemical parameters 125
5.2.4. Samples analysis 126
5.2.5. Data calculations 127
5.3. Results 128
5.3.1. Pore-water characteristics 128
5.3.2. Physico-chemical parameters variability in the tidal creek 130
5.3.3. Variability of dissolved metals concentrations (M_D) in the tidal creek 130
5.3.4. Variability of particulate metal concentrations (M_P) in the tidal creek 132
5.4. Discussion 133
5.4.1. Temporal variability of physico-chemical parameters in the tidal creek 133
5.4.2. Trace metals dynamics in the mangrove tidal creek 134
5.4.2.1 Manganese dynamic 134
5.4.2.2 Iron dynamics 138
5.4.2.3 Cobalt and Nickel dynamics 141
5.5. Conclusions 143
6. Chapter 6 - Conclusions and Perspectives 145
6.1. Conclusions 145
6.2. Research Perspectives 148
6.2.1. Seasonal effect on trace metals geochemistry in mangrove sediments 148
6.2.2. Estimate trace metals budget in mangrove ecosystem 148
6.2.3. Trace metals bioaccumulations in coastal trophic chain 149
6.2.4. Comparison of trace metals exports with other mangroves characterized by higher trace metals loads. 149
REFERENCES .....

LIST OF FIGURES

Fig. 1-1. (a) Schematic diagram of a mangrove (Selvam and Karunagaran 2004); (b) Physical and biological components of mangrove ecosystem, adapted from Kathiresan and Bingham (2001).. 1
Fig. 1-2. Mangrove Species Richness: Native distributions of mangrove species (Polidoro et al. 2010)– colors represent the number of species. 2
Fig. 1-3. Conceptual model of physical, chemical and biological variables and processes for metal behaviors (de Souza Machado et al. 2016)(de Souza Machado et al. 2016). 4
Fig. 1-4. Representation of post-deposition mobilization of trace metals in coastal sediments (Lacerda 1998). 11
Fig. 1-5. A hypothetical plot showing change in terminal electron-accepting processes for a soil containing a finite supply of bioavailable organic matter and soil oxidation capacity (Chadwick and Chorover 2001). 13
Fig. 1-6. Concept of a model with selected (a) abiotic and (b) biotic redox processes that influence the fate of arsenic in the environment (Borch et al. 2009)(Borch et al. 2009). 15
Fig. 1-7. Map of study area showing: i) the location of Viet nam in the Southeast Asia, ii) the location of Can Gio mangrove in the edge of Ho Chi Minh City, iii) the zonation of Can Gio Mangrove Biosphere Reserve Adapted from (Kuenzer and Tuan 2013) and (UNESCO 2000). 18
Fig. 1-8. (a) The corner of Long Tau river in Can Gio mangrove with the Rhizophora in the background; (b) high density of saplings on the ground of the Rhizophora stand. 19
Fig. 1-9. The view of a tidal creek in Can Gio mangrove with the Avicennia along the banks: (a) flooding and (b) ebbing periods. 20
Fig. 1-10. The distribution of mangrove species in Can Gio Mangrove Biosphere Reserve (Kuenzer and Tuan 2013).. 22
Fig. 1-11. The foreground image of (a) the mudflat with crabs activity and (b) beneath the Avicennia alba stand. 23
Fig. 2-1. Satellite image of Can Gio mangrove forest (black area) and sampling locations along the estuary. Site 1 characterizing the riverine and urban end-member; Site 2 characterizing aquaculture activities (mainly shrimps) and the buffer zone of mangrove forest; Site 3 characterizing the core of mangrove forest; site 4 characterizing the marine end-member. 32
Fig. 2-2. Spatio-temporal variations in pH, DO, POC DOC and TSS along the salinity gradient during the dry and the wet seasons. 39
Fig. 2-3. Relationship between the total metal concentrations (i.e. dissolved plus particulate metal concentrations, expressed in µg L-1) of Fe, Cr, Ni, Pb, Mn, Cu, As, Co and TSS concentration during the dry and the wet seasons. 42
Fig. 2-4. Distribution of dissolved, particulate, log Kd of metals in the Can Gio mangrove estuary during the dry (gray dots) and the wet seasons (black dots), with circles, squares, multiplication signs and triangles representing the site 1, site 2, site 3 and site 4 respectively: Fe (a), Mn (b), Cr (c), As (d), Cu (e), Ni (f), Co (g) and Pb (h) 45
Fig. 2-5. Interrelations between dissolved metal concentrations and relationships between log KD of metal with physico-chemical parameters during the dry and the wet seasons: (a) Log KDMn and DO; (b) Log KDMn and pH; (c) CrD and POC; (d) log KDCr and POC ; (e) log K_D^{Cr} and DO;

(f) Cr_D and Fe_D; (g) As_p and Fe_p; (h) $LogK_D^{As}$ and POC; (i) Cu_D and Fe_D; (j) Ni_D and Mn_D; (k) Co_D and Fe_D; (l) Pb_D and Fe_D 50
Fig. 3-1. Location of Can Gio mangrove and collected samples. Three cores (90 cm depth) were collected in the mudflat, beneath the Avicennia and the Rhizophora stands..... 62
Fig. 3-2. Depth distribution of (a) pH, (b) Eh, (c) Salinity and (d) Total organic carbon in the mudflat, the Avicennia stand and the Rhizophora stand in the Can Gio mangrove. 68
Fig. 3-3. Depth profile of Sequential extraction of Fe (a), Mn (b), Ni (c), Cr (d), Cu (e), Co (f) and As (g) in the mudflat, the Avicennia stand and the Rhizophora stand in Can Gio mangrove (continued in next page)..... 72
Fig. 3-4. Depth profile of dissolved metals concentrations (µg L-1) in the pore-waters of the mudflat, Avicennia and Rhizophora stands. Asterisks highlight extreme values that could not be shown in the graph even with cut axis (i.e. values of 14.4 for Cr and 13.9 fo Cu). Continued in next page. 76
Fig. 3-5. Risk Assessment Code of metals in the sediment cores of the mudflat, the Avicennia stand and the Rhizophora stand in Can Gio mangrove..... 89
Fig. 4-1. Map of the study area showing: i) the location of Can Gio mangrove in Viet nam and ii) the location of the collected biological samples in the mangrove. 99
Fig. 5-1. Map of the study area showing: i) the location of Can Gio mangrove in Viet nam and ii) the location of the tidal creek in the mangrove (red star). 124
Fig. 5-2. Temporal variations of water level, salinity, pH, DO, TSS, POC and DOC observed in neap and spring tidal cycles during the dry season (04-2015) and the wet season (10-2015). The 222Rn were measured only during the wet season..... 129
Fig. 5-3. Temporal distribution of dissolved concentrations of trace metals (MD) over the neap and the spring tidal cycles during the dry season (04.2015) and the wet season (10.2015). Dissolved Ni concentrations were measured only during the rainy season..... 131
Fig. 5-4. Distributions of the particulate metal concentrations (Mp) over neap and spring tidal cycles during the dry season (04.2015) and the wet season (10.2015). The data of all trace metals within the neap tidal cycle in the dry season are not available..... 132
Fig. 5-5. Correlations between dissolved, particulate metal concentrations, physico-chemical parameters, and water level over all tidal cycles. The interrelationships between Log K_D of trace metals and physico-chemical parameters are also presented..... 136
Fig. 5-6. Interrelationships between trace metals and 222Rn in the ebb periods during the wet season (black dots), and during the dry (gray dots): (a) Mn_D, (b) Fe_D, (c) Co_D, (d) Ni_D and $_{222}Rn$; (e) DOC and ^{222}Rn, (f) Mn_D and DOC, (g) Co_D and Mn_D, (h) Co_D and DOC. 140
Fig. 5-7. Correlations between Log K_D of trace metals and water level in all tidal cycles in the creek during the dry (gray dots) and the wet seasons (black dots). 141

LIST OF TABLES

Table 2-1. Quality control of analytical methods applied for dissolved and particulate metal concentrations analysis: a) accuracy, precision and detection limit using estuarine water SLEW-3; b) BCR-277R for wet digestion method. a) Dissolved metal concentration analysis 35
Table 2-2. Bi-hourly water level (m), salinity, pH, DO (mgO2 L-1), DOC (mgC L-1), POC (%) and TSS (mg L-1) measured at the four sampling sites (site 1, site 2, site 3, site 4) during the dry and the wet seasons. 38
Table 2-3. Supplementary data 2.1: Original data of dissolved and particulate metal concentrations during the wet season (expressed in µg L^{-1} and mg kg^{-1}, respectively): S1 to S4 showed sampling sites; h0 to h24 are the hours of the 24 h tidal cycling, with a sampling every 2 h. 54
Table 2-4. Supplementary data 2.2: Original data of dissolved and particulate metal concentrations during the dry season (expressed in µg L^{-1} and mg kg^{-1}, respectively): S1 to S4 showed sampling sites; h0 to h24 are the hours of the 24 h tidal cycling, with a sampling every 2 h. 55
Table 3-1. Quality control of analytical methods applied for dissolved and total metal concentrations analysis: a) accuracy, precision and detection limit using estuarine water SLEW-3; b) BCR-277R for wet digestion method. 64
Table 3-2. Depth distribution of total metals concentrations (Fe, Mn, Ni, Cr, Cu, Co and As) in the mudflat, the Avicennia stand and the Rhizophora stand, expressed in mg kg^{-1}. 70
Table 3-3. Trace metals stocks in the sediments of the mudflat, the Avicennia stand and the Rhizophora stand in Can Gio mangrove (expressed in t ha-1, values were obtained based on the mean metal concentration and bulk density of each core on 50 cm depth). The stocks of each metal beneath Avicennia and Rhizophora stands were compared with those measured in the mudflat (%). 71
Table 4-1. Trace metal concentrations (expressed in µg g-1) in mangrove sediments of the Avicennia and the Rhizophora stands (data from the chapter 3). The data presenting the available concentrations (sum of exchangeable/carbonate bound, oxidizable and reducible fractions) and non-available concentration of each metal. 101
Table 4-2. Metal concentrations in the different tissues of the Avicennia and the Rhizophora trees(saplings and mature trees), expressed in µg g-1 (mean, SD). The roots samples of trees were collected in the upper part of 50 cm depth of the sediments. 102
Table 4-3. Bioconcentration factors (BCF = metal concentration in tissues/ metal concentration in sediment of the various plants developing in the studied mangrove in Can Gio,Viet nam. 103
Table 4-4. Translocation factors (TF = metal concentration in leaves/ metal concentration in roots) of the various plants developing in the studied mangrove in Can Gio, Viet nam. 104
Table 4-5. Metal concentrations in soft tissues of various snails (expressed in µg g-1): Checoreus (predator), Littoraria (leaves eater), Cerithidea (sediment eater) and Nerita (algae eater). 105
Table 4-6. Bioconcentration factors (BCF = metal concentration in soft tissues/ metal concentration correspond to metal concentration in feeding of individual type) of various snails in the Can Gio mangrove. 105
Table 5-1. Quality control of analytical methods applied for dissolved and particulate metal concentrations analysis:a) Accuracy, precision and detection limit using estuarine water SLEW-3; b) BCR-277R for wet digestion method. 127

Table 5-2. Average concentrations of dissolved trace metals (µg L-1, ± SD), pH, and salinity measured in the pore-water beneath the mangrove stands during the dry and the wet seasons. NA: non-available 129

Chapter 1. General introduction

1.1. Mangroves, global distribution and ecological roles

1.1.1. Definition of mangroves

Mangroves are assemblage of trees and shrubs that grow at the interface between land and sea in tropical and subtropical foreshore areas, where river water mixes with sea water (Fig. 1.1a). These plants, and the associated microbes, fungi, and animals, constitute mangrove forests community or mangal (Kathiresan and Bingham 2001). The mangal and its associated abiotic factors form the mangrove ecosystem (Fig. 1.1b). In ecological terms, mangrove forest, mangrove swamp and mangrove wetland are synonymously used to indicate a biodiverse community of species, to describe specific individual plant that can adapt to saline environment (Mitsch and Gosselink 2000) or to indicate salt-tolerant trees and shrubs that are native to the intertidal zones. Full knowledge of mangrove species classification is essential in differentiating between main plants and plant associations.

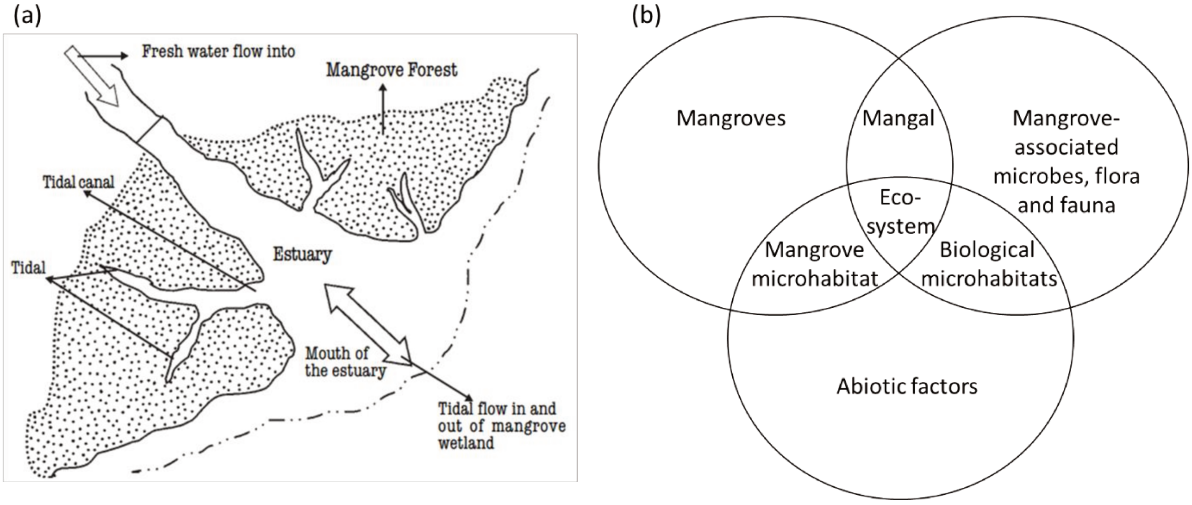

Fig. 1-1. (a) Schematic diagram of a mangrove (Selvam and Karunagaran 2004); (b) Physical and biological components of mangrove ecosystem, adapted from Kathiresan and Bingham (2001).

1.1.2. Global distribution and ecological roles of mangroves

Mangrove forests cover close to 140,000 km^2 and extend over a latitudinal range from 30 °N to 38 °S (Fig. 1.2) (Giri et al. 2011). Mangrove distribution in the world is: Asia (42 %), Africa (20 %), North and Central America (15 %), Oceania (12 %) and South America (11 %) (Giri et al. 2011). The more developed mangroves can be found in Sundarbans, Mekong Delta, Amazon, Madagascar, Papua New Guinea and Southeast Asia. The above pattern clearly indicates that mangrove distribution is limited by temperature (Duke 1992). The number of mangrove species varies according to a geographical location, position within an estuary, and the position along the intertidal profile (Duke et al. 1998). They prefer a humid climate with fresh water inflow that contains abundant nutrients and silts. Mangrove species worldwide comprise approximately 14 to 16 families and 54 to 75 species, with greatest biodiversity occurring in Southeast Asia (Tomlinson 2016). They are abundant in broad, sheltered, low-lying coastal plains, where topographic gradient are small and tidal amplitudes are large.

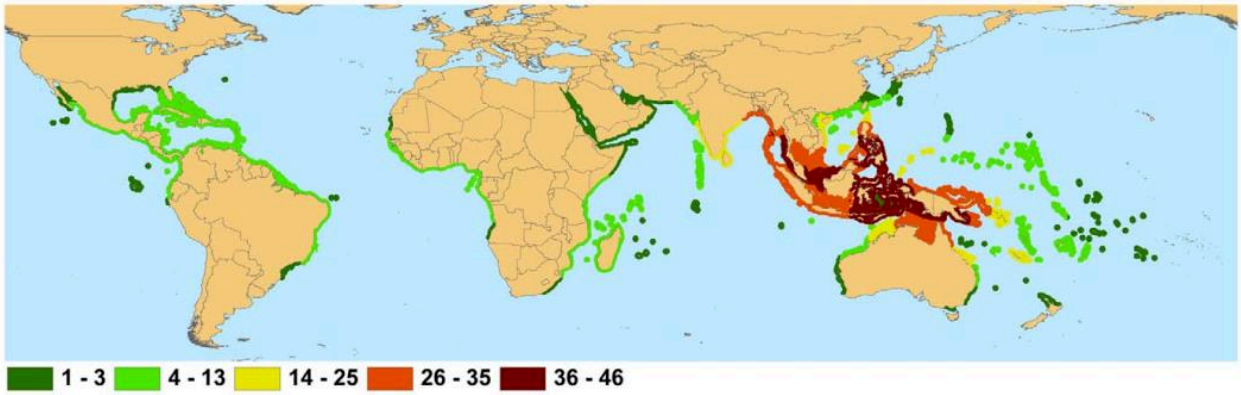

Fig. 1-2. Mangrove Species Richness: Native distributions of mangrove species (Polidoro et al. 2010)– colors represent the number of species.

The ecological, environmental, and socioeconomic importance of mangrove wetlands has been widely recognized (Kathiresan 2012). They have an extraordinary high rate of primary productivity (Alongi 2002), acting as both an atmospheric CO_2 sink and an essential source of oceanic carbon, protect coastal erosion and maintain shore stability (Mumby et al. 2004). In

addition, mangrove forests provide many ecosystem services, such as support for local livelihood through provision of fuels, foods, construction materials (Bandaranayake 1998) and aquatic products. Mangroves host wide variety of biodiversity, providing habitats for fauna including aquatic and terrestrial insects, fish, crustaceans, amphibian, mammalian, reptilian and avian species (Hogarth 2015).

As a transit zone between terrestrial and marine environments, mangrove wetlands also inevitably receive contaminants from tidal water, rivers, and storm runoff (Tam and Wong 1996,1993). It is estimated that from 75 % to 90 % of the total flux of continental materials to the oceans is trapped in coastal environments (Berner and Raiswell 1983)**.** Mangroves have been reported to serve as reservoirs of contaminations, including nitrogen and phosphorus (Tam et al. 1995), and organic pollutants (Maskaoui et al. 2002). Due to the capacity of mangroves to efficiently trap suspended materials from the water column (Furukawa et al. 1997) and the high affinity of organic matter (OM) for metals, mangroves sediments have a large capacity to accumulate these pollutants (Harbison 1986, Marchand et al. 2011b, Tam and Wong 2000). Therefore, coastal areas can act as filters, retaining materials supplied by the rivers, the atmosphere and the oceans for relatively long periods of time (Berner 1984, Kjerfve and Magill 1989).

Despite their importance for local livelihood, biodiversity and carbon sequestration, mangrove forests are greatly threatened, being destroyed at a rate close to 1 % per year (Duke et al. 2007). Losses in mangrove forest extent were observed globally, due to anthropogenic and natural factors, with majority of loss and degradation occurring in Southeast Asia, where aquaculture practices were widespread (Thomas et al. 2017). As a result of mangrove degradation, the release of carbon into the atmosphere has been estimated to range from 0.02 to 0.12 Pg per year (Donato et al. 2011). Furthermore, mangrove forest destruction can result in sediment oxidation, inducing the

modification in physico-chemical properties of sediments and subsequent oxidation of the stored organic matter (Dent 1986).

1.2. Sources, distribution of trace metals in mangrove.

1.2.1. Sources of trace metals

Trace metal is a general collective term applied to the group of metal and metalloid with an atomic density greater than 5 g cm^{-3} (Berkowitz et al. 2008). Another definition of trace metal is that its molecular weight is above 40 g mol^{-1}. They can be divided into two groups including essential trace metals and toxic trace metals based on their importance to human being and living organisms. The sources of trace metals entering the estuarine system are point sources (e.g. municipal sewage treatment plants, industrial facilities, combined sewer overflow), non-point sources (e.g. the runoff of agriculture, urban, construction, mining regions, landfills/ spills) and atmospheric deposition (Fig. 1.3) (de Souza Machado et al. 2016). Pollutants commonly reported in estuaries and in the coastal ocean include trace metals accumulating from smelting, sewage-sludge dumping, ash and dredged material disposal, antifouling paints, seed dressings and slimicides, power station corrosion products, oil refinery effluents and other industrial processes (Idrees 2009, Nriagu and Pacyna 1988).

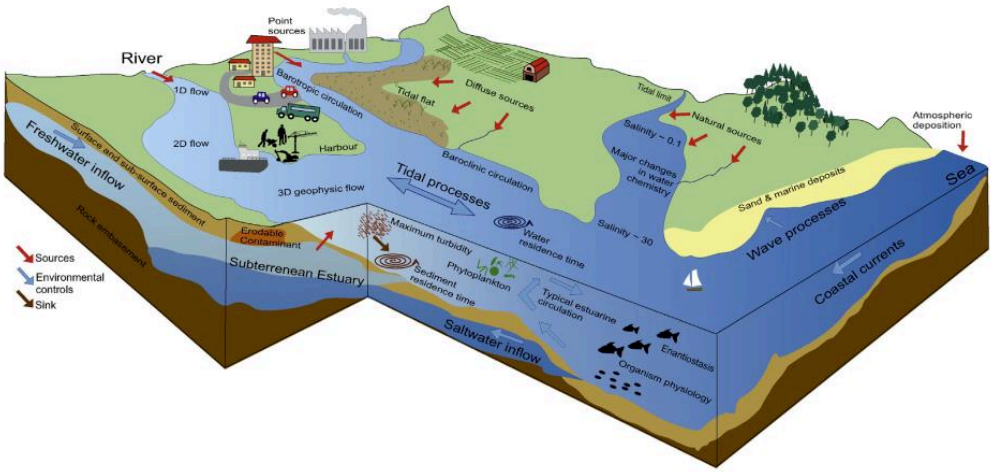

Fig. 1-3. Conceptual model of physical, chemical and biological variables and processes for metal behaviors (de Souza Machado et al. 2016)(de Souza Machado et al. 2016).

Among the many industrial sources of trace metals, the most important are pyrometallurgy processes in mining and smelting (Larison et al. 2000). Burning of fossil fuels, incineration of wastes and release of non-treated domestic and urban sewage are also important sources of trace metals to the environment. Most sources of trace metals were associated with large urban centers which, throughout the world are preferably located along the seashore, and this is particular true for tropical regions. Globally, there has been an agreement that the reported levels of trace metals within mangrove sediments are increasing every year as a result of pollution caused by developmental growth and urbanization (Sekabira et al. 2010).

Mangrove ecosystems receive considerable quantities of riverine and coastal watershed discharge, which includes high loads of nutrients, sediments, suspended particulate matter, trace metals and petroleum hydrocarbons associated with municipal wastewater and agricultural runoff that impact the water and sediment quality, productivity, biodiversity and functioning of coastal ecosystems. For instance, the investigations of trace metal pollution in grey mangrove biota within the Red Sea coastal areas of Saudi Arabia have documented very high concentrations of copper and chromium (Usman et al. 2013). Similary in India and Hong Kong, the intense development and industrialization have posed an ecological threat to the nearby mangroves, which have revealed elevated levels of trace metals that exceed sediment quality guidelines particularly in lead (Defew et al. 2005, Sarika and Chandramohanakumar 2008). Thus, coastal and marine resources are under relentless pressure from rapid population growth and industrialization.

1.2.2. Distribution of trace metals in mangroves

Many coastal areas act as an intermediate step in the transport of water and substances from land to sea. This transition zone induce drastic physical and chemical changes of the water body. Decreasing river topography gradients towards the sea results in descending water velocity and

transport capability, which affects the deposition of particles by gravity. As a results of these changes, some suspended particulate load, including trace metals, which cannot be biologically or chemically degraded, may accumulate locally. Other long-lasting pollutants are trapped and deposited, and only a minor fraction of continental load is exported to the open ocean (Salomons et al. 1988). In addition, mangrove muds have intrinsic physico-chemical properties and an extraordinary capacity to accumulate materials discharged to the near shore marine environment (Harbison 1986). The sheltered and stagnant water environment of mangroves allow extensive sedimentation of the finest clay, silt and detrital particles. This material is bound and stabilized by a tangled mat of root hairs growing horizontally just below the mud surface. These particles provide optimum surfaces for trace metal transport. However during prolonged period of water immersion, changes in pH may affect the migration of metals at the sediment surface and the concentration of free metal ions in overlying water. In mangrove sediments, trace metals can be subject to adsorption, precipitation and co-precipitation, and uptake by plants (Wood and Shelley 1999, Yu et al. 2001). Mangrove plants can retain contaminants in their tissues (Dunbabin and Bowner 1992), but also favor the settlement of suspended solids, carry oxygen from the aerial parts to the roots, create the proper environment in the rhizosphere and promote a variety of chemical and biochemical reactions, which enhance metal retention (Kadlec et al. 2000). The high levels of sulfide production in mangroves favor the precipitation and immobilization of trace metals (Ambus and Lowrance 1991, Dunbabin and Bowner 1992). Conversely, the radial oxygen loss (ROL) of mangrove plants would aerate the rhizosphere and increase the mobilization of trace metals due to sulfide oxidation and dissolution. The ROL would also cause the formation of Fe plaque, which provides some extra binding sites for trace metal on root surface (Cheng et al. 2013).

Due to the fact that mangrove roots usually act as a physical barrier, retaining most of trace metals and reducing their translocation to aerial parts (Yim and Tam 1999).

1.2.2.1 Trace metals in mangrove waters

The concentrations of trace metals in estuarine and coastal marine waters are controlled by advective transport, mixing, and differential settling of sediment-sorbed metals, leading to substantial variation in trace metal composition along the estuary. In addition, biogeochemical processes occurring at the water-sediment interface or in the water column will influence trace metals distribution in these systems. Trace metals dynamic in mangrove waters are less studied than in their sediments. Studies concerning trace metals in the water of some mangrove forests were developed in Singapore (Cuong et al. 2005), Taiwan (Leaño and Pang 2010), Australia (Melville and Pulkownik 2006), United State (Jara-Marini et al. 2009), Nigeria (Essien et al. 2009). Bayen (2012), in his review, reported the ranges for detectible concentrations ($\mu g\ L^{-1}$) of trace metal in mangrove rivers, estuaries and adjacent coastal: 0.470 – 3.1 (As), 0.094 – 21 (Cr), 0.1 – 109 (Cu), 0.272 – 20 (Ni), 0.104 – 17 (Pb).

1.2.2.2 Trace metals in mangrove sediments

Natural background levels of trace metals are present in the majority of sediments due to mineral weathering and natural soil erosion. Sediments with low trace metal concentrations are not necessarily natural just because the levels are really low. They may represent a mixture of small quantity of pollutants diluted by a large amount of natural sediment with low trace metal contents. Suspended particles are by far the most important metals carriers from rivers to coastal areas (Yao et al. 2016). When entering brackish water, deposition of fine particles, due to the decrease in current velocity, flocculation of negatively charged clay particles, and the general decrease of metal species solubility occur, leading to a gradual accumulation of trace metals in sediments (Salomons and Forstner 1984). Bayen (2012) showed that trace metal concentrations

have been reported for sediments collected from mangrove ecosystems like in Hong Kong (Chan 1992, Ong Che and Cheung 1998, Tam and Wong 1995), Peoples Republic of China (Jingchun et al. 2006), United Kingdom (Emmerson et al. 1997), Malaysia (Kamaruzzaman et al. 2008), Australia (McConchie et al. 1988), Philippines (Prudente et al. 1994), Mexico (Soto-Jiménez and Páez-Osuna 2001), Brazil (Lacerda and Abrao 1984), Viet Nam (Tue et al. 2011), New Caledonia (Marchand et al. 2011a). The most investigated trace metals in mangrove habitat are nickel, chromium, arsenic, cobalt, copper and lead, with a ranges of concentrations (µg g^{-1} dry weight) of: 0.3 – 208.4 (Ni), 0.55 – 6240 (Cr), 8 – 40 (As), 0.6 – 58 (Co), 0.01 – 4050 (Cu), 0.08 – 1950 (Pb).

1.2.2.3 Trace metals in mangrove plants

Mangrove plants have developed physiological, morphological and anatomical adaptations, such as salt regulation, aerenchyma, and highly specialized root systems (knee joints, pneumatophores or aerial roots, cable roots, and buttress/prop roots), to cope with anoxic and saline environments (Marchand et al. 2004). These adaptive changes in mangrove plants, together with the harsh growth conditions (environmental extremes and pollution) suggest the possibility of using mangrove plants in phytoremediation of contaminated water and sediments. Because of their predominance, *Avicennia* and *Rhizophora* species have been widely used as bioindicators for understanding uptake and distribution of metals (Kamaruzzaman et al. 2011, Marchand et al. 2016). Mangrove roots often act as a barrier, retain most of the trace metals and reduce the translocation of trace metals to other plant parts (Yim and Tam 1999). The variation in the levels of trace metal tolerance exhibited by different types of mangroves, the grey mangrove *Avicennia marina* has a relatively higher tolerance level when compared with other mangrove species (Agoramoorthy et al. 2008, MacFarlane et al. 2003). It is speculated that *Avicennia* marina could be more tolerant to trace metals by developing several adaption mechanisms including avoiding the uptake of metals actively and ions excretion at their leaf surfaces. Numerous studies have

utilized mangrove species and their sediment as reliable bio-indicators for trace metal pollution and contamination (Defew et al. 2005, MacFarlane et al. 2003). Wetland plants can accumulate trace metals in their tissues and have the ability to take up greater than 0.5 % dry weight of a given element and bioconcentrate the element in their tissues to 1,000-fold the initial element supply concentration (Yang and Ye 2009). Most studies report concentrations for multiple trace metals (MacFarlane and Burchett 2002). Range of detectable levels of contaminants (μg g^{-1} dry weight) for all species and tissues in mangrove plants were: 0.2 – 347 (Cr), 0.1 – 207 (Cu), 0.42 – 2472 (Mn), 0.4 – 108 (Ni), 0.02 – 225 (Pb), and 0.41 – 2.47 (Co) (Bayen 2012).

1.2.2.4 Trace metals in mangrove-associated gastropods

Gastropods are one of the most abundant mangrove-associated animals. They can tolerate a wide range of trace metals concentrations and physical variables (i.e. salinity). Pinocytosis and ingestion are processes by which metals are taken up into their body (Luoma and Bryan 1981). Among gastropods, snails offer the possibility to assess metals contaminations. Zhou et al. (2008) reported that snails can accumulate higher metal concentrations than any other groups of invertebrates, and were, thus, revealed as potential bioindicators. An understanding of the metal concentrations in their different tissues also gives an idea regarding the safety of these snails for human consumption (Cheng and Yap 2015). The metal occurrence in whole body and different parts of various snails in the mangroves were reported by several scientists (Cheng et al. 2016, Yap and Cheng 2013). They showed that the different metals concentrations in snails tissues depended not only on metal characteristics (i.e. physiological properties and biological functions), and metabolic requirements of each species. Furthermore, metals bioavailability to snails also depend on their feeding regime, their digging activities, and metal partitioning in their foods. Essential elements as Fe, Mn and Cu presented higher concentrations in snail soft tissues than As, Ni, Cr and As, which can be toxic (Dias and Nayak 2016, Palpandi and Kesavan 2012, Vargas et

al. 2015). Metal bioaccumulations in snails have been addressed in the past two decades (Berandah et al. 2010, Dias and Nayak 2016, Reed-Judkins et al. 1997). The link between metal concentrations in sediment with a number of snails species were found to be negative (Amin et al. 2009). De Wolf and Rashid (2008) also found that *Littoraria* density was higher in non-polluted area than the polluted one.

1.2.3. Geochemistry of trace metals in mangrove sediments.

1.2.4. Possible reactions affecting the cycling of trace metals in mangrove sediments

Trace metals are transported mostly associated with suspended particles, in coastal water (Turner 1996, Wang et al. 2016) and this is the major form under which trace metals reach mangrove areas. Once inside the mangrove forest, trace metals will suffer a series of processes typical of the mangrove water and sediment conditions, which are different from those occurring in the marine and riverine environments. Sheltered, slack water conditions allow deposition of fine particles normally enriched with trace metals. High organic matter and sulfide content helps in fixing trace metals as insoluble sulfides and precipitated organic-metal complexes (Marchand et al. 2012).

Microbial degradation of the high content of organic matter in mangrove muds generally removes most oxygen from sediments below the surface layer, creating ideal condition for bacterial sulphate reduction (Berner and Raiswell 1983). When photosynthetic oxygen production end during the night, H_2S diffuses upwards through the mud and escapes to shallow water covering the sediments. Metals dissolved in this water as free ions or metal-humic complexes, are deposited as sulphides (Harbison 1986). Fig. 1.4 shows a schematic representation of the major physical-chemical processes involving trace metal post-deposition mobilization in coastal sediments. The enrichment of pore water metal concentrations occurs due (i) to the solubilization of substances and metal complexes subject to redox processes, in particular oxidized compounds of Fe and Mn,

and most probably of As; (ii) to desorption processes as consequence of the lower pH typical of pore waters; and (iii) to the partial mineralization of organic matter and subsequent solubilization of metal complexes with dissolved organic species, which readily react with free amino acids and amino sugars and polyphenols of low to medium molecular weight (Lacerda et al. 1987, Salomons and Forstner 1984). The permanence of most metals in solution will depend on the possibility of complex formation with organic and inorganic ligands because autochthonous organic production is high in coastal waters as compared to most waters of the continental shelf, as land derived nutrients and those regenerated in bottom sediments sustain a continuous growth of phytoplankton. Also, shallow depth facilities the colonization by macrophytes such as seagrasses, saltmarshes and mangrove species which contribute to the supply of organic matter.

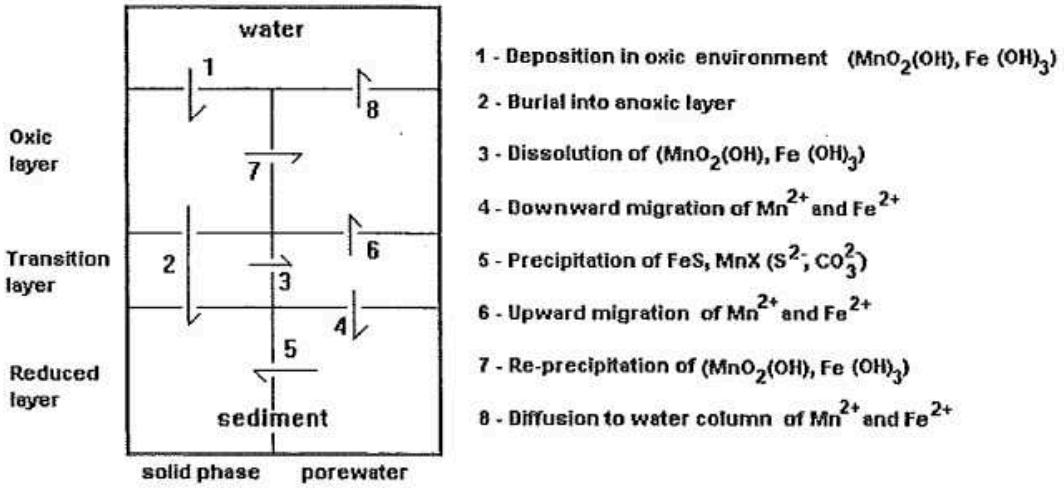

Fig. 1-4. Representation of post-deposition mobilization of trace metals in coastal sediments (Lacerda 1998).

Dissolved metals resulting from reductive dissolution of trace metals during OM decay process may be incorporated by the mangrove biota with various forms. Eventually, they can be transferred through food chains to terrestrial and marine ecosystems and be exported to the continental shelf associated with dissolved and particulate detritus. Mangrove sediments are known as redox-stratified, with a succession of oxic, suboxic and anoxic zone from the surface to depth (Marchand

et al. 2011a). The strong redox gradient in mangrove sediments plays a dominant role in speciation and solubility of redox sensitive elements as trace metals (Otero et al. 2009) and usually act as a sink for anthropogenic contaminations (especially trace metals) in coastal areas. Metallic speciation in mangrove sediments depend on one or several combination of sediment properties: pH, organic matter, clay content, redox potential, salinity, the quality and quantity of suspended matter (e.g. organic and inorganic), iron and manganese (hydr)oxides (Marchand et al. 2012) which are dependent on tidal amplitude and flooding characteristics, season and meteorological conditions. Complex redox cycling in mangrove sediments may thus significantly impact the speciation of metallic elements across the intertidal zone (Clark et al. 1998, Tam and Wong 2000).

1.2.5. Factors controlling the geochemistry of trace metals in mangrove sediments

1.2.5.1 Organic matter

The sources of sedimentary organic matter are multiple and include mangrove litter or imported suspended organic matter (terrestrial sources, microalgae, macroalgae, riverine and marine material, etc.). The most common surface functional group in organic matter are –COOH (carboxyl), -OH (hydroxyl), -C6H4-OH (phenolic), -NH2 (amino) and -NH (imino) compounds, which are capable of binding cations (Stevenson 1976). Among these, metals are mainly bound to –COOH and –OH groups ,due to their ionization, and can form stable complexes with positively charged trace metal, which will affect their mobility and bioavailability (Antoniadis and Alloway 2002).

1.2.5.2 Redox cycling

It is generally accepted that sediment ORP is also a most important factors controlling trace metal mobility. Fig. 1.5 shows sequence of reactions for a hypothetical soil containing a finite supply of bioavailable organic matter and sediment oxidation capacity (Chadwick and Chorover 2001). Oxygen (O_2) can be depleted rapidly by microbial and root respiration in sediment subjected

to limited influx of air or oxygenated water because it is sparingly soluble in water (0.25 mM at 25ºC). At this point, dissolved nitrate and available Mn(IV) solids are utilized as alternative electron acceptors during the oxidation of organic material (Chadwick and Chorover 2001). If these reactants are exhausted, further reduction results in the successive use of Fe (III) solids (ferric reduction), SO_4^{2-} (sulfate reduction), and eventually organic matter itself (fermentation) or CO_2 (methanogenesis). Sediments tend to undergo a series of sequential redox reactions when the redox status of the sediment changes from aerobic to anaerobic conditions during flooding (Yu et al. 2007).

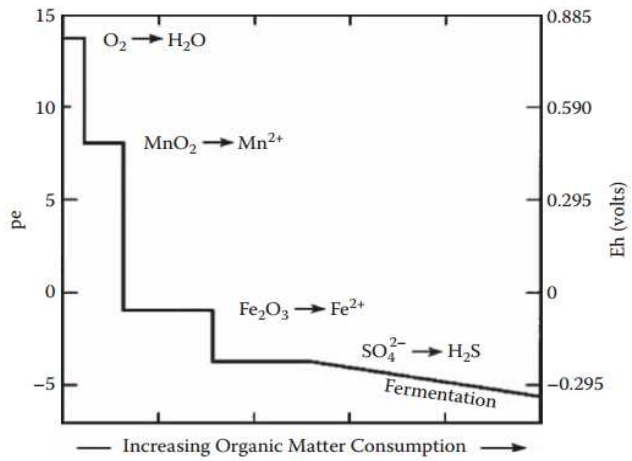

Fig. 1-5. A hypothetical plot showing change in terminal electron-accepting processes for a soil containing a finite supply of bioavailable organic matter and soil oxidation capacity (Chadwick and Chorover 2001).

In anaerobic sediment, acid volatile sulfide (AVS), a key component controlling the activities of some divalent cationic metals, are usually present naturally. Initially, the majority of ASV contained in the anaerobic sediment is bound to iron as soil iron monosulfide (FeS), greigite (Fe_3S_4) or exits as free sulfides. However, if divalent metals, such as copper, chromium or lead are present, the iron in iron-sulfide are displaced and one of these heavy metals rapidly bind to AVS with stronger affinity (Hansen et al. 1996). Finally, in those sediments contaminated, the metal bound with sulfide usually takes up a rather high proportion. When ORP in sediment increases,

the oxidation rate of metal sulfides and the degradation rate of organic compounds will increase correspondingly. Both can accelerate the release of the adsorbed/ complexing trace metals. The reaction can be expressed as: $MS_2 + (15/4)O_2 + (7/2)\ H_2O \rightarrow M(OH)_3 + 2SO_4^{2-} + 4H^+$. The release of H^+ ions into pore-water would decrease the pH of sediment and then cause a secondary release of trace metals. Part of this released material will be re-adsorbed, especially onto the more labile binding fractions. For instance, reduced conditions result in the reduction of Cr (VI) to Cr (III) (Pardue and Patrick 2018) and the immobilization of chromates (Reddy and DeLaune 2008). Conversely, Cr (VI) will be mobilized at high E_h values. Several electron donors (Fe (II), sulfur compounds), and bacteria acting as catalysts, may be involved in the Cu(II) to Cu(I) reduction process under slightly alkaline and anaerobic conditions (Simpson et al. 2000), subsequently leading to Cu_2S precipitation (Du Laing et al. 2009).

1.2.5.3 Iron and manganese oxihydroxides

As a result of temporal inundations and the establishment of lower ORP, Fe and Mn oxihydroxides in the sediment are reduced to Mn^{2+} and Fe^{2+}, being present as soluble metals and organic complexes. This transition zone is called postoxic or suboxic, and extends for a few millimeters to a few centimeters in most coastal areas, (Alongi et al. 1996). Trace metals associated with Fe and Mn oxihydroxides, are released from these complexes when reaching this transition zone, and are transformed into more mobile and plant-available forms. However, these dissolved elements can also be immobilized due to co-precipitation with or adsorption to Fe and Mn oxihydroxides if the redox conditions evolve towards oxia. For example, Borch et al. (2009) showed that the mobility, dynamic, bioavailability, toxicity and environmental fate of As are controlled by biogeochemical transformations involving Fe that can form or destroy As- bearing carrier phases, or modify the redox state and chemical speciation of As (Fig 1.6). The stability of

Fe^{2+} and Fe oxihydroxides depends on a combination of the E_h and pH values of the sediment. The nearly amorphous $Fe(OH)_3$ minerals (ferrihydrite) are reduced at a higher E_h for a given pH than are the crystalline minerals of FeOOH (goethite) or Fe_2O_3 (hematite) (Du Laing et al. 2009). Fe occurs in soluble forms under acid conditions. At neutral pH, Fe is soluble at low redox potentials or as a soluble organic complex in oxic sediments. The absence of As in the dissolved phase is related to the presence of poorly soluble iron (hydr)oxides that are able to sorb arsenite-As(III) and arsenate-As(V).

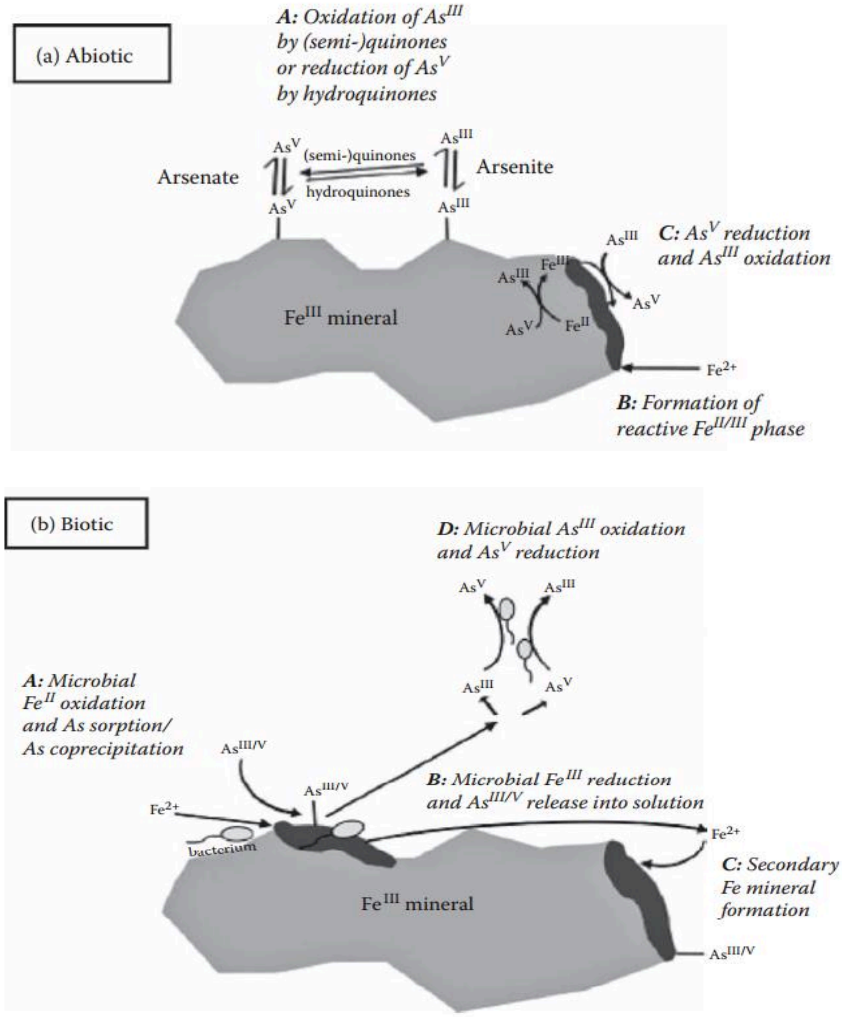

Fig. 1-6. Concept of a model with selected (a) abiotic and (b) biotic redox processes that influence the fate of arsenic in the environment (Borch et al. 2009)(Borch et al. 2009).

Although Mn oxides are typically less abundant in sediments than Fe oxides, they are particularly involved in sorption reactions with trace metals, as they adsorb them more strongly, thus reducing their mobility. The range of redox potential during a tidal cycles is sufficient to change Mn species equilibrium as Mn(II) and Mn (IV), resulting in dissolution or precipitation of Mn oxihydroxides and consequently of any trace metal associated with them. Guo et al. (1997) reported an increasing affinity between both Fe and Mn oxides and As, Cr with increasing redox potential in the sediment.

1.2.5.4 pH and carbonates

The pH is a key parameter controlling trace metal transfer in sediments. Changes of pH can be induced by different parameters (tides, season, mangrove species, depth, etc) (Marchand et al. 2012) and can affect indirectly the mobility of metals. When pH decreases in sediment, the competition between H^+ and the dissolved metals for ligands (e.g. OH^-, CO_3^{2-}, SO_4^{2-}, Cl^-, S^{2-} and phosphates) becomes more and more significant. It subsequently decreases the adsorption abilities, and then increases the mobility of trace metals. In the sediments, due to the organic matter degradation and the acid volatile sulfide oxidation, the pH usually decreases from neutral to acid (Otero et al. 2009), sometimes even decreasing to pH 1.2, which results in some metals release into the water even under stable water conditions (Bonnissel-Gissinger et al. 1998). This processes would occurred for pH range of Ni (5.0 – 6.0), As (5.5 – 6.0), Cu (4.5), Pb (4.0) and Fe (2.5).

The presence of carbonates in calcareous floodplain sediments constitutes an effective buffer against a pH decrease. These carbonates, which may directly precipitate metals (Guo et al. 1997), can be (bio)geochemically formed and deposited within frequently flooded sediments. On the other hand, decalcification can also occur which may result in acidification of the pore waters (Du Laing et al. 2007). These authors demonstrated that a pH drop during partial decalcification can cause an

increased release of metals in a calcareous sediment layer of a contaminated overbank sedimentation zone.

1.2.5.5 Salinity

Tidal variations in estuaries result in varying salinities of the river water and pore water of the floodplain sediment. Seawater of high ionic strength (0.6 mol L^{-1}) is diluted by river water (ionic strength 10^{-3} – 4. 10^{-3} mol L^{-1}), leading to axial salinity gradients and the formation of the fresh water-seawater interface (Millward 1995). When negatively charged clay particles move from freshwater to salt water, free cations neutralize the negatively charged surfaces, allowing molecular attractive forces to dominate when the particles are brought close enough. They flocculate and their settling velocity increases, leading to increased deposition of sediment in the floodplains. Because trace metals are often strongly sorbed to particles, they will also tend to accumulate in floodplains. In addition to salinity-induced flocculation of metal-containing particles, salinity can also affect metal fate in different other ways. Due to chloride concentrations increase when inland fresh river water mixes with seawater, metals may be mobilized from sediments as soluble chloride complexes (Hahne and Kroontje 1973). Moreover, an increase of salinity is also associated with an increase of major element concentrations (Na, K, Ca, Mg), which compete with trace metals for the sorption sites. The addition of Ca salts results in a higher release of exchangeable metals in the solution compared to the addition of Na salts, which are less competitive for sorption (Khattak et al. 1989).

1.3. The Can Gio Mangrove Biosphere Reserve

1.3.1. Geo-physical characteristics

The Can Gio Mangrove Biosphere Reserve (Fig. 1.7) is located in the South of Viet Nam (10º22’14’’-10º40’09’’N; 106º46’12’’-107º00’59’’E), being situated in Can Gio district of Ho Chi Minh City (HCMC: a Vietnam biggest industrial city with almost 10 million inhabitants). The total

area of the Can Gio Mangrove Biosphere Reserve is 75,740 ha and can be divided into three zones (the core, the buffer, and the transition zones): (1) the core zone covers an area of 4,720 ha and was established with the long term purpose of landscape conservation, species biodiversity and research. Human activities are prohibited in this zone; (2) the buffer zone surrounds the core zone and covers an area of 37,340 ha. Its purpose is to act as a buffer and to prevent any harmful activities impacting the core zone while creating large spaces for wildlife, providing a natural landscape, and serving as a cultural and ecological tourist destination; (3) the transition zone covers approximately 29,3110 ha and is the outermost surrounding area, and is important for maintaining socio-economic activities (Nam et al. 2014).

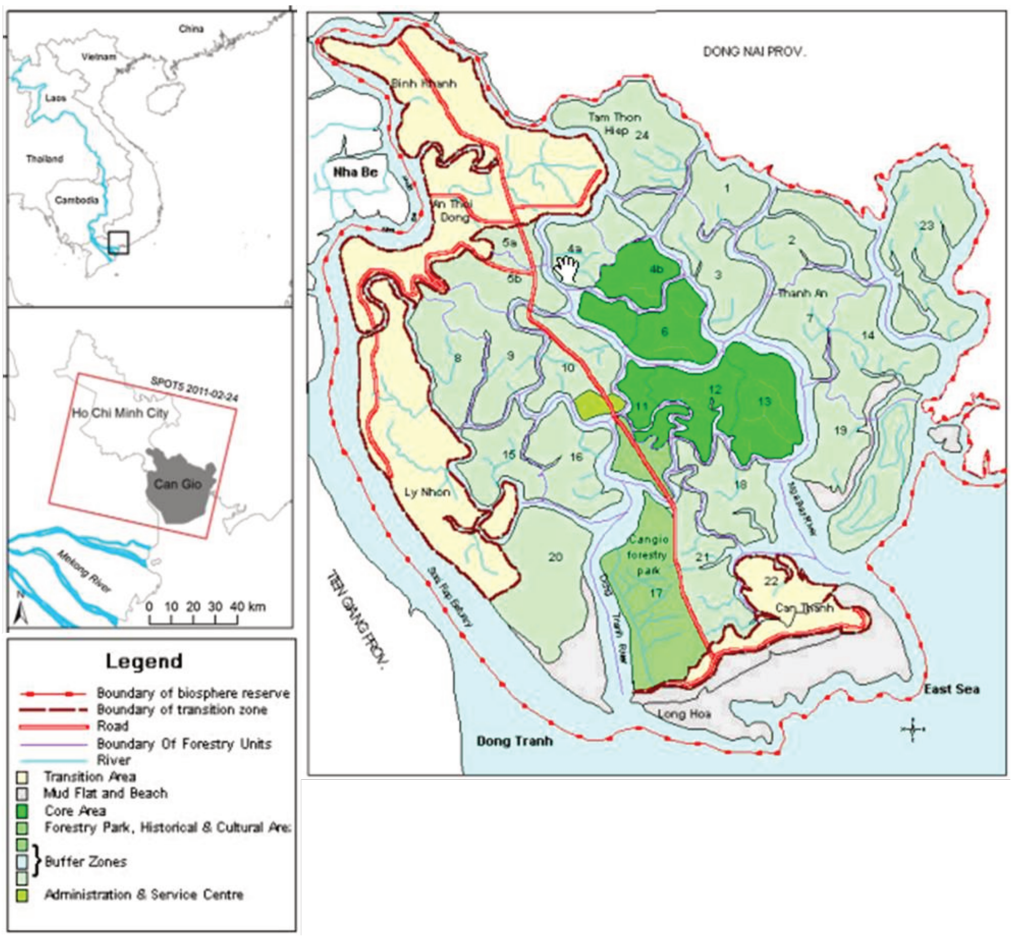

Fig. 1-7. Map of study area showing: i) the location of Viet nam in the Southeast Asia, ii) the location of Can Gio mangrove in the edge of Ho Chi Minh City, iii) the zonation of Can Gio Mangrove Biosphere Reserve Adapted from (Kuenzer and Tuan 2013) and (UNESCO 2000).

The Can Gio mangrove has a complex network of rivers. Freshwater originates from the Sai Gon and Dong Nai Rivers, emptying out via the Long Tau and Soai Rap Rivers (the main branches) to the East Sea (South China Sea). There is a considerable mixing of saline and fresh water at those estuaries, namely Dong Tranh Bay and Ganh Rai Bay. The rivers flow in a general southeasterly direction and their courses affect the local topography, and vegetation distribution (Luong 2011). Long Tau and Soai Rap Rivers, the two main terminal branches, affect the hydrographic regime of other subsidiary branches.

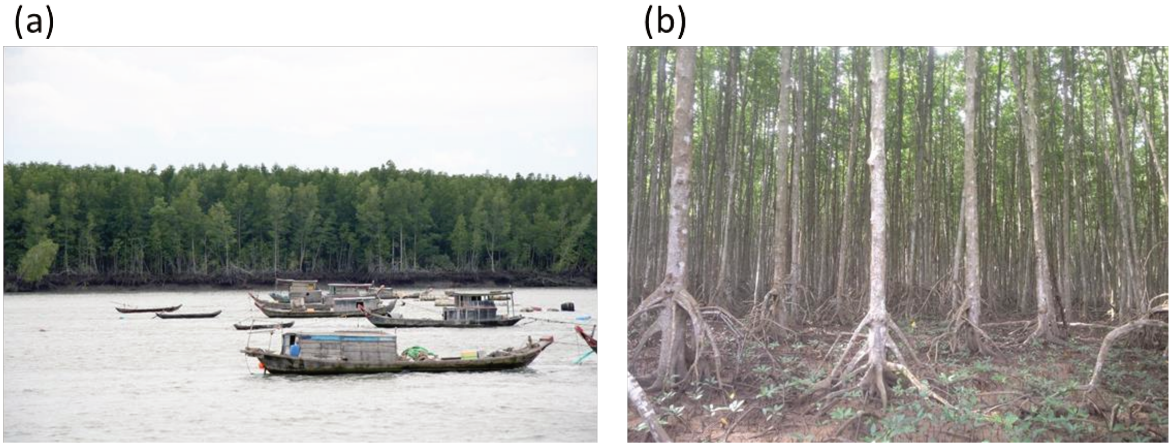

Fig. 1-8. (a) The corner of Long Tau river in Can Gio mangrove with the Rhizophora in the background; (b) high density of saplings on the ground of the Rhizophora stand.

The Can Gio mangrove forest lies in a zone with a semi-diurnal tidal regime (i.e. two ebb and flow tides per day). Tidal amplitudes range from about 2 m at mean tide to 4 m during spring tides. It has been observed that the two daily high and low tides differ in height. Tidal amplitude decreases with distance north (i.e. inland), relating to the proximity of the East Sea (South China Sea).

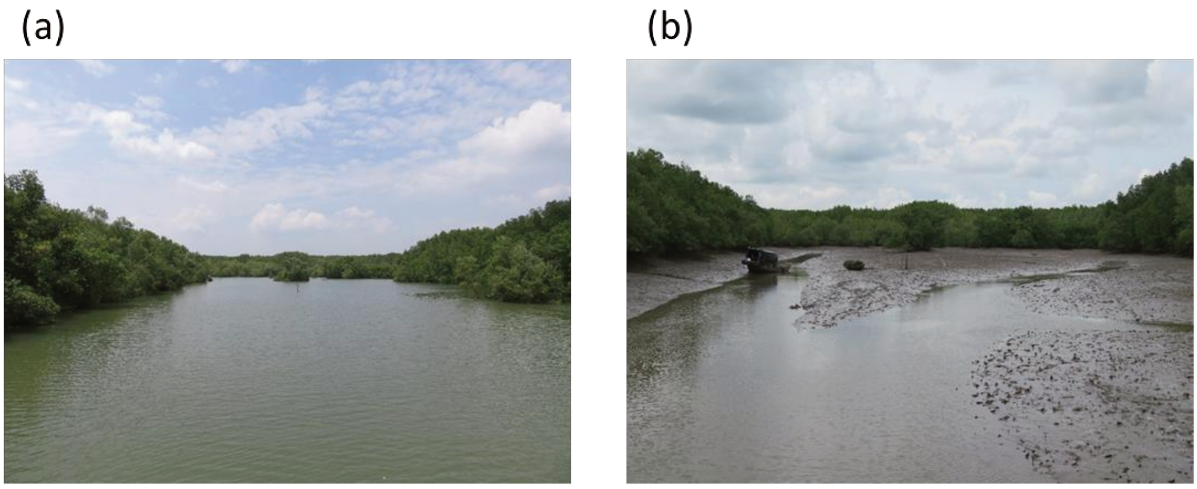

Fig. 1-9. The view of a tidal creek in Can Gio mangrove with the Avicennia along the banks: (a) flooding and (b) ebbing periods.

The climate in the Can Gio mangrove is subject to the tropical monsoon type with high humidity, high temperature, and a wet season from May to October and a dry season from November to April. The average annual precipitation ranges from 1,300 to 1,400 mm with the highest rainfall in September (300 to 400 mm). The annual average temperature is 25.8 ºC and the monthly average temperature varies from 25.5 to 29.0 ºC, with the highest temperatures occurring from March to May and the lowest from December to January (Luong 2011). During the wet season, humidity varies from 79 % to 83 % and is highest in September. During the dry season, humidity varies from 74 % to 77 % and is lowest in April.

1.3.2. The destruction and reforestation of the Can Gio mangrove

During the two Indochina wars, most of the mangroves in Can Gio were destroyed (Hong 1997) and the species *Rhizophora apiculata, Rhizophora mucronata* disappeared. Some species remained in small groups. The *Ceriops tagal* and *Eceocaria agallocha* regenerated naturally along the waterways, *Avicennia sp.* can be found in flooded areas, and *Phoenix paludosa* and *Acrostichum aureum* can be found on higher land.

In 1978, with the support of the HCMC government, *Rhizophora apiculata* was planted in any uncovered lands as part of a reforestation program. After 22 years, the Can Gio replanted mangrove have become one of the largest reforestation areas in Vietnam, covering over 40% of the Can Gio district (approximately 35,000 ha) (UNESCO 2000). It is now considered to be among the most developed mangrove forests in Southeast Asia and was recognized as an international biosphere reserve on January 21, 2000. Like other biosphere reserves on the world, the Can Gio Mangrove Biosphere Reserve has three functions: 1) biodiversity restoration, 2) stimulation of environmentally responsible cultural and economic development; and 3) training, research, and education with regard to mangrove ecosystems.

To date in global studies, the Can Gio mangrove is usually classified as a 'Mangrove afforestation and re-forestation area" (Blasco et al. 2001). According to the Management Board of the Can Gio Mangrove Biosphere Reserve, several hundreds of plant species, 77 mangrove species or associated, 130 species of algae, 63 zooplankton species, 127 species of fish, 30 species of reptiles, 100 species of invertebrate benthic animals, 145 bird species, and 19 mammal species are found in the mangrove. The observed 77 mangrove species (35 true mangroves and 42 associates) include both salt water and brackish water species (e.g. *Bruguiera gymnorrhiza, Bruguiera parviflora, Ceriopssp, Kandelia candel, Rhizophora mucronata, Sonneratia alba, Sonneratia ovata, Sonneratia casedar, Avicennia officinalis, A. lanata, Aegiceras majus, Thespesia populnea, Hibiscus tiliaceus, Lumnitzerara cemose, Xylocarpus granatum, Excoecaria agallocha* (Luong et al. 2015). The three dominant species are namely *Rhizophora apiculata, Avicennia alba,* and *Phoenix paludosa* (Fig. 1.10). The *Rhizophora apiculata* has a high commercial timber value and was widely replanted after the war. The *Avicennia alba* is a pioneering species and has a higher saline tolerance and ability to grow on weak, unconsolidated sediment. The *Phoenix paludosa* is

often found on elevated ground, forming mixed communities with other mangrove species such as *Acrostitum aureum* and *Nypa fruticans*. Mangroves and sea grass beds act as a breeding ground for many other species of mollusks, crustaceans, fish, amphibians, and birds-as well as terrestrial animals. About 150 species of aquatic fauna are known in this region.

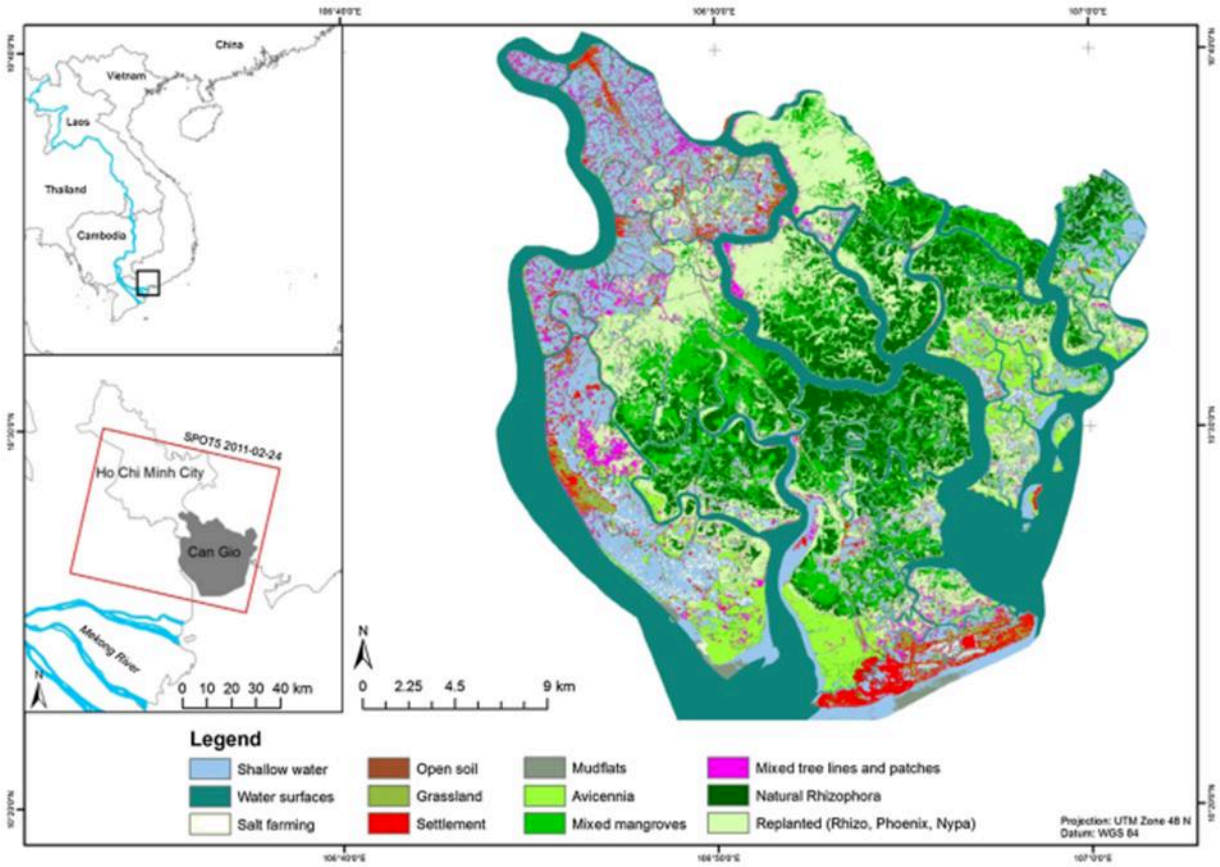

Fig. 1-10. The distribution of mangrove species in Can Gio Mangrove Biosphere Reserve (Kuenzer and Tuan 2013)..

Human benefits not only from the direct use of these ecosystem goods, but also from its important ecological functions and services. For example, mangroves act as a cleansing system for water and sediments. Thus, they provide hydrological services to local inhabitants. Furthermore, mangrove ecosystems maintain high biodiversity within forests and water grounds, protect coastal zones from erosion through the moderation of the force of winds and waves, and stabilize climate

through carbon sequestration, as well as the moderation of temperature extremes (Kuenzer and Tuan 2013).

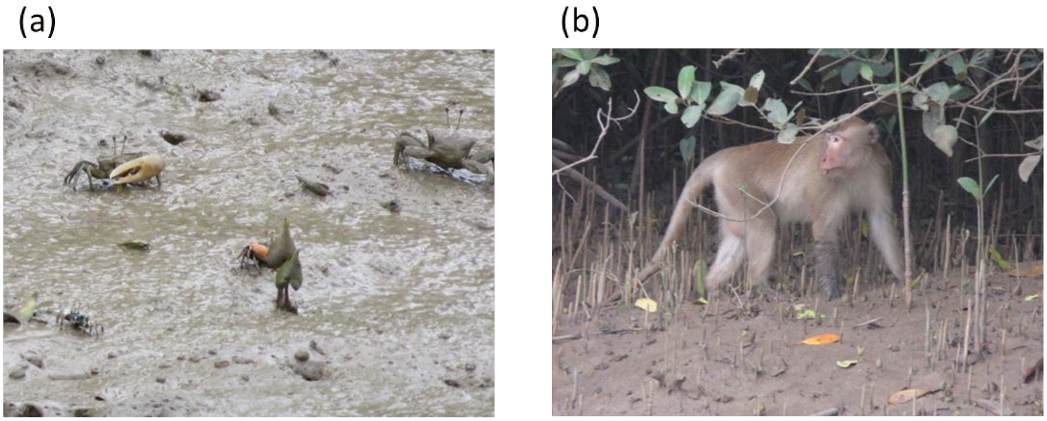

Fig. 1-11. The foreground image of (a) the mudflat with crabs activity and (b) beneath the Avicennia alba stand.

1.3.3. Research projects conducted in the Can Gio mangrove

Because of the importance of the mangrove forest, many scientists have carried out extensive studies on different aspects of the Can Gio mangrove ecology. For instance, the factors that affect the development and distribution of mangrove forests, the components and characteristics of the mangrove flora, and mangrove degradation (Hong 1997, Nam et al. 2014). Kuenzer and Tuan (2013) assessed the ecosystem service values of Can Gio mangrove. Some studies have emphasized the effects of hydrology on the structure and function of the mangrove (Van Loon et al. 2016), the geographical range, zonation of mangrove forests (Luong et al. 2015). Several publications interested the sedimentation rates (MacKenzie et al. 2016, Schwarzer et al. 2016) and but also the effects of sediment physico-chemical parameters on organic nutrient cycling (Oxmann et al. 2010, Oxmann et al. 2009). However, there is a lack of published studies on trace metals dynamics within the Can Gio mangrove: (Costa-Boddeker et al. 2017) reported trace metal accumulation in sediments fringing the mangrove while Strady et al. (2017a) stated that untreated wastewaters combined with industrial discharges conducted to the degradation of the Saigon River water quality, upstream the mangrove. Because of their toxicity, bio-accumulation capacity and

persistence, trace metals may represent a major threat to the mangrove biodiversity and also for human health. Thus, a better understanding in the fate of trace metals in the Can Gio mangrove ecosystem is required.

1.4. Objectives of the dissertation

The overall goals of this PhD thesis was to elucidate the fate of trace metals in the Can Gio mangrove forest, Viet Nam. Especially, I wanted to answer the following questions:

(1) What are the main parameters controlling trace metals partitioning between dissolved and particulate phases in the Can Gio mangrove estuary?

(2) What are the trace metal distributions and speciation in the mangrove sediments?

(3) What are the main parameters controlling trace metals distribution in the mangrove sediments?

(4) In which quantity trace metals are exported from the mangrove sediments?

(5) What are the main drivers of trace metal exports from mangrove sediments to tidal creek?

(6) Is there any transfer of trace metals from mangrove sediments to mangrove biota?

The objectives will be addressed in the following chapter:

The chapter 2 emphasizes the distribution and partitioning of metals (Fe, Mn, Cr, As, Cu, Ni, Co and Pb) between particulate and dissolved phases along the salinity gradient in the Can Gio mangrove estuary. This chapter was published in the journal *Chemosphere* (Chemosphere 196 (2018) 311-322.

The chapter 3 investigates the trace metals geochemistry (Fe, Mn, Cr, As, Cu, Ni and Co) in the sediments and their ecological risks on mangrove organisms. This chapter will be submitted to the journal *Chemosphere*.

The chapter 4 provides the degree and distribution of trace metals (Fe, Mn, Cr, As, Cu, Ni and Co) in mangrove biota, plants and snails. This chapter will be submitted to the journal *Ecotoxicology and Environmental Safety*

The chapter 5 investigates the influence of pore-water seepage on the trace metals dynamics (Fe, Mn, Ni and Co) in a tidal creek of the Can Gio mangrove. This chapter will be submitted to the journal *Science of the Total Environment*.

Eventually, the last chapter of this dissertation is a conclusion that summarizes the main results obtained during my PhD thesis, and I also developed some research perspectives.

Chapter 2 - Trace metals partitioning between particulate and dissolved phases along a tropical mangrove estuary

This chapter was published in the journal *Chemosphere* (Chemosphere 196 (2018) 311-322).

Highlights:

- Partitioning and distribution of 8 trace metals were studied in a mangrove estuary
- TSS was the main trace metals carrier during their transit in the estuary
- The monsoon induced increased metal inputs to the estuary
- Most of dissolved metals exhibited a non-conservative behavior whatever the season
- Mn, Cr and As were highly reactive, OM or DO playing a key role in their dynamics

Keywords: biogeochemical processes; salinity gradient; monsoon effect; non-conservative behavior; Vietnam

ABSTRACT

Mangroves can be considered as biogeochemical reactors along (sub) tropical coastlines, acting both as sinks or sources for trace metals depending on environmental factors. In this study, we characterized the role of a mangrove estuary, developing downstream a densely populated megacity (Ho Chi Minh City, Vietnam), on the fate and partitioning of trace metals. Surface water and suspended particulate matter were collected at four sites along the estuarine salinity gradient during 24 h cycling in dry and rainy seasons. Salinity, pH, DO, TSS, POC, DOC, dissolved and particulate Fe, Mn, Cr, As, Cu, Ni, Co and Pb were measured. TSS was the main trace metals carrier during their transit in the estuary. However, TSS variations did not explain the whole variability of metals distribution. Mn, Cr and As were highly reactive metals while the other metals (Fe, Ni, Cu, Co and Pb) presented stable log K_D values along the estuary. Organic matter dynamic appeared to play a key role in metals fractioning. Its decomposition during water transit in the estuary induced metal desorption, especially for Cr and As. Conversely, dissolved Mn concentrations decreased along the estuary, which was suggested to result from Mn oxidative precipitation onto solid phase due to oxidation and pH changes. Extra sources as pore-water release, runoff from adjacent soils, or aquaculture effluents were suggested to be involved in trace metal dynamic in this estuary. In addition, the monsoon increased metal loads, notably dissolved and particulate Fe, Cr, Ni and Pb.

2.1. Introduction

Estuaries are key environment for the transfer of trace metals from land to open ocean (Fu et al. 2013, Wang et al. 2016). They are characterized by strong physico-chemical gradients, e.g. salinity, dissolved oxygen (DO), pH, redox condition (Elliott and McLusky 2002), as well as gradients of organic matter quantity and quality (Abril et al. 2002), which may affect trace metal speciation and distribution. Some elements may have a conservative behavior along the estuary, and their distribution is controlled by physical mixing of river and sea waters (de Souza Machado et al. 2016). Conversely, others may have a non-conservative additive or subtractive behavior, which means that due to biogeochemical processes a gain or a loss of dissolved metal concentrations in comparison to the theoretical dilution line will be observed. Metals also have affinities with suspended solid (Lacerda et al. 1988), which are by far the most important metal carriers from the rivers to the coastal area (Yao et al. 2016). Consequently, the distribution and partitioning of trace metals between the particulate and the dissolved phases may vary along the estuarine salinity gradient due mainly to changes in water chemistry (pH, DO, organic matter) and ionic strength (Benoit et al. 1994, de Souza Machado et al. 2016) which can induce trace metal desorption by metal complexation with chloride and sulfate forming soluble inorganic complexes (Acosta et al. 2011, Greger et al. 1995) or metal adsorption by cation exchange capacity (Wang et al. 2016, Yang and Wang 2017).

In developing countries, the capacity of wastewater treatment plants are not sufficient enough to treat the metal loads from urban, domestic or industrial activities, which are thus released into the rivers and then estuaries. As most of the tropical estuaries are colonized by mangrove forests (Giri et al. 2011), those inorganic contaminants can thus be deposited in these ecosystems. Mangrove sediments are known to act as a sink of trace metals due to their richness in organic matter, their clay content, and their dense root systems that can efficiently trap suspended matter

and their associated metals from the water column (Chu et al. 1998, Harbison 1986, Marchand et al. 2006b, Natesan et al. 2014). However, because of the reactivity of these sediments and the alternation between oxic and anoxic conditions, trace metals bearing phases may be dissolved (Marchand et al. 2016, Noël et al. 2014) and metals can, thus, be exported to adjacent tidal creeks (Holloway et al. 2016). As mangroves have specific ecological, sociological and economical roles, notably for the local population and the fishing resources (Lee et al. 2014), their ecological status and the understanding of the metal fate in their water column is highly relevant.

Can Gio is the biggest mangrove forest in Vietnam, being a well-known sea-food producing area, and having its core zone registered as a UNESCO biosphere reserve. Can Gio is also an estuary located at the confluence of Sai Gon and Dong Nai Rivers, which drain a megacity of almost 10 million inhabitants, Ho Chi Minh City. In addition, this estuary is acting as a unique gate for water traffic connecting Ho Chi Minh City to the South China Sea. Despite the long list of ecosystem services provided by the Can Gio mangrove and the increasing anthropogenic pressure on this zone (Kuenzer and Tuan 2013), there is a lack of published studies along this estuary, especially on trace metal dynamics. Some publications were interested in organic compounds (Minh et al. 2007, Oxmann et al. 2010), and recently accumulation of trace metal in sediments fringing the mangrove was studied (Costa-Boddeker et al. 2017). The only available data concerning trace metals distribution was reported in surface water of the Sai Gon River, upstream the mangrove (Strady et al. 2017a).

Within this context, our main objectives were to determine: i) the spatio-temporal variations of salinity, pH, DO, total suspended solids (TSS), particulate organic carbon (POC) and dissolved organic carbon (DOC) along this mangrove estuary, from the downstream end of Ho Chi Minh City to the South China Sea; ii) the distribution and partitioning of metals between the particulate

and dissolved phases along the salinity gradient; iii) the potential influence of the monsoon on the fate of trace metals. Our main hypothesis are: i) a decrease of trace metals concentrations due to the dilution with marine waters and/or desorption from bearing phase resulting from increased oxygen content; ii) increased inputs during the monsoon caused by elevated runoff and soil leaching. To reach our goals, water and suspended matter samples were collected for organic carbon and trace metals analysis during 24 h cycling in order to take into account the whole tidal cycling at four sites along the estuary during two distinct seasons.

2.2. Materials and Methods

2.2.1. Study area

The Can Gio mangrove is located in the south of Vietnam (10°22'14"-10°40'09"N; 106°46'12"-107°00'59"E) and is part of the densely populated megacity of Ho Chi Minh City (HCMC; almost 10 million of inhabitants), 35 km downstream of the City urban center and industrial zones (Strady et al. 2017a, Vo 2007). This mangrove covers an area of 35,000 ha (Fig. 2.1) and is a UNESCO biosphere reserve which can be divided into three areas according to their anthropogenic pressure and level of conservation (Nam et al. 2014): (i) a core zone protected for long term conservation of biodiversity, in which human activities are prohibited, (ii) a buffer zone to protect the core zone with limited human activities and (iii) a transition zone with humans activities like agriculture, aquaculture, fishing, salt-pan, trading and tourism. Can Gio mangrove is home to high biodiversity with more than 200 species of fauna (e.g. planktonic and benthic organism, fishes, reptiles and amphibians) and 20 species of flora, in which three mangrove species are dominant *Avicenia alba*, *Rhizophora apiculata*, *Phoenix paludosa* (Kuenzer and Tuan 2013). Freshwater inputs originate from the Sai Gon and Dong Nai Rivers, emptying out the South China Sea via the Long Tau and Soai Rap Rivers. The hydrology is affected by a semi-diurnal tidal regime with a tidal amplitude up to 4 meters, and by typical tropical monsoon climate, with a rainy

season lasting from May to October and a dry season extending from November to April. The annual average temperature and precipitation are 25.8 ^{o}C and 1,400 mm, respectively. During the rainy season, highest precipitation can reach up 400 mm in September while it is usually less than 80 mm per month during the dry season.

The main economic activities of local people are: aquaculture, in which shrimp farming dominate with approximately 3,160 ha, fisheries, agriculture and salt production (Tuan and Kuenzer 2012). The industrial activities are excluded of the three zones (core, buffer and transition zones) of the Can Gio mangroves but are developed to 35km upstream the mangrove close to HCMCity urban center and along the Dong Nai river (mainly plastic and rubber production, mechanical engineering, electrical engineering, packaging, textile and dyes industry, oil activities and cement production).

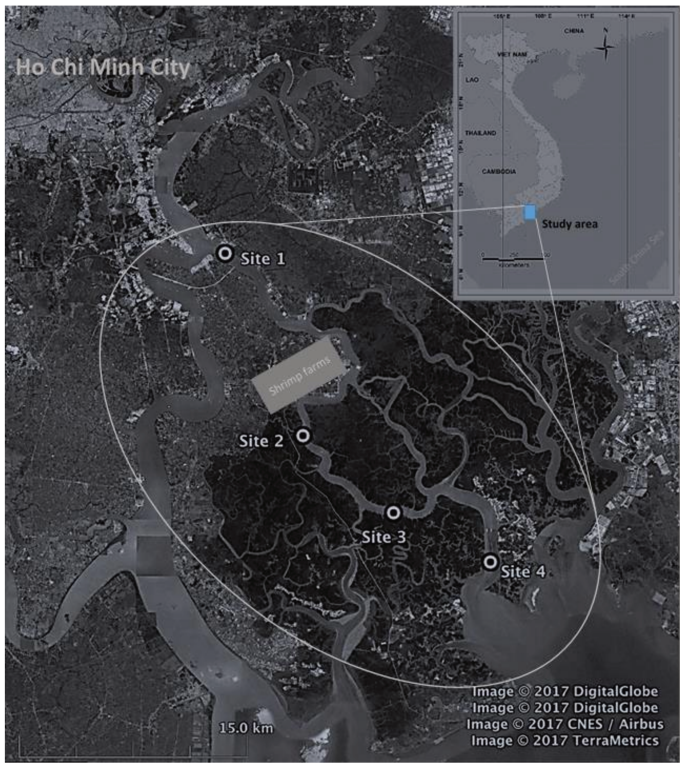

Fig. 2-1. Satellite image of Can Gio mangrove forest (black area) and sampling locations along the estuary. Site 1 characterizing the riverine and urban end-member; Site 2 characterizing aquaculture activities (mainly shrimps) and the buffer zone of mangrove forest; Site 3 characterizing the core of mangrove forest; site 4 characterizing the marine end-member.

2.2.2. *Field sampling and measurements*

Samples were collected during 24 h tidal cycles, with a sampling every 2 h, at four sites along the Long Tau River according to their environmental characteristics and their locations into the different zones of the mangrove described in the section above: site 1 (10°39'55"N - 106°47'30"E) characterizing the riverine and urban end-member; site 2 (10°34'19"N - 106°50'11"E) located in the buffer zone of the mangrove forest characterizing aquaculture activities (mainly shrimps); site 3 (10°31'04"N - 106°53'13"E) located in the core zone of the mangrove forest; site 4 (10°29'32"N - 106°56'55"E) characterizing the marine end-member (Fig. 2.1). The sampling campaigns were carried out during dry season (January and February, 2015) and rainy season (September and October, 2015).

The physico–chemical parameters such as salinity, pH and temperature (^{o}C) were logged continuously *in-situ* using a multi-probe (Yellow Spring Instrument® meters YSI 6920). DO was monitored with a HOBO Dissolved Oxygen data logger (HOBO U26-001). pH probes were pre-calibrated using buffer solutions: 4, 7 and 10 (NIST scale) at the same day prior of sampling. Probes were immerged 50 cm below the air-water interface and data were recorded every at 5 min.

At each sampling site and time, surface waters (50 cm below the air-water interface) were collected in duplicates using a bucket, immediately transferred into acid pre-cleaned polypropylene bottles (1 L) - previously rinsed with surface water. Then, a first aliquot of surface water was filtered through 0.2 µm PTFE Omnipore™ Membrane Filters for trace metal analysis. The filtrate was transferred into pre-cleaned 50 mL polypropylene, immediately acidified to pH < 2 using concentrated suprapur® HNO_3 (HNO_3/ sample = 1/1000 (*v/v*)) for dissolved trace metals M_D, while the filters were kept in pre-cleaned plastic petri dishes for suspended particulate trace metals analysis (M_P). Both samples were maintained in cool box during sampling campaign and

stored at 4 ºC in the laboratory for dissolved metal and at -18 ºC for particulate metal (Strady et al. 2017b). Filters were then freeze dried, weighed and preserved at room temperature until analysis. A second aliquot of surface water was filtered in triplicates through pre-combusted (500 °C) and pre-weighted glass fiber filters (Whatman® GF/F 0.7 µm): the filter was stored at -18 ºC for particulate organic carbon (POC) and total suspended solid (TSS) determinations while the filtrate was transferred into sterile 15 mL polypropylene, acidified using concentrated suprapur® HCl and stored at 4 ºC in fridge for dissolved organic carbon (DOC) analysis.

2.2.3. Samples analysis

Dissolved metals concentrations (M_D)

Dissolved Mn, Fe, Cr, Co, Ni, Cu, As and Pb concentrations were directly measured by Thermo Scientific iCAPQ ICP-MS using internal standard calibration (AETE-ISO platform, OSU-OREME/Université de Montpellier), with a Kinetic Energy Discrimination – Argon Gas Dilution module (KED – AGD mode) (Kutscher et al. 2014). Accuracy and precision were controlled using certificate reference material: riverine water (SLRS6) for salinity lower than 1 and estuarine water (SLEW-3) for salinity higher than 1 (Table 2.1a).

Particulate metal concentrations (M_P)

Particulate Mn, Fe, Cr, Co, Ni, Cu, As and Pb concentrations were analyzed according to a total extractable metal digestion adapted from the USEPA 3051a method (USEPA 2007). Filters were put on PTFE vessel in which 6 mL of concentrated HNO_3 and 2 mL of concentrated HCl were added. The vessels were placed into ultrasonic bath during 15 min and were then heated at 110 °C during 12 h in the electrical oven. After cooling, the digestions were put again in ultrasonic bath during 15 min, and temperature was then increased up to 160 ºC during 4 h. The samples were cooled and filtrated to reject residue, then diluted to 25 mL with deionized water and stored

in pre-cleaned PP tubes at 4 °C until analysis. All reagents were of analysis grade (Merck) and were purified using a sub-boiling quartz distillation equipment prior digestion.

Concentrations of Cr, Co, Ni, Cu, As and Pb were measured by ICP –MS (Agilent 7700x) using spiked ^{103}Rh and ^{197}Au as internal standard while Fe and Mn concentrations were determined by Flame Atomic Absorption Spectrophotometer (Shimadzu AA-6650). The analytical precision and accuracy were insured by analyzing certificate reference material estuarine sediments (BCR-277R) (Table 2.1b).

Table 2-1. Quality control of analytical methods applied for dissolved and particulate metal concentrations analysis: a) accuracy, precision and detection limit using estuarine water SLEW-3; b) BCR-277R for wet digestion method.

a) Dissolved metal concentration analysis

Element	*Detection limit ($\mu g\ L^{-1}$)*	*Certificated values ($\mu g\ L^{-1}$)*	*Measured values ($\mu g\ L^{-1}$)*	*Recovery (%)*	*Relative standard deviation (%)*
Cr	0.022	0.183 ± 0.019	0.0182 ± 0.020	99	11
Mn	0.013	1.61 ± 0.22	1.469 ± 0.016	91	1
Fe	0.031	0.568 ± 0.059	0.661 ± 0.073	116	11
Co	0.0092	0.042 ± 0.010	0.0464 ± 0.0025	110	5
Ni	0.011	1.23 ± 0.07	1.230 ± 0.014	100	1
Cu	0.011	1.55 ± 0.12	1.491 ± 0.041	96	3
As	0.0062	1.36 ± 0.09	1.569 ± 0.013	115	1
Pb	0.003	0.009 ± 0.0014	0.0115 ± 0.0017	130	15

b) Particulate metal concentration analysis

Element	Certificated values ($mg\ kg^{-1}$)	Measured values ($mg\ kg^{-1}$, n = 9)	Recovery (%)	Relative standard deviation (%)	Analytical method
As	18.3 ± 1.8	17.56 ± 0.87	96	5.0	ICP-MS
Pb	NA	28 ± 1.3	-	4.8	ICP-MS
Co	22.5 ± 1.4	22.9 ± 0.7	102	2.8	ICP-MS
Cr	188 ± 14	171.3 ± 5.4	91	3.2	ICP-MS
Cu	63 ± 7	60.5 ± 1.8	96	2.9	ICP-MS
Ni	130 ± 8	128.9 ± 3.2	99	2.5	ICP-MS
Mn	NA	835 ± 29	-	3.5	FAAS
Fe	NA	51855 ± 3146	-	6.1	FAAS

Dissolved organic carbon (DOC) and particulate organic carbon (POC) analysis

The DOC analysis were performed on a Shimadzu® TOC-L series analyzer employing a 680 °C combustion catalytic oxidation method. The analyzer was combined with a solid sample module (SSM-5000A) heated up to 900 ºC for POC measurement (Leopold et al. 2013). For both, 40% glucose standard was used for calibrations. Repeated measurements of the standard at different concentrations indicated a measurement deviation < 2%.

2.2.4. Data analysis

In order to better understand the interaction of trace metals between dissolved and particulate phases along the salinity gradient, the partitioning coefficient (K_D) was calculated. The K_D provide a quantitative value for the partitioning of metal concentration between solution and particle. It is defined as the ratio of particulate metal concentration (M_P) to dissolved metal concentration (M_D) in the water column (Turner et al. 1993).

$K_D = M_P / M_D$, where M_p is the particulate metal concentration; M_D is the dissolved metal concentration.

The Pearson correlation coefficient and the one-way ANOVA were performed using statistical package software (SPSS; version 23) to identify major relationships between metal concentrations and physico-chemical parameters as well as interrelations between metals together in order to identify the main factors controlling metal partitioning.

2.3. Results and discussion

2.3.1. Spatial and seasonal variations of physico-chemical parameters

Can Gio is a tropical mangrove-dominated estuary characterized by semi-diurnal tidal regime and subject to a monsoon season. All the studied parameters varied from the upstream site, at the edge of Ho Chi Minh City, to the downstream site, at the mouth of the estuary (Table 2.2, Fig. 2.2). In addition, some seasonal variations were observed. Salinity, DO and DOC were affected by seasonal change (ANOVA, $p < 0.01$), whereas pH, TSS and POC were not (ANOVA, $p > 0.05$). From the upstream site to the sea, salinity varied from 0 to 25 during the rainy season and from 5 to 25 during the dry season. The very low salinity (< 2) observed at the upstream site during the rainy season, whatever the tides, was attributed to intense rainfall increasing the freshwater inflow and limiting the saline intrusion. The pH values varied from 6.8 to 7.8 during the dry season and from 6.4 to 7.5 during the rainy season, and were positively correlated to salinity ($r = 0.96$ and

0.97 during the dry and the rainy season, respectively). DO ranged from 3.5 to 7.0 mgO_2 L^{-1} and from 1.2 to 5.3 mgO_2 L^{-1} during the dry and the rainy seasons respectively, also increasing with salinity (r = 0.86 and 0.94 for the dry and the rainy season, respectively). Both pH and DO reflected the mixing of fresh and sea waters (Fig. 2.2). The acidic pH values measured at the upstream site during the monsoon are likely related to the contribution of the Sai Gon River, which is characterized by low pH, down to 5.7 (Strady et al. 2017a), possibly due to the leaching of the surrounding acidic sulfate soils (Nguyen et al. 2011), but also to the decay processes of organic inputs. The latter may also be responsible for the drastic decrease of DO values measured at this site, down to 1.2 mgO_2 L^{-1}. These organic inputs may originate from domestic and urban discharges of Ho Chi Minh City urban center and also from the industrial areas located along the Sai Gon and Dong Nai Rivers.

The POC concentrations decreased along the salinity gradient but not linearly, from 3.8% to 1.3%, and from 5.0% to 1.7% during dry and rainy seasons, respectively. Those patterns suggest that POC distributions resulted both from the dilution by seawater and from the decomposition processes occurring during its transit in the estuary (Fig. 2.2). Decreasing POC concentrations have also been observed in most estuaries like in temperate European estuaries (Abril et al. 2002, Etcheber et al. 2007) or tropical estuaries like in the Mandovi Estuary (Shynu et al. 2015). At the upstream site, DOC concentrations ranged from 1.22 mgC L^{-1} to 5.89 mgC L^{-1} during the rainy season and could be related to intense inputs from the city and industrial zones (Strady et al. 2017a). Along the salinity gradient, DOC concentrations varied from 1.64 mgC L^{-1} to 3.54 mgC L^{-1} and were stable during the rainy season. However, during the dry season, DOC values slightly increased in the downstream part of the estuary, which might be the result of intense carbon

degradation processes in well oxygenated waters (Ni et al. 2008), and possible inputs from the adjacent mangrove forest (Dittmar and Lara 2001).

Table 2-2. Bi-hourly water level (m), salinity, pH, DO (mgO2 L-1), DOC (mgC L-1), POC (%) and TSS (mg L-1) measured at the four sampling sites (site 1, site 2, site 3, site 4) during the dry and the wet seasons.

		Dry season							*Wet season*						
Site	*Label*	Water level m	Sal	pH	DO mgO_2 L^{-1}	DOC mgC L^{-1}	POC %	TSS mg L^{-1}	Water level m	Sal	pH	DO mgO_2 L^{-1}	DOC mgC L^{-1}	POC %	TSS mg L^{-1}
S1	h0	12.8	8.84	6.87	3.89	2.8	3.76	16.6	11	0.55	6.57	1.84	2.36	5.05	44.53
S1	h2	13.6	7.4	6.81	3.47	3.25	3.84	17.23	10.6	0.2	6.55	1.21	3.88	5.04	45.66
S1	h4	14.6	7.92	6.93	4.07	3.18	3.4	18.96	10.8	0.3	6.55	1.32	5.89	4.35	58.46
S1	h6	16.2	10.68	7.09	4.62	2.94	2.6	29.03	11.3	0.64	6.59	1.8	NA	3.94	62.23
S1	h8	15.1	12.56	7.17	4.15	2.92	2.95	21.53	11.9	1.92	6.68	2.33	3.42	2.92	136.76
S1	h10	14.2	11.01	7.1	4.1	3.33	2.41	33.46	12.2	3.19	6.75	2.57	2.52	4.96	22.8
S1	h12	13.1	10.05	7.09	3.52	2.92	2.73	25.1	12	0.91	6.62	1.72	2.04	4.73	34.00
S1	h14	12.9	9.77	7.04	3.6	3.59	2.39	60.26	11.8	0.75	6.6	1.59	3.18	4.00	42.53
S1	h16	12.4	8.15	6.97	4.17	3.35	2.7	43.06	11.9	0.69	6.6	1.64	2.42	4.04	42.96
S1	h18	13.6	8.44	7	4.65	2.54	2.98	22.96	12.1	0.84	6.61	1.77	1.22	4.36	32.9
S1	h20	15.3	10.19	6.99	4.04	3.12	3.12	27.53	11.8	0.83	6.64	2.26	2.44	4.45	37.7
S1	h22	15.3	11.43	6.84	4.65	3.88	2.52	42.56	11.5	0.85	6.66	2.3	1.97	4.74	33.36
S1	h24	13.5	9.17	6.87	4.08	3.83	3.61	15.96	11	0.57	6.63	2.12	1.41	4.26	47.23
S2	h0	11.7	21.33	7.32	4.98	4.41	1.98	198.26	10.8	17.76	7.59	4.6	2.35	2.78	53.00
S2	h2	10.8	21.71	7.43	4.93	2.47	1.94	139.43	10.6	16.7	7.37	4.28	1.96	2.31	75.96
S2	h4	9.3	21.32	7.4	4.89	4.32	1.62	168.66	8	15.06	7.42	4.27	1.94	1.93	236.26
S2	h6	9.4	20.22	7.39	4.96	2.3	2.02	151.16	7.3	11.78	7.24	3.88	1.99	1.99	178.33
S2	h8	10.5	20.17	7.38	4.87	2.62	1.28	70	8.2	6.49	7.01	3.16	2.12	2.64	50.76
S2	h10	11.1	21.56	7.42	4.84	2.39	1.31	61.53	10.8	8.78	7.28	3.93	2.3	2.01	178.63
S2	h12	11.1	22.67	7.45	4.8	4.11	NA	147.9	13.3	16.28	7.46	4.07	1.64	1.67	266.8
S2	h14	9.7	21.69	7.36	4.87	4.02	NA	108.96	13.6	17.07	7.49	4.12	1.86	2.03	82.56
S2	h16	8.2	20.9	7.38	4.85	4.72	NA	206.6	8.6	15.97	7.39	4.05	1.89	2.29	190.7
S2	h18	7.5	18.8	7.33	4.85	3.62	NA	361.16	7.6	14.88	7.38	3.94	2.82	2.11	283.06
S2	h20	8.1	13.89	7.19	4.52	2.8	NA	93.96	7.3	10.31	7.17	3.51	3.54	2.22	80.23
S2	h22	10.3	17.55	7.3	4.75	3.19	NA	55.13	9.8	10.92	7.26	3.98	2.38	2.62	67.36
S2	h24	10.8	21.17	7.38	4.83	3.13	NA	281.33	10.5	15.82	7.43	3.93	2.03	2.25	170.23
S3	h0	NA	NA	NA	NA	NA	NA	NA	11.8	15.86	7.43	3.58	2.09	2.65	30.76
S3	h2	12.6	NA	NA	4.93	3.77	1.66	77.8	11.2	14.71	7.35	3.25	2.07	2.47	51.16
S3	h4	12.7	NA	NA	5.13	2.22	1.7	167	11.4	13.47	7.29	3.11	2.01	2.51	48.26
S3	h6	12.8	NA	NA	5.36	2.3	1.49	73.8	12.3	13.47	7.31	3.34	2.24	2.92	33.3
S3	h8	11.7	NA	NA	5.55	2.54	1.51	44.66	12.9	17.05	7.45	3.61	1.78	2.46	38.8
S3	h10	NA	NA	NA	NA	NA	NA	NA	13.3	18.93	7.56	3.8	2.41	2.92	43.83
S3	h12	10.3	NA	NA	4.99	2.77	1.57	107.46	13.1	20.18	7.66	4.73	2.04	2.9	36.53
S3	h14	10.6	NA	NA	4.91	2.36	1.77	52.46	12.9	16.48	7.48	4.17	1.82	3.51	31.5
S3	h16	12.4	NA	NA	4.98	3.94	1.29	53.9	12.7	16.68	7.47	3.79	2.39	2.65	33.23
S3	h18	12.7	NA	NA	5.11	2.82	1.53	54.96	12.6	16.98	7.48	3.58	2	2.86	36.86
S3	h20	11.3	NA	NA	5.17	3.1	1.48	39.7	13.1	16.9	7.48	3.72	2.08	2.92	24.56
S3	h24	10.6	NA	NA	5.22	2.79	1.5	66.8	12.9	17.21	7.5	3.88	2.14	2.78	24.5
S4	h0	12.6	26.06	7.75	6.82	3.66	1.66	73.56	12.6	16.52	7.5	4.2	2.21	3.06	23.23
S4	h2	12.3	26.1	7.81	7.01	4.48	1.58	45.43	12.3	18.93	7.39	3.86	2.2	2.22	41.96
S4	h4	12.1	25.91	7.81	6.85	3.64	1.26	42.3	13.5	23.01	7.59	4.52	1.66	1.85	62.36
S4	h6	12	24.17	7.73	6.49	3.64	1.58	40.66	14	25.61	7.7	5.27	3.19	1.87	50.06
S4	h8	12.6	25.24	7.76	6.65	4.32	2.09	34.83	12.3	22.92	7.59	4.97	2.32	1.82	60.73
S4	h10	13	25.78	7.79	6.75	4.16	2.9	34.83	12.4	21.43	7.48	4.29	2.24	1.83	89.66
S4	h12	12.5	25.56	7.77	6.61	4.84	2.37	28.66	14.1	20.09	7.44	4.09	1.89	1.84	42.8
S4	h14	11.3	23.63	7.69	6.24	3.28	1.77	78.73	14.5	23.09	7.57	4.51	1.91	2.02	51.06
S4	h16	11	22.78	7.64	5.97	3.92	2.33	121.86	13.8	24.09	7.63	4.63	2.71	2.18	48.43
S4	h18	11.4	20.98	7.58	5.84	4.44	2.38	50.63	13.1	23.74	7.59	4.83	2.35	2.09	46.46
S4	h20	11.9	23.59	7.64	5.99	4.46	1.97	93.93	11.7	21.92	7.52	4.53	3.46	2	120.93
S4	h22	12.8	25.97	7.75	6.57	3.79	1.85	98.8	11.4	19.44	7.41	4.37	2.78	2.09	102.76
S4	h24	13.1	25.82	7.76	6.6	3.8	1.89	54.33	12	18.01	7.38	3.95	3.14	2.42	39.73

The TSS concentrations varied from 16 to 361 mg L^{-1} and 23 to 283 mg L^{-1} during the dry and the rainy season, respectively, and did not present any conclusive distribution along the salinity

gradient (Fig. 2.2). They were in the same range than those measured upstream the mangrove by Strady et al. (2017a), whatever the seasons. However, higher values were measured at site 2, located within the outlet of small tributaries, which are suggested to be related to disturbance of bottom sediment due to confluences of watersheds (Cang et al. 2007) and the increased erosion of the river banks caused by the sinuous flow (Nam et al. 2014).

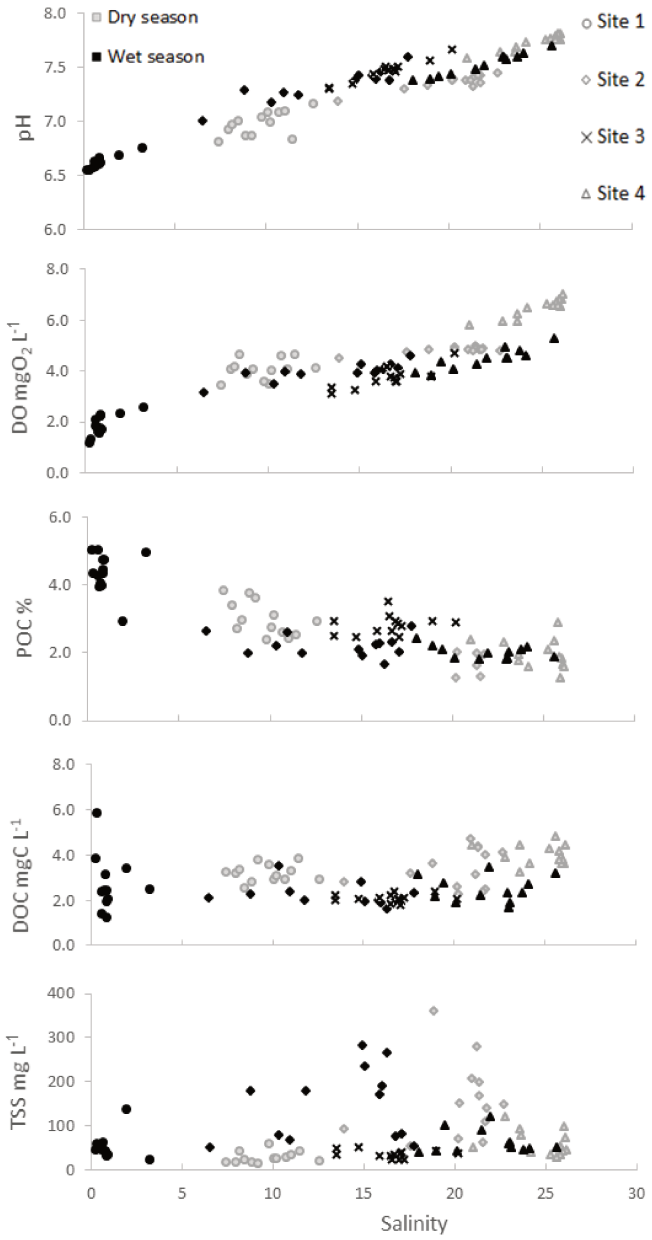

Fig. 2-2. Spatio-temporal variations in pH, DO, POC DOC and TSS along the salinity gradient during the dry and the wet seasons.

To summarize, the spatial and seasonal variations of the physico-chemical properties reflected well the mixing of the fresh and the sea waters in the estuary. The characteristics of the upstream site during the monsoon are those of the Saigon River: salinity almost null, acidic pH values, low DO concentrations, and high POC and DOC contents. We suggest that this site can be considered as the river end-member during this season. During the dry season, the characteristics of site 1 were estuarine ones, with a mix between fresh and sea waters, and thus cannot allow us to determine inputs in the estuary at this season. Concerning the downstream site, it exhibited similar salinity, pH and DO ranges during both seasons and was thus considered as the seawater end member of the studied system.

2.3.2. Trace metal distributions at the upstream site during the monsoon

The characteristics of the upstream site during the monsoon being those of the river end-member, and not those of estuarine waters, we choose to discuss them separately from the other data in order to evidence riverine trace metals inputs in the Can Gio Estuary. The dissolved concentrations measured during this period were (µg L^{-1}): Mn_D, 3.4 – 37; Fe_D, 2.4 – 18; Cu_D, 0.2 – 1.5; Pb_D, 0.15 – 2.1; Ni_D, 0.3 – 1.37; As_D, 0.09 – 1.4; Cr_D, 0.053 – 0.26 and Co_D, 0.01 – 0.5 (Fig. 2.4; supplementary data 2.1) while the particulate concentrations were (mg kg^{-1}): Fe_p, 42,959 – 55,238; Mn_p, 306 – 822; Cr_p, 73 – 131; Ni_p, 57 – 93; Cu_p, 43 – 76; Pb_p, 18 – 27; Co_p, 10 – 19 and As_p, 9 – 14 (Fig. 2.4; supplementary data 2.1). Both dissolved and particulate concentrations were in the same range as previously measured in the Sai Gon River (Nguyen et al. 2011, Strady et al. 2017a) and were in the low range of World River average concentrations (Gaillardet et al. 2014, Viers et al. 2009). We noticed that the higher dissolved and particulate concentrations were measured during the ebb tide, namely during riverine water flowing, attesting their inputs from urban and anthropogenic sources (Strady et al. 2017a). Elevated Cr_p, Cu_p and Ni_p concentrations coincided with high POC values, as previously observed by Strady et al. (2017a) suggesting that

organic matter might be an important factor affecting those metal distributions. The decrease and variation of Cr_p, Cu_p and Ni_p concentrations, at the riverine part and the beginning of estuary (Fig. 2.4c, 2.4e and 2.4f), may be thus related to the organic matter degradation.

3.3. Relationship between TSS and total trace metal concentrations

To assess the control of TSS concentrations on metal transfer in the Can Gio Estuary, the total metal concentrations in a volume of water (i.e. the particulate concentrations, expressed in $\mu g\ L^{-1}$, plus dissolved concentrations) were calculated (Strady et al. 2017b, Wang et al. 2016) and expressed in $\mu g\ L^{-1}$ (Fig. 2.3). All total metal concentrations increased with increasing TSS concentrations along the estuary ($r > 0.95$, $p < 0.01$ for all metals during the dry season, and $r > 0.9$ for Mn, Fe, Cr, Ni and Pb; $r = 0.80$ for Co; $r = 0.75$ for Cu and $r = 0.46$ for As; $p < 0.01$ during the rainy season) supporting the fact that the total metal concentrations transfer in the Can Gio Estuary is controlled by the change of TSS concentrations whatever the season, like in the Mekong Delta, Vietnam (Strady et al. 2017b), in the Huanghe River Estuary, China (Wang et al. 2016) or in the Changjiang River Estuary, China (Yang et al. 2014). However, for a given TSS concentration, total concentrations in Fe, Cr, Ni and Pb were higher during the monsoon than the dry season (Fig. 2.3) suggesting enhanced metal transport from land to sea during the monsoon. The particulate phase was the dominant one for Fe, Cr and Co, representing more than 99% of the total for Fe, 75 to 99% for Cr and 70 to 98% for Co, while the percentage of Ni_p, Cu_p, As_p, Pb_p and Mn_p varied from 22 to 91%, 28 to 95%, 13 to 94%, 24 to 99% and 29 to 99%, respectively. This result suggests different partitioning between particulate and dissolved metal phases during their transit along the Can Gio mangrove Estuary.

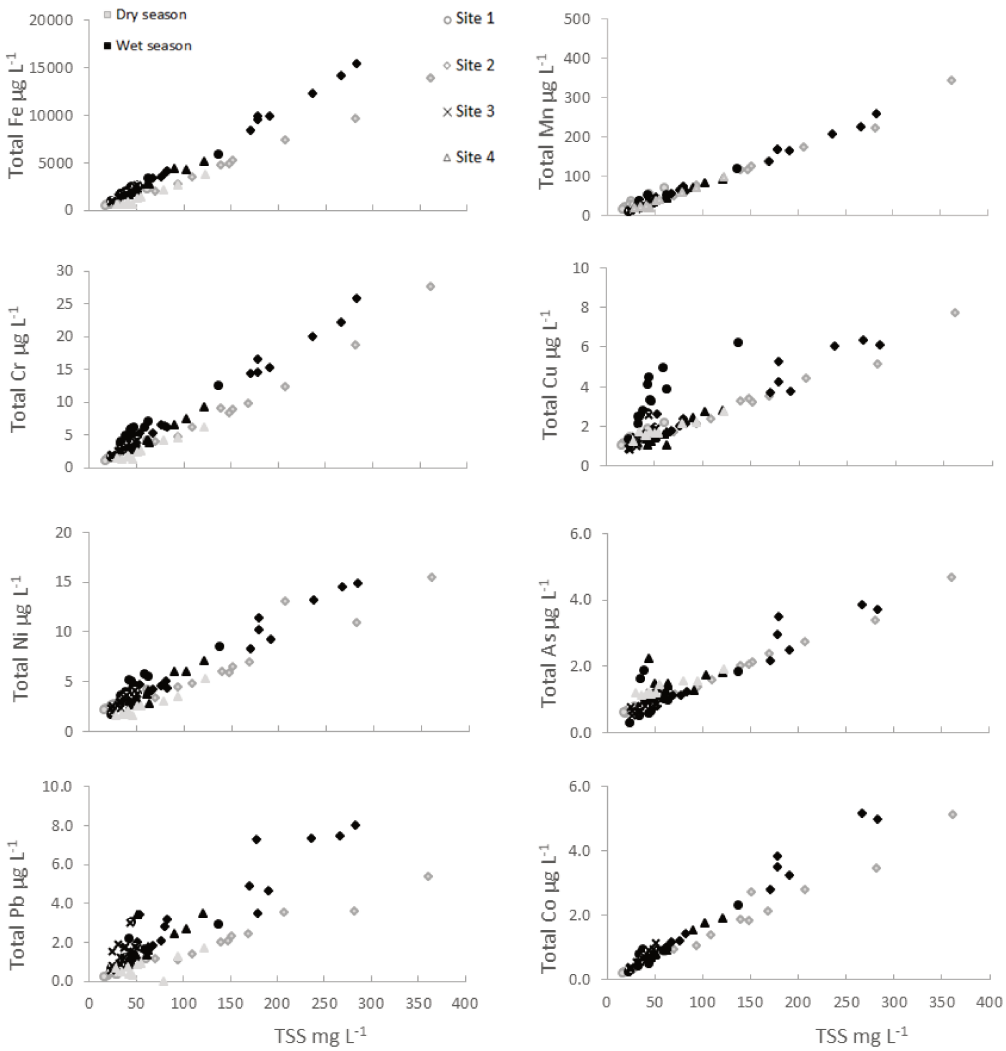

Fig. 2-3. Relationship between the total metal concentrations (i.e. dissolved plus particulate metal concentrations, expressed in µg L-1) of Fe, Cr, Ni, Pb, Mn, Cu, As, Co and TSS concentration during the dry and the wet seasons.

2.3.3. Trace metal partitioning in the estuarine zone

2.3.3.1 *Iron*

Along the salinity gradient, Fe_P varied from 35,276 to 55,302 mg kg^{-1} during the monsoon, and from 13,917 to 41,328 mg kg^{-1} during the dry season with minimum values reached at the seaside of the estuary (Fig. 2.4a). These lower values during the dry season could be attributed to the dilution with the sea water (i.e. Fe_p concentrations of 15,000 mg kg^{-1} in coastal zones of the Pacific Ocean (Hatje et al. 2001). During the monsoon, dilution was not observed, probably due to intense leaching of Fe from the surrounded mangrove soils, Fe being a rich element of mangrove soils

(Marchand et al. 2006b, Miola et al. 2016, Noël et al. 2014). The Fe_D varied between 1.01 to 3.3 µg L^{-1} during the dry season and 1.6 to 5.0 µg L^{-1} during the rainy season. Along the salinity gradient, Fe_D showed a non-conservative behavior with additive concentrations at mid salinity (site 2 and 3) (Fig. 2.4a, supplementary data 2.1 and 2.2). During the dry season at site 2, these higher concentrations might be attributed first to the contribution of the pore-water inputs from mangrove sediments, as observed in mangrove estuaries like in Australia (Santos et al. 2011). These authors reported extremely high dissolved iron concentration up to 374 mg L^{-1} in pore-water. They also evidenced that iron in surface water originated from mangrove soils by pore-water discharge, using radio-isotopes (Radon, ^{222}Rn). In fact, mangrove soils can be rich in dissolved iron as described in the Pai Matos mangrove system, Brazil (Otero et al. 2009) or in the French Guiana mangrove (Marchand et al. 2006b). This richness result from the alternation of different redox processes, notably iron oxide reduction and iron sulphide oxidation, leading both to the release of dissolved iron in pore-waters, which can thus be exported to adjacent ecosystems through pore-water seepage (Deborde et al. 2015, Sanders et al. 2015). Secondly, we assumed that irregular inputs from the shrimp farms might also be a source of dissolved iron concentration to the water column as observed in the Estuaries of East-Hainan, China (Fu et al. 2013). The Fe_D concentrations were influenced by pH changes, associated to the cultivation cycles (Azevedo et al. 2009), reaching approximately 2 mg L^{-1} in ponds on acid sulfate soils (Jayasinghe et al. 2010). Unfortunately, we were not able to determine the Fe_D concentrations at site 3 during the dry season, which was only surrounded by mangrove forest. During the rainy season, scattered Fe_D were also measured at site 2 and at site 3 at both ebb and flood tides, which may be related to pore-water releases from mangrove sediments, aquaculture ponds or runoff from the surrounding watershed. Along the Can Gio mangrove Estuary, log K_D^{Fe} was stable whatever the season, ranging from 6.1 to 7.6 (Fig.

2.4a). The absences of significant correlations between log K_D^{Fe} and salinity, pH, DO, DOC, POC or TSS do not allow us to better characterize Fe partitioning along this mangrove estuary.

2.3.3.2 *Manganese*

Mn_p ranged from 402 to 1,055 mg kg^{-1} during the dry season and from 397 to 922 mg kg^{-1} during the monsoon along the salinity gradient (Fig. 2.4b), showing an absence of seasonal effect. These values were in the same range than those measured at the upstream site during the rainy season, and in tropical estuaries like the Tanshui Estuary, Northern Taiwan (Fang and Lin 2002). The high Mn_p fluctuations and its absence of conclusive distribution along the salinity gradient indicated that the Mn_p distribution in the Can Gio Estuary was not dominated by a simple mixing of the two end members, and might be influenced by biogeochemical processes. The Mn_D varied between 15.2 to 0.93 µg L^{-1} and 12.5 to 0.98 µg L^{-1} during the dry and the rainy season, respectively (Fig. 2.4b, supplementary data 2.1 and 2.2). Additionally, it decreased along the salinity gradient exhibiting a non-conservative subtractive behavior whatever the season. Both in laboratory experiments (Hatje et al. 2003) and in the field (Fang and Lin 2002), it was observed that DO increase can result in Mn_D adsorption onto particles surface by the oxidation of dissolved Mn (II) to insoluble Mn (III) and Mn (IV) (hydr)-oxides. Log K_D^{Mn} increased from 4.0 to 5.8 along the salinity gradient whatever the seasons (Fig. 2.4b) exhibiting good correlation with both DO and pH (Fig. 2.5a and 2.5b), suggesting that Mn partitioning is probably affected by the change of oxygenation in the estuary. During the dry season, higher Mn_D were measured at site 2, similarly to Fe_D, and could also originate from mangrove sediment pore-waters (Holloway et al. 2016, Sanders et al. 2015) or shrimp ponds effluents (Inoue and Asano 2013). During the rainy season, Mn_D presented scattered values at flood tide that might be related to runoff inputs of the adjacent watershed. Consequently, Mn dynamic along the estuary was strongly influenced by geochemical processes, mainly Mn precipitation resulting from oxygenation and pH changes with water mixing.

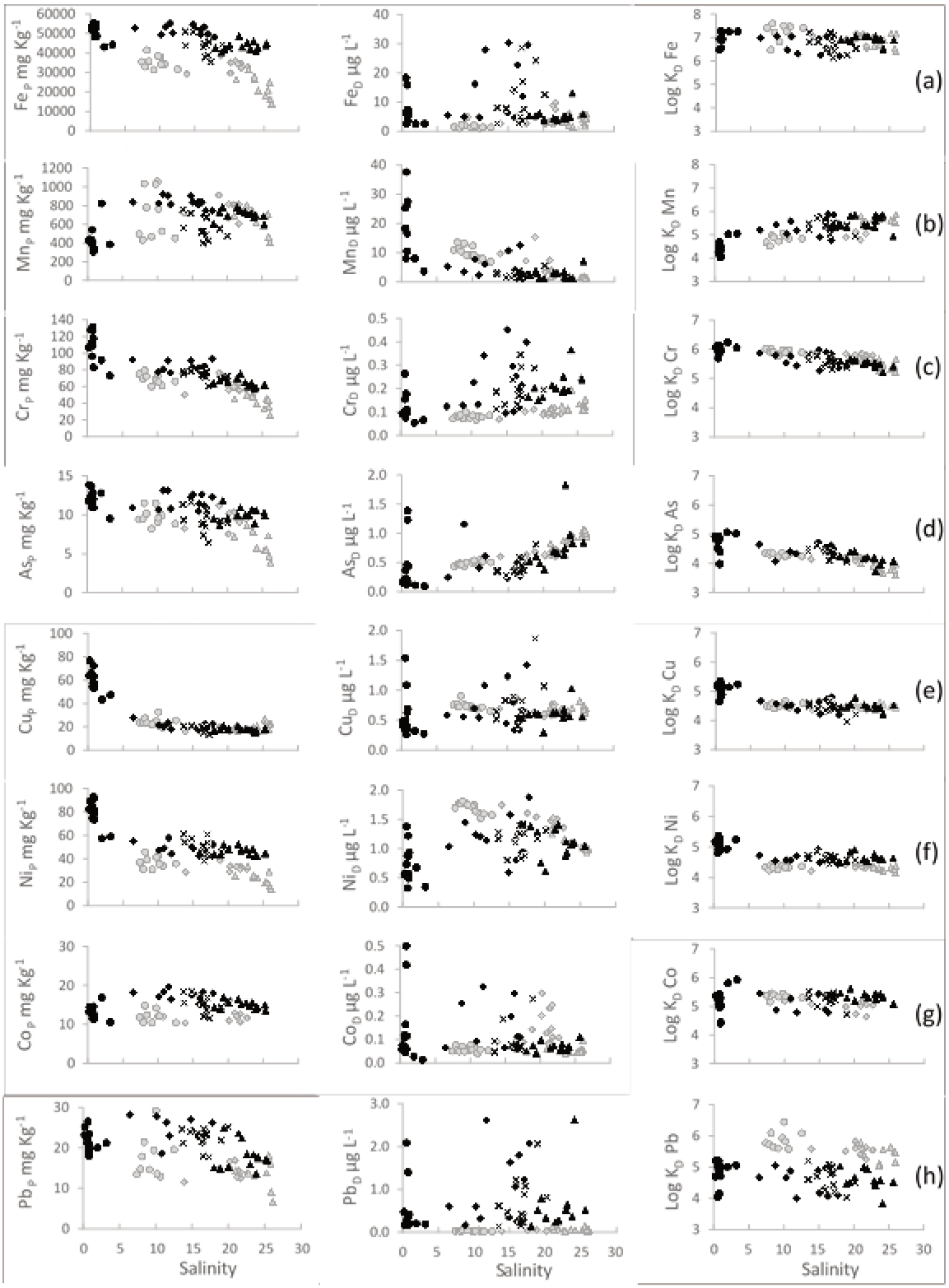

Fig. 2-4. Distribution of dissolved, particulate, log Kd of metals in the Can Gio mangrove estuary during the dry (gray dots) and the wet seasons (black dots), with circles, squares, multiplication signs and triangles representing the site 1, site 2, site 3 and site 4 respectively: Fe (a), Mn (b), Cr (c), As (d), Cu (e), Ni (f), Co (g) and Pb (h)

2.3.3.3 *Chromium*

The Cr_P ranged from 25 to 79 mg kg^{-1} during the dry season and from 57 to 94 mg kg^{-1} during the rainy season (Supplementary data 2.1 and 2.2), showing seasonal variations and decreasing concentrations along the salinity gradient (Fig. 2.4c). The Cr_p in the estuarine zone were slightly lower than in the riverine part (upstream site during the rainy season), while the Cr_p at the seaside of the estuary were close to the Cr_p reported in the coastal area of South China Sea (Cenci and Martin 2004). Therefore, the Cr_p concentrations decrease along the salinity gradient might be attributed to both dilution with seawater containing low Cr_p and to its desorption processes during organic matter degradation in the estuary, Cr having a strong affinity for organic matter (Masscheleyn et al. 1992). We observed that later process may play an important role on Cr_p distribution during the rainy season (i.e. a positive correlation observed between Cr_p and POC, r = 0.71) and a minor role during the dry season (r = 0.53), affecting also Cr partitioning (Fig. 2.5c). The Cr_D showed distinct behaviors along the salinity gradient between seasons: i) conservative distribution with gradually Cr_D increase seaward during the dry season, and ii) non-conservative with a gain of Cr_D at mid salinity during the rainy season (Fig. 2.4c, supplementary data 1 and 2). Scattered and higher Cr_D at site 2 and site 3 observed during the monsoon might be originated from the same sources as Fe_D (positive correlation between Cr_D and Fe_D; Fig. 2.5f), i.e. mangrove sediment pore-water releases (Szymczycha et al. 2016), runoff and/or shrimp pond effluents inputs. Along the estuary, Log K_D^{Cr} decreased from 6.2 to 5.2 and presented a low variation range. The combination of Cr_D increase, Log K_D^{Cr} decrease from the upstream site to the seaside and the positive correlation between Log K_D^{Cr} and POC (Fig. 2.4c and Fig 2.5d) confirm the Cr desorption from particulate organic matter during the water transit in the estuary. We suggest that the oxidation level may also influence Cr partitioning as evidenced by the negative correlation observed between Log K_D^{Cr} and DO (Fig. 2.5e). Thus, Cr partitioning in the Can Gio mangrove

Estuary was controlled by physical mixing and also biochemical processes, notably OM decomposition and increased oxygenation along the estuary.

2.3.3.4 *Arsenic*

The As_p varied from 6.4 to 13.8 mg kg^{-1} during the rainy season, and from 3.9 to 11.5 mg kg^{-1} during the dry season. Values were stable along the salinity gradient during the rainy season and presented a drop of concentrations at site 4 during the dry season (Fig. 2.4d). The concentrations at the seaside during the dry season were in the same range than those measured in the coastal zone of South China Sea (Cenci and Martin 2004) and in the Bohai Sea (Wang et al. 2016). The As_P distribution in the Can Gio mangrove Estuary reflected thus the water mixing between the river and the sea end-members but also biogeochemical processes. Along the estuary, As_P exhibited a strong correlation to Fe_P ($r > 0.8$, for both seasons, Fig. 2.5g) implying that Fe_p was the main carrier phase of As (Strady et al. 2017a) and an important factor controlling As_p distribution in the estuary. Both metals probably had a terrigenous origin (Cances et al. 2005, Oursel et al. 2014). Actually in Vietnam, many soils are naturally enriched in As, which is a public health problem for the local populations (Gustafsson and Tin 1994, Nguyen et al. 2016, Phuong et al. 2010). Along the estuary, As_D concentrations increased from 0.5 to 0.95 during the dry season and from 0.15 to 0.65 µg L^{-1} during the rainy season, which might be caused by dilution with sea water i.e. 1.5 µg L^{-1} of As_D in the Bohai Sea (Wang et al. 2016) and probably by As_D release during degradation of organoarsenic compounds from particulate phase (i.e. negative correlations were observed between As_D and POC, $r = 0.64$). This hypothesis is supported by the $LogK_D^{As}$ decrease along the salinity gradient, especially from mid salinity (Fig. 2.4d) and by positively correlations between $LogK_D^{As}$ and POC (Fig. 2.5h). In previous studies, some authors noticed that dissolved organic carbon plays an important role of As partitioning between dissolved and particulate phase because it can strongly interact with As species (Bauer and Blodau 2006, Liu and Cai 2010, Yanan et al. 2017). In the Can

Gio mangrove estuary, however, we observed the correlation coefficients between As_D concentrations and DOC being low during the dry season ($r < 0.4$) and very low during the rainy season ($p > 0.05$). As a consequence, we suggest that the As-DOC complexation may occur as a minor processes and possibly causing $logK_D^{As}$ decrease along the estuary. The As_D distributions presented conservative to non-conservative behavior with slightly subtractive concentrations at mid salinity during both seasons (Fig. 2.4d), which might be caused by the As_D adsorption onto particle phase containing rich (hydr)oxide Fe_p (Lenoble et al. 2013). We also noticed low $LogK_D^{As}$ values at the upstream site during the ebb tide, which could be related to the Sai Gon River inputs containing high As_D. In conclusion, As partitioning in the Can Gio Estuary was affected by both physical and biogeochemical processes, mainly organic matter decomposition.

2.3.3.5 *Copper*

During both seasons, Cu_P varied between 13 to 33 mg kg^{-1} (Fig. 2.4e, supplementary data 2.1 and 2.2) and presented stable values in the estuarine part (5 to 25 salinity), as observed in the East Hainan, China (Fu et al. 2013) and in the Pearl River Estuary, South China (Zhang et al. 2013). A drop of Cu_P was observed between the riverine part (e.g. 43 – 77 mg kg^{-1}, upstream site during the rainy season) and the beginning of the estuary. This loss of Cu_p at the fresh water - estuary interface could be related to intense organic matter degradation processes leading to desorption reaction due to the decomposition of organo-copper complexes; the urban water was characterized by both high POC and Cu_p. The higher $logK_D^{Cu}$ at the upstream site during the monsoon (Fig. 2.4e) confirmed those hypothesis. The Cu_D varied from 0.5 to 0.9 and 0.3 to 1.8 µg L^{-1} during the dry season and the monsoon, respectively, with a high variation range and no clear evolution along the salinity gradient. However, punctual elevated Cu_D at site 2 and site 3 were measured during the monsoon (Fig. 2.4e) and were positively correlated to Fe_D ($r = 0.73$, Fig. 2.5i) possibly suggesting the same sources as for Fe: inputs from adjacent ecosystems. However, these punctual Cu_D inputs did not

seem to affect the Cu partitioning, as evidenced by the stable $\log K_D^{Cu}$ along the estuary (Fig. 2.4e). These results suggest the biogeochemical processes might be minor factors influencing the Cu partitioning in this environment.

2.3.3.6 *Nickel*

The Ni_p distribution along the salinity gradient differed between seasons. During the rainy season, Ni_p varied from 61 to 38 mg kg^{-1}, with stable concentrations in the estuarine part, which were approximately 2–fold lower than in the riverine part (Fig. 2.4f, supplementary data 2.1). At the river end-member, high Ni_p were suggested to be related to the high POC concentrations. Like for Cu, the decrease of Ni_p at the river-estuary interface may result from Ni_p desorption due to organic matter degradation. The Ni_D, varied from 0.3 to 1.8 µg L^{-1} along the estuary with scattered concentrations. The absences of correlations between Ni_D and physico-chemical parameters or TSS or other metals do not allow us to identify the origin of scattered Ni_D concentrations. Log K_D^{Ni} was stable along the salinity gradient, except a slight decrease at the river-estuary interface (Fig. 2.4f), inferring that Ni was poorly reactive in the Can Gio mangrove Estuary during the rainy season. During the dry season, Ni_p slightly decreased along the salinity gradient and dramatically dropped to minimum values at the mouth of the estuary, from 45.6 mg kg^{-1} to 14.4 mg kg^{-1} (Fig. 2.4f, supplementary data 2.1). This phenomena might be induced by the marine dilution, the coastal area of South China Sea containing low Ni_p, 12 mg kg^{-1} (Cenci and Martin 2004). The decrease of Ni_p caused by sea water dilution was previously observed in the Tanshui Estuary, Northern Taiwan (Fang and Lin 2002) and in the East Hainan, China (Fu et al. 2013). The gradual Ni_D decrease during the dry season (1.81 µg L^{-1} to 0.93 µg L^{-1}) from site 1 to site 4 could be also related to sea water dilution, Ni_D were lower than 0.3 µg L^{-1} in the coastal area of South China Sea (Cenci and Martin 2004). This decrease can also be related to co-precipitation of Ni_D and Mn_D onto solid phase (i.e. a positive correlation between Ni_D and Mn_D, r = 0.88, Fig. 2.5j), like

previously observed in the Port Curtis Estuary, Australia (Angel et al. 2010) and in Yangtze River Estuary (Wen et al. 2013). During both seasons, the stability of Log K_D^{Ni} suggests that Ni was poorly reactive in the estuary. The physical mixing was thus the main factor controlling the Ni partitioning in the Can Gio mangrove Estuary.

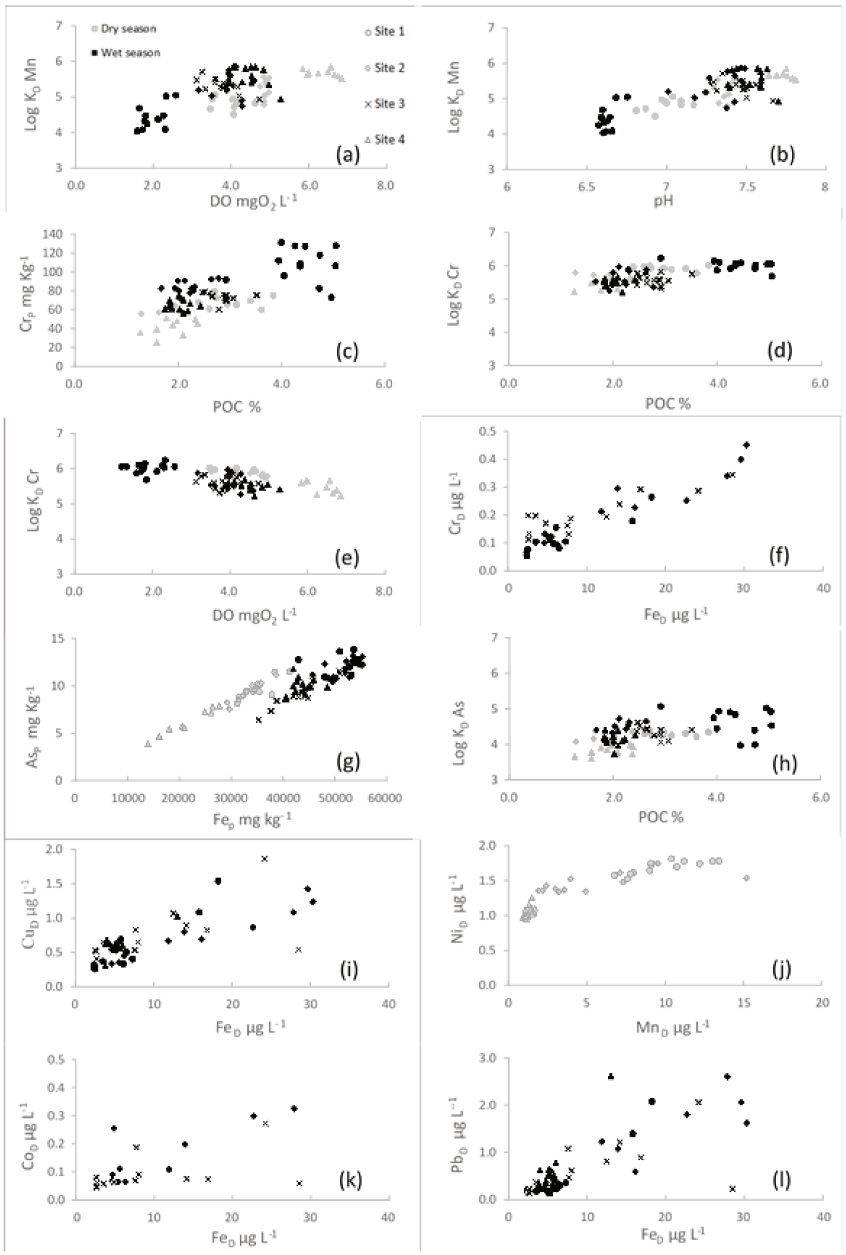

Fig. 2-5. Interrelations between dissolved metal concentrations and relationships between log KD of metal with physico-chemical parameters during the dry and the wet seasons: (a) Log KDMn and DO; (b) Log KDMn and pH; (c) CrD and POC; (d) log KDCr and POC ; (e) log K_D^{Cr} and DO; (f) Cr_D and Fe_D; (g) As_p and Fe_p; (h) LogK_D^{As} and POC; (i) Cu_D and Fe_D; (j) Ni_D and Mn_D; (k) Co_D and Fe_D; (l) Pb_D and Fe_D

2.3.3.7 *Cobalt and lead*

Because of their similar distributions in dissolved, particulate concentrations and partitions along the studied estuary, Co and Pb concentrations are presented and discussed together. The Pb_p presented scattered values close to 21 mg kg^{-1} and 15 mg kg^{-1} during the monsoon and the dry season respectively, while Co_p were varied around 13 mg kg^{-1} for both seasons (Fig. 2.4g and 2.4h, supplementary data 2.1 and 2.2). Those scattered concentrations were often observed in tropical estuaries, like in the Wenchang/Wenjiao River Estuary, East-Hainan, China (Fu et al. 2013) and in the Changjiang Estuary, Eastern China (Wang and Liu 2003). The physico-chemical parameters had a limited effect to Co_p and Pb_p distributions (e.g. no significant correlation with pH, DO or POC), implying that biogeochemical processes have a restricted control on the Co and Pb distribution in the estuary. The Co_D presented baseline concentration close to 0.05 µg L^{-1} during both seasons whereas the Pb_D were closed to 0.3 µg L^{-1} and 0.03 µg L^{-1} and the dry season, respectively, exhibiting a seasonal effect. The higher measured Pb_D during the rainy season might be attributed to intense leaching from mangrove soil (Defew et al. 2005) and/or to Pb enrichment by atmospheric deposition (Hien et al. 1997, Hien et al. 1999). Along the salinity gradient, both Co_D and Pb_D showed non-conservative additive behaviors (Fig. 2.4g and 2.4h), as previously observed in the Mekong delta (Cenci and Martin 2004) and in the Changjiang Estuary, Eastern China (Wang and Liu 2003). Scattered Co_D and Pb_D concentrations were observed at site 2 and site 3 during both flood and ebb tides in the rainy season that suggested similar sources between those metals and Fe_D (significant correlations with Fe_D: r = 0.56 for Co_D and r = 0.77 for Pb_D, Fig. 2.5k and 2.5l). In the Southern Baltic Sea, a significant pore-water discharge along the coastal area was reported to be a source of dissolved Co and Pb (Szymczycha et al. 2016). Log K_D^{Co} and Log K_D^{Pb} were stable and scattered along the estuary during both seasons but not correlated to any physico-chemical parameters, suggesting a poor reactivity (Fig. 2.4g and 2.4h). The scattered Log

K_D^{Co} and Log K_D^{Pb} evidenced thus that the contribution of extra sources played an important role in Co and Pb distributions in the Can Gio Estuary.

2.4. Conclusions

The Can Gio mangrove Estuary is a dynamic environment at the edge between the biggest City in Vietnam and the South China Sea. The water delivered to the estuary during the rainy season was acidic, almost anoxic, and rich in organic matter and in trace metals, evidencing strong anthropogenic pressure on the ecosystem. We suggest that during the monsoon season, heavy rainfall induced increased runoff and soil leaching, resulting in enhanced trace metal inputs to the estuary, both in particulate and dissolved phases. However, as soon as the trace metals enter the estuary, their distribution and partitioning changed due to the physical mixing with seawater and/or biogeochemical processes. The first parameter controlling metal dynamics and transport from Ho Chi Minh City to the South China Sea was the concentration of suspended solids, which can vary as a function of tide and season. Strong correlations were measured between total trace metal concentrations and TSS, whatever the element, but they did not explain the whole variability of trace metal dynamics along the estuary. Organic matter played also a key role on these dynamics. First, we suggest that the elevated inputs of Cu_p, Ni_p and Cr_p were related to the high POC concentrations at the upstream site during the monsoon season. Then, OM decomposition along the estuary resulted in metal release in the dissolved phase, with increasing concentrations with the salinity gradient, specifically for As and Cr. Conversely, concentrations of other dissolved elements decreased along the salinity gradient, either due to water mass mixing, or geochemical processes, which was the case for Mn. Fe, Co and Pb which were poorly reactive during their transit, as evidenced by the absence of any specific correlation between their log K_D and the physico-chemical parameters studied. For the latter metals, water mass mixing was suggested to be the main factor driving their distribution along this mangrove Estuary. Regarding the potential

impacts of extra sources on metal partitioning like: i) pore-waters flushed out from mangrove soils at low tide, ii) runoff from adjacent soils, or iii) shrimp pond effluents, a further detailed investigation should be carried out at sites without freshwater discharge to get a better assessment of their role in trace metals dynamic along the estuary. Furthermore, trace metal geochemistry should be studied in the whole ecosystem (e.g. mangrove soils, trees, animals) and not only in the water column, to understand their potentially bioavailability and ecologically risks.

Table 2-3. Supplementary data 2.1: Original data of dissolved and particulate metal concentrations during the wet season (expressed in µg L^{-1} and mg kg^{-1}, respectively): S1 to S4 showed sampling sites; h0 to h24 are the hours of the 24 h tidal cycling, with a sampling every 2 h.

Site	Label	Mn µg L^{-1}	Fe µg L^{-1}	Cr µg L^{-1}	Co µg L^{-1}	Ni µg L^{-1}	Cu µg L^{-1}	As µg L^{-1}	Pb µg L^{-1}	Mn mg kg^{-1}	Fe mg kg^{-1}	Cr mg kg^{-1}	Co mg kg^{-1}	Ni mg kg^{-1}	Cu mg kg^{-1}	As mg kg^{-1}	Pb mg kg^{-1}
S1	h0	25.2	18.2	0.26	0.12	1.37	1.54	0.36	2.08	436	55237	127.6	13.5	84.1	65.8	12.2	22.5
S1	h2	NA	NA	0.09	0.06	0.56	0.42	0.14	0.46	423	51945	106.3	13.2	82.1	63.9	11.7	23.2
S1	h4	NA	NA	0.09	0.07	0.57	0.48	0.20	0.16	437	53710	105.9	14.4	89.0	76.6	13.8	25.2
S1	h6	18.3	6.50	0.08	0.11	0.88	0.50	0.22	0.29	541	53856	112.0	14.1	74.8	54.2	12.4	22.0
S1	h8	7.92	2.40	0.05	0.03	0.68	0.32	0.11	0.20	822	42951	91.4	16.8	57.3	43.2	12.8	20.0
S1	h10	3.47	2.39	0.06	0.01	0.34	0.27	0.09	0.18	383	44242	72.9	10.5	58.7	47.1	9.5	21.2
S1	h12	27.4	5.82	0.10	0.11	0.93	0.68	0.44	0.41	320	48526	82.5	11.4	73.4	53.0	10.9	20.9
S1	h14	37.5	15.8	0.18	0.16	1.22	1.08	0.46	1.40	404	54572	131.1	14.6	92.8	72.3	12.7	19.6
S1	h16	7.92	2.51	0.08	0.04	0.32	0.26	0.13	0.17	380	48062	95.9	11.4	74.0	57.2	10.9	26.5
S1	h18	16.4	3.54	0.10	0.06	0.57	0.36	0.16	0.18	346	53245	108.8	11.3	78.0	54.7	11.1	18.7
S1	h20	10.4	7.30	0.10	0.50	0.49	0.40	1.39	0.36	306	54602	126.9	12.6	91.4	63.3	12.8	23.5
S1	h22	26.4	5.35	0.11	0.42	0.88	0.63	1.22	0.19	319	52784	117.4	11.5	82.0	57.2	12.0	17.9
S2	h0	2.61	29.6	0.40	NA	1.88	1.42	NA	2.07	744	48120	93.6	18.1	52.3	22.4	12.3	26.2
S2	h2	12.6	5.57	0.12	0.11	0.93	0.35	0.27	0.30	690	45778	84.1	14.8	48.5	22.3	11.2	23.2
S2	h4	10.6	30.3	0.45	NA	1.58	1.23	NA	1.62	839	52234	82.5	17.9	49.0	20.5	12.6	24.3
S2	h6	6.03	27.8	0.34	0.33	1.14	1.09	0.62	2.61	909	55301	90.6	19.6	57.8	23.5	13.1	26.3
S2	h8	5.25	5.43	0.12	0.06	1.04	0.58	0.25	0.60	836	52821	92.2	18.2	55.1	27.8	11.0	28.1
S2	h10	3.35	4.85	0.13	0.25	1.45	0.56	1.15	0.16	922	53590	80.5	18.3	49.0	20.6	13.2	18.6
S2	h12	1.13	22.7	0.25	0.30	1.25	0.86	0.50	1.80	838	53328	82.6	18.3	49.6	20.6	12.6	21.3
S2	h14	1.05	11.9	0.21	0.11	0.93	0.66	0.34	1.23	743	49753	71.9	16.3	41.0	18.0	11.0	24.1
S2	h16	4.07	4.60	0.10	0.07	0.81	0.34	0.33	0.25	841	51957	79.8	16.7	44.5	18.0	11.4	23.3
S2	h18	1.58	6.27	0.10	0.06	0.60	0.45	0.23	0.35	906	54629	90.8	17.4	50.4	20.1	12.2	27.0
S2	h20	7.74	16.1	0.23	NA	1.24	0.69	NA	0.60	824	49309	77.4	17.2	47.4	21.2	10.6	27.8
S2	h22	2.11	4.66	0.13	0.09	1.20	0.55	0.41	0.31	812	50294	76.5	16.4	44.4	18.2	10.8	22.9
S2	h24	1.83	13.9	0.30	0.20	1.14	0.80	0.38	1.07	806	49549	82.4	15.3	42.1	17.0	10.4	22.6
S3	h0	2.07	14.2	0.24	0.08	1.10	0.89	0.35	1.22	513	42993	73.7	15.1	50.6	20.3	8.82	23.0
S3	h2	1.41	7.69	0.13	0.19	0.80	0.83	0.28	0.47	717	50862	78.2	18.4	57.4	20.7	11.6	24.0
S3	h4	2.55	7.99	0.19	0.09	1.17	0.65	0.34	0.61	755	51016	79.0	18.4	61.1	20.6	11.3	24.6
S3	h6	3.30	2.61	0.11	0.05	1.27	0.52	0.37	0.13	559	43635	75.3	15.6	54.0	20.5	9.31	21.2
S3	h8	2.09	16.8	0.29	0.07	1.26	0.82	0.42	0.89	671	45396	78.6	16.8	60.8	19.9	9.89	23.5
S3	h10	2.23	24.2	0.29	0.27	1.17	1.86	0.81	2.06	551	44237	69.1	14.4	45.7	16.8	9.16	21.8
S3	h12	5.52	12.5	0.19	NA	1.31	1.07	NA	0.81	476	41992	72.5	16.1	48.2	17.3	8.92	25.1
S3	h14	2.78	2.67	0.13	0.06	1.26	0.41	0.34	0.22	526	44799	75.4	15.1	51.4	18.4	8.72	21.5
S3	h16	2.93	4.83	0.17	0.06	0.83	0.52	0.32	0.42	528	44188	74.7	15.3	45.7	18.1	8.91	24.7
S3	h18	2.11	3.52	0.20	0.06	1.43	0.65	0.58	0.36	681	45789	76.0	16.9	53.6	19.5	10.5	23.3
S3	h20	2.55	28.5	0.35	0.06	1.41	0.54	0.45	0.23	483	38796	71.0	13.6	47.1	17.0	8.42	23.0
S3	h22	2.18	7.57	0.16	0.07	0.88	0.53	0.36	1.08	424	35276	60.3	11.5	42.0	13.2	6.39	17.7
S3	h24	3.72	2.56	0.20	0.08	1.40	0.53	0.59	0.15	397	37700	72.1	12.0	38.2	15.2	7.35	18.0
S4	h0	3.58	5.16	0.20	0.07	1.28	0.62	0.61	0.51	732	40434	66.5	13.9	43.1	17.6	8.64	14.8
S4	h2	1.83	4.00	0.25	0.06	1.11	0.68	0.75	0.62	716	45898	63.4	15.6	48.2	17.1	10.6	18.3
S4	h6	6.98	5.79	0.24	0.11	1.04	0.55	0.84	0.51	594	44907	61.4	13.4	44.5	18.1	9.86	16.8
S4	h8	3.37	5.07	0.19	0.06	0.86	0.54	0.64	0.52	728	45239	64.8	15.5	48.2	17.7	9.94	18.4
S4	h10	2.97	4.42	0.21	0.06	1.33	0.62	0.68	0.24	778	48608	69.9	16.4	52.4	20.7	9.88	23.5
S4	h12	0.98	3.83	0.16	0.10	0.61	0.30	0.38	0.33	685	43900	66.0	15.4	48.1	18.0	9.53	15.3
S4	h14	1.01	5.14	0.20	0.08	0.93	0.62	1.83	0.64	701	41979	60.3	14.6	43.4	17.3	10.0	15.9
S4	h16	1.02	13.01	0.37	0.07	1.11	1.02	0.83	2.62	697	42647	58.4	14.5	42.2	17.0	10.5	17.7
S4	h18	1.16	4.72	0.19	0.05	1.07	0.56	0.98	0.36	673	40613	56.5	13.8	42.0	15.4	8.84	13.5
S4	h20	2.93	3.90	0.20	0.07	1.40	0.63	0.66	0.26	747	42974	75.1	15.1	47.0	17.8	10.9	22.3
S4	h22	1.25	6.00	0.15	0.04	0.75	0.59	0.48	0.78	786	41993	70.5	17.0	51.8	20.7	11.8	24.8

Table 2-4. Supplementary data 2.2: Original data of dissolved and particulate metal concentrations during the dry season (expressed in µg L^{-1} and mg kg^{-1}, respectively): S1 to S4 showed sampling sites; h0 to h24 are the hours of the 24 h tidal cycling, with a sampling every 2 h.

Site	Label	Mn µg L^{-1}	Fe µg L^{-1}	Cr µg L^{-1}	Co µg L^{-1}	Ni µg L^{-1}	Cu µg L^{-1}	As µg L^{-1}	Pb µg L^{-1}	Mn mg kg^{-1}	Fe mg kg^{-1}	Cr mg kg^{-1}	Co mg kg^{-1}	Ni mg kg^{-1}	Cu mg kg^{-1}	As mg kg^{-1}	Pb mg kg^{-1}
S1	h0	13.0	1.89	0.07	0.07	1.77	0.76	0.44	0.06	NA	NA	NA	NA	NA	NA	NA	NA
S1	h2	10.8	1.36	0.07	0.05	1.69	0.76	0.43	0.02	495	35403	74.8	11.8	36.9	23.1	9.38	13.4
S1	h4	13.5	NA	0.08	0.07	1.78	0.77	0.47	0.03	429	32861	69.1	10.5	31.0	23.4	9.41	14.7
S1	h6	7.95	1.17	0.07	0.06	1.61	0.69	0.49	0.03	524	34251	60.8	12.0	33.8	19.4	9.87	12.8
S1	h8	6.76	1.21	0.08	0.05	1.57	0.65	0.50	0.02	449	31550	65.7	10.4	35.8	25.5	8.82	19.5
S1	h10	7.60	1.01	0.08	0.04	1.52	0.69	0.54	0.01	NA	NA	NA	NA	NA	NA	NA	NA
S1	h12	12.2	1.42	0.08	0.07	1.74	0.69	0.50	0.01	1054	37869	72.0	12.1	42.5	32.5	9.05	29.2
S1	h14	9.12	1.20	0.07	0.05	1.71	0.73	0.50	0.02	1026	38398	67.6	14.1	41.2	24.6	11.5	19.4
S1	h16	11.2	1.03	0.08	0.05	1.77	0.72	0.48	0.01	1032	41327	79.2	14.8	45.6	27.4	11.5	17.8
S1	h18	10.4	2.12	0.09	0.05	1.81	0.91	0.46	0.05	780	35496	71.9	12.4	39.1	23.0	10.1	21.4
S1	h20	9.02	1.85	0.08	0.06	1.64	0.70	0.53	0.02	763	34044	65.2	12.1	35.4	21.0	9.57	13.5
S1	h22	7.79	1.20	0.08	0.05	1.59	0.72	0.52	0.01	NA	NA	NA	NA	NA	NA	NA	NA
S1	h24	9.12	4.72	0.10	0.05	1.74	0.73	0.50	0.04	467	31182	59.7	10.4	30.5	22.0	8.16	14.6
S2	h0	3.01	8.76	0.12	0.23	1.38	0.77	0.73	0.15	NA	NA	NA	NA	NA	NA	NA	NA
S2	h2	2.39	9.83	0.12	0.11	1.42	0.76	0.72	0.08	812	34278	64.6	12.7	33.2	18.1	9.30	14.0
S2	h4	3.57	NA	0.11	0.09	1.36	0.58	0.71	0.06	802	34096	57.4	12.2	33.4	17.4	10.0	14.4
S2	h6	3.21	2.36	0.10	0.30	1.33	0.55	0.61	0.04	816	35027	58.8	16.2	33.8	17.5	10.2	15.0
S2	h8	4.93	3.27	0.09	0.20	1.33	0.61	0.63	0.02	663	29655	55.9	11.0	28.8	15.9	7.53	16.7
S2	h10	1.94	2.70	0.09	0.15	1.35	0.73	0.71	0.11	NA	NA	NA	NA	NA	NA	NA	NA
S2	h12	2.16	3.25	0.09	0.11	1.35	0.69	0.69	0.04	766	32928	56.1	11.7	31.2	18.5	9.40	13.8
S2	h14	NA	7.50	0.09	0.25	1.50	0.58	0.61	0.03	606	32294	55.5	10.7	30.8	16.5	8.96	12.5
S2	h16	7.31	3.37	0.09	0.13	1.47	0.62	0.62	0.07	806	35839	59.4	13.0	0.00	18.5	10.3	16.9
S2	h18	15.2	4.56	0.11	0.14	1.53	0.64	0.68	0.05	911	38689	76.4	13.8	38.6	19.6	11.1	14.8
S2	h20	9.54	2.42	0.07	0.09	1.74	0.70	0.60	0.03	716	29197	50.2	10.4	28.6	15.5	8.24	11.5
S2	h22	7.13	2.61	0.10	0.09	1.60	0.64	0.63	0.03	NA	NA	NA	NA	NA	NA	NA	NA
S2	h24	3.96	2.41	0.09	0.08	1.52	0.59	0.69	0.03	783	34467	66.2	12.1	33.4	16.3	9.57	12.7
S3	h2	NA	NA	NA	NA	NA	NA	NA	NA	650	31525	57.1	11.4	33.1	16.7	8.64	13.1
S3	h4	NA	NA	NA	NA	NA	NA	NA	NA	754	34692	59.1	12.4	34.5	17.7	9.16	13.1
S3	h6	NA	NA	NA	NA	NA	NA	NA	NA	686	32459	69.2	11.6	33.3	17.4	8.24	13.5
S3	h8	NA	NA	NA	NA	NA	NA	NA	NA	499	24761	46.2	8.34	26.3	13.4	6.66	10.1
S3	h12	NA	NA	NA	NA	NA	NA	NA	NA	674	30284	53.4	10.9	30.6	15.2	8.28	11.6
S3	h14	NA	NA	NA	NA	NA	NA	NA	NA	581	28277	53.2	9.67	28.6	15.4	7.99	11.4
S3	h16	NA	NA	NA	NA	NA	NA	NA	NA	527	26269	48.9	8.92	29.3	14.5	7.10	13.6
S3	h18	NA	NA	NA	NA	NA	NA	NA	NA	642	30459	57.9	10.7	30.6	18.2	8.20	12.9
S3	h20	NA	NA	NA	NA	NA	NA	NA	NA	415	30826	57.5	10.4	31.8	15.7	7.11	12.2
S3	h24	NA	NA	NA	NA	NA	NA	NA	NA	695	32849	57.6	11.5	32.0	16.5	9.17	12.9
S4	h0	1.22	4.25	0.12	0.10	0.97	0.61	0.94	0.07	NA	NA	NA	NA	NA	NA	NA	NA
S4	h2	1.23	5.69	0.15	0.06	1.00	0.70	0.99	0.05	406	13917	25.4	NA	14.4	22.8	3.88	6.60
S4	h4	0.93	2.08	0.12	0.05	0.97	0.62	1.00	0.02	466	16124	35.4	NA	16.6	22.4	4.67	9.06
S4	h6	1.46	1.36	0.20	0.04	1.10	0.70	0.95	0.04	617	20548	39.3	NA	23.5	20.6	5.74	17.1
S4	h8	1.55	5.31	0.13	0.05	1.02	0.82	0.93	0.04	584	18027	33.1	NA	19.2	26.7	5.45	13.8
S4	h10	1.63	2.84	0.11	0.06	1.04	0.74	0.99	0.09	NA	NA	NA	NA	NA	NA	NA	NA
S4	h12	1.50	3.96	0.25	0.05	1.01	0.57	1.05	0.14	682	20970	45.2	NA	19.7	24.4	5.52	18.2
S4	h14	1.70	6.25	0.11	0.05	1.10	0.61	0.95	0.04	738	26396	50.9	NA	24.2	19.7	7.79	0.00
S4	h16	1.31	2.91	0.13	0.05	1.15	0.64	0.87	0.02	805	31430	49.7	NA	33.8	17.3	8.58	13.8
S4	h18	1.49	2.98	0.10	0.06	1.25	0.69	0.83	0.13	694	26159	44.7	NA	25.2	19.4	7.17	14.2
S4	h20	1.06	1.92	0.11	0.04	1.08	0.65	0.83	0.05	747	27720	47.8	NA	25.8	16.8	7.88	13.1
S4	h22	1.14	4.22	0.11	0.05	0.93	0.63	1.00	0.03	NA	NA	NA	NA	NA	NA	NA	NA
S4	h24	1.09	1.72	0.11	0.04	0.98	0.67	1.06	0.04	707	24921	43.8	NA	28.9	18.2	7.29	16.1

Chapter 3 - Trace metal geochemistry and ecological risks in a tropical mangrove

Highlights:

- Trace metals geochemistry was studied in the sediment of the Can Gio mangrove forest
- The residual fraction was the major geochemical phase of trace metals
- Trace metals partitioning was strongly linked to organic matter cycling.
- Most of estimated trace metal stocks presented higher values in the *Avicennia* stand
- Trace metals presented low ecological risks to the ecosystem, except Mn, Ni and As

Keywords: Sequential extraction; Metal geochemistry; Partitioning; Ecological risk; Vietnam.

ABSTRACT

Mangrove sediments can act as natural biogeochemical reactors, modifying trace metals partitioning after their deposition. The objectives of this study were i) to determine the distribution and partitioning of some trace metals (Fe, Mn, Ni, Cr, Cu, Co and As) in sediments and pore-waters of the Can Gio mangrove, which is located at the edge of a megacity (Ho Chi Minh City, Vietnam), and ii) to assess their ecological risks to mangrove ecosystem based on the Risk Assessment Code (RAC). Three cores were collected from the tidal creek to inner mangrove, i.e. within a mudflat, beneath an *Avicennia alba* stand and beneath a *Rhizophora apiculata* stand. We suggest that metals had a natural origin, being deposited in the mangrove mainly as oxihydroxides coming from the upstream lateritic soils. However, the enrichment of mangrove-derived organic matter from the mudflat to the *Rhizophora* stand played a key role in controlling the studied metals partitioning. We suggest that reductive dissolution of Fe-Mn oxihydroxides by bacteria for organic matter decay processes may be a major source of dissolved trace metals in pore-waters. Subsequently, these metals co-precipitated with organic compounds, sulphides or carbonates. Despite of the increasing trend of metals concentrations in bioavailable fractions towards the inland forest, only Mn exhibited a potential high risk to the ecosystem, and possibly Ni and As due to their elevated concentrations in pore-waters. Most of estimated trace metals stocks in the sediments were higher in the *Avicennia* stand than the *Rhizophora* and the *mudflat* with the exception of Fe and As, which presented higher values in the mudflat.

3.1. Introduction

Rapid demographic increase and industrial developments have induced serious environmental degradations, including the accumulation of organic and inorganic pollutants in coastal and estuarine ecosystems. Due to their specific characteristics, e.g. their richness in fine particles and in organic matter, and the occurrence of sulfate-reduction processes, mangrove sediments can act as natural sinks for trace metals originating from natural and anthropized watersheds (Clark et al. 1998, Marchand et al. 2011a, Tam and Wong 1996). In contrast to organic pollutants, metals cannot be chemically or biologically degraded. Within mangrove sediments, trace metals are either adsorbed or precipitated with different bearing phases such as carbonate, organic matter, sulphide, iron–manganese oxide-hydroxides, etc. (Tam and Wong 1996). However, mangrove sediments are highly reactive systems, and due to depth or seasonal evolutions of the redox conditions, pH, salinity, organic matter, etc., bearing phases can be dissolved, releasing trace metals in pore-waters and increasing their bioavailability (Marchand et al. 2016). Trace metals can subsequently re-precipitate with another bearing phase (Noël et al. 2014) or be transferred to adjacent ecosystems (Holloway et al. 2016, Sanders et al. 2012) or mangrove living organisms (trees, fishes, crabs, snails, etc.) (De Wolf and Rashid 2008, Parvaresh et al. 2011). To date, mangroves are being destroyed at a rate close to 1 % per year (Duke et al. 2007), notably for implanting shrimp farming activities. The destruction of mangrove forests can generate sediment perturbation and their oxidation, inducing the dissolution of sulfide minerals, which can result in sediment acidification and trace metal release into the environment (Dent 1986). Furthermore, mangrove ecosystems provide many ecosystems services for the local populations of the (sub)tropical coastlines, being notably a famous fishing area (Lee et al. 2014). Thus, understanding the fate of trace metals in mangrove ecosystems is also highly relevant for human health.

In Vietnam, large mangrove areas were devastated by herbicide mixture during the war in the 70's. Can Gio mangrove was one of the most heavily sprayed areas. Mangrove restoration efforts have been realized and almost 40 years after, the rehabilitated mangrove is now more diverse in community structure than prior the war (Hong 2001). The mangrove forest is now largely dominated by the *Rhizophora apiculata* species, with fringing by mainly *Avicennia alba* toward tidal creek and the sea. The Can Gio mangrove is located downstream of Ho Chi Minh City, the economic capital of Vietnam with almost 10 million inhabitants. Mangrove river network acts as a unique gate for water outlet from Ho Chi Minh City to the South China Sea. Industrial activities, economic development and rapid population growth are inducing high pressure on water and sediment quality. However, Strady et al. (2017a) stated that the main rivers and canals in the city were moderately contaminated by major metal(oid)s. Recently, Thanh-Nho et al. (2018) highlighted that trace metals can be transferred over long distance from the downstream Ho Chi Minh City to the mangrove forest, and that during the monsoon season, heavily rainfall induced enhanced runoff and soil leaching, resulting in elevated trace metals inputs in the estuary. Consequently, taking into account the mangrove specific geochemical characteristics, the lack of treatment plants in emerging countries as Vietnam and the fishing activities in mangrove waters, more attention should be paid on trace metals distributions, speciation, bioaccumulation and transfer in mangrove ecosystems.

Within this context, our objectives were: *i)* to investigate the geochemistry of some trace metals (Fe, Mn, Ni, Cr, Cu, Co and As) in the sediment of the Can Gio planted mangrove forest, beneath the two main species: *Rhizophora* and *Avicennia*, and in the adjacent mudflat; *ii)* to assess the potential ecological risks of these trace metals on mangrove ecosystem. We hypothesize that

metals distribution and speciation will vary with depth and between zones because of different organic content and different redox condition, influencing their bioavailability.

3.2. Materials and methods

3.2.1. Study site

The Can Gio mangrove (approximately 35,000 ha, extending from 10º22'-10º44'N and 106º46'-107º01'E (Tuan and Kuenzer 2012)) is located in the south of Vietnam at the downstream part of the Sai Gon and Dong Nai Rivers watershed and in the South China Sea coastal zone (Fig. 3.1). It is a Biosphere Reserve of UNESCO since 2000 and it is also a well-known example of "mangrove afforestation and reforestation area'' (Blasco et al. 2001). The Can Gio mangrove is home to more than 20 mangrove species with two dominant ones: *Rhizophora apiculata* and *Avicennia alba* (Luong et al. 2015), and 200 species of fauna (e.g. amphibians, fishes, benthic organisms, etc.). The main economic activities of the local people are forest management, aquaculture, fishing and salt production (Kuenzer and Tuan 2013). The Can Gio mangrove is subject to the typical tropical monsoon climate, with two distinct seasons. The dry season lasts from November to April and the monsoon season from May to October. The annual mean precipitation is about 1,300 to 1,400 mm, with ~ 90 % of the precipitation falling during the wet season and the annual mean temperature ranges from 26.5 °C to 30 °C. It is also subject to a semi-diurnal tidal regime. The topography of the Can Gio mangrove is generally low-lying. The sediment is composed of alluvial deposits derived from upstream of the Sai Gon and Dong Nai Rivers (Luong 2011).

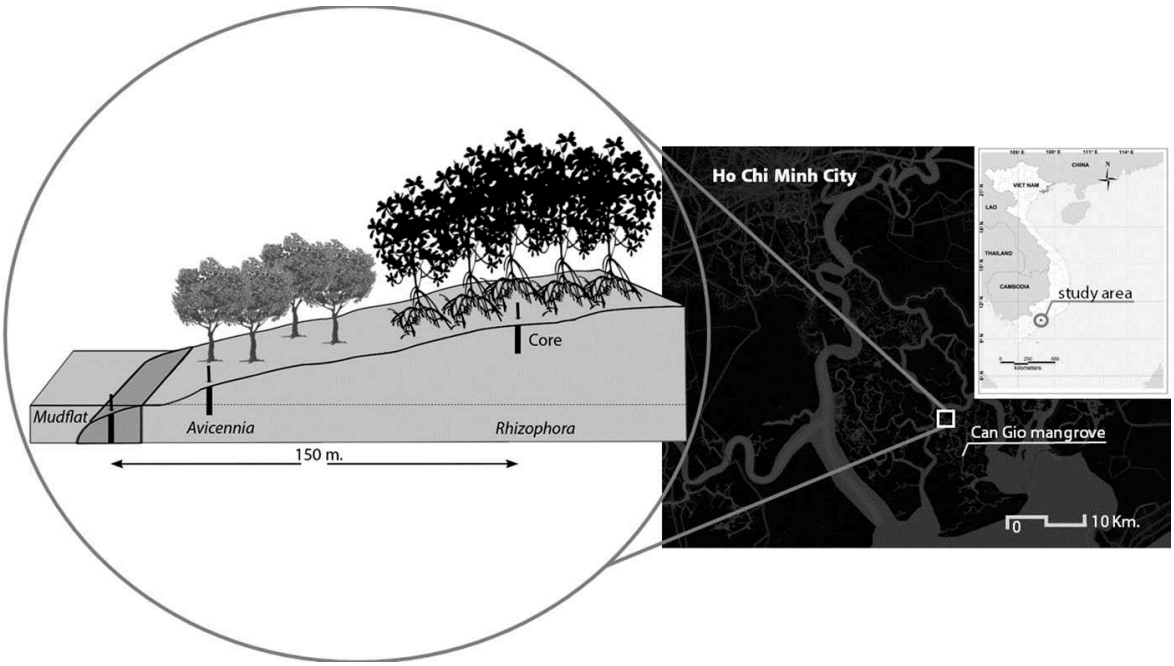

Fig. 3-1. Location of Can Gio mangrove and collected samples. Three cores (90 cm depth) were collected in the mudflat, beneath the Avicennia and the Rhizophora stands.

3.2.2. Sample collections and preservations

Sampling was carried out in the core zone of the Can Gio mangrove during the monsoon season (October 2016). Three cores (90 cm depth) were collected with an Eijkelkamp gouge auger at low tide in the mudflat (lower elevation than the mangrove stands), beneath an *Avicennia alba* stand and a *Rhizophora apiculata* stand (Fig. 3.1). Cores were immediately sectioned into 10 samples: every 5 cm from the surface to 30 cm depth, every 10 cm from 30 to 50 cm depth, and every 20 cm from 50 to 90 cm depth. Samples were stored in polythene bags, stored in a cooler box for their transfer to the laboratory and were then preserved frozen (-20 °C) until drying. Dried samples were grinded using an agate pestle and mortar, and sieved using 100 µm pore size for sequential extraction of trace metal fractions and for total organic carbon (TOC) analysis.

For dissolved metal analysis, pore-waters were extracted on the day of coring with soil moister sampler Rhizon®, which were directly inserted into the center of the cores (Marchand et al. 2012). All samples were then filtered through 0.45 µm Sartorius® filter membranes and acidified to pH <

2 by Suprapur® concentrated HNO_3 (Merck). The samples were then preserved in cleaned 14 ml polypropylene tubes at 4 °C until analysis.

3.2.3. Analytical methods and calculations

3.2.3.1 Salinity, pH and redox measurements

Additional cores beneath each mangrove stand and in the mudflat were collected to measure salinity, pH and redox. These parameters were measured in-situ. Salinities were determined using an ATAGO refractometer (S-10, Japan) after extracting a drop of pore-water from each sediment layer. pH was measured using a glass electrode (pH 3110-WTW), which was pre-calibrated using pH 4, 7 and 10 standard buffer solution (NIST scale). Redox potential was measured using digital voltmeter with Pt and Ag/AgCl (reference) electrode connected to pH/mV/T meter (pH100-YSI), which was periodically checked using 0.43V standard solution and deionized water. Redox data are reported relative to a standard hydrogen electrode i.e. after adding 194 mV to the original mV values obtained with an Ag/AgCl (reference electrode) at 30 °C. The redox scale was fully described by Marchand et al. (2011a), as follows: (i) oxic > 400 mV, containing measurable dissolved oxygen; (ii) 100 mV < suboxic < 400 mV, with a lack of measurable oxygen or sulfide, containing dissolved iron or manganese, with no reduction of sulfate; (iii) anoxic < 100 mV, with sulfate reduction.

3.2.3.2 Metal concentrations in pore-waters

Dissolved Fe, Mn, Ni, Cr, Cu, Co and As concentrations were directly measured by Thermo Scientific iCAPQ ICP-MS with a Kinetic Energy Discrimination-Argon Gas Dilution module (KED - AGD mode) (Kutscher et al. 2014) using internal standard calibration (AETE-ISO platform, OSU-OREME/Université de Montpellier). Accuracy and precision were controlled using the certificate reference material SLEW-3 (Table 3.1a).

Table 3-1. Quality control of analytical methods applied for dissolved and total metal concentrations analysis: a) accuracy, precision and detection limit using estuarine water SLEW-3; b) BCR-277R for wet digestion method.

a) Dissolved metal concentration analysis.

Element	*Detection limit ($\mu g\ L^{-1}$)*	*Certificated values ($\mu g\ L^{-1}$)*	*Measured values ($\mu g\ L^{-1}$)*	*Recovery (%)*	*Relative standard deviation (%)*
Fe	0.031	0.568 ± 0.059	0.661 ± 0.073	116	11
Mn	0.013	1.61 ± 0.22	1.469 ± 0.016	91	1
Ni	0.011	1.23 ± 0.07	1.230 ± 0.014	100	1
Cr	0.022	0.183 ± 0.019	0.0182 ± 0.020	99	11
Cu	0.011	1.55 ± 0.12	1.491 ± 0.041	96	3
Co	0.0092	0.042 ± 0.010	0.0464 ± 0.0025	110	5
As	0.0062	1.36 ± 0.09	1.569 ± 0.013	115	1

b) Total metal concentration analysis

Element	Certificated values ($mg\ kg^{-1}$)	Measured values ($mg\ kg^{-1}$, n = 9)	Recovery (%)	Relative standard deviation (%)	Analytical method
Fe	NA	50,843 ± 3029	-	5.8	FAAS
Mn	NA	897 ± 37	-	4.2	FAAS
Ni	130 ± 8	125.9 ± 6.1	96.9	4.9	ICP-MS
Cr	188 ± 14	179.9 ± 16.1	95.7	9.0	ICP-MS
Cu	63 ± 7	58.9 ± 4.6	93.6	7.9	ICP-MS
Co	22.5 ± 1.4	23.1 ± 1.7	102.6	7.5	ICP-MS
As	18.3 ± 1.8	18.1 ± 1.5	98.9	8.2	ICP-MS

3.2.3.3 Total metal concentrations in sediments

Total Fe, Mn, Ni, Cr, Cu, Co and As concentrations were digested using 10 mL of concentrated HNO_3/HCl/HF (3:1:1 = *v/v*) in polytetrafluoroethylene (PTFE) vessel at 110 ^{o}C for 48h. After cooling, 2 mL of concentrated HNO_3 (n = 2) was added into these samples for eliminating residual HF. For each adding, the solution were evaporated near to dryness at 160 ^{o}C. The samples were filtrated and adjusted using deionized water into 25 mL, and were then stored in pre-cleaned polypropylene (PP) tubes at 4 ^{o}C until analysis.

The analytical precision and accuracy were insured by analyzing certificate reference material estuarine sediment (BCR-277R). The quantification of Fe and Mn concentrations were performed by Flame Atomic Absorption (Shimadzu AA-6650) while the other metals (Co, Ni, Cu, As and Cr) were analyzed by ICP-MS (Agilent 7700x) using spiked ^{103}Rh and ^{197}Au as internal standard (Table 3.1b). Certificate reference material (BCR-277R) were always intercalated in each batch of sample digestion for controlling the analytical method. All reagents were purchased from analysis grade (Merck) and all the containers were de-contaminated by soaking in 5 % nitric acid for 24 h and rinsed in deionized water.

3.2.3.4 Sequential extraction of metal chemical fractions

To evaluate the geochemistry and availability of trace metals (Fe, Mn, Ni, Cr, Cu, Co and As) in these sediment cores, a sequential extraction procedure was carried out based on the method developed by Tessier et al. (1979) and Ure et al. (1993). Each element was divided into four operationally-defined geochemical fractions: exchangeable/carbonate fraction (acid-soluble phase), Fe – Mn oxides fraction (reducible phase), organic fraction (oxidizable phase) and a residual fraction. Briefly, the various single extractions were performed as following: 1 g of fine dry sediments were put into 50 mL PP tubes with caps, which were also used for shaking time and centrifugation to minimize the possible loss in the centrifuge – washing step. For the determination of the acid-soluble fraction (F1), we used 8 mL of 1M buffer acidic solution (CH_3COOH/CH_3COONH_4, pH = 5) at room temperature during 5 h; for the reducible fraction (F2), we used 20 mL of 0.04 M $NH_2OH.HCl$ in 25 % CH_3COOH (*m/v*) at 96 ºC during 6 h; for the oxidizable fraction (F3), we used 3 mL of 0.02 M HNO_3 and 8 mL of 30 % H_2O_2. 5 mL of 3.2 M CH_3COONH_4 was added into the solution to prevent reabsorb of those metals onto particles

surface; for the residual fraction (F4), it was digested according to the same procedure described above for total metals analysis.

3.2.3.5 Total organic carbon (TOC)

TOC analysis were carried out on a Shimadzu® TOC-L series analyzer combined with a solid sample module (SSM-5000A) heating at 900 ^{o}C. Glucose standard (40 %, Sigma Aldrich) was used for calibrations. Repeated measurements of the standards at different concentrations indicated a measurement deviation < 2 %.

3.2.3.6 Sediment bulk density and trace metal stock estimation

The bulk density is defined as the ratio of dry sediment mass to sediment volume (including pore space). Bulk density is typically expressed in g cm^{-3}. To calculate the sediment bulk density in the present study, subsamples of known volume in the mudflat, the *Avicennia* and *Rhizophora* stands were collected and dried to a constant weight.

To compare trace metal stocks in the Can Gio mangrove sediments to those measured in the literature, we determined them to a depth of 50 cm depth using the following equation:

$$\text{Metal Stock (t ha}^{-1}) = (C_{sediment} * BD * 50 * 100)/10^6$$

where, $C_{sediment}$: mean trace metal concentration in the upper 50 cm (mg kg^{-1})

BD: mean bulk density in the upper 50 cm (g cm^{-3})

50: length of the core used for estimation of trace metal stock (cm)

100: conversion factor from g cm^{-2} to t ha^{-1}

10^6: conversion factor of a metal concentration in mg kg^{-1}

3.2.3.7 Data analysis

The Pearson correlation coefficients were performed using statistical package software (SPSS: version 23) to identify major relationships between metal concentrations and physico-chemical parameters as well as interrelationships between metals together.

3.3. Results

3.3.1. Physico-chemical parameters in the sediment cores

The depth evolution of pH, redox potential (Eh), salinity and total organic carbon (TOC) in the mudflat and the mangrove stands are presented in Fig. 3.2. pH was stable with depth whatever the sites, being lower in the *Avicennia* stand (5.6 to 6.0) than in the *Rhizophora* stand (6.5 to 6.8) and in the mudflat (6.8 to 7.1) (Fig. 3.2a). Eh distributions and values differed in the three environments. The mudflat was characterized by anoxic conditions in whole core, ranging between 73 mV and -88 mV. The sediment beneath mangroves stands were characterized from suboxic to anoxic conditions toward the bottom of the cores. In the *Avicennia* stand, Eh values decreased from 254 mV at the top of the core to 43 mV at 30 cm depth, and then slightly increased without being higher than 140 mV. In the *Rhizophora* stand, redox values decreased from the top of the core (224 mV) to 20 cm depth (- 90 mV) and then fluctuated between of -20 mV to -115mV (Fig. 3.2b). Salinity increased with depth in the three cores with similar distribution patterns, from 14 to 22 (Fig. 3.2c). TOC contents vary with depth in the mudflat (from 2.7 % to 2.1 %) and in the *Avicennia* stand (from 2.8 % to 2.3 %) without specific distributions patterns (Fig. 3.2d), while in the *Rhizophora* stand TOC concentrations decreased with depth (from 4.62 % to 2.1 %).

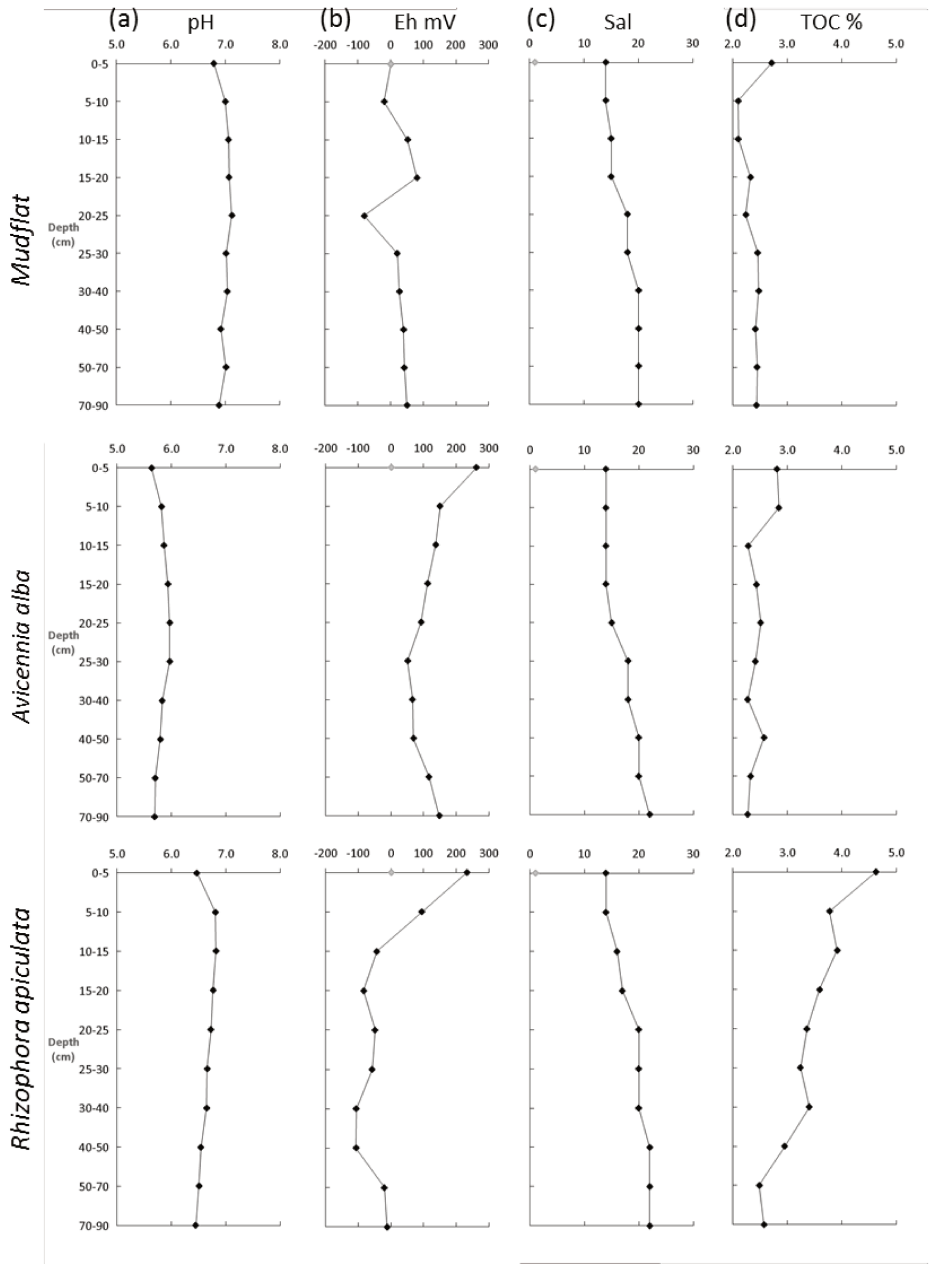

Fig. 3-2. Depth distribution of (a) pH, (b) Eh, (c) Salinity and (d) Total organic carbon in the mudflat, the Avicennia stand and the Rhizophora stand in the Can Gio mangrove.

3.3.2. Total metal concentrations in the sediment cores

The depth's distribution of total metal concentrations (Fe, Mn, Ni, Cr, Cu, Co and As) measured in the mudflat, the *Avicennia* stand, the *Rhizophora* stand and their calculated mean concentrations are presented in Table 3.2. Total Fe concentrations did not vary with depth in the three environments. The mean total Fe concentrations over depth presented decreasing mean

values from the mudflat to the mangrove stands (i.e. mean concentration of 53,110 ± 1,423 mg kg^{-1}, 49,335 ± 2,198 mg kg^{-1} and 46,079 ± 2,371 mg kg^{-1} in the mudflat, the *Avicennia* stand and the *Rhizophora* stand, respectively). The distribution of total Mn concentrations decreased with depth in each environment, from 653 mg kg^{-1} to 310 mg kg^{-1} in the mudflat, from 800 mg kg^{-1} to 227 mg kg^{-1} in the *Avicennia* stand and from 350 mg kg^{-1} to 160 mg kg^{-1} in the *Rhizophora* stand. Total Ni and Cr concentrations did not vary with depth in the three environments but their mean concentrations in each core evidenced higher mean values in the *Avicennia* and *Rhizophora* stands than in the mudflat. Total Co concentrations presented similar distribution between environments, being stable in the upper horizons from 0 to 40 cm depth and then increasing to reach a maximum values of 24.2 mg kg^{-1}, 29.7 mg kg^{-1} and 25.8 mg kg^{-1} in the mudflat, the *Avicennia* stand and the *Rhizophora* stand respectively. Finally, total As and Cu concentrations did not present any specific vertical distributions pattern, and their mean concentrations were similar in all environments (between 11.6 and 14.9 mg kg^{-1} for As and between 16.7 and 20.6 mg kg^{-1} for Cu).

3.3.3. Trace metal stock estimation

The estimated stock of metals down to 50 cm depth differed between the mangrove stands and the mudflat (Table 3.3). The estimated Fe stock presented decreasing values from the mudflat (169.2 ± 4.2 t ha^{-1}) to the inner mangrove (i.e. the *Rhizophora* stand, 126.4 ± 6.2 t ha^{-1}). Conversely, the estimated stock of Mn was higher beneath the *Avicennia* stand (1.62 ± 0.57 t ha^{-1}) than in the mudflat (1.44 ± 0.41 t ha^{-1}) and was even lower in the *Rhizophora* stand (0.74 ± 0.12 t ha^{-1}). Except As stock, which was higher in the mudflat, the estimated stocks of Co, Ni, Cr and Cu showed higher values in the *Avicennia* stand than in the *Rhizophora* zone and in the mudflat. They varied (expressed in t ha^{-1}) from 0.16 ± 0.004 to 0.19 ± 0.01 for Ni, from 0.25 ± 0.01 to 0.29 ± 0.003 for Cr, and from 0.053 ± 0.003 to 0.057 ± 0.002 for Cu, from 0.060 ± 0.004 to 0.067 ± 0.010 for Co, from 0.035 ± 0.005 to 0.045 ± 0.008 for As.

Table 3-2. Depth distribution of total metals concentrations (Fe, Mn, Ni, Cr, Cu, Co and As) in the mudflat, the Avicennia stand and the Rhizophora stand, expressed in mg kg^{-1}.

Stand	Depth (cm)	**Fe**	**Mn**	**Ni**	**Cr**	**Cu**	**Co**	**As**
Mudflat	0-5	53,711	653	54.3	95.5	17.1	19.5	12.7
	5-10	50,864	567	48.2	83.6	15.7	18.2	13.1
	10-15	52,382	560	49.9	81.4	15.4	18.7	12.2
	15-20	52,049	438	49.4	86.1	16.0	18.4	13.4
	20-25	51,827	388	48.2	83.3	15.7	18.5	11.9
	25-30	53,368	350	52.0	87.4	16.7	19.4	13.7
	30-40	54,404	338	53.6	86.2	17.4	21.6	16.7
	40-50	54,478	310	56.8	89.4	18.1	23.7	18.9
	50-70	55,526	316	58.6	87.7	17.2	24.2	13.5
	70-90	52,851	310	56.3	85.6	16.9	22.5	12.4
	Mean	*53,110*	*369*	*52.8*	*86.1*	*16.8*	*19.5*	*13.2*
	SD	*1423*	*126*	*3.8*	*3.9*	*0.9*	*2.3*	*2.2*
Avicennia alba	0-5	52,590	800	61.1	97.3	17.9	21.6	11.2
	5-10	50,314	643	59.3	96.5	18.7	21.7	13.4
	10-15	50,843	473	62.1	95.3	17.9	21.1	11.7
	15-20	47,228	458	64.0	96.2	18.3	22.0	10.6
	20-25	50,044	728	61.3	94.8	18.8	21.3	11.3
	25-30	51,427	543	61.6	94.0	18.6	19.8	11.8
	30-40	45,054	338	61.5	96.6	18.5	19.2	9.0
	40-50	48,358	256	69.2	94.9	19.4	29.7	13.8
	50-70	48,627	236	62.6	92.4	18.0	26.3	12.1
	70-90	48,575	227	62.7	95.5	19.0	22.8	11.6
	Mean	*49,335*	*465*	*61.9*	*95.4*	*18.6*	*21.7*	*11.6*
	SD	*2,198*	*208*	*2.6*	*1.4*	*0.5*	*3.1*	*1.3*
Rhizophora apiculata	0-5	45,554	231	60.4	88.7	20.7	21.6	13.3
	5-10	49,517	263	59.4	93.0	20.7	21.3	14.9
	10-15	48,695	302	60.2	93.3	20.6	22.9	14.9
	15-20	52,187	317	59.6	93.1	20.1	22.0	18.4
	20-25	46,128	253	59.5	98.9	20.1	22.3	12.1
	25-30	47,628	350	60.7	93.5	19.8	22.7	14.5
	30-40	45,773	297	60.9	98.8	21.2	23.2	13.8
	40-50	46,030	219	63.5	100.8	21.6	25.8	16.9
	50-70	44,512	166	63.6	95.8	20.0	25.7	14.9
	70-90	45,334	160	63.5	102.0	22.6	24.8	17.6
	Mean	*46,079*	*258*	*60.5*	*94.7*	*20.6*	*22.8*	*14.9*
	SD	*2,371*	*63*	*1.7*	*4.2*	*0.9*	*1.6*	*2.0*

Table 3-3. Trace metals stocks in the sediments of the mudflat, the Avicennia stand and the Rhizophora stand in Can Gio mangrove (expressed in t ha-1, values were obtained based on the mean metal concentration and bulk density of each core on 50 cm depth). The stocks of each metal beneath Avicennia and Rhizophora stands were compared with those measured in the mudflat (%).

Stand	Bulk density ($g\ cm^{-3}$)	Fe	Mn	Ni	Cr	Cu	Co	As
Mud flat	0.64	169.2 ± 4.2	1.44 ± 0.41	0.16 ± 0.01	0.28 ± 0.01	0.053 ± 0.003	0.063 ± 0.006	0.045 ± 0.008
Avicennia	0.61	150.9 ± 7.5	1.62 ± 0.57	0.19 ± 0.01	0.29 ± 0.003	0.057 ± 0.002	0.067 ± 0.010	0.035 ± 0.005
(% mud flat)		89	112	116	105	107	106	79
Rhizophora	0.53	126.4 ± 6.2	0.74 ± 0.12	0.16 ± 0.004	0.25 ± 0.01	0.055 ± 0.002	0.060 ± 0.004	0.039 ± 0.005
(% mud flat)		75	51	97	91	103	95	87

3.3.4. Metal partitioning in mangrove sediments

The metals (Fe, Mn, Ni, Cr, Cu, Co and As) partitioning in each sediment core layer collected in the mudflat, the *Avicennia* stand and the *Rhizophora* stand is determined based on their concentrations in the exchangeable/carbonate fraction (F1), the oxides fraction (F2), the organic fraction (F3) and the residual fraction (F4). Their respective percentage in each phase are evaluated based on their total concentrations (sum of metal concentrations in the four fractions) (Fig. 3.3).

3.3.4.1 Fe and Mn

The partitioning of Fe and Mn presented different vertical distribution according to environments. In the mudflat and in the *Avicennia* stand, the partitioning was F4 > F2 > F3 ~ F1 (Fig. 3.3a) whereas for Mn it was: F4~ F1 > F2 > F3 (Fig. 3.3b). Fe in F4 was stable with depth, representing 72 % in the mudflat and 78 % in the *Avicennia* stand, whereas Mn in F4 increased with depth, from 22 % to 38 % in the mudflat and from 18 % to 62 % in the *Avicennia* stand. Mn was characterized by an important exchangeable/carbonate fraction, which decreased from 42 % to 27 % in the mudflat and from 51 % to 22 % in the *Avicennia* stand. F2 of both Fe and Mn decreased with depth in the mudflat and in the *Avicennia* stand, respectively from 20 % to 12 % and from 20 % to 12 % for Fe and from 42 % to 27 % and 51 % to 22 % for Mn. F3 of Fe and Mn presented increasing values with depth in the mudflat, from 8 % to 15% for Fe and from 6 % to 13 % for Mn, while it is stable in the *Avicennia* stand with a mean value of 3 % for Fe and values

ranging from 2 % to 6 % for Mn. F1 of Fe was stable with depth with mean values of 2 % and 3% in the mudflat and in the *Avicennia* stand, respectively.

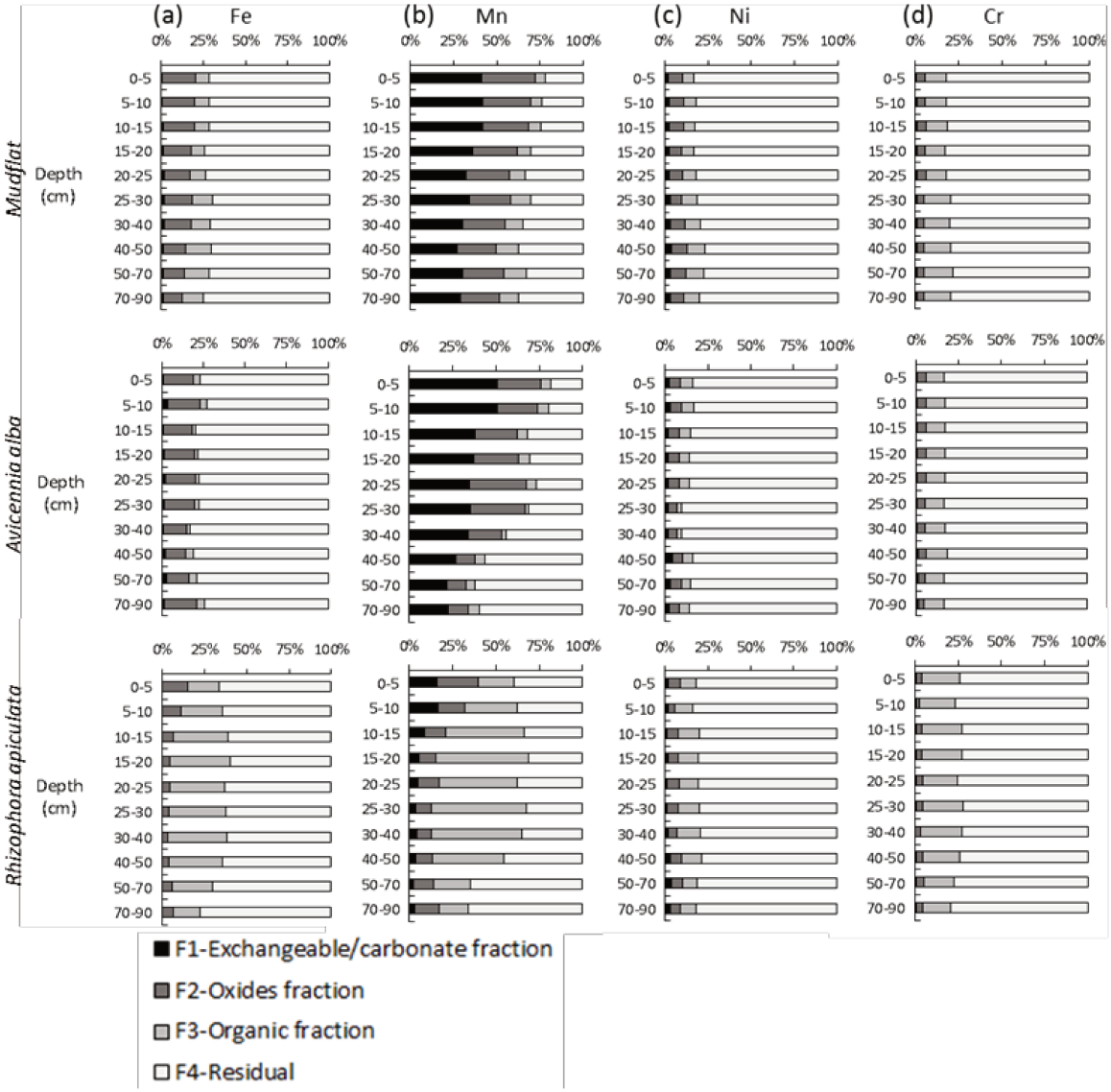

Fig. 3-3. Depth profile of Sequential extraction of Fe (a), Mn (b), Ni (c), Cr (d), Cu (e), Co (f) and As (g) in the mudflat, the Avicennia stand and the Rhizophora stand in Can Gio mangrove (continued in next page).

In the *Rhizophora* stand, Fe and Mn exhibited the same partitioning: F4 > F3 > F2 > F1. The residual fraction was stable from the top to the 40 cm depth, and then gradually increased with depth from 62 % to 78 % for Fe and from 35 % to 66 % for Mn. The organic fraction of both Fe and Mn was higher in the *Rhizophora* stand than in the *Avicennia* stand and the mudflat.

Conversely to F4, the proportion of Fe and Mn in F3 increased from the top to 40cm depth (i.e. ranging from 18 to 36 % for Fe and 21 to 54 % for Mn), then decreased to the bottom of the core (i.e. ranged from 35 to 16 % and from 52 to 17 % for Fe and Mn, respectively). Fe and Mn in F2 decreased toward the bottom of the core, from 15 % to 3 % for Fe and from 23 % to 8 % for Mn. Eventually, the exchangeable/carbonate fraction of Fe represented less than 1 % of total Fe concentrations, while F1 of Mn decreases with depth from 16 % to 3 %.

3.3.4.2 Ni, Cr, Cu, Co and As

Ni partitioning was characterized by F4 > F2 ~ F3 > F1 in the mudflat and the *Avicennia* stand and by F4 > F3 > F2 > F1 in the *Rhizophora* stand (Fig. 3.3c). F4 was in the same range (from 76 % to 84 %) in the mudflat and in the *Rhizophora* stand, but higher (from 83 to 91 %) in the *Avicennia* stand, without clear vertical distributions in all cores. F3 was stable with depth and presented a higher proportion in the *Rhizophora* stand (11 %) than in the mudflat (8 %) and in *Avicennia* stand (5 %). F2 and F1 were stable with depth at all sites, and represented less than 8% for F2 and less than 3% for F1.

Cr partitioning was by F4 > F3 > F2 > F1, without any clear depth evolution (Fig. 3.3d). The residual fraction ranged from 78 % and 84 % in the mudflat and the *Avicennia* stand and from 72 % to 79 % in the *Rhizophora* stand. The organic fraction was characterized by higher proportion in the *Rhizophora* stand (16 % to 24 %) than in the mudflat (11 % to 17 %) and in the *Avicennia* stand (10 % to 13 %). The oxides fraction and the exchangeable/carbonate fraction presented low proportion (less than 5%) and same range of values in all environments.

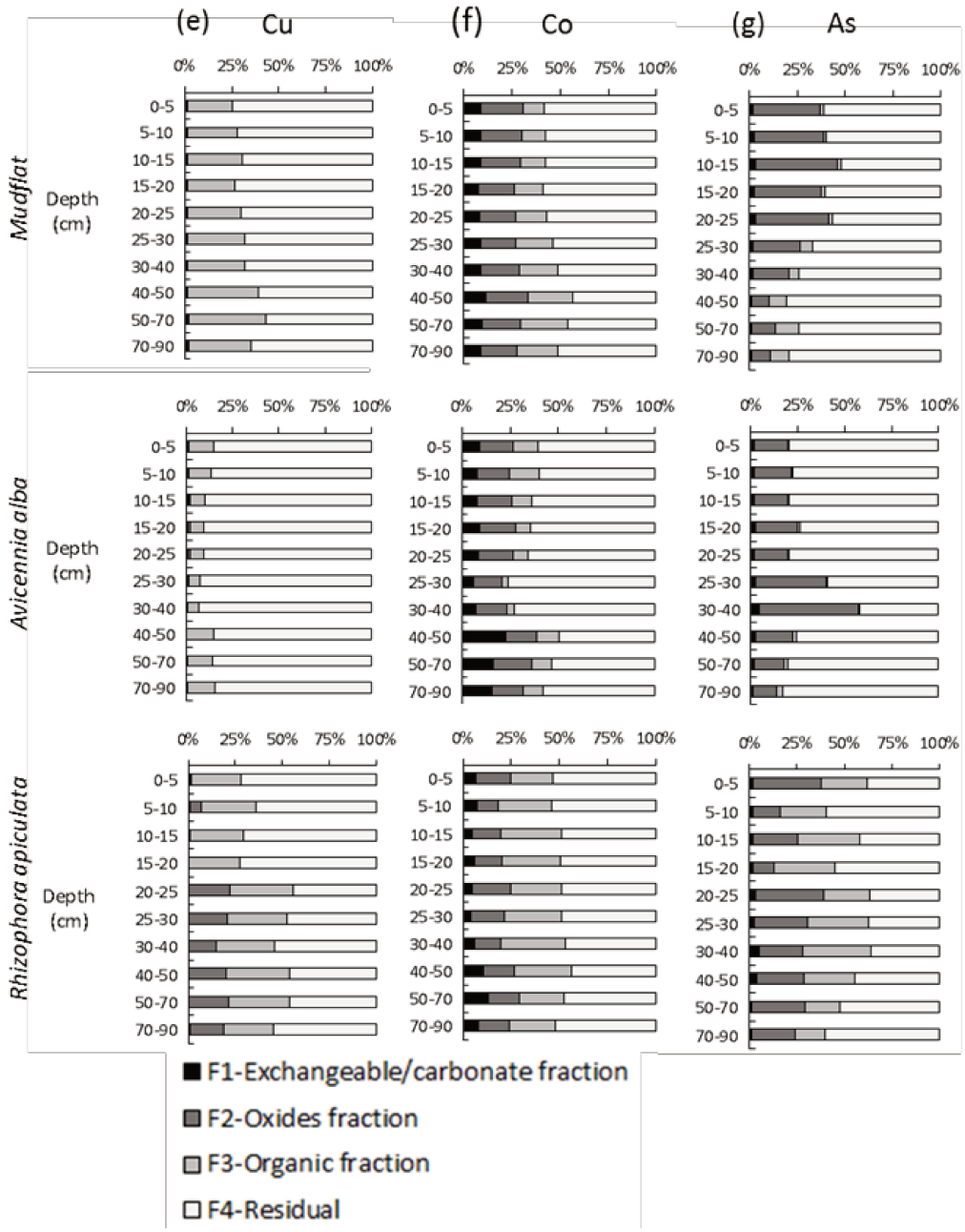

Fig. 3.3. (Continued)

Cu partitioning differed between sites: F4 > F3 > F1 > F2 in the mudflat, F4 > F3 > F2 ~ F1 in the *Avicennia* stand, and F4 > F3 > F2 > F1 in the *Rhizophora* stand (Fig. 3.3e). In F4, the proportion of Cu was higher in the *Avicennia* stand (85 % to 94 %) than in the *Rhizophora* stand (44 % to 73 %) and in the mudflat (57 % to 75 %). In the mudflat, the proportion of Cu in F4

decreased with depth while no specific distribution was observed in the mangrove stands. F3 ranged from 24 to 41 % in the mudflat and *Rhizophora* stand, and from 6 to 14 % in the *Avicennia* stand. F1 and F2 fractions were characterized by low proportion (< 2 %) in all environments except in the *Rhizophora* stand where the F2 increased from 20cm depth until the core bottom.

The Co partitioning also differed between cores: F4 > F2 ~ F3 > F1 in the mudflat, F4 > F2 > F1 ~ F3 in the *Avicennia* stand and F4 > F3 > F2 > F1 in the *Rhizophora* stand (Fig. 3.3f). The residual fraction was closed to 50% in both the mudflat and the *Rhizophora* stand, but ranging from 50 to 76% in the *Avicennia* stand with lower proportion at depth. F3 presented opposite pattern than F4 in the mudflat and the mangrove stands. F2 and the F1 were stable in all environments with lower proportion in the *Rhizophora* stand for F2 and increasing F1 proportion from 40cm depth in the *Avicennia* stand.

As partitioning was F4 > F2 > F3 > F1 in the mudflat, F4 > F2 > F3 ~ F1 in the *Avicennia* stand and F4 > F2 ~ F3 > F1 in the *Rhizophora* stand (Fig. 3.3g). In the upper part of the core in the mudflat (to 25 cm depth), all fractions presented stable proportions. Then, As in F3 and F4 increased with depth while As in F1 and F2 decreased. In the core beneath the *Avicennia* stand, As proportion in F4 gradually decreased from the top to the 40 cm depth and dramatically increased in deeper layers while the opposite distribution was observed for F3 ($r = -0.99$). F2 and F1 did not exhibit any specific distribution along the core. In the *Rhizophora* stand, the residual and the organic fractions were stable from the top of the core to 40 cm depth, then F4 increased toward the bottom while F3 decreased. The F2 and F1 fraction did not exhibit any specific distribution along the core.

3.3.5. Distribution of dissolved metals concentrations in mangroves pore-waters

Dissolved Fe concentrations (Fe_D) in pore-waters presented lower levels of concentrations in the *Rhizophora* stand (14 to 3,055 µg L^{-1}) and the mudflat (from 1,621 and 10,303 µg L^{-1}) pore-

waters than in the *Avicennia* stand pore-waters (333 to 40,771 µg L^{-1}). The Fe_D distributions was characterized by decreasing Fe_D from the surface to 15cm depth and then increasing values with depth in the stands (Fig. 3.4a). Dissolved Mn concentrations (Mn_D) presented higher concentration levels in the mudflat (from 6,812 to 15,106 µg L^{-1}) and in the *Avicennia* stand (25 to 13,648 µg L^{-1}) than in the *Rhizophora* stand (from 542 to 643 µg L^{-1}) pore-waters (Fig. 3.4b). In the mudflat stands, Mn_D decreased from the top to 10cm depth (in *Avicennia* stand) and to 40cm depth (in *Rhizophora* stand) and then increased again with depth.

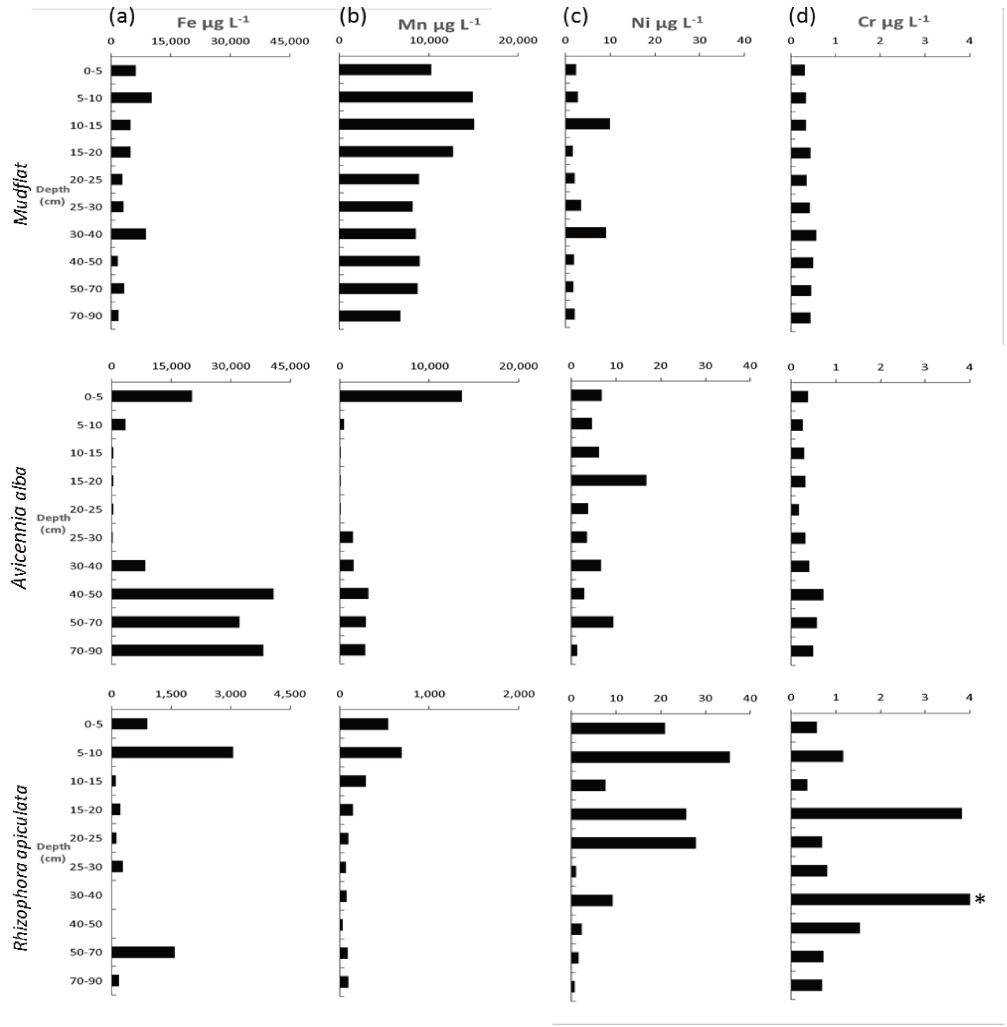

Fig. 3-4. Depth profile of dissolved metals concentrations (µg L-1) in the pore-waters of the mudflat, Avicennia and Rhizophora stands. Asterisks highlight extreme values that could not be shown in the graph even with cut axis (i.e. values of 14.4 for Cr and 13.9 fo Cu).
Continued in next page.

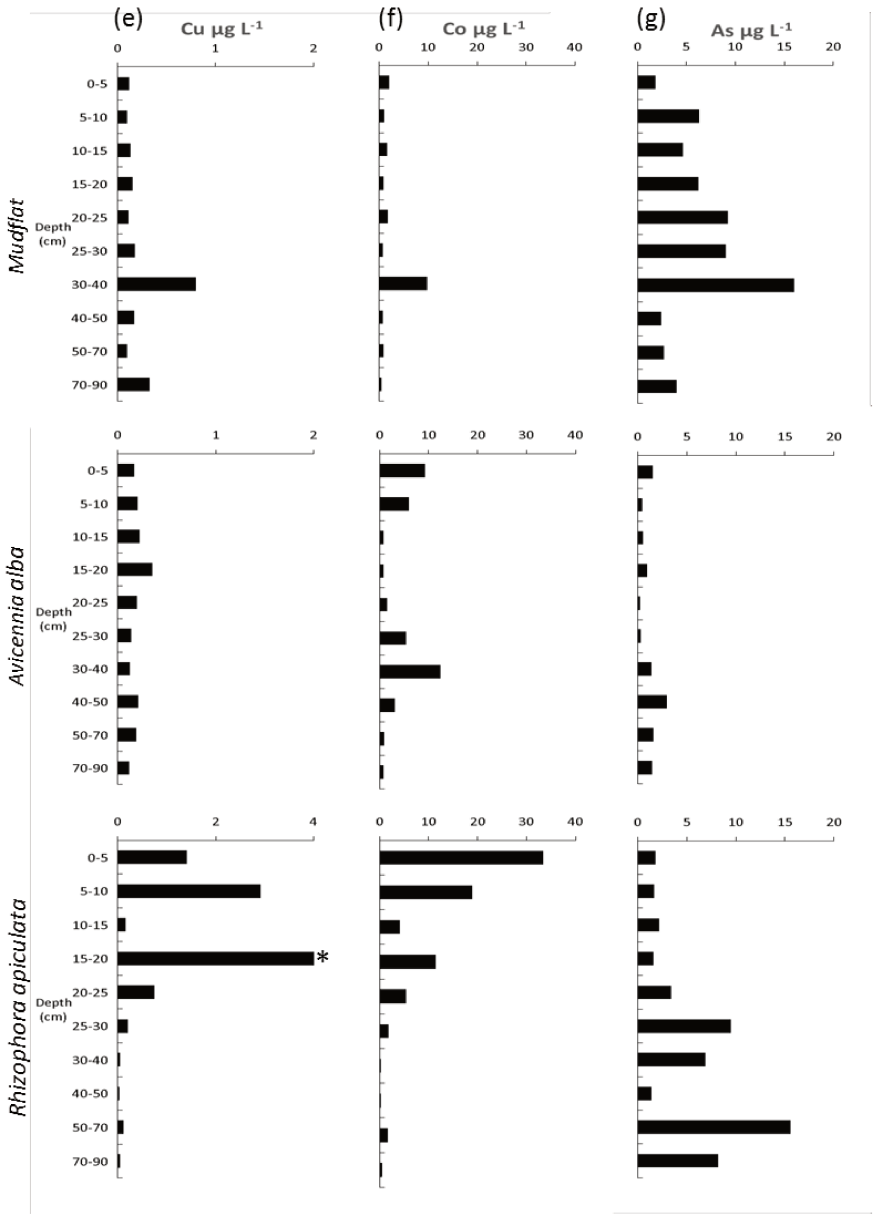

Fig. 3.4. (Continued)

The dissolved Ni (Ni_D), Cr (Cr_D) and Cu (Cu_D) concentrations in pore-waters presented similar patterns in the three cores (Fig. 3.4c, 3.4d and 3.4e). In the mudflat and the *Avicennia* stand, Ni_D, Cr_D and Cu_D were stable with depth with increasing concentrations at 30cm depth in the mudflat and at 15cm depth in the *Avicennia* stand. In the *Rhizophora* stand, Ni_D, Cr_D and Cu_D presented higher concentrations with a decreasing pattern from the top to the surface for Ni_D and Cu_D and a stable pattern with two peaks at 15cm and 30cm depth for Cr_D. The dissolved Co (Co_D) and As

(As_D) concentrations in pore waters (Fig. 3.4f, 3.4g) presented a stable vertical distribution with a peak at 30cm in the mudflat core while in the *Avicennia* stand, they presented decreasing concentrations from the top to 10cm depth, increasing concentrations until reaching a peak at 30cm and 40cm depth for Co_D and As_D respectively, and then decreasing concentrations towards the bottom. Finally in the *Rhizophora* stand, Co_D decreased with depth with a peak at 15cm depth while As_D is stable with two peaks at 25cm and 50cm depth.

3.4. Discussion

3.4.1. Mangrove sediments characteristics

Mangrove forests are known to be highly productive ecosystems (Bouillon et al. 2008), storing huge quantity of carbon in their soils. Kristensen et al. (2008a) showed that TOC values in mangrove soils usually range between 0.5 % and 15 %, with a median value around 2.2 %. In the Can Gio mangrove, TOC reached up to 4.6 % with increasing values from the tidal creek (the mudflat core) to the inner mangrove (the *Rhizophora* stand core) (Fig. 3.2d). The higher values measured beneath the *Rhizophora* stand than beneath the *Avicennia* stand may result from a higher productivity of the first species, including a more developed root system as it was observed in Australia (Alongi et al. 2000) or in New Caledonia (Marchand et al. 2011b). It may also be related to the elevation of the soil: the *Avicennia* trees in Can Gio mangrove developing at lower elevation than the *Rhizophora* ones may thus be subject to a more intense tidal export of leaf litter, which limits organic matter accumulation in the soil. Additionally, the oxygen released by the roots of *Avicennia* trees may induce more efficient organic matter decomposition (Marchand et al. 2004). Beneath the two mangrove stands, the redox values decreased with depth probably as a result of organic matter decomposition and the lack of electron acceptors renewal at depth (Otero et al. 2009). In the upper part of the sediments, the suboxic conditions ($100 < Eh < 260$ mV) may be explained by biological or physical factors (i.e. length of emersion, crab activity and bioturbation

by mangrove roots) (Marchand et al. 2012). The radial cable roots of *Avicennia* trees can also be important factor inducing higher Eh values than in the *Rhizophora* stand (Marchand et al. 2004). Whereas the mudflat is flooded almost all the time, the absence of air diffusion into the sediment can result to anoxic conditions despite its low organic content. We suggest that more intense organic decomposition and possible sulfide oxidation may cause lower pH in the *Avicennia* stand than in the *Rhizophora* and in the mudflat (Marchand et al. 2004). Finally, the upper sediment of every core was characterized by lower salinity values than deeper soil, which can be related to the period of coring, i.e. the end of the rainy season, the rainwater inducing a dilution of the saline pore-waters. The rainwater may also be responsible of an enhanced renewal of electron acceptors, influencing OM diagenesis.

3.4.2. Lateritic soil as main source of trace metal in mangrove sediments.

Mean trace metals concentrations (Fe, Mn, Ni, Cr, Co, Cu and As) in Can Gio mangrove sediments (Table 3.2) are in the range of other mangroves around the world (see review papers of Lewis et al. (2011) and Bayen (2012)) but are lower than those measured in mangroves subject to strong anthropogenic pressure as in India (Fernandes and Nayak 2012). Furthermore, these metals concentrations were also close to those measured in total suspended matter (TSM) in Can Gio mangrove estuary (Thanh-Nho et al. 2018). These authors stated that TSM acted as main carrier for trace metals during their transports to the ocean, and that trace metals distribution changed due to the physical mixing by the seawater and/or organic matter decay processes. Consequently, most metals concentrations in TSM collected in the estuary were lower than upstream, specifically during the monsoon. We suggest that despite being downstream of a developing megacity characterized by low urban wastewater treatments (only 10 %, (FAO 2014)), trace metals accumulation inside the mangrove forests was relatively limited. We consider that the main source of trace metals in the Can Gio mangrove was natural and originated from the rivers' watershed in

the central highland of Vietnam, composed of lateritic soil originating from the physico-chemical weathering processes of basaltic rocks (Egawa and Ooba 1963) rich in hematite and goethite minerals. This hypothesis may be supported by the high proportion of metals in the residual fraction (Fig. 3.3) and interrelationships of total metals concentrations in the mudflat, which reflect sediment inputs without the mangrove influence (Table 3.4).

3.4.3. Trace metal geochemistry in mangrove sediments.

3.4.3.1 Redox sensitive elements (Fe and Mn)

Iron geochemistry

As suggested earlier, the erosion of lateritic soils upstream Can Gio may induce the transfer of these Fe-oxihydroxides towards the estuary and then their deposition in the mangrove, explaining the high Fe concentrations measured in mangrove soils. In the main channel of the Can Gio estuary, we measured up to 55,302 µg g^{-1} of iron during the monsoon season (Thanh-Nho et al. 2018), which comfort our hypothesis. However, the oxide fraction was not the dominant one in mangrove soils. This may be attributed to the limitation of the selective extraction method offered by (Tessier et al. 1979), which is inefficient to extract iron from highly crystallized oxides and oxihydroxides, and which may explain the dominance of the residual fraction. (Ferreira et al. 2007) also stated that $NH_2OH.HCl$ only poorly extracts iron crystalized forms, like ferrihydrite or lepidocrocite. In the studied mangrove soils, Fe partitioning varied with depth and between stands. In addition, great variation of Fe_D concentrations were also observed between sites and with depth (Fig. 3.4a). We suggest that these variability resulted from the different redox conditions detailed earlier and driven by OM decomposition, bioturbation, root system, etc. Iron partitioning beneath the *Avicennia* stand and the mudflat was similar, but the one beneath the *Rhizophora* stand was different. In fact, we measured higher Fe concentrations in the oxidizable fraction but lower dissolved iron concentrations and lower Fe concentrations in residual, reducible and

exchangeable/carbonate bound fractions beneath the *Rhizophora* stand than beneath the *Avicennia* stand and in the mudflat (Fig. 3.3a and 3.4a). With the selective extraction method used, metals associated with organic matter are included in the oxidizable fraction. We, thus, suggest that the enrichment of the soil in OM along the studied transect may be responsible of these differences since Fe can form chelate complexes with OM (Thamdrup 2000). In addition, in the *Rhizophora* stand, TOC decrease with depth may affect Fe partitioning. Fe concentrations in the oxidizable fraction were negatively correlated with the concentrations in the reducible and the residual phases (r = - 0.67 and - 0.85, respectively). We suggest that toward the landside of the mangrove or with depth beneath the *Rhizophora* stand, Fe-oxihydroxydes, originated from the lateritic soil in the Sai Gon Dong Nai Rivers watersheds, were dissolved because of an increased organic content, and subsequently dissolved iron was complexed with OM as observed in other mangroves (Marchand et al. 2012). In anoxic conditions, Fe_D can also precipitate as sulphides, which can be reflected by the increased concentrations of Fe in the residual phase at depth in the *Rhizophora* stand. Unfortunately, we were not able to measure neither total sulfur (TS) nor sulphide in the studied mangrove sediments. However, it is known that mangrove sediments are characterized by high rate of sulfate reduction (Kristensen 2008b) and elevated TS content and pyrite are commonly observed in mangrove forest, especially at depth (Marchand et al. 2011a, Marchand et al. 2006b). Eventually and in addition to these reduction processes, Noël et al. (2014) suggested that re-oxidation of aqueous Fe(II) and pyrite can lead to the formation of poorly ordered ferrihydrite, lepidocrocite (c-FeOOH) and likely goethite. We suggest that this process possibly occurred in Can Gio in the upper suboxic sediments, but it was not possible to confirm it with the selective extraction we used.

Manganese geochemistry

Manganese is also known as highly redox sensitive (Lacerda et al. 1999). Like for Fe, the presence of Mn_D in the pore-waters may result from the reductive dissolution of Mn-oxihydroxides during the diagenetic processes (Froelich et al. 1979). This process can be responsible for the presence of high Mn_D concentrations in pore-waters, reaching more than 10,000 µg L^{-1} in the mudflat (Fig. 3.4b). The lower Mn_D observed in the *Avicennia* and *Rhizophora* stands than in the mudflat sediments may be related to (i) the loss of Mn_D by tidal drainage (Lacerda et al. 1999), Mn_D release from mangrove pore-waters being as a significant component of Mn oceanic budget (Holloway et al. 2016), (ii) to an uptake by mangrove plants (Wang et al. 2002), or iii) to more intense reprecipitation of Mn with other bearing phases after oxihydroxides dissolution. We suggest that those processes were more pronounced for the *Rhizophora* stand, with total Mn concentrations 2-fold lower than in the other site (Table 3.2). However and conversely to Fe, the dominant Mn fraction was the carbonate one in the two mangrove stands. Unlike Fe, Mn sulphides are unstable ($pK_{sp} = 1.3$) and the precipitation of Mn as sulphides may be severely limited by the presence of dissolved Fe^{2+} and carbonate. Because of similar ionic radii, Ca can be substituted by Mn in carbonate minerals (Costa-Boddeker et al. 2017, Rath et al. 2009). Previous studies, e.g. concerning mangrove sediments in the West coast of India (Noronha-D'Mello et al. 2015) or in Brazilia (Otero et al. 2009), reported that a considerable quantity of the free manganese was associated with carbonate (i.e. up to 2.5 µmol g^{-1}). Marchand et al. (2008) suggested that the decomposition of organic matter in mangrove sediments leads to the production of DIC that can migrate at depth, where carbonate minerals can precipitate because of the marked anoxic conditions that prevail there compared to the upper suboxic layers. This carbonate precipitation can be a sink for some elements, including Mn. In the *Rhizophora* stand, within the organic rich-

layers, oxidizable fraction was the predominant one for Mn, suggesting that Mn was adsorbed onto OM (Thamdrup 2000). This hypothesis may be supported by negative correlation between Mn concentrations in the oxidizable fraction with those in the reducible and in the residual phase (i.e. r = - 0.69 and – 0.79, respectively).

3.4.3.2 Geochemistry of Ni, Cr, Cu, Co and As

Nickel geochemistry

Under reducing condition, Ni-bearing Fe and Mn-oxihydroxides may be reduced by Fe and Mn reducing microorganisms during OM decay process, leading to the release of Ni_D (Klinkhammer 1980). In Can Gio mangrove sediments, the increase of OM in the *Rhizophora* stand implies intense diagenetic processes, which may induce increasing Ni_D toward the upper part of the *Rhizophora's* core (Fig. 3.4c) as supported by the positive correlation between TOC and Ni_D (i.e. r = 0.6). This result may also explain the higher Ni_D from the mudflat to the *Rhizophora* stand (Fig. 3.4c). We also found that the total Ni concentrations in the sediments beneath the mangrove stands were higher than in the mudflat, suggesting the poor mobility of Ni in the *Rhizophora* stand via pore-waters discharge in the Can Gio mangrove sediments. Beneath the *Avicennia* stand under anoxic condition, the increase of Ni concentrations in the residual fraction may be attributed to more intense precipitation of Ni pyrite and/or Ni sulphide (Noël et al. 2015). In anaerobic condition, Ni can be rapidly removed from the dissolved phase by co-precipitation with active sulphide (Clark et al. 1998). In the *Rhizophora* stand, we suggest that dissolved Ni was complexed by organic matter due to the richness of this sediment in OM and the adequate pH (i.e. 3.4 % of mean TOC concentrations and pH ranging from 6.4 to 6.8). Doig and Liber (2006) demonstrated that the organonickel complexes may be formed at pH 6 to 8, which may explain the higher concentrations of Ni in the organic fraction beneath *Rhizophora* than beneath the two other stands (i.e. 11.4 % in the *Rhizophora* stand vs. 5.4 % in the *Avicennia* stand and 8.2 % in the

mudflat, Fig. 3.3c). Finally, we conclude that the increase organic content and their decay processes in mangrove sediments modify the Ni partitioning, being deposited in the mangrove associated with Fe, Mn-oxihydroxydes. Those oxihydroxydes are then dissolved releasing Ni in pore-waters, which thus precipitated as sulphides or is complexed with organic matter.

Chromium geochemistry

As well as for Ni, we suggest that the organic enrichment in *Rhizophora* sediments induces a modification of Cr partitioning. The complexation of Cr_D by OM may result from the dissolution of Cr bound to Fe and Mn-oxihydroxides during diagenetic processes. The peak of Cr_D observed at 30-40 cm depth in the *Rhizophora* stand (Fig 3.4f) may be related to intense reductive dissolution of oxides, supported by the concomitantly decrease of Cr (down to 3.1%), Fe and Mn (drop to 3.1 % and 8.5 %) in oxides fraction, and the low Eh measured (-106 mV, Fig. 3.2b). The most striking evolution of Cr partitioning was the increasing organic fraction coinciding with the decreasing of the residual fraction and oxides one (Fig. 3.3d) like demonstrated in New Caledonia (Marchand et al. (2012). Lacerda et al. (1991) also observed in a Brazilian mangrove that Cr was immobilized in sediment as organochromium complexes. Furthermore, below 50 cm depth in the *Rhizophora* stand, the increasing Cr concentrations in the residual fraction may be related to the incorporation of Cr by pyrite, as supported by the positive correlation between Cr and Fe in the residual fraction (i.e. r = 0.86).

Copper geochemistry

Copper may be released in pore-waters upon OM decay processes and/or reductive dissolution of Fe-Mn oxihydroxides under suboxic conditions. Cu is a chalcophile element, being easily chemisorbed on or incorporated in several minerals such as chalcopyrite ($CuFeS_2$), covellite (CuS) and malachite $Cu_2CO_3(OH)_2$ (Pickering 1986). However, chalcopyrite and malachite are not stable

under acidic conditions, especially at pH values ranging from 5 to 6. Therefore, the high Cu concentrations in the residual fraction beneath the *Avicennia* stand (where pH values < 6), compared to the mudflat and the *Rhizophora* stand, may result from the intense precipitation of Cu as sulphides, mainly CuS and/or Cu_2S (Fernandes 1997, Morse and Luther 1999). In the Can Gio mangrove sediment, a negative correlation was observed between the organic fraction and the residual one whatever the sites (i.e. r = - 0.99, - 0.98 and – 0.83 in the mudflat, *Avicennia* stand and the *Rhizophora* stand, respectively). The well-known affinity of OM for Cu scavenging in mangrove sediments being widely documented (Chakraborty et al. 2015, Marchand et al. 2016, Silva et al. 2014), we suggest that the organic matter acts as a key factor controlling Cu partitioning and subsequently inducing the low concentrations of Cu in the other fractions (i.e. exchangeable/carbonate and oxides bound, Fig. 3.3e). We note that beneath the *Rhizophora* stand, Cu concentrations in the organic fraction were higher than in the two other sites (Fig. 3.3e). Overall, the Cu_D in the three cores are in the same range than those measured in the Can Gio mangrove estuary surface water (Thanh-Nho et al. 2018). Cu is known to be an essential element for plant growth (Yruela 2009) and to bioaccumulate up to a bioconcentration factors of 9 in leaves and 5 in roots of mangrove trees (MacFarlane et al. 2003, Usman et al. 2013). Therefore, we suggest that its low contents in pore-waters, in addition to its precipitation with OM and with sulphides, may be related to an uptake by the mangroves root systems (MacFarlane and Burchett 2002). However, some peaks of increasing Cu_D are observed at 5cm, 10cm and 20cm depth (1.4 µg L^{-1} 2.9 µg L^{-1} and 13.8 µg L^{-1}, respectively) in the *Rhizophora* stand (Fig. 3.4e), which may be attributed to a limited re-precipitation with oxides-bearing and supported by the Cu decreasing in the oxides fraction at these layers (Fig. 3.3e).

Cobalt geochemistry

In the *Rhizophora* stand, Co in the organic fraction represented almost 30% of total Co, while it represented 10 % and 18 % of the total in the *Avicennia* stand and in the mudflat, respectively (Fig. 3.3f). A negative correlation between the residual fraction and the organic one (r = - 0.76) was observed, evidencing one more time the key role of organic matter in trace metal partitioning in mangrove sediments either because of its decomposition that induce the dissolution of some bearing phase or because of dissolved trace metals complexion. However, beneath *Avicennia* trees, Co concentrations in the organic fraction were the lowest of the 3 stands despite of similar range of TOC in the mudflat. We suggest that in these soils, dissolved Co may be trapped into sulphides. In riverine sediments, Charriau et al. (2011) observed that sulphides compete with organic matter in scavenging soluble Co. However and conversely to Ni, Cr and Cu, Co concentrations in the exchangeable/carbonate bound fraction were elevated, reaching up to 23 % on total Co concentrations. Because of similar ionic radii, Co (III) can be substituted to Mn in Mn (III/IV) oxides (Manceau et al. 1997). This process can occur in the same Eh-pH space in which Mn (II) oxidation occurs (Murray and Dillard 1979). As explained earlier for Mn partitioning and the presence of Mn-carbonates, we suggest that the decomposition of organic matter can lead to DIC production, which can precipitate in specific redox-pH values, incorporating some elements, mainly Mn but also Co. However, Co and Mn proportions in the exchangeable/carbonate fraction showed the opposite distribution patterns with depth whatever the sites (Fig. 3.3f) which implies considerable competition of dissolved Mn on the formation of carbonate cobalt (i.e. negative correlation observed: r = -0.5 in the mudflat; r = -0.6 in both *Avicennia* and *Rhizophora* stands).

Arsenic geochemistry

Dissolved As concentrations were relatively high in the mudflat and at depth in the *Rhizophora* stand, reaching almost 20 µg L^{-1} (Fig. 3.4g). We suggest that the presence of As_D in pore-waters results from the reductive dissolution of As bound to oxides under suboxic/anoxic conditions (Masscheleyn et al. 1991, Nickson et al. 2000). Recent studies also supported that the reduction of Fe-oxihydroxides was a cause of As release into ground water in Bangladesh (Anawar et al. 2003, Zheng et al. 2004). Because of the stability of inorganic arsenic species under anoxic conditions (Rhine et al. 2005), As in the pore-waters of Can Gio mangrove sediments was probably dominated by arsenites such as H_3AsO_3, $H_2AsO_3^-$, as demonstrated by Hossain et al. (2012) in Sundarbans mangrove sediments in Bangladesh. Beneath the mudflat and the *Avicennia* stand, characterized by low TOC values, the depth distribution of As_D was similar with the dominance of the residual and organic fractions, which were characterized by a strong and negative correlation (i.e. r = - 0.98 in the mudflat and r = - 0.99 in the *Avicennia* stand). Conversely in the *Rhizophora* stand characterized by higher organic content, the organic fraction represents up to 36% of total As concentrations. The increase in OM content from the mudflat to the *Rhizophora* stand induces a modification of As partitioning by diagenetic processes. We also suggest that the increasing concentrations of arsenic in the residual fraction with depth in every sites may result from the incorporation of As into pyrite. In fact, the most common iron sulphide minerals have strong affinity for, and can incorporate large amounts of arsenic in its structure, up to 10 wt% (Abraitis et al. 2004, Qiu et al. 2017). Noël et al. (2014) stated that pyrite was the predominant Fe bearing phase at depth in mangrove sediments.

3.4.4. Trace metals stocks and ecological potential risk assessment

In the present study, we observed that the most of metals stocks in the upper 50 cm of the sedimentary column were lower in the *Rhizophora* stand compared to the *Avicennia* one and the mudflat. This may be related to the increase of sedimentary organic matter content in the sediment, which induces a decrease in the bulk density of the soils (0.55 g cm^{-3} in the *Rhizophora vs.* 0.61 g cm^{-3} in the *Avicennia* and 0.64 g cm^{-3} in the mud flat). It may also be related to a more reactive substrate like described in the previous discussion, which have induced the dissolution of some bearing phases and the export of dissolved metals through pore-water seepage, or the uptake of dissolved metals by mangrove plants. In addition, the metals stocks in Can Gio mangrove sediments were lower than those measured in other mangroves, like in New Caledonia (Marchand et al. 2016), confirming the moderate trace metals inputs in the system.

The bioavailability and potential toxicity of trace metals in the different geochemical fractions are expected to decrease in the following order: exchangeable/carbonate fraction > oxides fraction > organic fraction > residual fraction (Ma and Rao 1997). To assess trace metal availability and potentially ecological risks, we decided to use the Risk Assessment Code - RAC (Perin et al. 1985) and guideline (Benson et al. 2017, Passos et al. 2010) for the Can Gio mangrove sediments (Fig. 3.5).

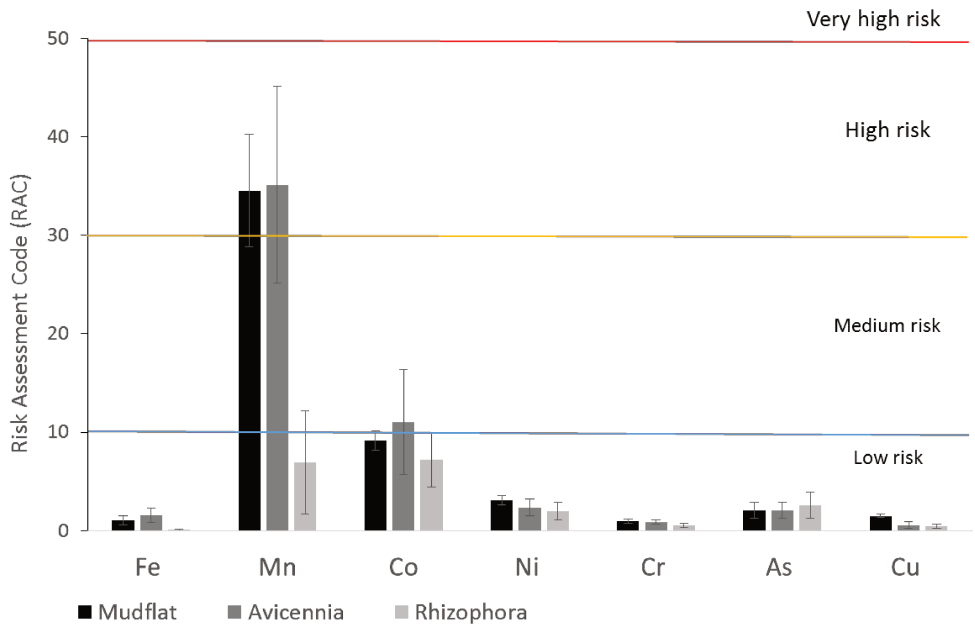

Fig. 3-5. Risk Assessment Code of metals in the sediment cores of the mudflat, the Avicennia stand and the Rhizophora stand in Can Gio mangrove.

The RAC is evaluated based on the percentage of metal concentrations that is representative in the bioavailable fraction (exchangeable/carbonate bound) to the total trace metal concentrations. According to the RAC guideline, metal with less than 1 % of exchangeable/carbonate fraction would be at no risk to the environment while higher ratio suggest: 1 % - 10 %: low risk; 11 %- 30 %: medium risk; 31 % - 50 %: high risk and > 50 %: very high risk. Consequently, in the Can Gio mangrove sediments, only Mn present a high risk in the mudflat and in the *Avicennia* stand (i.e. RAC > 33) and a low risk in the *Rhizophora* stand (i.e. RAC < 7). We note that in plants, Mn excess can damage the photosynthesis apparatus (Millaleo et al. 2010) and thus the plants productivity (Nguyen et al. 2018). Ni and As presented a low risk but their high dissolved concentrations in pore-waters, reaching up to ~40 µg L^{-1} for Ni and ~20 µg L^{-1} for As, may potentially be an additional ecological risk to organisms. Co, Fe and Cu showed low risks to the ecosystem while Cr was in the no risk category whatever the site. Along the mangrove, the RAC was lower in the *Rhizophora* stand than in the *Avicennia* stand and the mudflat, which may result

from the competition of organometallic complexation (see earlier discussion), reflecting the important role of organic matter in scavenging trace metals in mangrove sediments. Eventually, as a result of mangrove conversion for agriculture and/or aquaculture (i.e. salt production and shrimp farming, etc.), these sediments may be subject to an oxidation resulting in enhanced OM decomposition, sulphide oxidation, and thus sediments acidification. Noel et al. (2017) showed that increasing anthropogenic pressure on coastal areas altered the redox state of mangrove sediments from reducing condition to oxidizing condition, affecting the stability of Ni-accumulating Fe-sulfides and releasing significant dissolved trace metals at the redox boundary. Consequently, trace metals which were associated with OM and sulphides will be released in pore-waters, but also those associated with the exchangeable/carbonate bound due to the acidification, conducting all trace metals to be potentially at high ecological risks in the Can Gio mangrove sediments.

3.5. Conclusions

Despite being situated downstream the biggest city in Vietnam, Can Gio mangrove sediments do not present high trace metal concentrations. Their concentrations, close to those of the crust, and their bearing phases, suggest that studied metals originate from the lateritic soils of the Sai Gon–Dong Nai Rivers watersheds. Can Gio mangrove sediments acted thus as a natural biogeochemical reactor, inducing modification of trace metals bearing phases. Redox cycling in sediment impacted the Fe-Mn oxides dissolution, and subsequently the metals geochemistry across the intertidal zones. Metals were deposited mainly as Fe-Mn oxihydroxides, which were subsequently dissolved by bacteria in suboxic conditions, releasing them in pore-waters. Depending on the metal and on the redox conditions, they precipitated with OM, sulphides or carbonates. The OM enrichment of the sediments from the mudflat to the *Rhizophora* stand played

a key role in trace metals partitioning, either because its decay modify the redox conditions (inducing oxihydroxides dissolution and sulphides precipitation) or because of the formation of organometallic compounds.

According to the RAC index, most of the metals present low ecological risks to the mangrove ecosystem except Mn, and possibly Ni and As due to their elevated dissolved concentrations. However, we would like to underscore that any anthropogenic perturbation of the redox state of those mangrove sediments may result in a release of their trace metals contents in the adjacent ecosystems. We also suggest that *Avicennia* and *Rhizophora* trees may uptake dissolved trace metals and accumulate them into their tissues. In addition, pore-waters seepages may induce an export of trace metals from the mangrove sediments into the tidal creeks. A further detailed investigation on dissolved trace metals transfer and their accumulations into mangrove organisms should be carried out to get a better understanding of trace metal dynamics in the Can Gio mangrove ecosystem.

Chapter 4 - Trace metals accumulation in plants and snails of a tropical mangrove (Can Gio, Vietnam)

Highlights:

- Mangroves roots acted as barrier preventing Fe and As translocations to aerial parts
- *Rhizophora* trees presented high potential for Mn "phytoextraction".
- Low Ni, Cr in mangrove tissues may result from their low bioavailability in sediments.
- Fe, Cu and Mn were the dominant elements in soft tissues of all snail species.
- All snails contained high quantity of As, probably due to its bioavailability.

Keywords: Bioaccumulation; Gastropods, Mangrove plants, macroconcentrators; Vietnam.

ABSTRACT

Mangroves can store high amount of trace metals in their soils. Because of variable redox conditions, these metals can be more or less bioavailable and can sometimes being subject to an uptake by mangrove flora and biota. The main objectives of this study were: i) firstly to determine metals concentrations (Fe, Mn, Co, Ni, Cr, As and Cu) in various biological tissues (i.e. roots and leaves of *Avicennia alba*, *Rhizophora apiculata*; and snail species such as *Chicoreus capucinus*, *Littoraria melanostoma*, *Cerithidea obtusa*, *Nerita articulata*) living in a tropical mangrove located at the edge of a megacity with over 10 million inhabitants, ii) secondly to assess the effects of feeding habits and habitats on metals accumulation in snails soft tissues. In the present study, we suggest that the high degree of trace metals concentrations in organisms' tissues can result from both the biological requirements of individual species but also to the amount of trace metals in bioavailable forms in their habitat. For plants tissues, we suggest that the formation of iron plaque on the roots may have played a key role in preventing Fe and As translocations to the aerial parts of the trees. We suggest that mangroves can be considered as "phytostabilizators" for those metals, immobilizing them in the rhizosphere. Mn presented higher concentrations in the leaves than in the roots, with high BCF, possibly because of physiological requirements. We suggest that *Rhizophora* can be considered as a "phytoextractor" for Mn. Non-essential elements (Ni, Cr and Co) showed low BCF in both roots and leaves, which may result from their low bioavailability in mangrove sediment and pore-waters. Regarding snails species, essential elements (Fe, Mn and Cu) were the dominant trace metals in their tissues, with concentrations ranging from 271 to 1,517 µg g^{-1} for Fe, from 42.5 to 780 µg g^{-1} for Mn and from 7.84 to 481 µg g^{-1} for Cu. Most of snails were as "macroconcentrators" for Cu, with BCF values reaching up to 42.8 in *Cerithidea*. We suggest that high quantity of As in all snails may result from high bioavailability of As in their dietary intake and from their ability to metabolize As.

4.1. Introduction

Due to their persistence, bioaccumulation and toxicity, heavy metals pollution is one of the main problems to the marine ecosystems (Agoramoorthy et al. 2008). Mangroves, complex intertidal forests located at the interface between marine and terrestrial environments are considered as sinks for contaminants, including trace metals (Tam and Wong 2000). It was previously suggested that mangrove plants can play important roles in metals removal from mangrove sediments (Alongi et al. 2004, Yang et al. 2008). On the one hand, depending on the metal considered and on the mangrove species, they can provide "phytostabilization", meaning that metals are immobilized and stored in the sediment or in the below-ground biomass (MacFarlane et al. 2007). On the other hand, they can provide "phytoextraction", and the trees can be considered as accumulators, meaning that they can remove metals from the sediments and concentrate them in above-ground tissues (Kříbek et al. 2011). Because of different rates of metals uptake, and the specific influence of some roots on sediment geochemistry, metals dynamic in mangrove sediments may be affected by the composition of plant communities (Verkleij and Schat 1990). In fact, some mangrove trees can oxidize the sediments via their rhizosphere through the movement of oxygen downwards in aerenchyma tissues (Moorhead and Reddy 1988). This oxidation process can remobilize the stable forms of metals, e.g. the ones bound to sulphides (Marchand et al. 2006b, Noël et al. 2015), thus increasing metals' bioavailability. In addition, changes in Eh and pH conditions of sediments due to any anthropogenic pressure may alter metal speciation and solubility, releasing them in pore-water and being thus more bioavailable for organisms (Alongi et al. 1998). The bioaccumulation and/or fixation of trace metals in mangrove plant tissues may limit metals concentrations in the water column and restrict the entry of these contaminants into the food chain. However, some studies demonstrated that the excess of essential

metals and non-essential metals could affect the growth, metabolism activities and cell structure of plants (Cox and Hutchinson 1981, Wang et al. 2003).

Gastropods, which are potential indicators of environmental stress, also exhibit changes in diversity and community structure through chronic and acute effects of metals contamination (Traunspurger and Drews 1996). It was demonstrated that elevated heavy metal concentrations in sediments can influence negatively the number of gastropods species in an ecosystem (Amin et al. 2009). Among gastropods, snails offer the possibility to assess metals contaminations (De Wolf and Rashid 2008, Samsi et al. 2017, Yap and Cheng 2013). Zhou et al. (2008) reported that snails can accumulate higher metal concentrations than any other groups of invertebrates, and were, thus, revealed as potential bioindicators. Metals bioavailability to snails depend on their feeding regime, their digging activities, and metal partitioning. Metal bioaccumulations in snails have been addressed in many research projects in the past two decades (Berandah et al. 2010, Dias and Nayak 2016, Reed-Judkins et al. 1997).

In Vietnam, an emerging country, the fast economic development (i.e. urbanization, industrialization, etc.) and the population growth induce high pressure on sediments, rivers and estuaries. The Can Gio estuary is located at the edge of the biggest industrial city in Vietnam, Ho Chi Minh City (i.e. a megacity of almost 10 million inhabitants), and half of the Can Gio area is covered by mangrove forests. This estuary is also a unique gate for drainages of sewages from the land to the ocean. Hence, organic and inorganic contaminants can be deposited in mangrove sediments and transferred to the biota. However, it was surprising that Can Gio mangrove sediment did not show high trace metal concentrations, and only presented moderately polluted to unpolluted metals (see in Chapter 3). In fact, Can Gio mangrove is home to high biodiversity with 20 species of flora, in which two mangrove species are dominant: *Avicennia alba* and *Rhizophora*

apiculata (Luong et al. 2015), and with more than 200 species of fauna (e.g. benthic organisms, fish, gastropods, planktonic, etc.). In a previous study (Chapter 3 of this PhD thesis), we observed that trace metals stocks decreased from the mudflat to the mangrove stands (i.e. from the tidal creek to inner mangrove) due to organic enrichment that led to a modification of the bearing phase, some of them being more mobile and then exported from the system. Thus, knowledge of trace metals accumulation in different mangrove organisms would be useful to get a better understanding of the fate of these contaminants in the mangrove.

The objectives of this study were: i) to evaluate the transfer from the soil and the accumulation of some trace metals (Fe, Mn, Co, Ni, Cr, As and Cu) in the tissues of the main mangrove trees species developing in Can Gio, ii) to assess the effects of dietary habits and habitats on metals bioaccumulation in snails. To reach our goals, different parts (i.e. roots and leaves) of mangrove plants (i.e. *Avicennia* and *Rhizophora* trees), gastropods (i.e. snail species such as *Chicoreus capucinus*, *Littoraria melanostoma*, *Cerithidea obtusa* and *Nerita articulata*) were collected and analyzed for their total metals concentrations.

4.2. Materials and methods

4.2.1. Study area

The study was conducted in the Can Gio mangrove Biosphere Reserve (10°22'-10°44'N and 106°46'-107°01'E, Fig. 4.1). This mangrove covers approximately 35,000 ha (Tuan and Kuenzer 2012), being usually classified as a "Mangrove afforestation and re-forestation area" (Blasco et al. 2001). It is also a part of the densely populated megacity of Ho Chi Minh City (HCMC), with over 10 million of inhabitants. The Can Gio mangrove is situated 35 km downstream of the city urban center and industrial zones (Strady et al. 2017a, Vo 2007). The main economic activities of the local people are aquacultures, salt production, fishing and forest management. The topography of Can Gio mangrove is generally low-lying. This coastal area is subject to an asymmetric semi-

diurnal tidal regime and to the typical tropical monsoon climate, with two distinct seasons. The dry season extends from November to April and the monsoon season lasts from May to October. The highest precipitation can reach up to 400 mm in September, while it is usually less than 80 mm per month during the dry season. The annual mean precipitation is about 1,300 to 1,400 mm, with approximately 90 % of the precipitation falling during the rainy season and the annual mean temperature varies from 26.5 ºC to 30 ºC. The two dominant mangrove species are *Avicennia alba* and *Rhizophora apiculata.* Because of high commercial values, *Rhizophora apiculata* was widely replanted, being often found on elevated ground. *Avicennia alba* is a pioneering species with high salinity tolerance and the ability to grow on weak, unconsolidated sediment. Many marine organisms live within and around the mangroves, e.g. shrimp, fish, snail or crab, etc. Therefore, the mangrove ecosystem provides various goods and services to local people such as timber, seedlings, medicines, but also foods (Kuenzer and Tuan 2013).

4.2.2. Field sampling

The sampling campaign was carried out in the end of the monsoon season (October 2015) in the Can Gio mangrove (Fig. 4.1). Plants tissues (leaves and roots) were collected from saplings and mature trees in the *Rhizophora apiculata* and *Avicennia alba* stands. For leaf samples of both saplings and mature trees, they consisted of 30 leaves from 15 trees. The root samples were collected in upper 50 cm depth. All samples were rinsed with deionized water and were then dried at 50 ºC for > 48h to constant mass in an oven.

Four species of snails were collected in the mangrove stands, including *Chicoreus capucinus*, *Littoraria melanostoma*, *Cerithidea obtusa* and *Nerita articulata*. Notably for Littoraria, they were collected on mangrove trees. In the *Rhizophora* stand, due to their excessive height (>15 m), most of *Litorraria* were collected on young trees. In the *Avicennia* stand, due to low density of saplings, most of *Littoraria* were collected on mature trees. Each sample comprised 15 to 20 snails and their

shell sizes (length and width) were measured prior to taking out their tissues. The whole bodies were kept at -18 ºC until freeze-drying. Samples were ground and sieved through 100 µm pore size for analysis.

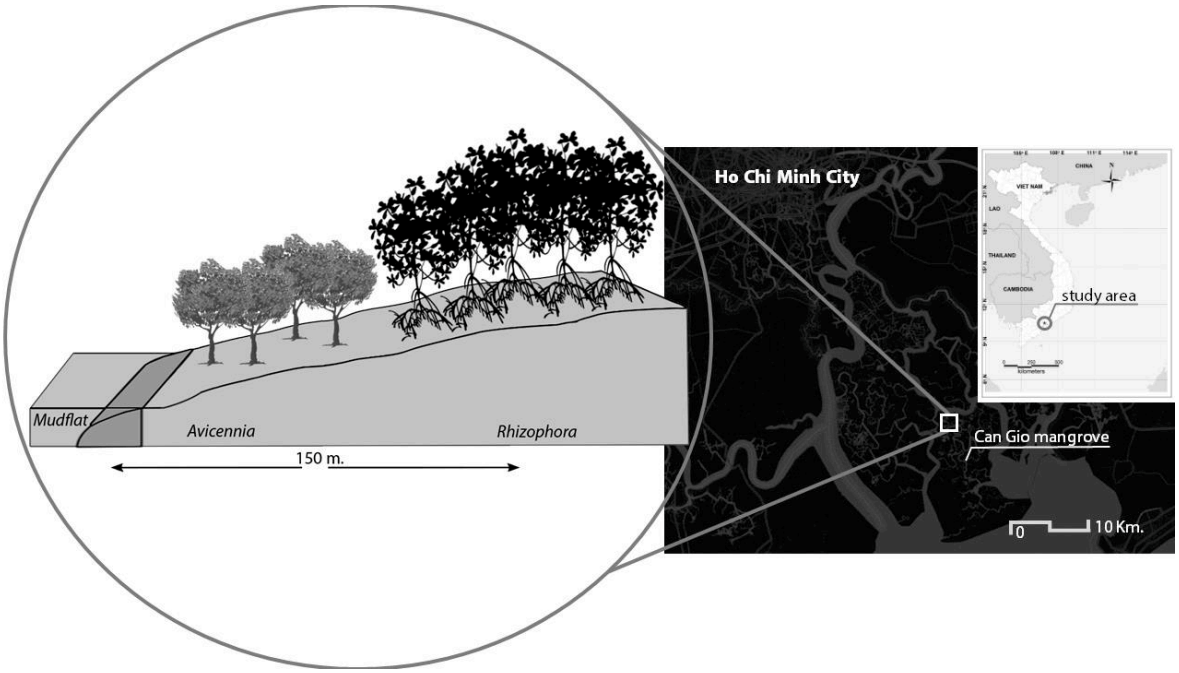

Fig. 4-1. Map of the study area showing: i) the location of Can Gio mangrove in Viet nam and ii) the location of the collected biological samples in the mangrove.

4.2.3. Analytical methods and calculations

4.2.3.1 Samples digestion

Samples were digested for metals analysis with concentrated nitric acid and hydrogen peroxide (MacFarlane et al. 2003). The samples (250 mg to 500 mg of tissues) were put into PTFE vessels, in which 10 mL of concentrated HNO_3 was added. These samples were homogenized in an ultrasonic bath for 15 min and were then digested at 110 °C for 12h in an electrical oven. After cooling, 2 mL of H_2O_2 was added into these samples, which were again digested at 110 °C for 30 min. The residual HNO_3 was eliminated at 160 °C. The samples were centrifuged to reject any residues and then diluted to 25 mL using deionized water and stored at 4 °C until analysis. The metals were determined by ICP – MS (Agilent 7700x) using spiked ^{103}Rh and ^{197}Au as internal

standards. All chemicals were analytical grade (Merck). HNO_3 was purified using a sub-boiling quartz distillation equipment.

4.2.3.2 Data calculations

Bioconcentration factor (BCF) was proposed by Babukutty and Chacko (1995) to assess the bioaccumulation of pollutants into an aquatic and terrestrial organisms via any route i.e., by active or/and passive accumulations. It is defined as $BCF = C_{tissues}/C_{sediment}$, where $C_{tissues}$ and $C_{sediment}$ are the total metal concentrations in organism tissues and the total metal concentrations in sediments, respectively. In this study, the mean concentrations of Fe, Mn, Co, Ni, Cr, Cu and As in the sediments were taken from the chapter 3 of this PhD thesis (Table 4.1). BCF of each metal was specifically calculated for each tissues.

Plant tissues

BCF was calculated from a mean total metal concentrations in sediments down to 50 cm depth. We choose this depth because in mangrove environment, the highest root density is in the upper soil, between 20 and 50 cm depth (Ha et al. 2018, Komiyama et al. 2000, Tamooh et al. 2012).

We also calculated translocation factors (TF), which are used to assess metal transfer from roots to aboveground plant tissues and to evaluate the potential phytoextraction of plant (Marchiol et al. 2004). It is defined as $TF = C_{leaves}/C_{root}$, where C_{leave} and C_{root} are the total metal concentration in leaves and the total concentration in roots of plants, respectively.

Snails

Depending on feeding regimes of individual snail species and their habitat, the BCF was calculated from a mean total concentration corresponding to a mean total concentration in each type of foods. *Littoraria* feeds on mangrove trees, mainly fresh leaves and material on the plant surfaces as phylloplane and fungi (Lee et al. 2001). Their BCF were estimated based on the mean metal concentration measured in *Avicennia* and *Rhizophora* leaves. *Cerithidea* is known as

sediment eater (Tue et al. 2012), BCF was calculated based on a mean metal concentration sediment corresponding to a mean metal concentration in available fractions of the upper 5 cm of the sediment. *Nerita* eats microalgae (Eichhorst 2016), and Chicoreus is a versatile predator of mollusks and crustaceans, seeking, attacking and consuming a wide variety of prey from different components of the mangrove habitat (Tan and Oh 2003). We were not able to sample their feeding sources, consequently, we did not calculate any BCF for these two snails species.

Table 4-1. Trace metal concentrations (expressed in µg g-1) in mangrove sediments of the Avicennia and the Rhizophora stands (data from the chapter 3). The data presenting the available concentrations (sum of exchangeable/carbonate bound, oxidizable and reducible fractions) and non-available concentration of each metal.

Avicennia stand					*Rhizophora stand*				
Element	Depth (cm)	mean concentration	Available fractions	Non-available fraction	Element	Depth (cm)	mean concentration	Available fractions	Non-available fraction
Fe	0-5	52,590	12,103	40,487	Fe	0-5	45,554	15,470	30,084
	0-50	49,482	10,649	38,833		0-50	47,689	17,693	29,996
Mn	0-5	800	653.0	147	Mn	0-5	231	140.1	91.2
	0-50	530	377.1	153		0-50	279	178.6	101
Co	0-5	21.6	8.6	13.0	Co	0-5	21.6	10.1	11.5
	0-50	22.1	8.1	13.9		0-50	22.7	11.6	11.1
Ni	0-5	61.1	9.7	51.4	Ni	0-5	60.4	11.0	49.4
	0-50	62.5	8.6	53.9		0-50	60.5	11.7	48.8
Cr	0-5	97.3	16.0	81.4	Cr	0-5	88.7	22.9	65.8
	0-50	95.7	17.3	78.3		0-50	95.0	24.7	70.3
As	0-5	11.2	2.3	8.9	As	0-5	13.3	8.2	5.1
	0-50	11.6	3.3	8.3		0-50	14.8	8.3	6.6
Cu	0-5	17.9	2.7	15.3	Cu	0-5	20.7	5.8	14.9
	0-50	18.5	2.0	16.6		0-50	20.6	8.5	12.1

4.3. Results

4.3.1. Plant tissues

The mean concentrations of Fe, Mn, Co, Ni, Cr, As and Cu (µg g^{-1}) in the roots and leaves of *Avicennia* and *Rhizophora* trees are presented in Table 4.2.

The mangrove roots of the saplings and mature *Avicennia* trees showed similar distribution of metals concentrations, as follows Fe > Mn > Cu > Cr > As > Ni > Co. Fe, Mn and Cu concentrations were higher in the Avicennia sapling roots than in the mature ones. In the *Rhizophora* trees, the metals concentrations in descending order were Fe > Mn > As > Cr > Cu ~ Ni > Co in the saplings and were Fe > Mn > Cr > Ni ~ Cu > As ~ Co in the mature trees. Notably, Fe and As concentrations were higher in the roots of the *Rhizophora* saplings than in the mature ones (Table 4.2). Concerning metal bioconcentration factors (Table 4.3), most metals were characterized by low values, i.e. less than 1 in all mangrove roots, except Cu and As for the roots *Avicennia* saplings (i.e. BCF: 1.02 for As and 2.95 for Cu).

Table 4-2. Metal concentrations in the different tissues of the Avicennia and the Rhizophora trees(saplings and mature trees), expressed in µg g-1 (mean, SD). The roots samples of trees were collected in the upper part of 50 cm depth of the sediments.

Root

	Depth(cm)	Type of trees	Fe	Mn	Co	Ni	Cr	As	Cu
Avicennia	< 50	Saplings	14,948 ± 239	376 ± 4	2.8 ± 0.06	5.1 ± 0.16	17.8 ± 0.11	11.9 ± 0.12	54.7 ± 1.8
	< 50	Mature trees	7,433 ± 308	217 ± 1.7	5.0 ± 0.13	5.8 ± 0.09	8.9 ± 0.42	7.5 ± 0.19	10.2 ± 0.29
Rhizophora	< 50	Saplings	19,897 ± 1265	60 ± 1.2	2.4 ± 0.05	5.0 ± 0.11	8.8 ± 0.25	12.7 ± 0.15	6.3 ± 0.12
	< 50	Mature trees	5,458 ± 145	57 ± 1.1	2.0 ± 0.01	5.4 ± 0.08	11.9 ± 0.33	2.0 ± 0.05	4.7 ± 0.13

Leaves

	Height of trees	Type of trees	Fe	Mn	Co	Ni	Cr	As	Cu
Avicennia	> 7 m	Saplings	2,287 ± 39	583 ± 5	1.43 ± 0.01	3.18 ± 0.28	7.31 ± 0.22	0.61 ± 0.02	22.14 ± 0.30
		Mature trees	359 ± 21	908 ± 20	0.29 ± 0.10	1.09 ± 0.14	2.13 ± 0.29	0.30 ± 0.03	8.93 ± 0.30
Rhizophora	< 80 cm	Saplings	1,416 ± 50	267 ± 3	0.48 ± 0.02	1.60 ± 0.02	13.19 ± 0.79	0.40 ± 0.01	10.63 ± 0.55
	> 15 m	Mature trees	498 ± 21	405 ± 38	0.07 ± 0.03	0.70 ± 0.25	3.72 ± 0.30	0.14 ± 0.03	15.92 ± 0.80

The mangrove leaves presented the following abundance of trace metal concentrations in the *Avicennia* saplings: Fe > Mn > Cu > Cr > Ni > Co ~ As, and in the mature *Avicennia* trees Mn > Fe > Cu > Cr > Ni > Co ~ As (Table 4.2). The Mn presented higher concentrations in the leaves of mature trees than in the ones of saplings while the other metals (Fe, Ni, Cr, Cu, As and Co) showed opposite distributions. In the *Rhizophora* trees, the trace metal concentrations were in the order Fe > Mn > Cr ~ Cu > Ni > Co ~ As in the saplings and Fe > Mn > Cu > Cr > Ni > As ~ Co in the mature trees. The Mn and Cu concentrations were higher in the leaves of the mature trees than in the young ones while Fe, Co, Ni, Cr and As presented opposite accumulation. The bioconcentration factors were lower than 1 for most metals, with the exception of Mn in both saplings and mature leaves of the two mangrove species, and of Cu in sapling leaves (Table 4.3).

Table 4-3. Bioconcentration factors (BCF = metal concentration in tissues/ metal concentration in sediment of the various plants developing in the studied mangrove in Can Gio,Viet nam.

BioConcentration Factor

Root	Depth (cm)	Type of trees	Fe	Mn	Co	Ni	Cr	As	Cu
Avicennia	< 50	Saplings	0.30	0.71	0.13	0.082	0.19	**1.02**	**2.95**
	< 50	Mature trees	0.15	0.41	0.23	0.093	0.093	0.64	0.55
Rhizophora	< 50	Saplings	0.42	0.22	0.11	0.082	0.092	0.86	0.31
	< 50	Mature trees	0.11	0.21	0.09	0.090	0.13	0.13	0.23
Leaves	Height of trees	Type of trees	Fe	Mn	Co	Ni	Cr	As	Cu
Avicennia	> 7 m	Saplings	0.046	**1.10**	0.065	0.051	0.076	0.052	**1.19**
		Mature trees	0.007	**1.71**	0.013	0.018	0.022	0.026	0.48
Rhizophora	< 80 cm	Saplings	0.031	**1.15**	0.022	0.026	0.15	0.030	0.51
	> 15 m	Mature trees	0.011	**1.58**	0.003	0.011	0.039	0.009	0.77

The metal translocation factors (TF) were higher than 1 for Mn, Cu in the sapling and mature *Rhizophora* trees, Cr in the *Rhizophora* saplings while it was lower than 1 for other metals and tissues (Table 4.4).

Table 4-4. Translocation factors (TF = metal concentration in leaves/ metal concentration in roots) of the various plants developing in the studied mangrove in Can Gio, Viet nam.

Translocation Factor	Height of tree	Type of trees	Fe	Mn	Co	Ni	Cr	As	Cu
Avicennia	> 7 m	Saplings	0.15	**1.55**	0.51	0.62	0.41	0.051	0.40
		Mature trees	0.048	**4.19**	0.058	0.19	0.24	0.040	0.88
Rhizophora	< 80 cm	Saplings	0.071	**4.43**	0.20	0.32	**1.51**	0.031	**1.69**
	> 15 m	Mature trees	0.091	**7.07**	0.038	0.13	0.31	0.068	**3.37**

4.3.2. Snails

The mean concentrations of Fe, Mn, Co, Ni, Cr, As and Cu (µg g^{-1}) in snails soft tissues are given in Table 4.5. All snails presented higher concentrations in Fe, Mn and Cu than in As, Ni, Cr and Co. The *Chicoreus capucinus* presented metal concentrations in the following order: Fe > Cu > Mn > As > Ni ~ Cr ~ Co with some difference of concentrations between the *Avicennia* and the *Rhizophora* stands. The *Nerita articulata* showed similar metal abundance beneath the two mangrove zones: Fe > Mn > Cu > As ~ Ni ~ Cr > Co. Conversely, trace metals concentrations in *Littoraria melanostoma* and *Cerithidea obtusa* presented different abundance in metals concentrations depending on their habitat. The metals in *Littoraria melanostoma* beneath the *Avicennia* stand were Mn > Fe > Cu > As > Ni ~ Cr ~ Co, while beneath the *Rhizophora* stand they were Fe > Mn ~ Cu > As > Ni ~ Cr ~ Co. The metals in *Cerithidea obtusa* were: Mn > Fe > Cu > Ni ~ As > Co > Cr beneath the *Avicennia* stand, while they were Fe > Mn ~ Cu > Ni ~ As > Cr > Co beneath the *Rhizophora* stand.

Table 4-5. Metal concentrations in soft tissues of various snails (expressed in µg g-1): Checoreus (predator), Littoraria (leaves eater), Cerithidea (sediment eater) and Nerita (algae eater).

Mangrove stand	Species	Length (cm)	Width (cm)	Fe	Mn	Co	Ni	Cr	As	Cu
Avicennia	Chicoreus	2.5 - 4	1 - 1.5	536 ± 40	139 ± 10	0.88 ± 0.11	1.52 ± 0.16	1.11 ± 0.17	10.9 ± 1.1	481 ± 38
	Littoraria	1.5 - 2.5	1 - 2	714 ± 95	766 ± 29	1.04 ± 0.03	2.14 ± 0.08	0.61 ± 0.12	3.64 ± 0.17	120.6 ± 9.1
	Cerithidea	2 -4	1 - 1.5	360 ± 44	780 ± 81	2.64 ± 0.26	5.93 ± 0.44	0.70 ± 0.11	4.32 ± 0.88	113.9 ± 5.7
	Nerita	2 - 2.6	1.5 - 2	271 ± 26	42.5 ± 2.6	0.20 ± 0.13	1.16 ± 0.15	0.90 ± 0.25	2.83 ± 0.22	7.84 ± 0.65
Rhizophora	Chicoreus	3 - 4	1.5 - 2.5	885 ± 80	119 ± 11	1.14 ± 0.03	2.07 ± 0.12	1.27 ± 0.31	14.3 ± 2.2	389 ± 13
	Littoraria	1.5 - 3	1 - 2	1,517 ± 120	201 ± 20	1.41 ± 0.02	3.34 ± 0.30	2.5 ± 1.3	5.39 ± 0.25	163 ± 17
	Cerithidea	3 - 4	1 - 1.2	338 ± 29	158 ± 16	0.99 ± 0.09	6.15 ± 0.74	1.58 ± 0.41	6.95 ± 1.15	120 ± 20
	Nerita	1.8 - 2.5	1.2 - 1.5	795 ± 82	96 ± 14	0.88 ± 0.27	3.58 ± 1.74	5.99 ± 1.43	6.45 ± 1.69	16.6 ± 0.9

The bioconcentration factors of all metals are presented in Table 4.6. The BCF of each metal varied between snail species. The BCF of Fe ranged from 0.02 to 1.58, with the highest value for *Littoraria* collected beneath the *Rhizophora* stand. The BCF of Mn varied from 0.6 to 1.13, with the highest value for *Cethididea* in the *Rhizophora* zone. The BCF of Cu in all snail species ranged from 7.7 to 42.8, with highest value for *Cerithidea* in the *Avicennia* zone. Arsenic also showed high amplitude in BCF, ranging from 0.85 to 20.1, with the highest values in *Littoraria* collected beneath the *Rhizophora* zone. The Co and Ni presented same BCF range from 0.1 to 5.09 for Co and 0.56 to 2.9 for Ni, with the highest BCF observed in the *Littoraria* collected beneath the *Rhizophora* stand. Finally, BCF of Cr was basically lower than 1 for all snails whatever the stands, ranging from 0.04 to 0.3.

Table 4-6. Bioconcentration factors (BCF = metal concentration in soft tissues/ metal concentration correspond to metal concentration in feeding of individual type) of various snails in the Can Gio mangrove.

Mangrove stand	Species	Length (cm)	Width (cm)	Fe	Mn	Co	Ni	Cr	As	Cu
Avicennia	*Littoraria* (leaves eater)	1.5 - 2.5	1 - 2	0.54	1.05	1.21	1.00	0.13	8.03	7.77
	Cerithidea (sediment eater)	2 -4	1 - 1.5	0.03	1.22	0.31	0.61	0.04	1.88	42.8
Rhizophora	*Littoraria* (leaves eater)	1.5 - 3	1 - 2	1.58	0.60	5.09	2.90	0.30	20.10	12.29
	Cerithidea (sediment eater)	3 - 4	1 - 1.2	0.02	1.13	0.10	0.56	0.07	0.85	20.74

4.4. Discussions

4.4.1. Trace metal bioaccumulation in Avicennia and Rhizophora mangrove tissues

4.4.1.1 Essential elements: Fe, Mn, Cu

Iron is an important component of chlorophyll, being useful for protein synthesis and root growth (Jones Jr et al. 1991). In the present study, despite low bioconcentration factors (BCF), Fe was the most abundant element in the roots whatever the mangrove species, reaching up to 19,897 $\mu g\ g^{-1}$ (Table 4.2). These mean iron concentrations in Can Gio mangrove root's tissues were substantially higher than other mangrove on the world like in roots of *Avicennia marina* in Indian mangroves (Kathiresan et al. 2014). We suggest that the measured high iron concentrations in the mangrove roots resulted from the high iron concentrations measured in the sediments (Table 4.1) and in the pore-waters (see Chapter 3) (e.g. where it can be highly bioavailable (Abohassan 2013)), as observed for *Avicennia marina* and *Rhizophora stylosa* in New Caledonian mangroves, where the mangrove sediments are rich in iron because these ecosystems develop downstream of lateritic sediments (Marchand et al. 2016). However, if the concentrations were high in the roots, the translocation factors to the leaves were low for this element (Table 4.4), suggesting that the root acted as a barrier preventing iron translocation to aerial parts. Machado et al. (2005) suggested that the seedlings of mangrove species can exclude some trace metals through iron plaque formation on the roots. The oxygen released by the roots of some mangrove species may promote oxidizing conditions within the rhizosphere that result in trace metal precipitation at the root surface, creating iron-rich root coatings, generally called iron plaques (Chaudhuri et al. 2014, Koch and Mendelssohn 1989, Zhou et al. 2011). Machado et al. (2005) also demonstrated that the washing of the roots prior analysis influences the fixation of the iron plaque on the roots: in contrary to distilled water, the dithionite–citrate–bicarbonate (DCB) solution is able to extract the iron plaque from the roots. Considering that we only washed the roots with deionized water, the presence of

iron plaques at the root surface may be a possible explanation for the elevated iron concentrations in the Can Gio mangrove tree's roots. For the mature trees, Fe concentrations were higher in the *Avicennia* roots than in the *Rhizophora* ones which may be the results of the higher Fe concentrations both in the solid and the dissolved phases in the sediment beneath *Avicennia* stand (see in chapter 3). Also, the *Avicennia* root system is known to release oxygen (Marchand et al. 2004, Scholander et al. 1955) which may in return increase the iron plaque precipitation. Notably, whatever mangrove species, the Fe concentrations in leaves of saplings presented higher values than the mature ones despite the roots of saplings contained higher Fe concentrations (Table 4.2). We suggest that iron plaque may be a source of Fe for plants uptake by bacterial reductive dissolution of plaque during OM decay processes on death roots surface. Additionally, the root system of the saplings may develop in the upper layer, and not as deep as the one of the mature trees. This upper layer is more subject to variations in the redox conditions, and possibly to enhanced alternation of precipitations/dissolution processes. Consequently, trace metals, and specifically iron, may be more available at the level of the saplings' roots. Eventually, is it possible that the adaptation strategy of the mangrove trees were not fully develop at the sapling stage, and that consequently the role of barrier of the root system may be limited.

Manganese is as a major contributor to various biological processes, including photosynthesis (Millaleo et al. 2010). In the Can Gio mangrove, whatever the plants species, Mn was the second abundant element in their tissues, with average concentrations in the range of those measured worldwide in mangroves (see review of Lewis et al. (2011) and Bayen (2012)). Conversely to Fe, Mn accumulated more in the leaves than in the roots (Table 4.2), as observed in New Caledonia by Marchand et al. (2016). The TF values and Mn concentrations in plants tissues measured in this New Caledonia (e.g. maximum TF: 4.08) were lower than in the present study (e.g. TF reached up

to 7.07). We suggest that the high dissolved Mn concentrations measured in the pore-waters and the difference of Mn partitioning in the mangrove sediments may be responsible of the elevated values measured in the present study. Within the top 50 cm of the sediments in Can Gio mangrove, approximately 60 % of Mn was associated with the bioavailable fractions whereas in New Caledonia, 90 % of Mn was bound to the refractory fraction, preventing its transfer to mangrove plants (Marchand et al. 2016). We remind that Mn was the only metal potentially presenting an ecological risk due to its high bioavailability (ratio of metal concentrations in the bioavailable fractions (exchangeable/carbonate bound) to the total trace metal concentrations) (see Chapter 3 of this thesis). Since high Mn TF were already reported for *Rhizophora*, we suggest that it may be related to metabolic requirements, this element playing an important role in enzymes reactions is also needed for water splitting at photosystemII (McEvoy and Brudvig 2006). Consequently, the *Rhizophora* trees have a high potential for Mn phytoextraction.

Regarding copper, it is known as an essential element for plants growth, being required in enzyme system related to photosystemII electron transport, mitochondria and chloroplast reaction, carbohydrate metabolism, cell wall lignification and protein synthesis (Yruela 2009). The Cu concentrations in plant tissues measured in this study were in the range of those measured in other mangroves (Bayen 2012) like in China (He et al. 2014), in southern Brazil (Madi et al. 2015), or in Indonesia (Martuti et al. 2016). We observed that the Cu partitioning in sediments of the Can Gio mangrove was mainly related to sulphide precipitation and to its complexation with organic compounds (see in chapter 3 of this thesis). Thus, we suggest that the low Cu concentrations measured in the mangrove roots may be related to Cu association with sulphide, which limit its bioavailability. However, this element presented the second highest TF values, beside Mn, with TF reaching 1.69 for mature *Avicennia* trees and 3.37 for mature *Rhizophor*a ones. MacFarlane

and Burchett (2002) showed that Cu can be toxic to plants growth if its concentration in the sediments exceeds 400 µg g^{-1}, which is almost 20 times higher than the concentrations measured in the Can Gio mangrove sediments. Consequently, we suggest that the high Cu TF values results from specific metabolic requirements (Baker 1981, Dudani et al. 2017) as Cu has a direct impact on photosynthesis I, being a constituent of plastocyanin, which is involved in the photosynthetic electron transport chain (Maksymiec 1998).

4.4.1.2 Non-essential elements: As, Ni, Cr, Co

In the Can Gio mangrove trees, the non-essential elements such as As, Ni, Cr and Co mainly accumulated in the roots (Table 4.2), with low translocation to the leaves (Table 4.4). This phenomenon may result from different mechanisms developed by mangrove trees to prevent the uptake of toxic elements and to limit their transport within the plants (Almeida et al. 2006), notably through cell wall immobilization and/or sequestration in the epidermal layers (MacFarlane et al. 2007). They, thus, accumulate in the perennial tissues, especially the roots (Carbonell et al. 1998, Zhou et al. 2011).

Concerning Arsenic, some forms can be subject to plant uptake, involving arsenites-As(III) and arsenates-As(V) (Asher and Reay 1979). However, arsenites can be toxic for radicular membranes because of As reaction with sulfhydryl groups in proteins, causing disruption of roots functions and cellular death (Speer 1973, Wu et al. 2015). In the present study, arsenic concentrations in the mangrove tissues were higher than in most mangrove forests, like in the Indian Sundarban (Chowdhury et al. 2015), or in the Chinese Futian (He et al. 2014). Arsenic was also characterized by higher BCF in the roots, specifically in the *Avicennia* forest. These results may be related to the high As concentrations in bioavailable fractions in the Can Gio mangrove sediments (Table 4.1). In Vietnam, soils are naturally rich in As (Gustafsson and Tin 1994, Nguyen et al. 2016), which may explain its accumulation in mangrove sediments and then its transfer to

mangrove roots. We suggest that As may be incorporated into iron plaque at the roots surface, which restricted As transfer to aerial parts. This hypothesis is supported by a positive correlation between the concentrations of Fe and As in the roots (i.e. r = 0.91). Like for iron, As was more bioavailable beneath the *Rhizophora* stand, where the sediments were more enriched in organic matter and the oxidizable fraction represented up to 36 % of total As concentrations. However, As BCF was higher for the *Avicennia* than for *Rhizophora* roots, which comforts our hypothesis of enhanced plaque formation in the *Avicennia* rhizosphere due to specific redox conditions resulting from oxygen release by the roots. Similar to Fe, As concentration in sapling leaves of both *Avicennia* and *Rhizophora* species were higher than for mature ones. We suggest that the As incorporated in iron plaque may be a As source for plant uptake from Fe reductive dissolution by bacteria during organic matter decay processes of death roots tissues. The uptake of As by mangrove leaves may occur at the same time with Fe (i.e. a positive correlation was observed between As and Fe in the leaves, r = 0.91). And again, the extension of the root system in the upper layer and possibly the less developed adaptation strategy of saplings may also be responsible for the transfer of trace metals to saplings' leaves.

Regarding Ni and Cr, their concentrations in the plant tissues of the Can Gio mangrove trees were in the range of those presented in the review of Lewis et al. (2011) but lower than measured in the Indian Sundarban mangroves (Chowdhury et al. 2017) or in New Caledonia (Marchand et al. (2016). In the later environments, the authors reported higher Ni concentrations in mangrove tissues, with values up 700 $\mu g\ g^{-1}$ due to high Ni concentrations in mangrove sediments resulting from the proximity of lateritic soils enriched in Ni. Thus, we suggest that the moderate Ni and Cr concentrations measured in the Can Gio mangrove plants may result from their bound to the refractory fraction (i.e. more than 80 %), as demonstrated by Weis and Weis (2004). For plants,

Ni is a micronutrient which is required at very low concentration (Gajewska and Skłodowska 2007) and which can inhibit plant growth at high concentration (Rao and Sresty 2000). The effect of Ni on plants varies according to plant species as well as the Ni concentration in sediment; one example of its toxic symptom is chlorosis or yellowing of the leaves (Mishra and Kar 1974). The Cr is also toxic for plant growth (Shanker et al. 2005). When mangrove seedlings are exposed to excessive Cr concentrations, their roots would be shortened, and their height and biomass would be limited (Fang et al. 2008). However, considering the low BCF and the low concentrations factors for these metals in the Can Gio mangrove trees, their impact on plant growth is probably limited. The Cr concentrations in the roots of *Rhizophora* trees was lower despite that its bioavailable amount was higher than in the *Avicennia* (Table 4.1). This phenomenon, supported by higher TF values in the *Rhizophora* trees, may be related to a more intense phytoextraction of *Rhizophora* species. In addition, Cr TF in young *Avicennia* and *Rhizophora* trees was higher than in mature ones which may be due to the shorter distance in translocation of saplings than mature trees. Similar result was also observed for Ni (Table 4.4).

The Co is a micronutrient, which can be used in redox processes to stabilize molecules through electrostatic interactions as components of various plant enzymes. However in excess, it can be toxic, inducing enzyme modification, disturbing cellular function (Palit et al. 1994). In the present study, Co concentrations in the tissues of the different mangrove species were higher than in mangroves in Australia (Nath et al. 2014), in French Guiana (Marchand et al. 2006b), or New Caledonia (Marchand et al. 2016). We suggest that the high Co concentrations in the Can Gio mangrove plants may result from its high concentrations in the bioavailable fractions in the sediments, reaching up to 44 % (Table 4.1). However if the Co concentrations in the roots were relatively high, TF were lower than 0.5 (Table 4.4), which suggest its limited physiological role

and/or the fact that the roots acted as a physical barrier. As a consequence, the present study showed a narrow range of Co level in the leaves (i.e. 0.07 to 1.43 µg g^{-1}). The BCF values of Co in the tissues of *Avicennia* were much higher than in the *Rhizophora*, which may reflect the specific physiological requirements of the trees considering that its bioavailability was higher beneath *Rhizophora* stand (Table 4.1).

4.4.2. Trace metal bioaccumulation in snails

In the Can Gio mangrove forest, whatever the snails species and their habitat, Fe, Mn and Cu were the most abundant trace metals in their soft tissues, while non-essential elements (Ni, Cr, Co and As) presented lower concentrations (Table 4.5). Previous studies showed that soft tissues of mollusks accumulated higher concentrations of Cu and Fe than in the shells because of specific physiological requirements (Szefer et al. 1999, Vukašinović-Pešić et al. 2017, Yap and Cheng 2009). In fact, Fe, Mn and Cu play important roles in metabolic biomolecules like enzymes or metalloenzymes (Langston et al. 1998, Rainbow 1997). Snails also need elevated amount of Cu, being a constituent of hemocyanin (Dallinger et al. 2005). Conversely, the other elements studied can be toxic, inducing growth retardation, edema and thinning of the shell (Factor and de Chavez 2012). Similar results were reported concerning snails and different mollusks in mangroves in Malaysia (Yap and Cheng 2013), in India (Palpandi and Kesavan 2012), in Costa Rica (Vargas et al. 2015), or in Senegal (Sidoumou et al. 2006).

We also suggest that the different metal amount in the food sources and feeding habits of individual snail affect the degree and extent of heavy metal accumulation in their tissues. The snail *Cerithidea,* a sediment eater, exhibited higher metals concentrations in their tissues in the *Rhizophora* stand than in the *Avicennia* one, except Mn and Co. This result could result from higher metal concentrations in the available fractions in sediments in the *Rhizophora* stand (Table 4.1). We evidenced that because of the enhanced sediment organic enrichment beneath the

Rhizophora stand, reductive dissolution of Fe-Mn oxihydroxides by bacteria for organic matter decay processes was a source of dissolved trace metals in pore-waters, these metals being more bioavailable. As a consequence, trace metals concentrations in *Cerithidea* tissues in the present study were far higher than those measured in other mangroves (Joseph and Ramesh 2016) or estuary with strong anthropogenic pressure (Kesavan et al. 2013). Concerning *Littoraria*, a leaf eater, we suggest that the higher metals concentrations (except Mn), combined to higher BCF (Table 4.6), in snails tissues in the *Rhizophora* stand than the *Avicennia* one (Table 4.5) is likely related to the higher trace metals concentrations in the *Rhizophora* leaves than the *Avicennia* ones (Table 4.2). In addition, *Littoraria* presented the highest concentrations Fe and Mn in their tissues of all snail species in the Can Gio mangrove. This result may suggest that leaf eater may be more sensitive to metals accumulation or than metals in leaves are more bioavailable. In addition, *Litoraria* in the present study showed higher Fe and Mn concentrations than those measured in *Littoraria scabra* collected from a polluted mangrove (De Wolf and Rashid 2008). *Chicoreus,* a predator of barnacles, bivalves and other gastropods (Berandah et al. 2010), presented the highest Cu concentrations, which may result from copper biomagnification via their food chains because Cu is known to be very compatible with protein binding in organisms (Jiang and Qiu 2009). Cu biomagnification in snails body is usually observed, and they are considered as "macroconcentrators" species for Cu (Nica et al. 2012). However, concerning *Nerita*, the microalgae eater, Mn and Cu concentration in their tissues were lower than those in other species whatever the mangrove stands, and were lower than those measured in *Nerita* living in other mangroves like in Malaysia (Yap and Cheng 2013) or Southeast coast of India (Palpandi and Kesavan 2012). This result may be related to low Mn and Cu accumulation in microalgae in Can Gio mangrove. Unfortunately, in the present study, we were not able to measure trace metal

concentrations in microalgae. Considering the key role of microphytobenthos in mangrove trophic food chain, we suggest that further investigation should be carried on trace metals accumulation in these microalgae.

Eventually, among non-essential elements, all snails contained high quantity of As, which can result from its availability in their diet, and snails' ability to metabolize it and retain it (Kirby et al. 2002, Zhang et al. 2013). As also presented the highest BCF whatever the snail species (Table 4.6). In the Can Gio, dissolved As concentrations in mangrove pore-waters reached almost 20 µg L^{-1}. In addition in the *Rhizophora* stand, characterized by higher organic content, the organic fraction, being bioavailable, represented up to 36% of total As concentrations (See chapter 3 of this thesis). Khokiattiwong et al. (2009) studied two gastropod species (*Chicoreus capucinus* and *Telescopium telescopium*), and they showed that *Chicoreus*, as a predator, contained more As than the detritus and algae eater species, *Telescopium*. In the Can Gio, we also observed that *Chicoreus* contained the highest As concentrations in their body (2 to 4 fold higher level tissues than other snail species), which may be related to his predator diet and magnification along food chain (Goessler et al. 1997).

According to Dallinger (1993), snail tissues can be classified in macroconcentrators (BCF > 2), microconcentrators (1< BCF < 2) or deconcentrators (BCF < 1). Thus, the *Littoraria and Cerithidea* can be classified as macroconcentrators for Cu. The *Littoraria* was macroconcentrators for As, Co and Ni. Conversely, all snails were deconcentrators to microconcentrators for Mn and Fe. Due to negative effects of heavy metals on community structure, gender, size of snails (Amin et al. 2009, Yap and Cheng 2013). The results obtained in the present study provided a further claim that these snails can be used as good bioindicators/ biomonitors for environmental quality (Samsi et al. 2017).

4.5. Conclusions

Trace metals accumulation in the tissues of mangrove plants and snails studied in Can Gio mangrove reflected their concentrations in the sediment, their bioavailability, and specific adaptation strategies or physiological processes. We suggest that the formation of iron plaque on roots by oxygen release in the rhizosphere may be main factor preventing Fe and As translocation to the aerial parts. Consequently, mangroves roots can be considered as "phytostabilizator", immobilizing trace metals and limiting their transfer. Co exhibited higher concentrations in roots and leaves than world average, but with low BCF and TF. These results may be related to high concentrations in available forms in the sediment, and to specific physiological processes to limit the toxicity of this element. Conversely, Mn and Cu presented high translocation factors, possibly due to physiological requirements, being both useful in photosynthetic processes, and enhanced bioavailability in the sediment. We also suggest that the *Rhizophora* trees have a high potential for Mn "phytoextraction". Ni and Cr were characterized by low BCF and TF whatever the mangrove plant, which may result from their low bioavailability in the sediment and from the limited physiological roles of those elements.

The great variability of studied metals concentrations in the various snails indicated that trace metals accumulation depended not only on metal characteristics (i.e. physiological properties and biological functions), and metabolic requirements of each species but also on available concentrations of these metals in their food. Fe, Mn and Cu, which are essential elements, presented higher concentrations in all snail tissues than As, Ni, Cr and Co, which can be toxic. Most of the snails living in the *Rhizophora* stand presented higher level of trace metals concentrations (except Mn and Co) than those living in the *Avicennia* stand, specifically for *Littoraria* and *Cerithidea*, due to higher concentrations of trace metals in the leave or in the bioavailable fraction in the sediment. Concerning the predators, Chicoreus, possible

biomagnification of Cu via the food chain induced elevated Cu concentrations in their tissues. In this study, we also measured that all snails contained high amount of As, most probably because it is highly bioavailable in mangrove sediments. Eventually, most snails can be classified as "maroconcentrators" of some trace metals such as Cu, As, Co and Ni. Because of their potential toxic effects, a further study should be performed to assess the possibility of using snails as bioindicators of environmental quality.

Chapter 5 - Trace metals dynamic in a tropical mangrove tidal creek, influence of pore-water seepage

Highlights:

- Trace metals geochemistry was studied in the tidal creek of the Can Gio mangrove forest
- During ebb tides, dissolved trace metals were exported from mangrove sediments
- Mangroves can be a great source of dissolved Mn for adjacent ecosystems
- In the tidal creek, particulate Fe precipitated and was exported to the estuary
- Seasons and type of tides influenced pore-water seepage

Keywords: Trace metals; Mangroves; Tidal flushing; Ecological risk; Vietnam

ABSTRACT

Mangrove sediments are considered as sinks for trace metals, protecting coastal waters from pollutions. However, the fate of trace metals in mangroves is complex due to various biogeochemical processes across the intertidal zone, and notably the dissolution of some bearing phases resulting in high trace metals concentrations in mangrove pore-waters. Previous studies demonstrated a decrease of trace metals stocks in mangrove sediments due to the export of dissolved metals through tidal pumping. Can Gio is a tropical mangrove, being the largest one in Vietnam, and developing just downstream Ho Chi Minh City (Viet Nam's biggest industrial city). The objectives of this study were to characterize trace metals dynamics in a tidal creek of the Can Gio mangrove, and to identify the role of pore-water seepage on these dynamics. At high tide in the creek, trace metals concentrations, both in the dissolved and the particulate phases, were in the same range that those measured in Can Gio estuary, being thus considered as an end-member of the system. Then during the ebb, we clearly evidenced high inputs of dissolved Fe, Mn, Co and Ni from mangrove sediments, being the second end-member of the system. However, the fate of these inputs differed depending on the element considered. We suggest that Mn was exported from the tidal creek in its dissolved form. However for iron, and possibly to a lesser extent for Co and Ni, we suggest that, when they were delivered in the creek under dissolved forms, precipitation occurred because of different physico-chemical characteristics between mangrove sediments and tidal creek, notably higher DO and higher pH. Consequently, these elements were exported to the estuary under particulate forms. This study confirms that if mangroves can act as sinks for trace metals, they can also be sources of both dissolved and particulate trace metals for adjacent ecosystems. Consequently, we suggest that trace metals budget studies in mangroves should be developed like the ones concerning carbon, in order to efficiently determine their role of barrier for pollutants between land and sea.

5.1. Introduction

One of the most important functions of mangroves is trapping sediments and suspended solids, with their load of trace metals, originating from upstream soils, rocks or anthropogenic activities (Furukawa et al. 1997, Tam and Wong 1999, Wolanski 1995). Mangroves are, thus, considered as efficient barriers between land and sea, being sinks for trace metals and protecting coastal waters from pollutions. However, this ability may depend on sediment characteristics and hydrology (Kaly et al. 1997). The fate of trace metals in mangroves is complex due to various biogeochemical processes across the intertidal zone (Marchand et al. 2011a, McKee 1993, Noël et al. 2015). Numerous physico-chemical parameters, such as redox, pH, sulfides, and salinity can influence the distribution of trace metals between solid and liquid phases in the sediment, and their transfer at the sediment-water interface (Patrick and Jugsujinda 1992, Van Ryssen et al. 1998). Because of metal toxicities to mangrove biodiversity and also to human health, their cycling is a serious question addressed by many authors during the last few decades (Clark et al. 1998, Ferreira et al. 2007, Lacerda et al. 1988) and nowadays (Marchand et al. 2016, Xiao et al. 2015). In most of the published studies, authors focused on trace metal distributions and dynamics between sediments, pore-waters and plants. Only few and recent publications showed the transfer of trace metals from mangrove soils to tidal creeks through tidal pumping and pore-waters seepages (Holloway et al. 2016, Sanders et al. 2015). Tidal pumping induces advective flushing of permeable sediments and the transport of organic and inorganic products to the open water column (Maher et al. 2013). In New Caledonia, some studies demonstrated a decrease of the stocks of Fe, Ni and P in mangrove sediments from the landside to the seaside of the mangrove due to a more reactive substrate that lead to increased dissolution of metals bearing phases, and probably to the export of dissolved metals through tidal pumping (Deborde et al. 2015, Marchand et al. 2016, Noël et al. 2014). In the Chapter three of this thesis, we also observed a decrease of total metal concentrations in the

mangrove stands compared to mudflat. Thus, studies dealing with the export of trace metal via pore-waters discharges in mangrove system are highly relevant, and may be useful to decipher the roles of mangroves as sinks or sources of trace metals along coastal environment.

Within this context, we were interested in trace metals dynamics in a mangrove tidal creek of the Can Gio mangrove. The objective of our study was to understand the variability of trace metals (Fe, Mn, Co, Ni) concentrations and distributions between the particulate and the dissolved phases as a function of tides and seasons in a tidal creek. We were also interested in the relationships between physico-chemical parameters (pH, salinity, dissolved oxygen, dissolved organic carbon, particulate organic carbon, total suspended solid) and trace metals behaviors. Our main hypothesis was that dissolved metal concentrations in the tidal creek will increase during the ebb tide as a result of inputs from mangrove soils. To reach our goals, we collected suspended matters and waters every two hours during 24 h at different tidal cycles and in distinct seasons (dry and rainy). Physico-chemical parameters of the water column were also monitored continuously during the 24 h cycles, and groundwater tracer (^{222}Rn) was measured during the wet season.

5.2. Materials and Methods

5.2.1. Study site

Can Gio mangrove, 35,000 ha, represents 20% of the total mangrove area in Vietnam, and is situated just downstream Ho Chi Minh City (Viet Nam's biggest industrial city). The studied tidal creek, without any direct fresh-water inputs than rain, is situated in the core zone of Can Gio mangrove (10°30.399N-106°52.943E), and is its length is approximately 1,400 m (Fig. 5.1). The main economic activities of the local people in Can Gio are forest managements, aquacultures, fishing and salt production (Kuenzer and Tuan 2013). The mangrove forest covers over 40 % of the Can Gio district while rivers, creeks and water areas of the land – ocean cover 30 % involving

a complex estuarine system, where the Sai Gon, Dong Nai and Vam Co Rivers discharge into the South China Sea.

Can Gio mangrove is considered as one of the most beautiful mangrove forest of Southeast Asia, and is usually classified as "Mangrove afforestation and re-forestation area" (Blasco et al. 2001), and has been declared as a World's Biosphere Reserve by the UNESCO since 2000. The area of the reserve extends for 35 km from North to South and 30 km from East to West, comprising mostly a flat alluvial plain area with a basement of Neogene to Quaternary sediments below 3 m depths (Hirose 2004). The tidal regime is irregular semi-diurnal. The climate is typical of monsoonal zone with two distinct seasons, in which the dry season starts in November and lasts until the end of May, the wet season starts from the end of May until the end of October. The annual mean precipitation is about 1,300 to 1,400 mm, with ~ 90 % of the precipitation falling during the wet season and the annual mean temperature ranges from 26.5 °C to 30 °C. Can Gio Mangrove Biosphere Reserve has a high biodiversity with more than 200 species of fauna and 52 species of flora, the main mangrove species being *Rhizophora apiculata* and *Avicenia alba*, (Luong et al. 2015).

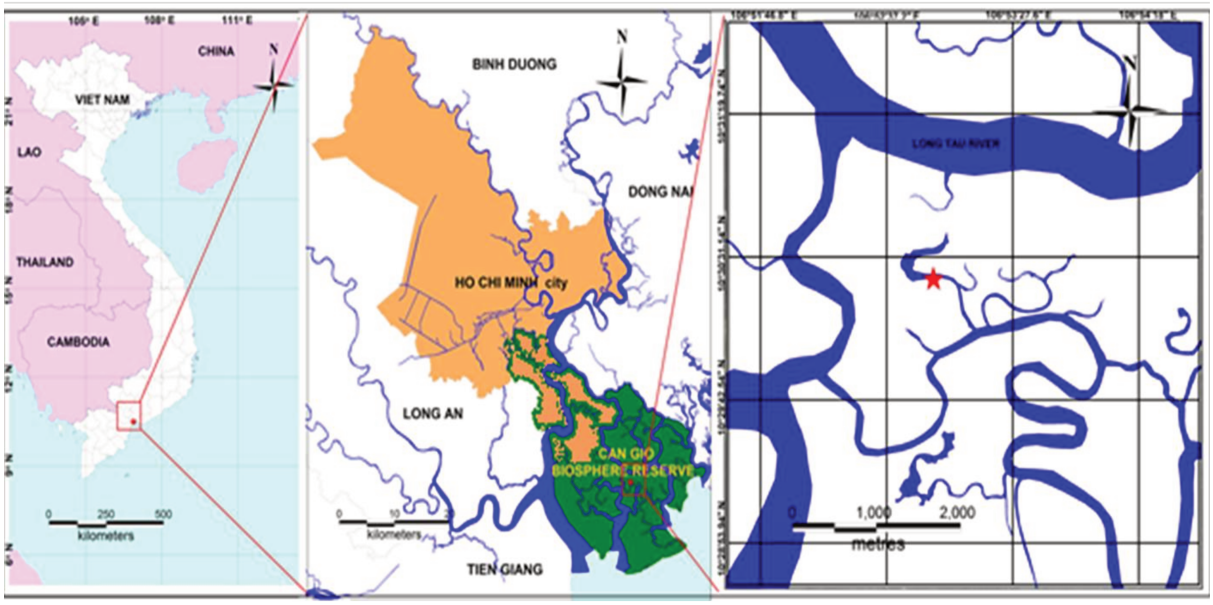

Fig. 5-1. Map of the study area showing: i) the location of Can Gio mangrove in Viet nam and ii) the location of the tidal creek in the mangrove (red star).

5.2.2. Field sampling

For each sampling period, during the dry season (April 11 – 12th and 18 -19th, 2015) and the wet season (October 18 – 19th and 26 – 27th, 2015), a boat was anchored in the middle of the tidal creek (Fig. 5.1). For each season, two 24-h time series were conducted during the asymmetric and symmetric tidal cycle. During each sampling campaign, surface waters (50 cm below the water surface) were collected every two hours (13 samples for 24 hours) in duplicates using pre-decontaminated bucket. Samples were immediately transferred into acid pre-cleaned polypropylene bottles (1 L) - previously rinsed with estuarine water. After that, a maximum volume of samples was filtered through 0.2 µm JG PTFE Omnipore™ Membrane Filters: the filtrates were then transferred into pre-cleaned 50 mL polypropylene tubes, immediately acidified to pH < 2 using concentrated suprapur® HNO_3 (*HNO_3:sample = 1:1000 (v/v)*) for dissolved trace metals analysis (Strady et al. 2009). The filters were kept in small plastic boxes with closed cover fir future analyzes of total trace metals in suspended particulate matter. Both types of samples were maintained in cooler box during sampling and stored at 4 °C at laboratory until metals analysis.

Filtration for the determination of total suspended solid (TSS) and future measurements of particulate organic carbon (POC), and dissolved organic carbon (DOC) were also simultaneously carried out as follows: water samples were filtered through pre-combusted and pre-weighted glass fiber filters (Whatman® GF/F 0.7 µm). Filters were stored at -20 °C, and the filtrates were transferred into sterile 15 mL polypropylene and then acidified using concentrated suprapur® HCl and stored at 4 °C until DOC analysis (Thanh-Nho et al. 2018).

Between the two 24-h time series (per sampling period), mangrove pore-waters were collected across two elevation/land cover transects, extending from the mangrove towards the tidal creek. Three holes beneath each zone, i.e. *R. apiculata*, *A. alba*, mudflat, were dug to approximately 1 m depth at low tide, using an Eijkelkamp gouge auger. The holes were purged at least two times with a hand pump, before sampling. All samples were filtered through 0.45 µm Sartorius® filter, kept in pre-cleaned 50 mL polypropylene and were then acidified to pH < 2 by concentrated suprapur® HNO_3 (Merck), and stored at 4 °C until analysis.

5.2.3. In situ measurements of physico-chemical parameters

Surface water salinity and pH were logged continuously using a multi-probe (Yellow Spring Instrument® meters YSI 6920). The pH probe was pre-calibrated using buffer solutions: 4, 7 and 10 (NIST scale). Dissolved Oxygen (DO) was monitored with a HOBO Dissolved Oxygen data logger (HOBO U26-001). These probes were immerged 50 cm below the water sruface and data were recorded every 5 min. Water level profile were measured using Hondex PS-7.

Three sediment cores (1 m depth) beneath each stand were collected using an Eijkelkamp gouge auger in the different stands for in-situ measurements of soil pH and salinity. For each parameter, the value was recorded every 10 cm. pH was measured using a glass electrode (pH 3110-WTW), which was pre-calibrated using pH 4, 7 and 10 standard buffer solution (NIST scale).

Salinities were determined using an ATAGO refractometer (S-10, Japan) after extracting a drop of pore-water from each sediment layer.

^{222}Rn is considered as a natural groundwater tracer, being widely used to quantify pore-water exchange in mangrove system (Maher et al. 2013, Tait et al. 2016). ^{222}Rn concentrations in water were measured during the wet season only, with the same equilibration technique, but using a showerhead equilibrator. The head-space gas was streamed into an automated ^{222}Rn-in-air analyzer with the Rad Aqua package installed (RAD 7, Durridge Co.) (Burnett et al. 2001). The ^{222}Rn monitor logged data at 30 min intervals, resulting in analytical uncertainty <10% for individual concentrations, except during the first three hours when the analytical uncertainty was 30%.

5.2.4. Samples analysis

Dissolved metals concentrations (M_D)

The Mn_D, Co_D and Ni_D concentrations were analyzed after matrix separation and pre-concentration by solid–liquid extraction, using 6 mL *DigiSEP* Blue® cartridges (SCP SCIENCE), with amino–di–acetate as the functional group. The experimental steps were described in details by Strady et al. (2009). The Fe_D was analyzed after 2-folds dilution with deionized water. These metal concentrations were then measured by ICP-MS (Agilent 7700x) using spike ^{103}Rh and ^{197}Au as internal standards. The analytical precision and accuracy were evaluated using certified reference material estuarine water (SLEW-3, Table 5.1a). All reagents were suprapur grade (Merck).

Particulate metal concentrations (M_p)

Particulate Fe, Mn, Co and Ni concentrations were quantified according to a total extractable metal digestion adapted from the USEPA 3051a method (USEPA 2007). The experimental steps and analytical evaluations were described in details by Thanh-Nho et al. (2018). In brief, the mixture of 6 mL concentrated HNO_3 and 2 mL concentrated HCl were used for samples

preparation. The Co_p and Ni_p concentrations were analyzed by ICP-MS (Agilent 7700x) using ^{103}Rh and ^{197}Au as internal standards. The Fe_p and Mn_p concentrations were measured using Flame Atomic Absorption Spectrophotometer (Shimadzu AA-6650). The analytical precision and accuracy were insured by analyzing certified reference material estuarine sediment (BCR-277R), which were also intercalated in each batch of samples digestion (Table 5.1b).

Table 5-1. Quality control of analytical methods applied for dissolved and particulate metal concentrations analysis:a) Accuracy, precision and detection limit using estuarine water SLEW-3; b) BCR-277R for wet digestion method.

a) Dissolved metal concentration analysis

Element	*Detection limit ($\mu g\ L^{-1}$)*	*Certificated values ($\mu g\ L^{-1}$)*	*Measured values ($\mu g\ L^{-1}$)*	*Recovery (%)*	*Relative standard deviation (%)*
Fe	0.20	0.568 ± 0.059	0.682 ± 0.068	120	10
Mn	0.09	1.61 ± 0.22	1.48 ± 0.10	92	7
Co	0.05	0.042 ± 0.010	0.0464 ± 0.0025	116	15
Ni	0.11	1.23 ± 0.07	1.37 ± 0.11	112	8

b) Particulate metal concentration analysis

Element	Certificated values ($mg\ kg^{-1}$)	Measured values ($mg\ kg^{-1}$, n = 9)	Recovery (%)	Relative standard deviation (%)	Analytical method
Fe	NA	51855 ± 3146	-	6.1	FAAS
Mn	NA	835 ± 29	-	3.5	FAAS
Co	22.5 ± 1.4	22.9 ± 0.7	102	2.8	ICP-MS
Ni	130 ± 8	128.9 ± 3.2	99	2.5	ICP-MS

Particulate organic carbon (POC) and dissolved organic carbon (DOC)

The DOC was measured on Shimadzu® TOC-L series analyzer employing a 680 ºC combustion catalytic oxidation method. The analyzer was coupled with a solid sample module (SSM-5000A) heated up to 900 ºC for the POC determinations (Leopold et al. 2013). A 40 % glucose standard was used for calibrations. Repeated measurements of different standards concentrations indicated deviations < 2 %.

5.2.5. Data calculations

The partitioning coefficient (K_D) was calculated to get a better understanding in the interaction of trace metals between dissolved and particulate phases during tidal cycles. K_D is defined as the

ratio of particulate metal concentration (M_P) to dissolved metal concentration in the water column (Turner et al. 1993).

$K_D = M_P / M_D$,

where, M_P is the particulate metal concentration and M_D is a dissolved metal concentration.

The Pearson correlation coefficient was performed using statistical package software (SPSS: version 23) to identify major relationships between metal concentrations and the physico-chemical parameters as well as interrelationships between metals together, which help to identify the main factors controlling metal partitioning.

5.3. Results

5.3.1. Pore-water characteristics

Salinity and pH values, as well as the average concentrations of trace metals (Fe, Mn, Co and Ni) in mangrove pore-waters at the two seasons, are presented in Table 5.2. They are mean values from all the samples collected in the three zones: mudflat, A. *alba*, *R. apiculata*. Salinity varied between 20 and 28 during the dry season, and between 14 and 22 during the rainy season. pH ranged between 4.6 and 6.7 during the dry season, and from 5.5 to 6.8 during the rainy season. Most of dissolved metals concentrations presented higher amplitudes during the wet season than the dry season with the exception of Co. Mean Fe concentrations were 1,203 ± 780 µg L^{-1} and 2,429 ± 2,744 µg L^{-1} during the dry and the wet season, respectively. Mean Mn concentrations were 1,523 ± 919 µg L^{-1} during the dry season, and 2891 ± 1768 µg L^{-1} during the monsoon. Co and Ni concentrations were far lower than Fe and Mn ones, being 9.4 ± 8.5 µg L^{-1} and 5.7 ± 0.9 µg L^{-1} for Co and 1.2 ± 0.8 µg L^{-1} and 9.0 ± 8.7 µg L^{-1} for Ni during the dry and the wet seasons, respectively.

Table 5-2. Average concentrations of dissolved trace metals (µg L-1, ± SD), pH, and salinity measured in the pore-water beneath the mangrove stands during the dry and the wet seasons. NA: non-available

	Fe (µg/L)	Mn (µg/L)	Co (µg/L)	Ni (µg/L)	pH	Sal
Dry season	1203 ± 780	1523 ± 919	9.4 ± 8.5	NA	4.6 - 6.7	20 – 28
Wet season	2429 ± 2744	2891 ± 1768	5.7 ± 0.9	9.0 ± 8.7	5.5 - 6.8	14 - 22

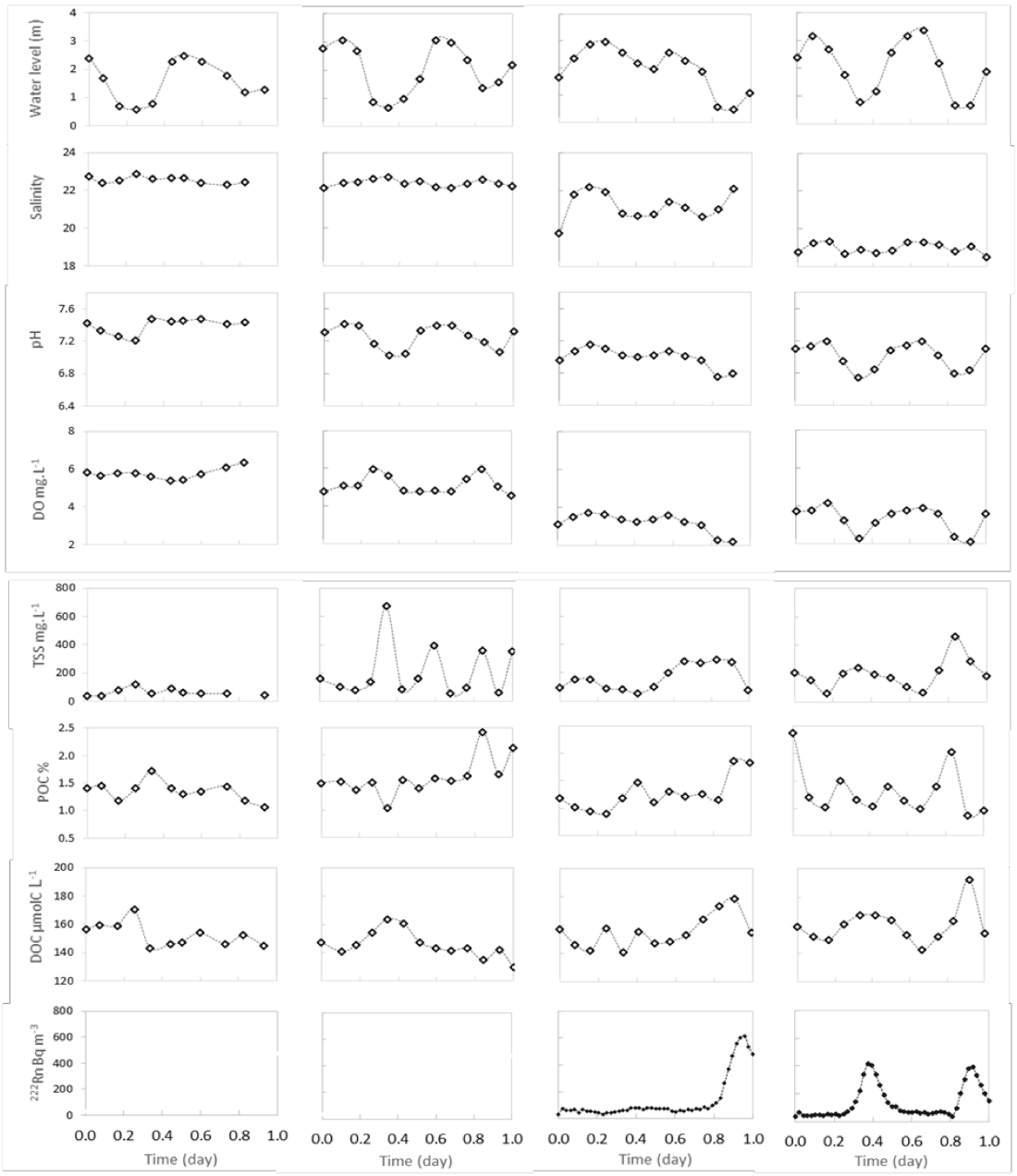

Fig. 5-2. Temporal variations of water level, salinity, pH, DO, TSS, POC and DOC observed in neap and spring tidal cycles during the dry season (04-2015) and the wet season (10-2015). The ^{222}Rn were measured only during the wet season.

5.3.2. Physico-chemical parameters variability in the tidal creek

The temporal variations of water levels, salinity, pH, DO, TSS, POC and DOC during the four tidal cycles are presented in Fig. 5.2. Salinity presented different distribution patterns between seasons, ranging between 22 and 23 and between 18.5 and 22 during the dry and wet seasons, respectively. The highest salinity values were measured at the lowest water levels during the dry season, while during the wet season, the opposite trend was observed. pH values varied from 7.0 to 7.5 during the dry season and from 6.7 to 7.2 during the wet season. DO was higher during the dry season than the wet one (4.6 to 6.4 mgO_2 L^{-1} versus 2.1 to 4.2 mgO_2 L^{-1}, respectively). TSS concentrations varied between the four tidal cycles (i.e. 36 to 119 mg L^{-1} in neap tide *vs* 60 to 675 mg L^{-1} in spring tide during the dry season; 54 to 291 mg L^{-1} *vs* 60 to 460 mg L^{-1} in neap and spring tides during the wet season, respectively). For each tidal cycle, the highest TSS concentrations were measured at the lowest water level. POC varied from 0.9 to 2.4 % for all tidal cycles. A higher POC amplitude was observed during spring tides (1.03 to 2.41 % and 0.87 to 2.37 % in the dry and the wet seasons, respectively) than neap ones (1.6 to 1.72 % and 0.9 to 1.6 % in the dry and wet seasons, respectively). The highest POC concentrations in each tidal cycle were measured at the lowest water level. DOC values were in the same range for all tidal cycles and varied from 129.5 to 192.1 µmolC L^{-1}. The maximum DOC values were observed at the lowest water level whatever the tidal cycle. ^{222}Rn concentrations in the surface water increased during the ebb and reached maximum values at the lowest water level for all tidal cycles (Fig. 5.2).

5.3.3. Variability of dissolved metals concentrations (M_D) in the tidal creek

The variations of Mn_D, Fe_D, Co_D and Ni_D during 24 h tidal cycles are presented in Fig. 5.3. Overall, all trace metals presented higher mean concentrations during the wet season than the dry season. Those metals showed higher concentrations in ebb periods compared with the flood periods. Mn_D increased during the ebb tides and reached up to maximum values at the lowest water

level for all tidal cycles i.e. 1,530 µg L^{-1} and 510 µg L^{-1} for neap and spring tides in the dry season, respectively whereas they were 1,779 µg L^{-1} for neap tide and 1,274 µg L^{-1} for spring tide during the wet season. The same patterns were observed for Fe_D with maximum values of 194 µg L^{-1}; 17 µg L^{-1}; 193 µg L^{-1} and 85 µg L^{-1} at lowest water levels for neap and spring tidal cycles in the dry season and the wet season, respectively. The Co_D concentrations varied from less than 0.1 µg L^{-1} up to approximately 2.0 µg L^{-1} during all tidal cycles. The highest Co_D was also observed during the periods of the lowest water levels. The Ni_D was unavailable during the dry season, and varied from 0.78 µg L^{-1} to 3.48 µg L^{-1} during the wet season, with high values also observed at low tidal periods.

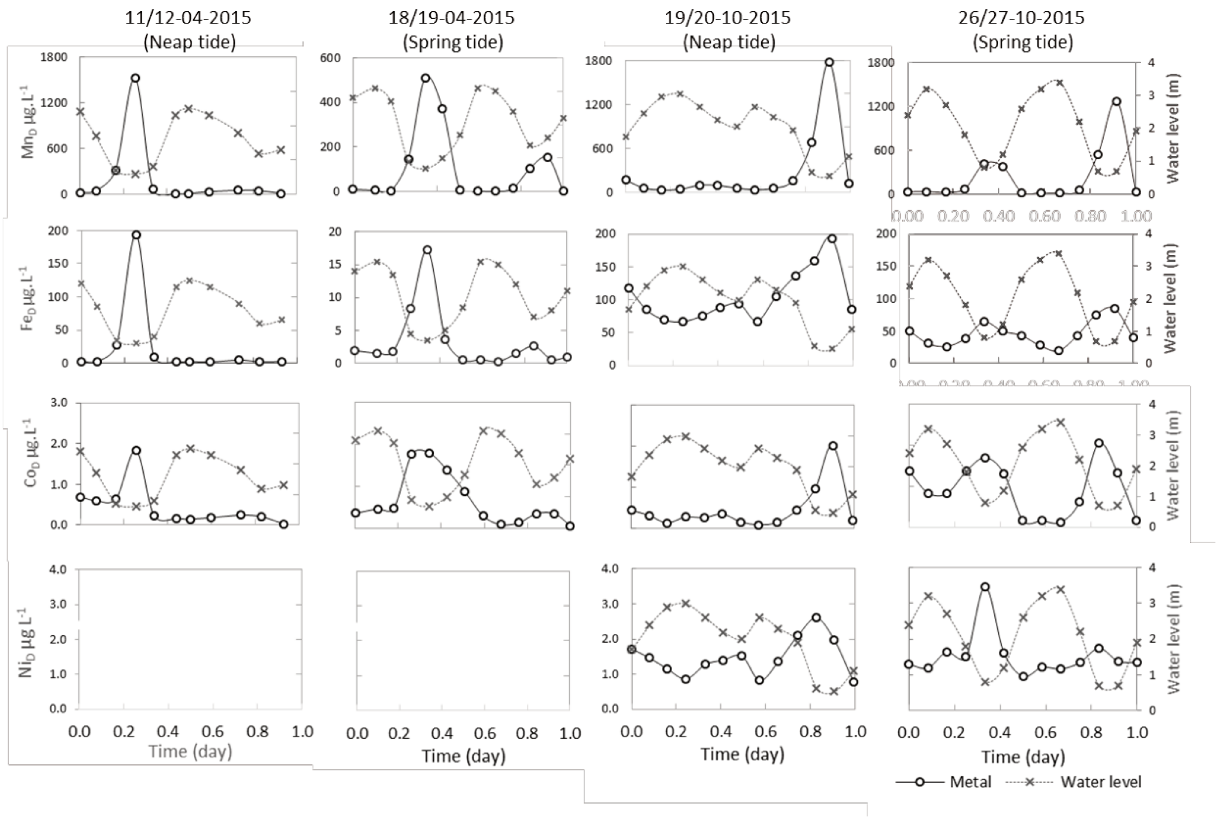

Fig. 5-3. Temporal distribution of dissolved concentrations of trace metals (MD) over the neap and the spring tidal cycles during the dry season (04.2015) and the wet season (10.2015). Dissolved Ni concentrations were measured only during the rainy season.

5.3.4. Variability of particulate metal concentrations (M_P) in the tidal creek

The fluctuations of Mn_p, Fe_p, Co_p and Ni_p concentrations during 24 h tidal cycles are showed in Fig. 5.4. The Mn_p and Fe_p showed an absence of seasonal effect. The Mn_P concentrations ranged from 320 mg kg^{-1} to 1,024 mg kg^{-1}, showing decreased values at ebb periods and dropping to minimum values at the lowest water levels. The Fe_p concentrations varied from 34,000 mg kg^{-1} to 50,000 mg kg^{-1} for all tidal cycles, with the highest values obtained at the lowest water levels. The Co_P concentrations were different range between seasons, ranging from 5.7 mg kg^{-1} to 11.7 mg kg^{-1} in the dry season and from 9.1 mg kg^{-1} to 19.8 mg kg^{-1} in the wet season. The Ni_P concentrations were quite constant during all sampling periods, showing higher concentrations in the wet season than in the dry season, with mean concentration of 42 mg kg^{-1} and 30.7 mg kg^{-1}, respectively.

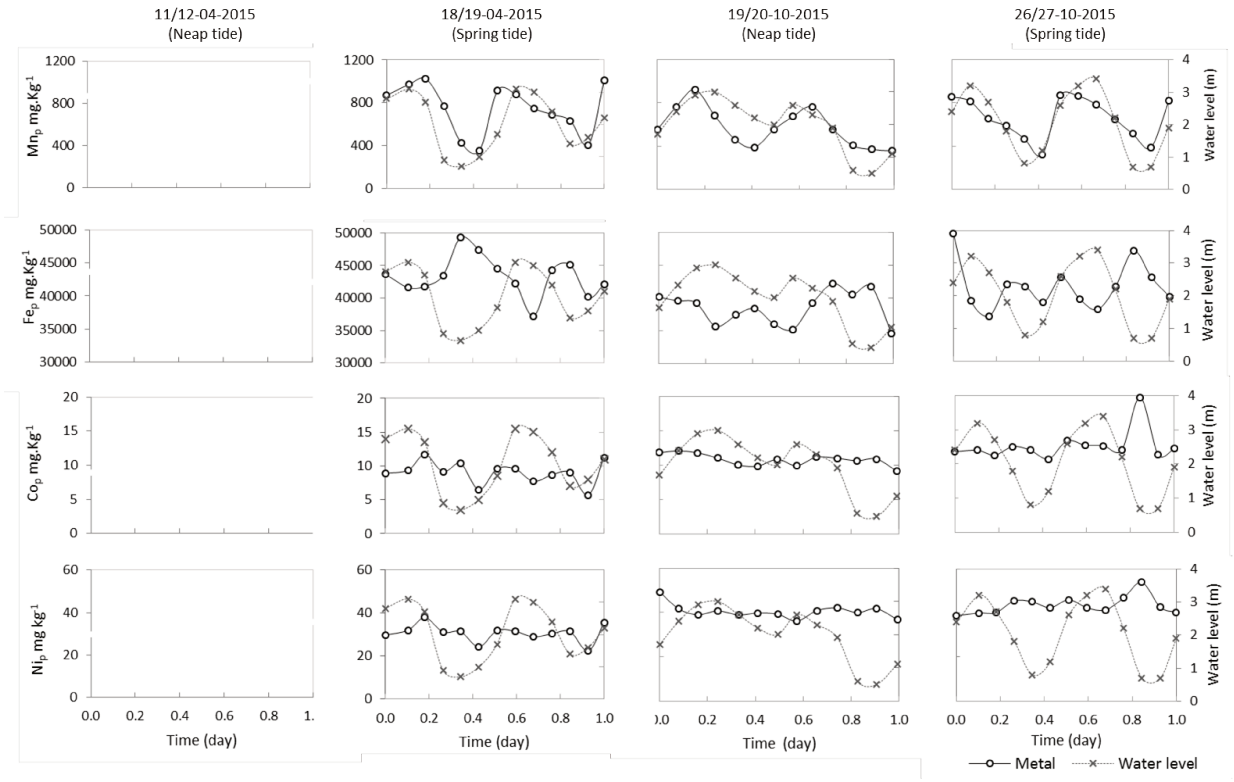

Fig. 5-4. Distributions of the particulate metal concentrations (Mp) over neap and spring tidal cycles during the dry season (04.2015) and the wet season (10.2015). The data of all trace metals within the neap tidal cycle in the dry season are not available.

5.4. Discussion

5.4.1. Temporal variability of physico-chemical parameters in the tidal creek

Because of the high productivity of mangrove forest, mangrove pore-waters are usually enriched in DOC (Marchand et al. 2006a). Additionally, mangrove soils are characterized by more acidic pH values than estuarine waters because of mangrove-derived organic matter decomposition and possible sulfide oxidation (Marchand et al. 2004, Marchand et al. 2012), which is consistent with our measurements on mangrove pore-waters. The observed correlations between ^{222}Rn and water level, pH, and DOC during ebb tide (Fig. 5.5a, 5.5b) provide strong evidences that tidal creek composition was partly controlled by pore-water inputs, even though other variables such as estuarine waters inflow during the flood and *in situ* biogeochemical processes may be involved. The key role of pore-water seepage on the composition of mangrove tidal creeks was recently evidenced in several studies (Bouillon et al. 2008, Call et al. 2015, Dittmar and Lara 2001, Maher et al. 2013). At low tide, DOC concentrations were higher and pH values were more acidic during the rainy season than during the dry season. These results may suggest a greater contribution of mangrove pore-waters to the tidal creek during the rainy season due to elevated volume of water exchanged between mangrove soils and mangrove creek, and also to a larger mangrove area immerged because of a higher water level. It can be also related to enhanced processes of organic matter decomposition in mangrove soils due to the higher temperature and the rainfall characterizing tropical regions (Taillardat et al., under revisions). In mangrove soils, salinity can be highly variable with depth and between mangrove stands, depending on the salinity of the incoming water (estuarine waters or rainfall) and on evapotranspiration processes (Marchand et al. 2004). However, the low salinity differences between the estuarine waters and the pore-waters, which was related to the tropical climate, prevent the use of salinity to trace pore-water inputs in the tidal creek studied. The intense rainfall occurring during the rainy season were responsible for

lower salinity values in the tidal creek. Concerning TSS, its variability in the tidal creek may depend on two processes; first it can increase during the ebb when the water column within the mangrove is low and the flow is rapid, which can induce an erosion of the upper mangrove soil; then it can increase at the lowest tide when bottom sediments of the tidal creek are re-suspended because of shallow waters. Mangrove soils are most of the time anoxic and contain thus very low oxygen content (Kristensen et al. 2017). Accordingly, at low tide during the rainy season, DO concentrations in the tidal creek were very low because of mangrove pore-water inputs, which is also consistent with our hypothesis of enhanced OM decomposition in mangrove soils during the rainy season. However and surprisingly during the spring tide of the dry season, we measured increased DO concentrations at low tide. (David et al. 2018) showed that algal cells can grow in tidal creek at low tide using nutrients and CO_2 provided by the tidal pumping of mangrove pore-water, and thus resulting in increased DO content, which can explain the observed results. There were no significant differences of POC concentrations between seasons, and most of the time POC concentrations were higher at low tide. In mangrove tidal creeks, POC concentrations significantly increased due to particle resuspension, either from mangrove soils or creek bottom (Bouillon et al. 2008).

5.4.2. Trace metals dynamics in the mangrove tidal creek

5.4.2.1 Manganese dynamic

The high Mn_p concentrations measured in the tidal creek during the flood periods irrespective of the seasons may be related to the high Mn_p concentrations measured at the mouth of the Can Gio mangrove estuary, reaching up to 800 mg kg^{-1} (Thanh-Nho et al. 2018). Consequently in the tidal creek studied, the positive correlations between Mn_p and the water levels during the dry and the wet seasons (r = 0.7 and 0.8, respectively, Fig. 5.5c) suggest that Mn_p mainly originated from the estuary. However, correlation between Mnp and TSS was low. As explained earlier TSS in the

tidal creek mainly depended on particle resuspension during the ebb, either from mangrove soils or creek bottom, while we consider that Mnp mainly originated from the estuary and thus increased in the tidal creek when the contribution of the estuarine waters increased, and thus with the flood. Variations of Mn_D concentrations in the tidal creek were the opposite of those of Mn_p, and increased with the ebb. In the Can Gio mangrove estuary, dissolved Mn concentrations were low, with a mean value of 1.3 µg L^{-1} (Thanh-Nho et al. 2018), which corresponds to what we measured in the creek at high tide. However at low tide, Mn_D concentrations in the tidal creek reached up to 1800 µg L^{-1} (Fig. 5.3). Therefore, the contribution of other sources of Mn_D to the creek is suggested. Considering that we measured positive correlations between Mn_D and ^{222}Rn (r = 0.94, Fig. 5.6a), but also between Mn_D and DOC (r = 0.72 and 0.79 during the dry and the wets seasons, respectively, Fig.6f), we suggest that Mn_D, like DOC, originated from mangrove soils, and were exported trough pore-water seepage as observed in Australian mangroves (Holloway et al. 2016). It is also possible that organo-manganese complexes were formed, explaining the correlation between DOC and Mn_D. Previous studies described the coupling between DOC and redox sensitive elements, like Mn (Dang et al. 2015).

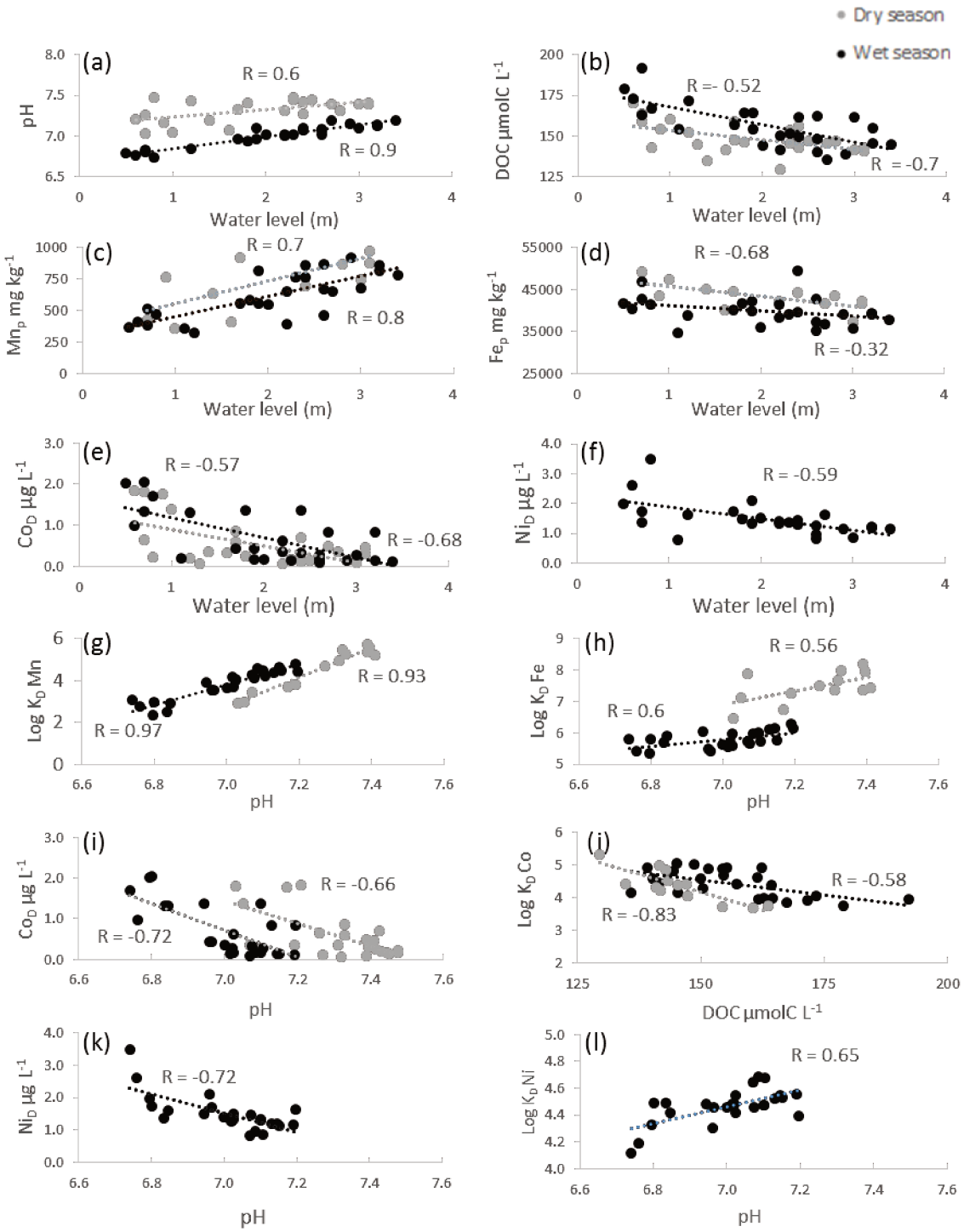

Fig. 5-5. Correlations between dissolved, particulate metal concentrations, physico-chemical parameters, and water level over all tidal cycles. The interrelationships between Log K_D of trace metals and physico-chemical parameters are also presented.

In Can Gio mangrove sediments, metals have a natural origin, being deposited in the mangrove mainly as oxihydroxides coming from the upstream lateritic soils (See Chapter three of this thesis).

However, the enrichment of mangrove-derived organic matter from the mudflat to the *Rhizophora* stand induced the reductive dissolution of Fe-Mn oxihydroxides by bacteria for organic matter decay processes, which were a source of dissolved trace metals in pore-waters, with MnD in pore-waters reaching up to 2891 ± 1768 µg L^{-1} (Table 5.2). In addition in the tidal creek, Log K_D^{Mn} varied in a larger range, from 2.32 to 5.72 (Fig. 5.7), than in the Can Gio estuary, from 4.5 to 5.8 (Thanh-Nho et al. 2018). We suggest that the drop of Log K_D^{Mn} observed at the low tides during both seasons may result from the increasing pore-water Mn_D inputs. The positive correlation between Log K_D^{Mn} and the water level may be related to the decrease of dissolved Mn by the physical mixing between pore-water and estuarine water, containing lower Mn_D concentrations. Additionally, we observed that the highest Mn_D concentrations were measured at the low tide of high amplitude cycle following a tidal cycle of low amplitude (Fig. 5.3). We suggest that due to the low amplitude of the previous tidal cycle, Mn_D produced by Mn oxi-hydroxide dissolution was not exported but accumulated in the soil, and was exported during the tidal cycle with a higher amplitude. Consequently, in the specific system of Can Gio, the intensity of the export of dissolved Mn was not only related to the alternation between spring tide and neap tide, but also to the irregularity of the tides. Eventually, we measured higher Mn_D concentrations in the tidal creek during the rainy season. We suggest that these higher concentrations were related to higher Mn_D concentrations in pore-waters (Table 5.2). Taillardat et al. (under revisions) suggested that during the rainy season, the elevated temperature and the high rainfall induced enhanced mineralization rates, which may have resulted in higher Mn_D production in mangrove soils. In addition during the rainy season, the water level of the river and thus of the tidal creek were higher. Consequently at high tide, mangrove immersion was more important during the rainy season, which may have induced increased exchanges between mangrove soils and tidal creek, also possibly partly

explaining the higher Mn_D in the tidal creek during the rainy season. These results confirm those of Holloway et al. (2016), who showed that pore-water exchange can release large amounts of dissolved Mn to mangrove creeks, and then to the nearby ocean surface water.

5.4.2.2 Iron dynamics

In the mangrove tidal creek studied, Fe, which is like Mn a redox sensitive element (Lacerda et al. 1999), presented the same variability than Mn in the dissolved phase but the opposite one in the particulate phase. In fact, the highest Fe_p concentrations were measured at low tide (Fig. 5.4) irrespective of the season or the tidal range, reaching almost 50,000 mg kg^{-1} during the rainy season. Conversely at high tide, Fe_p varied between ~35,000 and 45,000 mg kg^{-1}, which was the same range than what was measured in the Can Gio estuary for a similar range of salinity than in the tidal creek (Thanh-Nho et al. 2018). Consequently, we suggest that at high tide in the creek, Fe_p concentrations were related to the estuarine inputs and originated from the lateritic soils in Can Gio watersheds. In the Can Gio estuary, Fe_D concentrations were never higher than 30 µg L^{-1}, while at low tide in the tidal creek, they reached almost 200 µg L^{-1}. So like for Mn_D, another source than the estuarine waters must be considered. In mangrove pore-waters, mean Fe_D concentrations were 1,200 and 2,400 µg L^{-1} during the dry and the rainy season, respectively (Table 5.2). As explained for Mn, Fe oxihydroxide dissolution in suboxic conditions during OM diagenetic processes were responsible for these elevated concentrations (See chapter three of this thesis), and the high temperature and intense rainfall, enhancing OM decomposition, induced the higher concentrations measured during the rainy season. Consequently, we suggest that pore-water seepage was responsible for the high Fe_D concentrations measured in the tidal creek at low tide, which were even higher during the wet season because of increased geochemical processes in mangrove soils.

This hypothesis was confirmed by the positive correlations between dissolved Fe_D concentrations and ^{222}Rn (r = 0.63, Fig. 5.6b). However, the correlation was less strong than the one between Mn_D and ^{222}Rn (Fig. 5.6a), which possibly suggest that Fe_D was subject to biogeochemical processes. In addition, Fe_D and Mn_D concentrations in mangrove soil pore-waters were in the same range, but at low tide in the tidal creek, when pore-water inputs were maximum, Fe_D concentrations were 10 times lower than Mn_D. However and conversely to Mn_p, Fe_p concentrations in the tidal creek were maximum at low tides, with higher values than those we measured in the estuary. Consequently, we suggest that, because of different physico-chemical properties between the tidal creek and mangrove soils, notable O_2 and pH, part of the dissolved iron that was exported from mangrove soil precipitated in the creek, explaining the high Fe_p concentrations measured at low tide and the fact that Fe_D concentrations were 10 times lower than Mn_D. In mangrove soils, pH ranged from 4.6 to 6.8 (Table 5.2, and chapter three of this thesis), while in the tidal creek at low tide, it was always higher than 6.5, which can favor Fe_D precipitation (Hatje et al. 2003). This hypothesis could be supported by the positive correlation between Log K_D^{Fe} and pH (r = 0.56 and 0.60 during the dry and the wet season, respectively, Fig. 5.5h), and by the positive correlation between Log K_D^{Fe} and the water level. In addition in the tidal creek, Log K_D^{Fe} ranged from 5.33 to 8.19 (Fig. 5.7), while in the Can Gio estuary, Log K_D^{Fe} varied between 6.39 and 7.6 (Thanh-Nho et al. 2018).

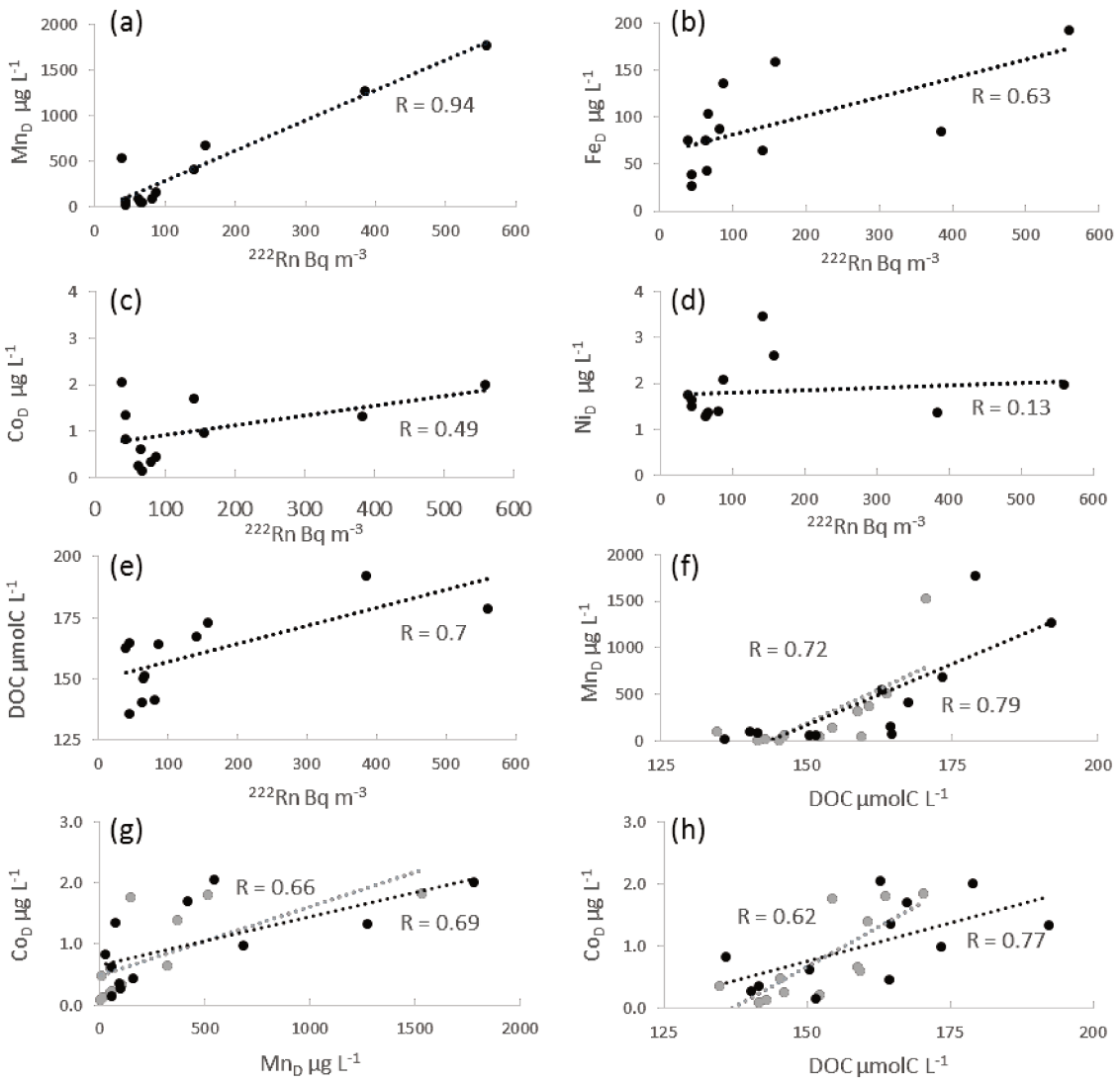

Fig. 5-6. Interrelationships between trace metals and 222Rn in the ebb periods during the wet season (black dots), and during the dry (gray dots): (a) Mn_D, (b) Fe_D, (c) Co_D, (d) Ni_D and $_{222}Rn$; (e) DOC and ^{222}Rn, (f) Mn_D and DOC, (g) Co_D and Mn_D, (h) Co_D and DOC.

Eventually at low tide, TSS increase in the tidal creek, because of resuspension of bottom sediments due to the low water depth, may also partly explain the higher Fe_p concentrations. However, the different dynamic between Fe and Mn in the creek evidenced that Fe_p distribution was not only related to physical processes but that geochemical processes were involved, like Fe_D precipitation or colloidal flocculation. These results confirmed those obtained by Sanders et al. (2015), who suggested that small tidal estuaries may be important conduits for dissolved Fe to the

ocean. However, we suggest that the great variability of pH and O_2 in mangrove ecosystems may limit this export under the dissolved form. Our results also confirm the hypothesis developed by Thanh-Nho et al. (2018) of an input of Fe_p from mangroves to the estuary, where they measured increased Fe_p concentrations at the "mangrove" station. In addition, like observed for different forms of carbon (Call et al. 2015, Maher et al. 2013), the type of tides and their ranges influenced Fe concentrations in the tidal creek, being higher when a large tidal range followed a small one because of elevated water residence time in the mangrove and larger mangrove area immerged.

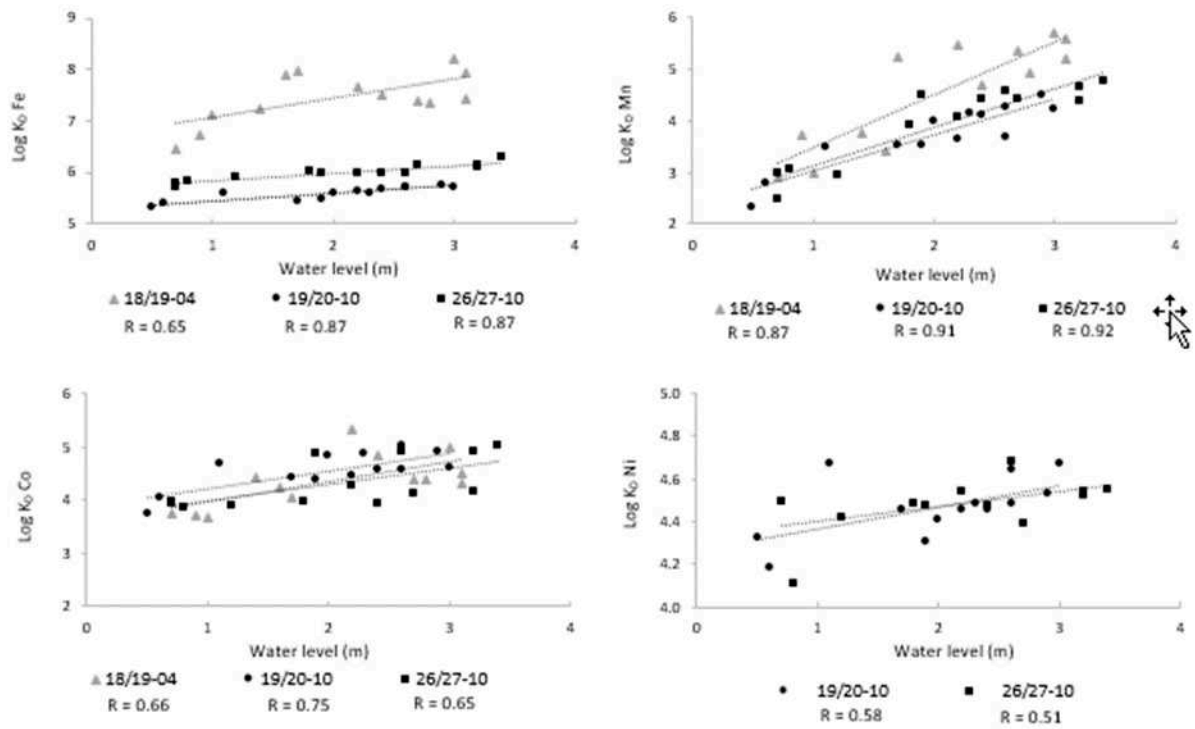

Fig. 5-7. Correlations between Log K_D of trace metals and water level in all tidal cycles in the creek during the dry (gray dots) and the wet seasons (black dots).

5.4.2.3 Cobalt and Nickel dynamics

Because of their similar distributions in dissolved and particulate phases in the mangrove tidal creek, Co and Ni were discussed together. Surprisingly, we did not observe any significant difference of Co_p and Ni_p concentrations between low tide and high tide. For similar salinity values in the estuary, Co_p concentrations ranged between 10 and 20 µg L^{-1}, and Ni_p between 40 and 50

μg L^{-1} (Thanh-Nho et al. 2018), which was similar to what we measured in the tidal creek. We, thus, consider that estuarine waters were the main sources of Co_p and Ni_p in the tidal creek. However, the highest concentrations of Co_p and Ni_p were measured at the lowest water level during spring tide in the wet season (Fig. 5.4), which may suggest that these two elements were subject to the same geochemical processes than iron, being exported from mangrove soils under dissolved form and precipitating in the creek. This process may also explain the almost stable concentrations measured in the creek whatever the tidal period, without Co and Ni precipitations at low tide, a decrease of their concentrations would have been observed. In fact, Co_D and Ni_D presented higher concentrations in the creek water than the mouth of the Can Gio mangrove estuary irrespective of the season, with mean concentrations lower than 0.1 μg L^{-1} for Co_D and lower than 1.0 μg L^{-1} for Ni_D irrespective of the season (Thanh-Nho et al. 2018). We suggest that the increasing Co_D and Ni_D concentrations during the ebb resulted from pore-water inputs, being consistent with the negative correlations between Co_D, Ni_D and water levels during the tidal cycles (r = -0.57; -0.68 for Co_D during the dry and the wet season, Fig. 5.5e; and r = -0.59 for Ni during the wet one, Fig. 5.5f). However, we did not observe good correlations between Co_D, Ni_D and ^{222}Rn (Fig. 5.6c and 6d), most probably because, like we suggested, these elements were subject to geochemical processes during their transfer from the soil to the creek and also in the creek. Like for Mn_D, Co_D concentrations in the tidal creek were positively correlated to DOC (r = 0.62; 0.77 with DOC during the dry season and the wet season, respectively) (Fig. 5.6h). Like for Mn, in addition to a common origin, i.e. mangrove pore-waters, we suggest the formation of organo-cobalt complexes, which may have increased the mobility of Co_D during its transfer from the pore-water to the tidal creek (Noble et al. 2008). Log K_D^{Co} presented a large range of values, from 3.7 to 5.3, being positively correlated with the water level (Fig. 5.7). As a result of pore-water inputs, Log K_D^{Co}

decreased during the ebb (Fig. 5.7). During the flood, Co_D may be adsorbed onto Fe-oxihydroxide as they precipitate because of variable redox and pH conditions (Murray and Dillard 1979). This hypothesis may be supported by the negative correlation between Co_D and pH (r = -0.66 and -0.72 during the dry and the wet season, respectively, Fig. 5.5i) and by the negative correlation between Log K_D^{Co} and DOC (r = -0.83 during the dry season and r = -0.58 during the wet season, Fig. 5.5j). Furthermore, the Co_D decrease during the flow can result from the physical mixing of the creek water with the estuarine water, containing lower Co_D concentrations.

Similarly to Co, Log K_D^{Ni} was positively correlated with the water level (Fig. 5.7), implying that physico-chemical processes also played key roles in Ni partitioning in the tidal creek. During the flood, decreasing Ni_D concentrations in the tidal creek most probably resulted from the dilution by the estuarine water, containing lower Ni_D, and/or from the adsorption onto TSS and the precipitation with Fe oxihydroxides. The later hypothesis may be supported by the negative correlation between Ni_D and pH (r = -0.72 during the dry season, Fig. 5.5k). This result was consistent with the positive correlation between Log K_D^{Ni} and pH (r = 0.65, Fig. 5.5l).

5.5. Conclusions

This study evidences that mangrove soils can lose part of their trace metals stocks, exporting dissolved trace metals in tidal creeks during ebb tide through pore-water seepage. Consequently, the role of trace metal sinks of mangrove may be questioned and budget studies must be developed. The main conclusions of this study can be summarized as follow:

1) Tidal ranges and irregularities of the tidal cycle influence trace metals concentrations in the tidal creek, by controlling pore-water seepage. A larger area of mangrove immerged and an increased residence time of the water in the mangrove, like what happened when a strong tide followed a small one, result in enhanced export of trace metals in the tidal creek during the ebb.

2) The high temperature characterizing tropical region, and the heavy rainfall occurring during the monsoon, may be responsible of enhanced geochemical processes in mangrove soils, resulting in elevated dissolution of metals bearing phases and thus in higher trace metals export during the rainy season.

3) Large amount of dissolved Mn, originated from mangrove soils, were exported from the tidal creek to the estuary and possibly to the coastal ocean.

4) Geochemical processes in the tidal creek modified trace metals partitioning. We suggest that part of the dissolved iron exported from mangrove soils, but also to a lesser extent dissolved nickel and cobalt, precipitated in the tidal creek due to different physico-chemical properties than in mangrove soils; colloidal flocculation may also be involved in particulate Fe, Ni, Co distribution in the creek. Consequently, these elements were mainly exported in the particulate form explaining the high concentrations measured in the estuary (See Chapter two of this thesis).

Chapter 6 - Conclusions and Perspectives

6.1. Conclusions

The purpose of this PhD thesis was to understand trace metals cycling in the Can Gio mangrove forest, which is located at the edge of the densely populated megacity - Ho Chi Minh City and the South China Sea.

Despite being situated downstream the biggest city in Vietnam, Can Gio mangrove sediments did not present high trace metal concentrations. We suggest that the main sources of trace metals in the mangrove were natural, and were the lateritic soils (i.e. rich in oxihydroxides) of the Sai Gon-Dong Nai Rivers watersheds (Chapter 3). During the wet season, heavy rainfall induced increased runoff and soil leaching, resulting in enhanced trace metal inputs to the estuary, both in particulate and dissolved phases (Chapter 2). However, as soon as trace metals enter the estuary, their distribution and partitioning changed due to the physical mixing with seawater and/or biogeochemical processes, notably organic matter (OM) decay processes. Total suspended matter (TSM) was proved to be the main carrier for trace metals during their transports to the ocean. However, TSM variations did not fully explain the fluctuations of trace metals distribution along the salinity gradient. Extra inputs, like runoff from adjacent mangrove sediments but also pore-water seepage, were suggested to be involved in trace metals dynamics in the Can Gio mangrove estuary. We suggest that the bacterial reductive dissolution of oxihydroxides in mangrove sediments during mineralization of OM in suboxic condition released dissolved trace metals in the pore-waters (chapter 3), which were then exported towards tidal creeks and eventually to the estuary. As a result of their high redox sensitive, dissolved Fe and Mn concentrations were dominant in mangrove pore-waters. Tidal ranges and irregularities of the tidal cycles influenced trace metals concentrations by controlling pore-water seepage. We also suggest that during the monsoon the change in temperature and heavy rainfall may be responsible for enhanced

biogeochemical processes in mangrove sediments, resulting in elevated dissolution of metals bearing phases and thus in higher trace metals exports during the rainy season. In addition, when delivered to the tidal creek under dissolved form, trace metals can precipitate because of different physico-chemical conditions, and be exported to the estuary under particulate form, like iron. Along the estuary, OM appeared to play a key role in trace metals partitioning, specifically for As and Cr. OM decomposition with increasing O_2 content resulted in As and Cr increases in dissolved phase. Conversely, Mn dynamic was strongly influenced by oxygenation and pH changes, which induced the decrease of dissolved Mn concentrations by precipitation of oxihydroxides. The absence of specific correlations between the Log K_D of Fe, Co, Pb and physico-chemical parameters did not allow us to better characterize these metals partitioning in this estuary. Irrespective of the season, Ni was poorly reactive, and physical mixing was the main factor controlling its distribution in the Can Gio mangrove estuary.

Furthermore, Can Gio mangrove sediments acted as a natural biogeochemical reactor, inducing modification of trace metals bearing phases (Chapter 3). Redox cycling in sediments impacted the Fe-Mn oxides dissolution, and subsequently the metals geochemistry across the intertidal zones. Depending on specific characteristic of metals and on the redox condition, dissolved metals from reductive dissolutions were re-precipitated with new bearing phases: organic matter, carbonates or sulphides. Most of metals partitioning beneath the *Avicennia* stand and the mudflat was similar with high proportion of the lithogenous fraction (except Mn, which was mostly present in the available fractions, especially in the exchangeable/carbonate bound one). Trace metals partitioning beneath the *Rhizophora* stand was different. We suggest that the organic enrichment of the sediment from the mudflat to the *Rhizophora* stand played a key roles on this difference, with a

decrease of the residual phases associated with increases in the organic fraction and in the total available fractions toward the inner mangrove forest.

We observed that trace metals can be transferred from mangrove sediments and the pore-waters into mangrove biota's tissues (plants and snails) via both active and passive processes, and that the degree of trace metals concentrations in their tissues depended on the availability of trace metals in their habitats (Chapter 4). For plants, mangrove roots can be considered as "phytostabilizators", immobilizing and limiting Fe and As translocation to aerial part. Conversely, Mn and Cu presented high translocation factors. As a result of high BCF in roots and leaves associated with high TF, *Rhizophora* trees can be considered as Mn "phytoextractors". We suggest that strong plants uptake and pore-water seepage of trace metals to the water column could induce the decrease of trace metals stocks in the sediment beneath mangrove vegetation, especially in the *Rhizophora* stands (Chapter 3). Cr and Ni showed low BCF in both roots and leaves as a result of their low bioavailability in the sediment. Concerning snails, the concentrations of Fe, Mn and Cu were higher than those As, Ni, Cr and Co in their tissues. Among non-essential elements, all snail contained higher As concentration in their tissues than other metals as a result of its high bioavailability in the sediment. Concerning *Littoraria* (leaves eater) and *Cerithidea* (sediment eater), metals concentrations in their tissues were related to the trace metals amount in their habitat. In fact, both snails species contained higher metals concentrations in the *Rhizophora* stand than in the *Avicennia* one, as a result of higher trace metals in available fractions in the sediment beneath *Rhizophora.*

The findings of my PhD thesis contribute in several ways to our understanding of the role of mangrove forest on trace metal cycling and provide basis for further investigations concerning trace metal pollutants in the Can Gio mangrove. This work also offers valuable insights into the

fate of trace metals in the tropical mangrove ecosystem and thus make several contributions to the current literature.

6.2. Research Perspectives

6.2.1. Seasonal effect on trace metals geochemistry in mangrove sediments

Metal speciation in mangrove sediments depends on one or several sediment properties: pH, organic matter, clay content, redox potential, salinity, the quality and quantity of suspended matter (e.g. organic and inorganic), iron and manganese oxihydroxides (Marchand et al. 2012). Seasonal and meteorological conditions associated with tidal amplitude and flooding characteristics are probably the most important variables to consider for describing the biogeochemical processes in mangrove sediments and pore-waters. Complex redox cycling in mangrove sediments may thus significantly impact the speciation of metal elements across the intertidal zone (Clark et al. 1998, Tam and Wong 2000). Thus, a further investigation on the trace metal geochemistry in the sediment collected during the dry season, with lower temperature and the absence of rainfall, should be carried out to get a better understanding of the full fate of trace metals in the Can Gio mangrove forest and to further provide a data of trace metals geochemistry in a tropical mangrove to current literature.

6.2.2. Estimate trace metals budget in mangrove ecosystem

The present study evidenced that mangrove sediments can lose part of their trace metals stocks beneath mangrove vegetation (chapter 3), exporting dissolved trace metals in tidal creeks during ebb tide through pore-water seepage (chapter 5). This processes lead to high concentration of Mn in tidal creeks. Consequently, the role of trace metal sinks of mangrove may be questioned and budget studies must be developed. In previous study, Holloway et al. (2016) reported that pore-water exchange can release large of dissolved Mn to mangrove creek with much of Mn subsequent exported to the nearby ocean surface water along the latitudinal gradient from 28°S to 12°S in

Australia. When compare to dissolved Mn concentrations of these mangrove in Australia, our findings are of higher order of magnitude both in the pore-waters and in the tidal. In addition, the Fe and Mn concentrations in Can Gio mangrove sediment were higher than those measured in the other tropical mangroves (Alongi et al. 1998, Sanders et al. 2015). Consequently, further research need be conducted to determine trace metals budgets in mangroves, to precisely quantify the amount of metals deposited each year and the one that is exported from the mangrove to the ocean. The further data could provide more understanding of the trace metals dynamics along the latitudinal gradient.

6.2.3. Trace metals bioaccumulations in coastal trophic chain

Trace metals can accumulate in the organs and tissues of aquatic organisms at higher concentrations than those in water. Moreover, some of them can be biomagnified in the food web and can cause negative biochemical and physiological effect to top predators, including human (Al-Reasi et al. 2007, Borrell et al. 2016). In particular, arsenic, a toxic metalloid with geogenic source (Järup 2003), presented high concentration in pore-waters and high bioavailability in Can Gio mangrove sediments (chapter 3). In addition, some trace metals were not studied in the present PhD as Cd, Pb, Hg, etc., which are known to be toxic for human health (Li et al. 2015). The fish is the important natural resources for local people, being high economic values (Kuenzer and Tuan 2013). Therefore, controlling the levels of trace metals accumulation in fishes may be required to protect human health in the future.

6.2.4. Comparison of trace metals exports with other mangroves characterized by higher trace metals loads.

In New Caledonia, one third of the island is composed of ultramafic rock, and lateritic soils rich in metals as Fe, Ni and Cr. Marchand et al. (2012) stated that the erosion can lead to the deposit of huge quantities of these metals in mangrove including Mn, and that the dissolved metals in pore-

water presented higher concentrations than those measured in Can Gio mangrove, specifically for dissolved Ni concentration presenting approximately 100-fold higher. Because of these differences in climate and tidal regime (i.e diurnal tidal range), we suggest an investigation to estimate quantify trace metals exports from New Caledonian mangrove sediment to tidal creeks and further to the lagoon, which is the biggest one in the world. These further findings could provide a significant data in the contribution of trace metals budgets to the ocean.

REFERENCES

Abohassan R. A. (2013). Heavy metal pollution in Avicennia marina Mangrove systems on the Red Sea Coast of Saudi Arabia. Journal of King Abdulaziz University: Metrology, Environment and Arid Land Agricultural Sciences 24(1), 35-53.

Abraitis P., Pattrick R. and Vaughan D. (2004). Variations in the compositional, textural and electrical properties of natural pyrite: a review. International Journal of Mineral Processing 74(1-4), 41-59.

Abril G., Nogueira M., Etcheber H., Cabeçadas G., Lemaire E. and Brogueira M. J. (2002). Behaviour of Organic Carbon in Nine Contrasting European Estuaries. Estuarine, Coastal and Shelf Science 54(2), 241-262.

Acosta J., Jansen B., Kalbitz K., Faz A. and Martínez-Martínez S. (2011). Salinity increases mobility of heavy metals in soils. Chemosphere 85(8), 1318-1324.

Agoramoorthy G., Chen F. A. and Hsu M. J. (2008). Threat of heavy metal pollution in halophytic and mangrove plants of Tamil Nadu, India. Environmental Pollution 155(2), 320-326.

Al-Reasi H. A., Ababneh F. A. and Lean D. R. (2007). Evaluating mercury biomagnification in fish from a tropical marine environment using stable isotopes (δ13C and δ15N). Environmental Toxicology and Chemistry 26(8), 1572-1581.

Almeida C. M. R., Mucha A. P. and Vasconcelos M. T. S. (2006). Comparison of the role of the sea club-rush Scirpus maritimus and the sea rush Juncus maritimus in terms of concentration, speciation and bioaccumulation of metals in the estuarine sediment. Environmental Pollution 142(1), 151-159.

Alongi D., Boyle S., Tirendi F. and Payn C. (1996). Composition and behaviour of trace metals in post-oxic sediments of the Gulf of Papua, Papua New Guinea. Estuarine, Coastal and Shelf Science 42(2), 197-211.

Alongi D., Sasekumar A., Tirendi F. and Dixon P. (1998). The influence of stand age on benthic decomposition and recycling of organic matter in managed mangrove forests of Malaysia. Journal of Experimental Marine Biology and Ecology 225(2), 197-218.

Alongi D., Tirendi F. and Clough B. (2000). Below-ground decomposition of organic matter in forests of the mangroves Rhizophorastylosa and Avicenniamarina along the arid coast of Western Australia. Aquatic Botany 68(2), 97-122.

Alongi D. M. (2002). Present state and future of the world's mangrove forests. Environmental Conservation 29(03), 331 - 349.

Alongi D. M., Wattayakorn G., Boyle S., Tirendi F., Payn C. and Dixon P. (2004). Influence of roots and climate on mineral and trace element storage and flux in tropical mangrove soils. Biogeochemistry 69, 105–123.

Ambus R. and Lowrance R. (1991). Comparision of denitrification in two riparian soils. Soil Science Society of America Journal 95, 994 - 997.

Amin B., Ismail A., Arshad A., Yap C. K. and Kamarudin M. S. (2009). Gastropod assemblages as indicators of sediment metal contamination in mangroves of Dumai, Sumatra, Indonesia. Water, Air, and Soil Pollution 201(1-4), 9-18.

Anawar H. M., Akai J., Komaki K., Terao H., Yoshioka T., Ishizuka T., Safiullah S. and Kato K. (2003). Geochemical occurrence of arsenic in groundwater of Bangladesh: sources and mobilization processes. Journal of Geochemical Exploration 77(2-3), 109-131.

Angel B., Hales L. T., Simpson S. L., Apte S. S., Chariton A. A., Shearer D. and Jolley D. F. (2010). Spatial variability of cadmium, copper, manganese, nickel and zinc in the Port Curtis Estuary, Queensland, Australia. Marine and Freshwater Research 61(2), 170-183.

Antoniadis V. and Alloway B. (2002). The role of dissolved organic carbon in the mobility of Cd, Ni and Zn in sewage sludge-amended soils. Environmental Pollution 117(3), 515-521.

Asher C. and Reay P. (1979). Arsenic uptake by barley seedlings. Functional Plant Biology 6(4), 459-466.

Azevedo A., Holanda J. and Scudelari A. (2009). Dynamic of Heavy Metals in the Shrimp Farm Environment. Journal of Coastal Research, 1174-1178.

Babukutty Y. and Chacko J. (1995). Chemical partitioning and bioavailability of lead and nickel in an estuarine system. Environmental Toxicology and Chemistry 4(13), 427-434.

Baker A. J. (1981). Accumulators and excluders-strategies in the response of plants to heavy metals. Journal of plant nutrition 3(1-4), 643-654.

Bandaranayake W. (1998). Traditional and medicinal uses of mangroves. Mangroves and Salt Marshes 2(3), 133-148.

Bauer M. and Blodau C. (2006). Mobilization of arsenic by dissolved organic matter from iron oxides, soils and sediments. Science of the Total Environment 354(2-3), 179-190.

Bayen S. (2012). Occurrence, bioavailability and toxic effects of trace metals and organic contaminants in mangrove ecosystems: a review. Environment International 48, 84-101.

Benoit G., Oktay-Marshall S., Cantu A., Hood E., Coleman C., Corapcioglu M. and Santschi P. (1994). Partitioning of Cu, Pb, Ag, Zn, Fe, Al, and Mn between filter-retained particles, colloids, and solution in six Texas estuaries. Marine Chemistry 45(4), 307-336.

Benson N. U., Udosen E. D., Essien J. P., Anake W. U., Adedapo A. E., Akintokun O. A., Fred-Ahmadu O. H. and Olajire A. A. (2017). Geochemical fractionation and ecological risks assessment of benthic sediment-bound heavy metals from coastal ecosystems off the Equatorial Atlantic Ocean. International Journal of Sediment Research 32(3), 410-420.

Berandah F. E., Kong Y. C. and Ismail A. (2010). Bioaccumulation and distribution of heavy metals (Cd, Cu, Fe, Ni, Pb and Zn) in the different tissues of Chicoreus capucinus lamarck (Mollusca: Muricidae) collected from Sungai Janggut, Kuala Langat, Malaysia. Environmental Asia 3(1), 65-71.

Berkowitz B., Dror I. and Yaron B. (2008). Contaminant Geochemistry: Interactions and Transport. In: The Subsurface Environment. Springer, Heidelberg, 412.

Berner R. A. (1984). Sedimentary pyrite formation: An update. Geochimica et Cosmochimica Acta 48, 605 - 615.

Berner R. A. and Raiswell R. (1983). Burial of organic carbon and pyrite sulfur in sediments over Phanerozoi~ time: a new theory. Geochimica et Cosmochimica Acta 47, 855 - 862.

Blasco F., Aizpuru M. and Gers C. (2001). Depletion of the mangroves of Continental Asia. Wetlands Ecology and Management 9, 245-256.

Bonnissel-Gissinger P., Alnot M., Ehrhardt J.-J. and Behra P. (1998). Surface oxidation of pyrite as a function of pH. Environmental Science and Technology 32(19), 2839-2845.

Borch T., Kretzschmar R., Kappler A., Cappellen P. V., Ginder-Vogel M., Voegelin A. and Campbell K. (2009). Biogeochemical redox processes and their impact on contaminant dynamics. Environmental Science and Technololy 44(1), 15-23.

Borrell A., Tornero V., Bhattacharjee D. and Aguilar A. (2016). Trace element accumulation and trophic relationships in aquatic organisms of the Sundarbans mangrove ecosystem (Bangladesh). Science of the Total Environment 545-546, 414-423.

Bouillon S., Borges A. V., Castañeda-Moya E., Diele K., Dittmar T., Duke N. C., Kristensen E., Lee S. Y., Marchand C. and Middelburg J. J. (2008). Mangrove production and carbon sinks: a revision of global budget estimates. Global Biogeochemical Cycles 22(2).

Burnett W., Kim G. and Lane-Smith D. (2001). A continuous monitor for assessment of 222Rn in the coastal ocean. Journal of Radioanalytical and Nuclear Chemistry 249(1), 167-172.

Call M., Maher D. T., Santos I. R., Ruiz-Halpern S., Mangion P., Sanders C. J., Erler D. V., Oakes J. M., Rosentreter J., Murray R. and Eyre B. D. (2015). Spatial and temporal variability of carbon dioxide and methane fluxes over semi-diurnal and spring–neap–spring timescales in a mangrove creek. Geochimica et Cosmochimica Acta 150, 211-225.

Cances B., Juillot F., Morin G., Laperche V., Alvarez L., Proux O., Hazemann J.-L., Brown G. and Calas G. (2005). XAS evidence of As (V) association with iron oxyhydroxides in a contaminated soil at a former arsenical pesticide processing plant. Environmental Science and Technology 39(24), 9398-9405.

Cang L. T., Czerniak P., Thanh N. C., Schwarzer K. and Ricklefs K. (2007). Suspended sediment dynamics in mangrove areas, Dong Tranh Estuary, Can Gio mangrove forest, Ho Chi Minh City, Southern Vietnam. Annual Report of FY 2007, The Core University Program between Japan Society for the Promotion of Science (JSPS) and Vietnamese Academy of Science and Technology (VAST), 439-450.

Carbonell A., Aarabi M., DeLaune R., Gambrell R. and Patrick Jr W. (1998). Arsenic in wetland vegetation: availability, phytotoxicity, uptake and effects on plant growth and nutrition. Science of The Total Environment 217(3), 189-199.

Cenci R. M. and Martin J. M. (2004). Concentration and fate of trace metals in Mekong River delta. Science of The Total Environment 332(1-3), 167-182.

Chadwick O. A. and Chorover J. (2001). The chemistry of pedogenic thresholds. Geoderma 100(3-4), 321-353.

Chakraborty P., Ramteke D. and Chakraborty S. (2015). Geochemical partitioning of Cu and Ni in mangrove sediments: relationships with their bioavailability. Marine Pollution Bulletin 93(1-2), 194-201.

Chan H. M. (1992). Heavy metal concentrations in coastal sea water and sediments from Tolo Harbour, Hong Kong. In: Morton, B. (Ed.), The Marine Flora and Fauna of Hong Kong and Southern China. Hong Kong University Press, Hong Kong, 621 - 628.

Charriau A., Lesven L., Gao Y., Leermakers M., Baeyens W., Ouddane B. and Billon G. (2011). Trace metal behaviour in riverine sediments: Role of organic matter and sulfides. Applied Geochemistry 26(1), 80-90.

Chaudhuri P., Nath B. and Birch G. (2014). Accumulation of trace metals in grey mangrove Avicennia marina fine nutritive roots: the role of rhizosphere processes. Marine Pollution Bulletin 79(1-2), 284-292.

Cheng H., Wang M., Wong M. H. and Ye Z. (2013). Does radial oxygen loss and iron plaque formation on roots alter Cd and Pb uptake and distribution in rice plant tissues? Plant and Soil 375(1-2), 137-148.

Cheng W. H. and Yap C. K. (2015). Potential human health risks from toxic metals via mangrove snail consumption and their ecological risk assessments in the habitat sediment from Peninsular Malaysia. Chemosphere 135, 156-165.

Cheng W. H., Yap C. K., Ahmad Z. A., Wong L. S. and Ong G. H. (2016). Cobalt in mangrove snails, Nerita lineata and sediments from Peninsular Malaysia.

Chowdhury R., Favas P. J. C., Jonathan M. P., Venkatachalam P., Raja P. and Sarkar S. K. (2017). Bioremoval of trace metals from rhizosediment by mangrove plants in Indian Sundarban Wetland. Marine Pollution Bulletin 124(2), 1078-1088.

Chowdhury R., Favas P. J. C., Pratas J., Jonathan M. P., Ganesh P. S. and Sarkar S. K. (2015). Accumulation of Trace Metals by Mangrove Plants in Indian Sundarban Wetland: Prospects for Phytoremediation. International Journal of Phytoremediation 17(9), 885-894.

Chu H., Chen N., Yeung M., Tam N. and Wong Y. (1998). Tide-tank system simulating mangrove wetland for removal of nutrients and heavy metals from wastewater. Water Science and Technology 38(1), 361-368.

Clark M. W., McConchie D., Lewis D. W. and Saenger P. (1998). Redox stratification and heavy metal partitioning in Avicennia-dominated mangrove sediments: a geochemical model. Chemical Geology 149(3-4), 147-171.

Costa-Boddeker S., Hoelzmann P., Thuyen L. X., Huy H. D., Nguyen H. A., Richter O. and Schwalb A. (2017). Ecological risk assessment of a coastal zone in Southern Vietnam: Spatial distribution and content of heavy metals in water and surface sediments of the Thi Vai Estuary and Can Gio Mangrove Forest. Marine Pollution Bulletin 114(2), 1141-1151.

Cox R. and Hutchinson T. (1981). Multiple and cotolerance to metals in the grass Despitosa Beauv from the sudbury smelting area. Journal of plant nutrition 3, 731-741.

Cuong D. T., Bayen S., Wurl O., Subramanian K., Wong K. K., Sivasothi N. and Obbard J. P. (2005). Heavy metal contamination in mangrove habitats of Singapore. Marine Pollution Bulletin 50(12), 1732-1738.

Dallinger R. (1993). Strategies of metal detoxification in terrestrial invertebrates. Ecotoxicology of metals in invertebrates 245.

Dallinger R., Chabicovsky M., Hödl E., Prem C., Hunziker P. and Manzl C. (2005). Copper in Helix pomatia (Gastropoda) is regulated by one single cell type: differently responsive metal pools in rhogocytes. American Journal of Physiology-Regulatory, Integrative and Comparative Physiology 289(4), R1185-R1195.

Dang D. H., Lenoble V., Durrieu G., Omanovic D., Mullot J. U., Mounier S. and Garnier C. (2015). Seasonal variations of coastal sedimentary trace metals cycling: insight on the effect of manganese and iron (oxy)hydroxides, sulphide and organic matter. Marine Pollution Bulletin 92(1-2), 113-124.

David F., Marchand C., Taillardat P., Thành-Nho N. and Meziane T. (2018). Nutritional composition of suspended particulate matter in a tropical mangrove creek during a tidal cycle (Can Gio, Vietnam). Estuarine, Coastal and Shelf Science 200, 126-130.

de Souza Machado A. A., Spencer K., Kloas W., Toffolon M. and Zarfl C. (2016). Metal fate and effects in estuaries: A review and conceptual model for better understanding of toxicity. Science of The Total Environment 541, 268-281.

De Wolf H. and Rashid R. (2008). Heavy metal accumulation in Littoraria scabra along polluted and pristine mangrove areas of Tanzania. Environmental Pollution 152(3), 636-643.

De Wolf H. and Rashid R. (2008). Heavy metal accumulation in Littoraria scabra along polluted and pristine mangrove areas of Tanzania. Environmental Pollution 152(3), 636-643.

Deborde J., Marchand C., Molnar N., Patrona L. and Meziane T. (2015). Concentrations and Fractionation of Carbon, Iron, Sulfur, Nitrogen and Phosphorus in Mangrove Sediments Along an Intertidal Gradient (Semi-Arid Climate, New Caledonia). Journal of Marine Science and Engineering 3(1), 52-72.

Defew L. H., Mair J. M. and Guzman H. M. (2005). An assessment of metal contamination in mangrove sediments and leaves from Punta Mala Bay, Pacific Panama. Marine Pollution Bulletin 50(5), 547-552.

(2005). An assessment of metal contamination in mangrove sediments and leaves from Punta Mala Bay, Pacific Panama. Marine Pollution Bulletin 50(5), 547-552.

Dent D. (1986). Acid sulphate soils: a baseline for research and development, ILRI.

Dias H. Q. and Nayak G. N. (2016). Geochemistry and bioavailability of mudflats and mangrove sediments and their effect on bioaccumulation in selected organisms within a tropical (Zuari) estuary, Goa, India. Marine Pollution Bulletin 105(1), 227-236.

Dittmar T. and Lara R. J. (2001). Driving Forces Behind Nutrient and Organic Matter Dynamics in a Mangrove Tidal Creek in North Brazil. Estuarine, Coastal and Shelf Science 52(2), 249-259.

Doig L. E. and Liber K. (2006). Nickel partitioning in formulated and natural freshwater sediments. Chemosphere 62(6), 968-979.

Donato D. C., Kauffman J. B., Murdiyarso D., Kurnianto S., Stidham M. and Kanninen M. (2011). Mangroves among the most carbon-rich forests in the tropics. Nature Geoscience 4(5), 293.

Du Laing G., Meers E., Dewispelaere M., Vandecasteele B., Rinklebe J., Tack F. M. and Verloo M. G. (2009). Heavy metal mobility in intertidal sediments of the Scheldt estuary: Field monitoring. Science of the Total Environment 407(8), 2919-2930.

Du Laing G., Vanthuyne D., Vandecasteele B., Tack F. and Verloo M. (2007). Influence of hydrological regime on pore water metal concentrations in a contaminated sediment-derived soil. Environmental Pollution 147(3), 615-625.

Dudani S. N., Lakhmapurkar J., Gavali D. and Patel T. (2017). Heavy Metal Accumulation in The Mangrove Ecosystem of South Gujarat Coast, India. Turkish Journal of Fisheries and Aquatic Sciences 17(4), 755-766.

Duke N. C. (1992). Mangrove floristics and biogeography. Tropical mangrove ecosystems, 63-100.

Duke N. C., Ball M. C. and Ellison J. C. (1998). Factors influencing biodiversity and distributional gradients in mangroves. Global Ecology and Biogeography Letters 7, 27-47.

Duke N. C., Meynecke J.-O., Dittmann S., Ellison A. M., Anger K., Berger U., Cannicci S., Diele K., Ewel K. C. and Field C. D. (2007). A world without mangroves? Science 317(5834), 41-42.

Dunbabin J. and Bowner K. (1992). Potential use of constructed wetlands for treatment of industrial wastewaters containing metals. Science of the Total Environment. 111, 151 - 168.

Egawa T. and Ooba Y. (1963). Mineralogical studies of some soils in the central highland of vietnam. Soil Science and Plant Nutrition 9(6), 14-20.

Eichhorst T. (2016). Neritidae of the world. Vol. 1. ConchBooks, Hackenheim, Germany.

Elliott M. and McLusky D. S. (2002). The Need for Definitions in Understanding Estuaries. Estuarine, Coastal and Shelf Science 55(6), 815-827.

Emmerson R. H. C., O'Riley-Wiese S. B., Macleod C. I. and Lester J. N. (1997). A multivariate assessment of metal distribution in intertidal sediments of the Blackwater Estuary UK. Marine Pollution Bulletin 34, 960 - 968.

Essien J. P., Essien V. and Olajire A. A. (2009). Heavy metal burdens in patches of asphyxiated swamp areas within the Qua Iboe estuary mangrove ecosystem. Environmental Research 109(6), 690-696.

Etcheber H., Taillez A., Abril G., Garnier J., Servais P., Moatar F. and Commarieu M.-V. (2007). Particulate organic carbon in the estuarine turbidity maxima of the Gironde, Loire and Seine estuaries: origin and lability. Hydrobiologia 588(1), 245-259.

Factor C. J. B. and de Chavez E. R. C. (2012). Toxicity of arsenic, aluminum, chromium and nickel to the embryos of the freshwater snail, Radix quadrasi von Möellendorf 1898. Philippine Journal of Science 141(2), 207-216.

Fang T. H. and Lin C. L. (2002). Dissolved and Particulate Trace Metals and Their Partitioning in a Hypoxic Estuary: The Tanshui Estuary in Northern Taiwan. Estuaries 25(4A), 598-607.

Fang Y., Zheng W., Wan Y., Chen C. and Sheng H. (2008). Effects of chromium (Ⅲ) on the seedling growth of mangrove species Avicennia marina [J]. Chinese Journal of Ecology 3, 021.

FAO (2014). Aquastat: Global information system on water and agriculture. www.fao.org/nr/water/aquastat/data/cf/readPdf.html?f=VNM-CF_eng.pdf.

Fernandes H. M. (1997). Heavy metal distribution in sediments and ecological risk assessment: the role of diagenetic processes in reducing metal toxicity in bottom sediments. Environmental Pollution 97(3), 317-325.

Fernandes L. L. and Nayak G. N. (2012). Heavy metals contamination in mudflat and mangrove sediments (Mumbai, India). Chemistry and Ecology 28(5), 435-455.

Ferreira T. O., Otero X. L., Vidal-Torrado P. and Macías F. (2007). Effects of bioturbation by root and crab activity on iron and sulfur biogeochemistry in mangrove substrate. Geoderma 142(1-2), 36-46.

Froelich P. N., Klinkhammer G., Bender M. L., Luedtke N., Heath G. R., Cullen D., Dauphin P., Hammond D., Hartman B. and Maynard V. (1979). Early oxidation of organic matter in pelagic sediments of the eastern equatorial Atlantic: suboxic diagenesis. Geochimica et Cosmochimica Acta 43(7), 1075-1090.

Fu J., Tang X. L., Zhang J. and Balzer W. (2013). Estuarine modification of dissolved and particulate trace metals in major rivers of East-Hainan, China. Continental Shelf Research 57, 59-72.

Furukawa K., Wolanski E. and Mueller H. (1997). Currents and sediment transport in mangrove forests, estuarine, coastal and shelf. Estuarine, Coastal and Shelf Science 44(3), 301-310.

Gaillardet J., Viers J. and Dupré B. (2014). Trace Element in river waters. In: Holland, H., D., Turekian, K. K. (Executive Editors), Treatise on Geochemistry, second ed. 7(Oxford Elsevier), 195-235.

Gajewska E. and Skłodowska M. (2007). Effect of nickel on ROS content and antioxidative enzyme activities in wheat leaves. Biometals 20(1), 27-36.

Giri C., Ochieng E., Tieszen L. L., Zhu Z., Singh A., Loveland T., Masek J. and Duke N. (2011). Status and distribution of mangrove forests of the world using earth observation satellite data. Global Ecology and Biogeography 20(1), 154-159.

Goessler W., Maher W., Irgolic K., Kuehnelt D., Schlagenhaufen C. and Kaise T. (1997). Arsenic compounds in a marine food chain. Fresenius' journal of analytical chemistry 359(4-5), 434-437.

Greger M., Kautsky L. and Sandberg T. (1995). A tentative model of Cd uptake in Potamogeton pectinatus in relation to salinity. Environmental and Experimental Botany 35(2), 215-225.

Guo T., DeLaune R. and Patrick W. (1997). The influence of sediment redox chemistry on chemically active forms of arsenic, cadmium, chromium, and zinc in estuarine sediment. Environment International 23(3), 305-316.

Gustafsson J. P. and Tin N. T. (1994). Arsenic and selenium in some Vietnamese acid sulphate soils. Science of The Total Environment 151(2), 153-158.

Ha T. H., Marchand C., Aimé J., Dang H. N., Phan N. H., Nguyen X. T. and Nguyen T. K. C. (2018). Belowground carbon sequestration in a mature planted mangroves (Northern Viet Nam). Forest Ecology and Management 407, 191-199.

Hahne H. and Kroontje W. (1973). Significance of pH and chloride concentration on behavior of heavy metal pollutants: mercury (II), cadmium (II), zinc (II), and lead (II) 1. Journal of Environmental Quality 2(4), 444-450.

Hansen D., Berry W., Boothman W., Pesch C., Mahony J., Di Toro D., Robson D., Ankley G., Ma D. and Yan Q. (1996). Predicting the toxicity of metal-contaminated field sediments using interstitial concentration of metals and acid-volatile sulfide normalizations. Environmental Toxicology and Chemistry 15(12), 2080-2094.

Harbison P. (1986). Mangrove muds—A sink and a source for trace metals. Marine Pollution Bulletin 17, 246-250.

Hatje V., Birch G. F. and Hill D. M. (2001). Spatial and Temporal Variability of Particulate Trace Metals in Port Jackson Estuary, Australia. Estuarine, Coastal and Shelf Science 53(1), 63-77.

Hatje V., Payne T. E., Hill D. M., McOrist G., Birch G. F. and Szymczak R. (2003). Kinetics of trace element uptake and release by particles in estuarine waters: effects of pH, salinity, and particle loading. Environment International 29(5), 619-629.

He B., Li R., Chai M. and Qiu G. (2014). Threat of heavy metal contamination in eight mangrove plants from the Futian mangrove forest, China. Environ Geochem Health 36(3), 467-476.

Hien P. D., Binh N. T., Ngo N. T., Ha V. T., Truong Y. and An N. H. (1997). Monitoring lead in suspended air particulate matter in Ho Chi Minh City. Atmospheric Environment 31(7), 1073-1076.

Hien P. D., Binh N. T., Truong Y. and Ngo N. T. (1999). Temporal variations of source impacts at the receptor, as derived from air particulate monitoring data in Ho Chi Minh City, Vietnam. Atmospheric Environment 33(19), 3133-3142.

Hirose K. (2004). Satellite data application for mangrove management. . International Symposium on Geoinfomatics for Spatial Infrastructure Development in Earth and Allied Sciences 2004.

Hogarth P. J. (2015). The biology of mangroves and seagrasses, Oxford University Press.

Holloway C. J., Santos I. R., Tait D. R., Sanders C. J., Rose A. L., Schnetger B., Brumsack H.-J., Macklin P. A., Sippo J. Z. and Maher D. T. (2016). Manganese and iron release from mangrove porewaters: A significant component of oceanic budgets? Marine Chemistry 184, 43-52.

Hong P. (1997). Assessment of the damages caused by chemical war on mangrove forests in Vietnam. Final Report of the National Project:“Assessment of the damages caused by chemical war on the nature in Vietnam”. National Environment Agency. 55pp (in Vietnamese).

Hong P. N. (2001). Reforestation of mangroves after severe impacts of herbicides during the the Viet Nam war: the case of Can Gio. Unasylva (FAO).

Hossain M., Williams P. N., Mestrot A., Norton G. J., Deacon C. M. and Meharg A. A. (2012). Spatial heterogeneity and kinetic regulation of arsenic dynamics in mangrove sediments: the Sundarbans, Bangladesh. Environmental Science and Technology 46(16), 8645-8652.

Idrees F. A. (2009). Assessment of Trace Metal Distribution and Contamination in Surface Soils of Amman, Jordan. Jordan Journal of Chemistry. 4(1), 77 - 87.

Inoue T. and Asano T. (2013). Characteristics of Water Quality and Nitrogen-Associated Bacterial Functions in Mekong Delta Mangroves. Global Environmental Research 17, 199-206.

Jara-Marini M. E., Soto-Jimenez M. F. and Paez-Osuna F. (2009). Trophic relationships and transference of cadmium, copper, lead and zinc in a subtropical coastal lagoon food web from SE Gulf of California. Chemosphere 77(10), 1366-1373.

Järup L. (2003). Hazards of heavy metal contamination. British medical bulletin 68(1), 167-182.

Jayasinghe J., Phillips M. and Anas M. (2010). Behaviour of environmental iron, manganese and aluminium in relation to brown/black gill syndrome in Penaeus monodon cultured in ponds on acid sulphate soils. Sri Lanka Journal of Aquatic Sciences 13.

Jiang J. and Qiu H. (2009). Assessment of content of heavy metals in seafood from sea area of Guangdong province. Journal of Environment and Health 26(9), 814-816.

Jingchun L., Chongling Y., MacNair M. R., Jun H. and Yuhong L. (2006). Distribution and speciation of some metals in mangrove sediments from Jiulong River Estuary, Peoples Republic of China. Bull Environ Contam Toxicol 76, 815 - 822.

Jones Jr J. B., Wolf B. and Mills H. A. (1991). Plant analysis handbook. A practical sampling, preparation, analysis, and interpretation guide, Micro-Macro Publishing, Inc.

Joseph T. and Ramesh K. (2016). Heavy Metal Risk Assessment in Bhavanapadu Creek Using Three Potamidid Snails-Telescopium telescopium, Cerithidea obtusa and Cerithidea cingulata. Journal of Environmental and Analytical Toxicology 6(385), 2161-0525.1000385.

Kadlec R. H., Knight R. L., Vymazal J., Brix H., Cooper P. and Haberl R. (2000). Contructed wetlands for pollution control: Processes, performance design and operation. IWA specialist group on use of macrophytes in water pollution control. IWA publishing.

Kaly U. L., Eugelink G. and Robertson A. I. (1997). Soil conditions in damaged North Queensland mangroves. Estuaries 20(2), 291-300.

Kamaruzzaman B. Y., Ong M. C., Azhar M. S. N., Shahbudin S. and Jalal K. C. A. (2008). Geochemistry of sediment in the major estuarine mangrove forest of Terengganu region, Malaysia. American Journal of Applied Science 5, 1707 - 1712.

Kamaruzzaman B. Y., Rina Sharlinda M. Z., Akbar John B. and Siti Waznah A. (2011). Accumulation and Distribution of Lead and Copper in Avicennia marina and Rhizophora apiculata from Balok Mangrove Forest, Pahang, Malaysia. Sains Malaysiana 40(6), 555–560.

Kathiresan K. (2012). Importance of mangrove ecosystem. International Journal of Marine Science 2(1).

Kathiresan K. and Bingham B. L. (2001). Biology of mangroves and mangrove ecosystems. Advances in marine biology 40, 84-254.

Kathiresan K., Saravanakumar K. and Mullai P. (2014). Bioaccumulation of trace elements by Avicennia marina. Journal of Coastal Life Medicine 2(11), 888-894.

Kesavan K., Murugan A., Venkatesan V. and Kumar V. (2013). Heavy metal accumulation in molluscs and sediment from Uppanar estuary, southeast coast of India. Thalassas 29(2), 15-21.

Khattak R. A., Page A. and Jarrell W. M. (1989). Mechanism of native manganese release in salt-treated soils. Soil Science Society of America Journal 53(3), 701-705.

Khokiattiwong S., Kornkanitnan N., Goessler W., Kokarnig S. and Francesconi K. A. (2009). Arsenic compounds in tropical marine ecosystems: similarities between mangrove forest and coral reef. Environmental Chemistry 6(3), 226-234.

Kirby J., Maher W., Chariton A. and Krikowa F. (2002). Arsenic concentrations and speciation in a temperate mangrove ecosystem, NSW, Australia. Applied Organometallic Chemistry 16(4), 192-201.

Kjerfve B. and Magill K. E. (1989). Geographic and hydrodynamic charactersistics of shallow coastal lagoons. Marine Geology 88, 187 - 199.

Klinkhammer G. P. (1980). Early diagenesis in sediments from the eastern equatorial Pacific, II. Pore water metal results. Earth and Planetary Science Letters 49(1), 81-101.

Koch M. S. and Mendelssohn I. (1989). Sulphide as a soil phytotoxin: differential responses in two marsh species. The Journal of Ecology, 565-578.

Komiyama A., Havanond S., Srisawatt W., Mochida Y., Fujimoto K., Ohnishi T., Ishihara S. and Miyagi T. (2000). Top/root biomass ratio of a secondary mangrove (Ceriops tagal (Perr.) CB Rob.) forest. Forest Ecology and Management 139(1-3), 127-134.

Kříbek B., Mihaljevič M., Sracek O., Knésl I., Ettler V. and Nyambe I. (2011). The extent of arsenic and of metal uptake by aboveground tissues of Pteris vittata and Cyperus involucratus growing in copper- and cobalt-rich tailings of the Zambian Copperbelt. Archives of Environmental Contamination and Toxicology 61(2), 228-242.

Kristensen E. (2008b). Mangrove crabs as ecosystem engineers; with emphasis on sediment processes. Journal of Sea Research 59(1-2), 30-43.

Kristensen E., Bouillon S., Dittmar T. and Marchand C. (2008a). Organic carbon dynamics in mangrove ecosystems: A review. Aquatic Botany 89(2), 201-219.

Kristensen E., Connolly R. M., Otero X. L., Marchand C., Ferreira T. O. and Rivera-Monroy V. H. (2017). Biogeochemical Cycles: Global Approaches and Perspectives. Mangrove Ecosystems: A Global Biogeographic Perspective, Springer**,** 163-209.

Kuenzer C. and Tuan V. Q. (2013). Assessing the ecosystem services value of Can Gio Mangrove Biosphere Reserve: Combining earth-observation- and household-survey-based analyses. Applied Geography 45, 167-184.

Kutscher D., Wills J. D. and McSheehy D. S. (2014). Analysis of High Matrix Samples using Argon Gas Dilution with the Thermo Scientifc iCAP Q ICP-MS. Technical Note 43202, Thermo Fisher Scientific, Bremen, Germany.

Lacerda L. (1998). Biogeochemistry of trace metals and diffuse pollution in mangrove ecosystems. International Society for Mangrove Ecosystems, Okinawa 65.

Lacerda L., Rezende C., Aragon G. and Ovalle A. (1991). Iron and chromium transport and accumulation in a mangrove ecosystem. Water, Air, and Soil Pollution 57(1), 513-520.

Lacerda L. D. and Abrao J. J. (1984). Heavy metal accumulation by mangrove and saltmarsh intertidal sediments. Revista Brasileira de Biologia 7, 49-52.

Lacerda L. D., Martinelli L. A., Rezende C. A., Mozetto A. A., Ovalle A. R. C., Victoria R. I., Silva C. A. R. and Nogueira F. B. (1988). The fate of heavy metals in suspended matter in a mangrove creek during a tidal cycle. Science of The Total Environment 75, 249-259.

Lacerda L. D., Pfeiffer W. C. and Fiszman M. (1987). Heavy metal distribution, availability and fate in Sepetiba Bay, SE Brazil. Science of the Total Environment 65, 163e173.

Lacerda L. D., Ribeiro Jr M. G. and Gueiros B. B. (1999). Manganese dynamics in a mangrove mud flat tidal creek in SE Brazil. Mangroves and Salt Marshes 3, 105-115.

Langston W. J., Bebianno M. J. and Burt G. R. (1998). Metal handling strategies in molluscs. Metal metabolism in aquatic environments, Springer**,** 219-283.

Larison J. R., Likens E., Fitzpatrick J. W. and Crock J. G. (2000). Cadmium toxicity among wildlife in the Colorado rocky mountains. Nature 406, 181 - 183.

Leaño E. M. and Pang K.-L. (2010). Effect of Copper(II), Lead(II), and Zinc(II) on Growth and Sporulation of Halophytophthora from Taiwan Mangroves. Water, Air, & Soil Pollution 213(1-4), 85-93.

Lee O. H., Williams G. A. and Hyde K. D. (2001). The diets of Littoraria ardouiniana and L. melanostoma in Hong Kong mangroves. Journal of the Marine Biological Association of the United Kingdom 81(6), 967-973.

Lee S. Y., Primavera J. H., Dahdouh-Guebas F., McKee K., Bosire J. O., Cannicci S., Diele K., Fromard F., Koedam N., Marchand C., Mendelssohn I., Mukherjee N. and Record S. (2014). Ecological role and services of tropical mangrove ecosystems: a reassessment. Global Ecology and Biogeography 23(7), 726-743.

Lenoble V., Omanovic D., Garnier C., Mounier S., Donlagic N., Le Poupon C. and Pizeta I. (2013). Distribution and chemical speciation of arsenic and heavy metals in highly contaminated waters used for health care purposes (Srebrenica, Bosnia and Herzegovina). Science of The Total Environment 443, 420-428.

Leopold A., Marchand C., Deborde J., Chaduteau C. and Allenbach M. (2013). Influence of mangrove zonation on CO2 fluxes at the sediment–air interface (New Caledonia). Geoderma 202-203, 62-70.

Lewis M., Pryor R. and Wilking L. (2011). Fate and effects of anthropogenic chemicals in mangrove ecosystems: a review. Environmental Pollution 159(10), 2328-2346.

Li P., Zhang J., Xie H., Liu C., Liang S., Ren Y. and Wang W. (2015). Heavy metal bioaccumulation and health hazard assessment for three fish species from Nansi Lake, China. Bulletin of Environmental Contamination and Toxicology 94(4), 431-436.

Liu G. and Cai Y. (2010). Complexation of arsenite with dissolved organic matter: conditional distribution coefficients and apparent stability constants. Chemosphere 81(7), 890-896.

Luoma S. N. and Bryan G. (1981). A statistical assessment of the form of trace metals in oxidized estuarine sediments employing chemical extractants. Science of The Total Environment 17(2), 165-196.

Luong N. V. (2011). Mangrove forest structure and coverage change analysis using remote sensing and geographical information system technology: A case study of Can Gio Mangrove Biosphere Reserve, Hi Chi Minh City, Vietnam. Final report submitted to Rufford Small Grants Foundation, 40pp.

Luong N. V., Tateishi R. and Hoan N. T. (2015). Analysis of an impact of succession in mangrove forest association using remote sensing and GIS technology. Journal of Geography and Geology 7(1), 106.

Ma L. Q. and Rao G. N. (1997). Chemical fractionation of cadmium, copper, nickel, and zinc in contaminated soils. Journal of Environmental Quality 26(1), 259-264.

MacFarlane G. and Burchett M. (2002). Toxicity, growth and accumulation relationships of copper, lead and zinc in the grey mangrove Avicennia marina (Forsk.) Vierh. Marine Environmental Research 54(1), 65-84.

MacFarlane G., Pulkownik A. and Burchett M. (2003). Accumulation and distribution of heavy metals in the grey mangrove, Avicennia marina (Forsk.) Vierh.: biological indication potential. Environmental Pollution 123(1), 139-151.

MacFarlane G. R., Koller C. E. and Blomberg S. P. (2007). Accumulation and partitioning of heavy metals in mangroves: a synthesis of field-based studies. Chemosphere 69(9), 1454-1464.

Machado W., Gueiros B. B., Lisboa-Filho S. D. and Lacerda L. D. (2005). Trace metals in mangrove seedlings: role of iron plaque formation. Wetlands Ecology and Management 13(2), 199-206.

MacKenzie R. A., Foulk P. B., Klump J. V., Weckerly K., Purbospito J., Murdiyarso D., Donato D. C. and Nam V. N. (2016). Sedimentation and belowground carbon accumulation rates in mangrove forests that differ in diversity and land use: a tale of two mangroves. Wetlands Ecology and Management 24(2), 245-261.

Madi A. P. L. M., Boeger M. R. T. and Reissmann C. B. (2015). Distribution of Cu, Fe, Mn, and Zn in Two Mangroves of Southern Brazil. Brazilian Archives of Biology and Technology 58(6), 970-976.

Maher D. T., Santos I. R., Golsby-Smith L., Gleeson J. and Eyre B. D. (2013). Groundwater-derived dissolved inorganic and organic carbon exports from a mangrove tidal creek: The missing mangrove carbon sink? Limnology and Oceanography 58(2), 475-488.

Maksymiec W. (1998). Effect of copper on cellular processes in higher plants. Photosynthetica 34(3), 321-342.

Manceau A., Silvester E., Bartoli C., Lanson B. and Drits V. A. (1997). Structural mechanism of Co2+ oxidation by the phyllomanganate buserite. American Mineralogist 82(11-12), 1150-1175.

Marchand C., Albéric P., Lallier-Vergès E. and Baltzer F. (2006a). Distribution and Characteristics of Dissolved Organic Matter in Mangrove Sediment Pore Waters along the Coastline of French Guiana. Biogeochemistry 81(1), 59-75.

Marchand C., Allenbach M. and Lallier-Vergès E. (2011b). Relationships between heavy metals distribution and organic matter cycling in mangrove sediments (Conception Bay, New Caledonia). Geoderma 160(3-4), 444-456.

Marchand C., Baltzer F., Lallier-Vergès E. and Albéric P. (2004). Pore-water chemistry in mangrove sediments: relationship with species composition and developmental stages (French Guiana). Marine geology 208(2-4), 361-381.

Marchand C., Fernandez J. M. and Moreton B. (2016). Trace metal geochemistry in mangrove sediments and their transfer to mangrove plants (New Caledonia). Science of The Total Environment 562, 216 - 227.

Marchand C., Fernandez J. M., Moreton B., Landi L., Lallier-Vergès E. and Baltzer F. (2012). The partitioning of transitional metals (Fe, Mn, Ni, Cr) in mangrove sediments downstream of a ferralitized ultramafic watershed (New Caledonia). Chemical Geology 300-301, 70-80.

Marchand C., Lallier-Vergès E. and Allenbach M. (2011a). Redox conditions and heavy metals distribution in mangrove forests receiving effluents from shrimp farms (Teremba Bay, New Caledonia). Journal of Soils and Sediments 11(3), 529-541.

Marchand C., Lallier-Vergès E., Baltzer F., Albéric P., Cossa D. and Baillif P. (2006b). Heavy metals distribution in mangrove sediments along the mobile coastline of French Guiana. Marine Chemistry 98(1), 1-17.

Marchand C., Lallier-Vergès E., Disnar J. R. and Kéravis D. (2008). Organic carbon sources and transformations in mangrove sediments: A Rock-Eval pyrolysis approach. Organic Geochemistry 39(4), 408-421.

Marchiol L., Assolari S., Sacco P. and Zerbi G. (2004). Phytoextraction of heavy metals by canola (Brassica napus) and radish (Raphanus sativus) grown on multicontaminated soil. Environmetal Pollution 132(1), 21-27.

Martuti N. K. T., Widianarko B. and Yulianto B. (2016). Copper Accumulation on Avicennia marina In Tapak, Tugurejo, Semarang, Indonesia. Waste Technology 4(1), 40-45.

Maskaoui K., Zhou J. L., Hong H. S. and Zhang Z. L. (2002). Contamination by polycyclic aromatic hydrocarbons in the Jiulong River Estuary and Western Xiamen Sea, China. Environmental Pollution 118, 109–122.

Masscheleyn P. H., Delaune R. D. and Patrick Jr W. H. (1991). Effect of redox potential and pH on arsenic speciation and solubility in a contaminated soil. Environmental Science and Technology 25(8), 1414-1419.

Masscheleyn P. H., Pardue J. H., Delaune R. D. and Patrick W. H. (1992). Chromium redox chemistry in a lower Mississippi Valley bottom land hardwood wetland. Environmental Science and Technology 26(6), 1217-1226.

McConchie D. M., Mann A. W., Linter M. J., Longman D., Talbot V. and Gabelish M. J. (1988). Heavy metals in marine biota, sediments, and waters from the Shark Bay area Western Australia. Journal of Coastal Research 4, 51 - 72.

McEvoy J. P. and Brudvig G. W. (2006). Water-splitting chemistry of photosystem II. Chemical reviews 106(11), 4455-4483.

McKee K. L. (1993). Soil physicochemical patterns and mangrove species distribution-reciprocal effects. Journal of Ecology 81(3), 477-487.

Melville F. and Pulkownik A. (2006). Investigation of mangrove macroalgae as bioindicators of estuarine contamination. Marine Pollution Bulletin 52(10), 1260-1269.

Millaleo R., Reyes-Díaz M., Ivanov A., Mora M. and Alberdi M. (2010). Manganese as essential and toxic element for plants: transport, accumulation and resistance mechanisms. Journal of soil science and plant nutrition 10(4), 470-481.

Millward G. E. (1995). Processes affecting trace element speciation in estuaries. A review. Analyst 120(3), 609-614.

Minh N. H., Minh T. B., Iwata H., Kajiwara N., Kunisue T., Takahashi S., Viet P. H., Tuyen B. C. and Tanabe S. (2007). Persistent organic pollutants in sediments from Sai Gon-Dong Nai River Basin, Vietnam: Levels and temporal trends. Archives of Environmental Contamination and Toxicology 52(4), 458-465.

Miola B., Morais J. O. and Pinheiro Lde S. (2016). Trace metal concentrations in tropical mangrove sediments, NE Brazil. Marine Pollution Bulletin 102(1), 206-209.

Mishra D. and Kar M. (1974). Nickel in plant growth and metabolism. The Botanical Review 40(4), 395-452.

Mitsch W. J. and Gosselink J. G. (2000). The value of wetlands: importance of scale and landscape setting. Ecological economics 35(1), 25-33.

Moorhead K. and Reddy K. R. (1988). Oxygen transport through selected aquatic macrophytes. Journal of Environmental Quality 17(1), 138-142.

Morse J. and Luther G. (1999). Chemical influences on trace metal-sulfide interactions in anoxic sediments. Geochimica et Cosmochimica Acta 63(19), 3373-3378.

Mumby P. J., Edwards A. J., Arisas-Gonzalez J. E., Lindeman K. C., Blackwell P. G., Gall A., Gorczynska M. I., Harborne A. R., Pescod C. L., Renken H., Wabnitz C. C. C. and Llewellyn G. (2004). Mangroves enhance the biomass of coral reef fish communities in the Caribbean. Nature 427, 533 - 536.

Murray J. W. and Dillard J. G. (1979). The oxidation of cobalt (II) adsorbed on manganese dioxide. Geochimica et Cosmochimica Acta 43(5), 781-787.

Nam V. N., Sinh L. V., Miyagi M., Baba S. and Chan H. T. (2014). Studies in Can Gio Mangrove Biosphere Reserve Ho Chi Minh city, Viet Nam. ISME Mangrove Ecosystems Technical Reports No. 6.

Natesan U., Madan Kumar M. and Deepthi K. (2014). Mangrove sediments a sink for heavy metals? An assessment of Muthupet mangroves of Tamil Nadu, southeast coast of India. Environmental Earth Sciences 72(4), 1255-1270.

Nath B., Birch G. and Chaudhuri P. (2014). Assessment of sediment quality in Avicennia marina-dominated embayments of Sydney Estuary: The potential use of pneumatophores (aerial roots) as a bio-indicator of trace metal contamination. Science of The Total Environment 472, 1010-1022.

Nguyen B. T., Do T. K., Tran T. V., Dang M. K., Dell C. J., Luu P. V. and Vo Q. T. K. (2018). High soil Mn and Al, as well as low leaf P concentration, may explain for low natural rubber productivity on a tropical acid soil in Vietnam. Journal of plant nutrition, 1-12.

Nguyen T. V. H., Takizawa S., Oguma K. and Phuoc N. V. (2011). Sources and leaching of manganese and iron in the Saigon River Basin, Vietnam. Water Science and Technology 63(10), 2231-2237.

Nguyen V. T., Ozaki A., Nguyen Tho H., Nguyen Duc A., Tran Thi Y. and Kurosawa K. (2016). Arsenic and Heavy Metal Contamination in Soils under Different Land Use in an Estuary in Northern Vietnam. International Journal of Environmental Research and Public Health 13(11).

Ni H. G., Lu F. H., Luo X. L., Tian H. Y. and Zeng E. Y. (2008). Riverine inputs of total organic carbon and suspended particulate matter from the Pearl River Delta to the coastal ocean off South China. Marine Pollution Bulletin 56(6), 1150-1157.

Nica D. V., Bura M., Gergen I., Harmanescu M. and Bordean D.-M. (2012). Bioaccumulative and conchological assessment of heavy metal transfer in a soil-plant-snail food chain. Chemistry Central Journal 6(1), 55.

Nickson R., McArthur J., Ravenscroft P., Burgess W. and Ahmed K. (2000). Mechanism of arsenic release to groundwater, Bangladesh and West Bengal. Applied Geochemistry 15(4), 403-413.

Noble A. E., Saito M. A., Maiti K. and Benitez-Nelson C. R. (2008). Cobalt, manganese, and iron near the Hawaiian Islands: A potential concentrating mechanism for cobalt within a cyclonic eddy and implications for the hybrid-type trace metals. Deep Sea Research Part II: Topical Studies in Oceanography 55(10-13), 1473-1490.

Noël V., Marchand C., Juillot F., Ona-Nguema G., Viollier E., Marakovic G., Olivi L., Delbes L., Gelebart F. and Morin G. (2014). EXAFS analysis of iron cycling in mangrove sediments downstream a lateritized ultramafic watershed (Vavouto Bay, New Caledonia). Geochimica et Cosmochimica Acta 136, 211-228.

Noël V., Morin G., Juillot F., Marchand C., Brest J., Bargar J. R., Muñoz M., Marakovic G., Ardo S. and Brown G. E. (2015). Ni cycling in mangrove sediments from New Caledonia. Geochimica et Cosmochimica Acta 169, 82-98.

Noronha-D'Mello, A. C. and Nayak G. N. (2015). Geochemical characterization of mangrove sediments of the Zuari estuarine system, West coast of India. Estuarine, Coastal and Shelf Science 167, 313-325.

Nriagu J. O. and Pacyna J. M. (1988). Quantitative assessment of worldwide contamination of air, water and soils with trace metals. Nature 333, 134 - 139.

Ong Che R. G. and Cheung S. G. (1998). Heavy metals in Metapenaeus ensis, Wriocheie sinensis and sediment from the Mai Po Marshes, Hong Kong. Science of the Total Environment 248, 87 - 97.

Otero X. L., Ferreira T. O., Huerta-Díaz M. A., Partiti C. S. M., Souza V., Vidal-Torrado P. and Macías F. (2009). Geochemistry of iron and manganese in soils and sediments of a mangrove system, Island of Pai Matos (Cananeia — SP, Brazil). Geoderma 148(3-4), 318-335.

Oursel B., Garnier C., Pairaud I., Omanović D., Durrieu G., Syakti A. D., Le Poupon C., Thouvenin B. and Lucas Y. (2014). Behaviour and fate of urban particles in coastal waters: Settling rate, size distribution and metals contamination characterization. Estuarine, Coastal and Shelf Science 138, 14-26.

Oxmann J. F., Pham Q. H., Schwendenmann L., Stellman J. M. and Lara R. J. (2010). Mangrove reforestation in Vietnam: the effect of sediment physicochemical properties on nutrient cycling. Plant and Soil 326(1-2), 225-241.

Oxmann J. F., Schwendenmann L. and Lara R. J. (2009). Interactions among phosphorus, pH and Eh in reforested mangroves, Vietnam: a three-dimensional spatial analysis. Biogeochemistry 96(1-3), 73-85.

Palit S., Sharma A. and Talukder G. (1994). Effects of cobalt on plants. The Botanical Review 60(2), 149-181.

Palpandi C. and Kesavan K. (2012). Heavy metal monitoring using Nerita crepidularia-mangrove mollusc from the Vellar estuary, Southeast coast of India. Asian Pacific Journal of Tropical Biomedicine 2(1), S358-S367.

Pardue J. H. and Patrick W. H. (2018). Changes in metal speciation following alteration of sediment redox status. Metal contaminated aquatic sediments, Routledge**,** 169-185.

Parvaresh H., Abedi Z., Farshchi P., Karami M., Khorasani N. and Karbassi A. (2011). Bioavailability and concentration of heavy metals in the sediments and leaves of grey mangrove, Avicennia marina (Forsk.) Vierh, in Sirik Azini Creek, Iran. Biological trace element research 143(2), 1121-1130.

Passos E. d. A., Alves J. C., dos Santos I. S., Alves J. d. P. H., Garcia C. A. B. and Spinola Costa A. C. (2010). Assessment of trace metals contamination in estuarine sediments using a sequential extraction technique and principal component analysis. Microchemical Journal 96(1), 50-57.

Patrick W. H. and Jugsujinda A. (1992). Sequential reduction and oxidation of inorganic nitrogen, manganese and iron in flooded soil. Soil Science Society of America Journal 56(4), 1071-1073.

Perin G., Craboledda L., Lucchese M., Cirillo R., Dotta L., Zanette M. and Orio A. (1985). Heavy metal speciation in the sediments of northern Adriatic Sea. A new approach for environmental toxicity determination. Heavy metals in the environment 2(1), 454-456.

Phuong N. M., Kang Y., Sakurai K., Iwasaki K., Kien C. N., Van Noi N. and Son L. T. (2010). Arsenic contents and physicochemical properties of agricultural soils from the Red River Delta, Vietnam. Soil Science and Plant Nutrition 54(6), 846-855.

Pickering W. (1986). Metal ion speciation—soils and sediments (a review). Ore Geology Reviews 1(1), 83-146.

Polidoro B. A., Carpenter K. E., Collins L., Duke N. C., Ellison A. M., Ellison J. C., Farnsworth E. J., Fernando E. S., Kathiresan K. and Koedam N. E. (2010). The loss of species: mangrove extinction risk and geographic areas of global concern. Plos One 5(4), e10095.

Prudente M. S., Ichihashi H. and Tatsukawa R. (1994). Heavy metal concentrations in sediments from Manila Bay, Philippines and inflowing rivers. Environmental Pollution 86, 83 - 88.

Qiu G., Gao T., Hong J., Tan W., Liu F. and Zheng L. (2017). Mechanisms of arsenic-containing pyrite oxidation by aqueous arsenate under anoxic conditions. Geochimica et Cosmochimica Acta 217, 306-319.

Rainbow P. S. (1997). Trace metal accumulation in marine invertebrates: marine biology or marine chemistry? Journal of the Marine Biological Association of the United Kingdom 77(1), 195-210.

Rao K. M. and Sresty T. (2000). Antioxidative parameters in the seedlings of pigeonpea (Cajanus cajan (L.) Millspaugh) in response to Zn and Ni stresses. Plant Science 157(1), 113-128.

Rath P., Panda U. C., Bhatta D. and Sahu K. C. (2009). Use of sequential leaching, mineralogy, morphology and multivariate statistical technique for quantifying metal pollution in highly polluted aquatic sediments--a case study: Brahmani and Nandira Rivers, India. Journal Hazardous and Materials 163(2-3), 632-644.

Reddy K. R. and DeLaune R. D. (2008). Biogeochemistry of wetlands: science and applications, CRC press.

Reed-Judkins D. K., Farris J. L., Cherry D. S. and Cairns J. (1997). Foodborne uptake and sublethal effects of copper and zinc to freshwater snails. Hydrobiologia 364(2-3), 105-118.

Rhine E. D., Garcia-Dominguez E., Phelps C. D. and Young L. (2005). Environmental microbes can speciate and cycle arsenic. Environmental Science and Technology 39(24), 9569-9573.

Salomons W. and Forstner U. (1984). Metal in the hydrocycle. Springer Verlag, Berline, 349 - 350.

Salomons W., Kerdijk H., Van Pagee H., Klomp R. and Schreur A. (1988). Behavious and impact assessment of heavy metal in estuarine and coastal zone. In: Seeliger, U., Lacerda, L. D., Patchineelan, S. R., Metals in coastal environments of Latin America. Springer – Verlag Berlin., 157 - 198.

Samsi A. N., Asaf R., Sahabuddin S., Santi A. and Wamnebo M. I. (2017). Gastropods As A Bioindicator and Biomonitoring Metal Pollution. Aquacultura Indonesiana 18(1), 1-8.

Sanders C. J., Santos I. R., Barcellos R. and Silva Filho E. V. (2012). Elevated concentrations of dissolved Ba, Fe and Mn in a mangrove subterranean estuary: Consequence of sea level rise? Continental Shelf Research 43, 86-94.

Sanders C. J., Santos I. R., Maher D. T., Sadat-Noori M., Schnetger B. and Brumsack H.-J. (2015). Dissolved iron exports from an estuary surrounded by coastal wetlands: Can small estuaries be a significant source of Fe to the ocean? Marine Chemistry 176, 75-82.

Santos I. R., de Weys J. and Eyre B. D. (2011). Groundwater or floodwater? Assessing the pathways of metal exports from a coastal acid sulfate soil catchment. Environmental Science and Technology 45(22), 9641-9648.

Sarika P. R. and Chandramohanakumar N. (2008). Distribution of heavy metals in mangrove sediments of Cochin estuary. Research Journal of Chemistry and Environment 12(3), 37-44.

Scholander P., Van Dam L. and Scholander S. I. (1955). Gas exchange in the roots of mangroves. American Journal of Botany, 92-98.

Schwarzer K., Thanh N. C. and Ricklefs K. (2016). Sediment re-deposition in the mangrove environment of Can Gio, Saigon River estuary (Vietnam). Journal of Coastal Research 75(sp1), 138-142.

Sekabira K., Oryem Origa H. O., Basamba T. A., Mutumba G. and Kakudidi E. (2010). Assessment of heavy metal pollution in the urban stream sediments and its tributaries. International Journal of Environmental Science and Technology 7(3), 435-446.

Selvam V. and Karunagaran V. M. (2004). Ecology and Biology of Mangroves. Orientation Guide.

Shanker A. K., Cervantes C., Loza-Tavera H. and Avudainayagam S. (2005). Chromium toxicity in plants. Environment International 31(5), 739-753.

Shynu R., Rao V. P., Sarma V. V. S. S., Kessarkar P. M. and Murali R. M. (2015). Sources and fate of organic matter in suspended and bottom sediments of the Mandovi and Zuari estuaries, western India. Current Science 108(2), 226 - 238.

Sidoumou Z., Gnassia-Barelli M., Siau Y., Morton V. and Romeo M. (2006). Heavy metal concentrations in molluscs from the Senegal coast. Environment International 32(3), 384-387.

Silva G. S. d., Nascimento A. S. d., Sousa E. R. d., Marques E. P., Marques A. L. B., Corrêa L. B. and Silva G. S. d. (2014). Distribution and Fractionation of Metals in Mangrove Sediment from the Tibiri River Estuary on Maranhão Island. Revista Virtual de Química 6(2).

Simpson S. L., Rosner J. and Ellis J. (2000). Competitive displacement reactions of cadmium, copper, and zinc added to a polluted, sulfidic estuarine sediment. Environmental Toxicology and Chemistry 19(8), 1992-1999.

Soto-Jiménez M. F. and Páez-Osuna F. (2001). Distribution and Normalization of Heavy Metal Concentrations in Mangrove and Lagoonal Sediments from Mazatlán Harbor (SE Gulf of California). Estuarine, Coastal and Shelf Science 53(3), 259-274.

Speer H. L. (1973). The effect of arsenate and other inhibitors on early events during the germination of lettuce seeds (Lactuca sativa L.). Plant physiology 52(2), 142-146.

Stevenson F. (1976). Stability Constants of Cu2+, Pb2+, and Cd2+ Complexes with Humic Acids 1. Soil Science Society of America Journal 40(5), 665-672.

Strady E., Blanc G., Schäfer J., Coynel A. and Dabrin A. (2009). Dissolved uranium, vanadium and molybdenum behaviours during contrasting freshwater discharges in the Gironde Estuary (SW France). Estuarine, Coastal and Shelf Science 83(4), 550-560.

Strady E., Dang V. B., Nemery J., Guedron S., Dinh Q. T., Denis H. and Nguyen P. D. (2017a). Baseline seasonal investigation of nutrients and trace metals in surface waters and sediments along the Saigon River basin impacted by the megacity of Ho Chi Minh (Vietnam). Environmental Science and Pollution Research International 24(4), 3226–3243.

Strady E., Tuc D. Q., Némery J., Nho N. T., Guédrone S., Sang N. N., Denis H. and Dan N. P. (2017b). Spatial variation and risk assessment of trace metals in water and sediment of the Mekong Delta. Chemosphere 179, 367-378.

Szefer P., Ali A., Ba-Haroon A., Rajeh A., Geldon J. and Nabrzyski M. (1999). Distribution and relationships of selected trace metals in molluscs and associated sediments from the Gulf of Aden, Yemen. Environmental Pollution 106(3), 299-314.

Szymczycha B., Kroeger K. D. and Pempkowiak J. (2016). Significance of groundwater discharge along the coast of Poland as a source of dissolved metals to the southern Baltic Sea. Marine Pollution Bulletin 109(1), 151-162.

Tait D. R., Maher D. T., Macklin P. A. and Santos I. R. (2016). Mangrove pore water exchange across a latitudinal gradient. Geophysical Research Letters 43(7), 3334-3341.

Tam N. and Wong Y. (1996). Retention and distribution of heavy metals in mangrove soils receiving wastewater. Environmental Pollution 94(3), 283-291.

Tam N. F. Y., Lie S. H., Lane C. Y., Chen G. Z., Li e M. S. and Wong Y. S. (1995). Nutrients and heavy metal contamination of plants and sediments in Futian mangrove forest. Hydrobiologia 295, 149-158.

Tam N. F. Y. and Wong Y. S. (1999). Mangrove soils in removing pollutants from municipal wastewater of different salinities. Journal of Environmental Quality 28(2), 556-564.

(1996). Retention and distribution of heavy metals in mangrove soils receiving wastewater. Environmental Pollution 94(3), 283-291.

(1993). Retention of nutrients and heavy metals in mangrove sediment receiving wastewater of different strengths. Environmental Technology 14(8), 719-729.

(1995). Spatial and temporal variations of heavy metal contamination in sediments of a mangrove swamp in Hong Kong. Marine Pollution Bulletin 31(4-12), 254-261.

(2000). Spatial variation of heavy metals in surface sediments of Hong Kong mangrove swamps. Environmental Pollution 110(2), 195-205.

Tam N. F. Y. and Wong Y. S. (2000). Spatial variation of heavy metals in surface sediments of Hong Kong mangrove swamps. Environmental Pollution 110 110, 195 - 205.

Tamooh F., Van den Meersche K., Meysman F., Marwick T. R., Borges A. V., Merckx R., Dehairs F., Schmidt S., Nyunja J. and Bouillon S. (2012). Distribution and origin of suspended matter and organic carbon pools in the Tana River Basin, Kenya. Biogeosciences 9(8), 2905-2920.

Tan K.-S. and Oh T. M. (2003). Feeding habits of Chicoreus capucinus (Neogastropoda: Muricidae) in a Singapore mangrove. Bollettino Malacologico 38, 43-50.

Tessier A., Campbell P. G. and Bisson M. (1979). Sequential extraction procedure for the speciation of particulate trace metals. Analytical Chemistry 51(7), 844-851.

Thamdrup B. (2000). Bacterial manganese and iron reduction in aquatic sediments. Advances in microbial ecology, Springer**,** 41-84.

Thanh-Nho N., Strady E., Nhu-Trang T. T., David F. and Marchand C. (2018). Trace metals partitioning between particulate and dissolved phases along a tropical mangrove estuary (Can Gio, Vietnam). Chemosphere 196, 311-322.

Thomas N., Lucas R., Bunting P., Hardy A., Rosenqvist A. and Simard M. (2017). Distribution and drivers of global mangrove forest change, 1996–2010. Plos One 12(6), e0179302.

Tomlinson P. B. (2016). The botany of mangroves, Cambridge University Press.

Traunspurger W. and Drews C. (1996). Toxicity analysis of freshwater and marine sediments with meio- and macrobenthic organisms: a review. Hydrobiologia 328(3), 215-261.

Tuan V. Q. and Kuenzer C. (2012). Can Gio Mangrove Biosphere Reserve Evaluation 2012: Current status, Dynamics and Ecosystem Services Ha Noi, Viet Nam: IUCN, 102 pp.

Tue N. T., Hamaoka H., Sogabe A., Quy T. D., Nhuan M. T. and Omori K. (2012). Food sources of macro-invertebrates in an important mangrove ecosystem of Vietnam determined by dual stable isotope signatures. Journal of Sea Research 72, 14-21.

Tue N. T., Quy T. D., Amano A., Hamaoka H., Tanabe S., Nhuan M. T. and Omori K. (2011). Historical Profiles of Trace Element Concentrations in Mangrove Sediments from the Ba Lat Estuary, Red River, Vietnam. Water, Air, & Soil Pollution 223(3), 1315-1330.

Turner A. (1996). Trace-metal partitioning in estuaries: importance of salinity and particle concentration. Marine Chemistry 54, 27 - 39.

Turner A., Millward G., Bale A. and Morris A. (1993). Application of the KD concept to the study of trace metal removal and desorption during estuarine mixing. Estuarine, Coastal and Shelf Science 36(1), 1-13.

UNESCO (2000). Valuation of the Mangrove Ecosystem in Can Gio Mangrove Biosphere Reserve, Vietnam. Final Report, Implemented by: The Vietnam MAB National Committee.

Ure A. M., Quevauviller P., Muntau H. and Griepink B. (1993). Speciation of heavy metals in soils and sediments - an account of the improvement and harmonization of extraction techniques undertaken

under the auspices of the BCR of the commission of the European comminities. International Journal of Environmental Analytical Chemistry 51(1-4), 135-151.

USEPA (2007). US Environmental Protection Agency, Method 3051A: Microwave Assisted Acid Digestion of Sediments, Sludges, Soils, and Oils, part of Test Methods for Evaluating Solid Waste. Physical/Chemical Methods.

Usman A. R., Alkredaa R. S. and Al-Wabel M. I. (2013). Heavy metal contamination in sediments and mangroves from the coast of Red Sea: Avicennia marina as potential metal bioaccumulator. Ecotoxicology and Environmental Safety 97, 263-270.

Van Loon A. F., Te Brake B., Van Huijgevoort M. H. and Dijksma R. (2016). Hydrological classification, a practical tool for mangrove restoration. Plos One 11(3)

Van Ryssen R., Alam M., Goeyens L. and Baeyens W. (1998). The use of flux-corer experiments in the determination of heavy metal re-distribution in and of potential leaching from the sediments. Water Science and Technology 37(6-7), 283-290.

Vargas J. A., Acuña-González J., Gómez E. and Molina J. (2015). Metals in coastal mollusks of Costa Rica. Revista de biologia tropical 63(4), 1007-1019.

Verkleij J. and Schat H. (1990). Mechanisms of metal tolerance in higher plants, CRC Press, Boca Raton, FL.

Viers J., Dupre B. and Gaillardet J. (2009). Chemical composition of suspended sediments in World Rivers: New insights from a new database. Science of The Total Environment 407(2), 853-868.

Vo P. L. (2007). Urbanization and water management in Ho Chi Minh City, Vietnam-issues, challenges and perspectives. GeoJournal 70(1), 75-89.

Vukašinović-Pešić V., Blagojević N., Vukanović S., Savić A. and Pešić V. (2017). Heavy Metal Concentrations in Different Tissues of the Snail Viviparus mamillatus (Küster, 1852) from Lacustrine and Riverine Environments in Montenegro. Turkish Journal of Fisheries and Aquatic Sciences 17(3), 557-563.

Wang S., Yang Z. and Xu L. (2003). Mechanisms of copper toxicity and resistance of plants. Ecology and Environment 3, 336-341.

Wang Y., Liu R. H., Zhang Y. Q., Cui X. Q., Tang A. K. and Zhang L. J. (2016). Transport of heavy metals in the Huanghe River estuary, China. Environmental Earth Sciences 75:288.

Wang Z.-L. and Liu C.-Q. (2003). Distribution and partition behavior of heavy metals between dissolved and acid-soluble fractions along a salinity gradient in the Changjiang Estuary, eastern China. Chemical Geology 202(3-4), 383-396.

Wang Z., Shan X.-q. and Zhang S. (2002). Comparison between fractionation and bioavailability of trace elements in rhizosphere and bulk soils. Chemosphere 46(8), 1163-1171.

Weis J. S. and Weis P. (2004). Metal uptake, transport and release by wetland plants: implications for phytoremediation and restoration. Environment International 30(5), 685-700.

Wen Y., Yang Z. and Xia X. (2013). Dissolved and particulate zinc and nickel in the Yangtze River (China): Distribution, sources and fluxes. Applied Geochemistry 31, 199-208.

Wolanski E. (1995). Transport of sediment in mangrove swamps. Hydrobiologia 295(1-3), 31-42.

Wood T. S. and Shelley M. L. (1999). A dynamic model of bioavailability of metals in constructed wetland sediments. Ecological Engineering 12, 231 - 252.

Wu G.-R., Hong H.-L. and Yan C.-L. (2015). Arsenic accumulation and translocation in mangrove (Aegiceras corniculatum L.) grown in Arsenic Contaminated Soils. International Journal of Environmental Research and Public Health 12(7), 7244-7253.

Xiao R., Bai J., Lu Q., Zhao Q., Gao Z., Wen X. and Liu X. (2015). Fractionation, transfer, and ecological risks of heavy metals in riparian and ditch wetlands across a 100-year chronosequence of reclamation in an estuary of China. Science of the Total Environment 517, 66-75.

Yanan Z., Li H., Kai Y. and Yiqun G. (2017). The Role of Dissolved Organic Matter in the Competitive Adsorption to Goethite, during Arsenic Mobilization. Procedia Earth and Planetary Science 17, 424-427.

Yang J. and Ye Z. (2009). Metal accumulation and tolerance in wetland plants. Frontiers of Biology in China 4(3), 282-288.

Yang Q., Tam N. F., Wong Y. S., Luan T., Su W., Lan C., Shin P. K. and Cheung S. G. (2008). Potential use of mangroves as constructed wetland for municipal sewage treatment in Futian, Shenzhen, China. Marine Pollution Bulletin 57(6-12), 735-743.

Yang X. and Wang Z. L. (2017). Distribution of Dissolved, Suspended, and Sedimentary Heavy Metals along a Salinized River Continuum. Journal of Coastal Research 33(5), 1189-1195.

Yang Z. F., Xia X. Q., Wang Y. P., Ji J. F., Wang D. C., Hou Q. Y. and Yu T. (2014). Dissolved and particulate partitioning of trace elements and their spatial-temporal distribution in the Changjiang River. Journal of Geochemical Exploration 145, 114-123.

Yao Q. Z., Wang X. J., Jian H. M., Chen H. T. and Yu Z. G. (2016). Behavior of suspended particles in the Changjiang Estuary: Size distribution and trace metal contamination. Marine Pollution Bulletin 103(1-2), 159-167.

Yap C. and Cheng W. (2013). Distributions of heavy metal concentrations in different tissues of the mangrove snail Nerita lineata. Sains Malaysiana 42(5), 597-603.

(2009). Heavy metal concentrations in Nerita lineata: the potential as a biomonitor for heavy metal bioavailability and contamination in the tropical intertidal area. Marine Biodiversity Records 2.

Yim M. and Tam N. (1999). Effects of wastewater-borne heavy metals on mangrove plants and soil microbial activities. Marine Pollution Bulletin 39(1), 179-186.

Yruela I. (2009). Copper in plants: acquisition, transport and interactions. Functional Plant Biology 36(5), 409-430.

Yu K., Böhme F., Rinklebe J., Neue H.-U. and DeLaune R. D. (2007). Major biogeochemical processes in soils-A microcosm incubation from reducing to oxidizing conditions. Soil Science Society of America Journal 71(4), 1406-1417.

Yu K. C., Tsai L. J., Chen S. H. and Ho S. T. (2001). Chemical binding of heavy metals in anoxic river sediments. Water Research 35(17), 4086 – 4094.

Zhang D., Zhang X., Tian L., Ye F., Huang X., Zeng Y. and Fan M. (2013). Seasonal and spatial dynamics of trace elements in water and sediment from Pearl River Estuary, South China. Environmental Earth Sciences 68(4), 1053-1063.

Zhang W., Wang W.-X. and Zhang L. (2013). Arsenic speciation and spatial and interspecies differences of metal concentrations in mollusks and crustaceans from a South China estuary. Ecotoxicology 22(4), 671-682.

Zheng Y., Stute M., Van Geen A., Gavrieli I., Dhar R., Simpson H., Schlosser P. and Ahmed K. (2004). Redox control of arsenic mobilization in Bangladesh groundwater. Applied Geochemistry 19(2), 201-214.

Zhou Q., Zhang J., Fu J., Shi J. and Jiang G. (2008). Biomonitoring: an appealing tool for assessment of metal pollution in the aquatic ecosystem. Analytica Chimica Acta 606(2), 135-150.

Zhou Y.-w., Peng Y.-s., Li X.-l. and Chen G.-z. (2011). Accumulation and partitioning of heavy metals in mangrove rhizosphere sediments. Environmental Earth Sciences 64(3), 799-807.

PERSONAL INFORMATION

NGUYEN THANH NHO

N° 380/36/2/8, Le Van Luong street, Tan Hung Ward, District 7, Ho Chi Minh city, 700000, Viet nam
(+84)28 38330733 (+84) 977603422
ntnho@hcmus.edu.vn

Sex Male | Date of birth 01/01/1987 | Nationality Vietnamese

STUDIES APPLIED FOR

Analysis of trace metals in soils, waters, wastewaters, foods, agriculture and medicinal products

WORK EXPERIENCE

Since September, 2009

Researcher and teaching assistant for special field of analytical chemistry at the department of analytical chemistry, Faculty of Chemistry, University of Science – Vietnam National University, Ho Chi Minh city, Vietnam.
Work with the equipment such as:
Atomic absorption spectrometry (F-AAS and HG-AAS) as well as ICP (MS/ OES)
Liquid chromatography (HPLC-UV)

EDUCATION

Since March, 2015

University of New Caledonia, France
PhD candidate: "Trace metals dynamics in a tropical mangrove estuary (Can Gio, Vietnam)"

March 2013

University of Science, Vietnam
Master degree: "Studying retention of As(III) and As(V) on SPE sorbents. Application to on-site sampling for arsenic speciation analysis in ground water"

Projects

2016-2018: Retention and distribution of metals in mangrove sediments, funded by Vietnam National University - Ho Chi Minh City (VNU-HCM) under grant number C2016-18-07.
2013 - 2015: Studying of determination of methyl and total mercury in sludge of Ho Chi Minh's creek, funded by Vietnam National University - Ho Chi Minh city, Vietnam.
2011 - 2012: Simplification of characterising the chemical composition of rock samples using microwave-assisted digestion system, funded by University of Science - Vietnam.

International Publications

- **Thanh-Nho N.,** Strady E., Nhu-Trang T–T., David F., Marchand C., Trace metals partitioning between particulate and dissolved phases along a tropical mangrove estuary (Can Gio, Vietnam). *Chemosphere,* 2018, 196, 311-322
- David F., Meziane T., Nhu-Trang T. T., Vinh T. V., **Thanh-Nho N.,** Taillardat P., Marchand C., Carbon biogeochemistry and CO2 emissions in a human impacted and 2 mangrove-dominated tropical estuary (Can Gio, Vietnam). *Biogeochemistry*, accepted 2018.
- Aimé J., Allenbach M., Bourgeois C., Léopold A., Jacotot A., Vinh T. V., **Thanh-Nho N.,** Patrona L. D., Marchand C., Variability of CO 2 emissions during the rearing cycle of a semi-intensive shrimp farm in a mangrove coastal zone (New Caledonia). *Marine Pollution Bulletin*, 2018, 129 (1), 194-206.
- Strady E., Tuc D. Q., Nemery J., **Thanh-Nho N.**, Guedrone S., Sang N. N., Denis H., Dan N. P., 2017. Spatial variation and risk assessment of trace metals in water and sediment of the Mekong Delta. *Chemosphere*, 179, 367 – 378.

National publications

- Trieu Quoc An, Le Thi Huynh Mai, **Nguyen Thanh Nho**, Nguyen van Dong. 2015. Studying of gold coated sand to apply for analysis of mercury. *Journal of Science and Technology Development*. Vol 18, No T3: 214-222.
- Hoang Thi Huynh Dieu, **Nguyen Thanh Nho**, Nguyen Van Đong. 2014. Studying of simultaneous extraction of As,

Cd, Cr, Pb in saline water and determination by non-flame atomic absorption spectrometry (GF-AAS). *Journal of Science and Technology Development.* Vol 17. No T3: 82-90.

Conferences

International conferences

- **Nguyen Thanh Nho**, Cyril Marchand, Emilie Strady, Frank David, Tran Thi Nhu Trang. 2017. Spatial and seasonal variability of trace metals in tropical mangrove estuary (can Gio, Viet nam), The 5th International Symposium on Environmental Analytical Chemistry (ISEAC 5 – ASIA), HCMC VietNam.
- **Nguyen ThanhNho**, Nguyen Van Dong. 2013. Selective retention of As(III) and As(V) on different SPE sorbents on – site sampling for arsenic speciation analysis in ground water, Analytica VietNam Processing,HCMC VietNam.

National Conferences

- **Nguyen Thanh Nho**, Vu Hoang Anh, Ho Ngoc Thien Khai. 2016. Studying of chemical extraction of Arsenic in contaminated soil. The 10th Scientific Conference of University of Science (VNU-HCM)
- **Nguyen Thanh Nho**, Le Hong Tuan Kiet, Phung Minh Chau, Trieu Quoc An, Nguyen Van Đong. 2014. Determination of inorganic and organic arsenic in rice and sea food by hydride generation atomic absorption spectrometry (HG-AAS). 9th Scientific Conference of University of Science (VNU-HCM).
- **Nguyen Thanh Nho**, Nguyen Thi Thanh Tuyen, Le Thanh Hai, Trieu Quoc An, Nguyen Van Đong. 2014. Determination of selenium in environmental sample and food by HG-AAS. 9th Scientific Conference of University of Science (VNU-HCM).
- Nguyen Tan Loc, **Nguyen Thanh Nho**, Trieu Quoc An, Nguyen Van Đong. 2014. Determination of inorganic and organic mercury in fish by cold vapour coupled atomic absorption spectrometry (CV-AAS). 9th Scientific Conference of University of Science (VNU-HCM).
- **Nguyen ThanhNho**, Tran ThiTuyet Mai, Nguyen Van Dong, Studying separation of arsenite – As(III) from orther arsenical species in water sample in form of As(III) – PDC complex by solid phase extraction using C18 cartridge, 8th Scientific Conference of University of Science (VNU-HCM), 2012.
- **Nguyen Thanh Nho**, Đo Minh Huy, Nguyen Van Đong. 2012. Responsibility of strong baz anion solid phase extraction for site sampling to analyse arsenic (V) in ground water.1st Conference of young scientist (VNU-HCM).
- Le Xuan Vinh, **Nguyen Thanh Nho**, Nguyen Van Dong. 2010. Determination of Bisphenol A in some polymer – based household materials using HPLC – UV, 7th Scientific Conference of University of Science.

ABSTRACT

Mangroves are considered as efficient barriers between land and sea, being sinks for trace metals and protecting coastal water from pollutions. However this ability may depend on sediment characteristics and hydrology. The fate of trace metal is complex due to various biogeochemical processes across the intertidal zone. Because of their toxicity to mangrove biodiversity and also to human health, the trace metal cycling is a serious question addressed by many scientists during the last few decades and nowadays. In contrast to the rest of the world, trace metal distribution in Viet Nam's mangrove forest has received little attention. The aim of this research was to characterize some trace metals dynamics in the Can Gio mangrove, which is located in the Southern Viet Nam, being situated at the edge of a densely populated megacity – Ho Chi Minh City (i.e. almost 10 million inhabitants) and the South China Sea. Along the Can Gio estuary, trace metals, which mainly originated from upstream lateritic soils, were transported mostly associated with suspended solids, mainly oxihydroxides forms. After being deposited in mangrove sediments, the oxihydroxides were dissolved by bacteria during organic matter decay processes under suboxic condition, releasing trace metals in pore-waters. The enrichment of mangrove derived-OM from the mudflat to the *Rhizophora* stand played a key role in controlling diagenetic processes. Dissolved metals were then reprecipitated with new bearing phases such as organometallic complexes, suphides, carbonate etc. depending on the redox condition and on metal characteristics. Furthermore, part of these dissolved metals were available for biota uptake or export to tidal creek by pore-water seepage. Consequently, this PhD thesis also demonstrated that mangrove ecosystems can be sources of trace metals for adjacent ecosystems.